



University of
Stavanger

Faculty of Science and Technology

MASTER'S THESIS

Study program/Specialization: Petroleum Engineering Drilling and Well Technology	Spring semester, 2016 Open
Writer: Anne May Haaland (Writer's signature)
Faculty supervisor: Mesfin Belayneh External supervisor(s): Ola M. Vestavik	
Thesis title: Numerical Simulation and Experimental Study of Reelwell's Heavy over Light Solution in Vertical Well Sections	
Credits (ECTS): 30	
Key words: Reelwell Heavy over Light Solution Numerical Simulation COMSOL Multiphysics Experimental work	Pages: 180 + enclosure: 59 Stavanger, 15.06.2016

ACKNOWLEDGEMENT

First and foremost, I would like to express my gratitude to my supervisor at the University of Stavanger, Professor Mesfin Belayneh. His guidance and support have been exceptional through the entire writing process of the thesis. His door was always open whenever I had questions.

I would also like to thank my external supervisor CTO Ola M. Vestavik from Reelwell, for giving me the opportunity to write the thesis for Reelwell. His knowledge and support have been most valuable.

Erlend Kristiansen and Bertil Nistad, both working for COMSOL, have been of great help whenever I had questions regarding COMSOL. Bertil was the lecturer of a COMSOL introduction course which I attended and Erlend helped building the HOL model in COMSOL. Without them it would have been difficult to implement the COMSOL simulation study in the thesis, and I would like to thank them both.

I also appreciate all the help I got from Theo Ivesdal and Paul Papatzacos at the University of Stavanger, who were always available whenever I had questions regarding technical support and COMSOL at the University.

Last, but not least, I would like to thank my proof-reader Anna Liisa Upsal, and my family and friends for all love and support through the process of writing this thesis.

Stavanger, June 2016

Anne May Haaland

ABSTRACT

Reelwell has developed the Reelwell Drilling Method (RDM), including the Heavy Over Light (HOL) solution. The HOL solution allows drilling with simultaneous use of two different drilling fluids, i.e. a near static drilling fluid with high density for pressure control on the outside of the drill string and a lighter drilling fluid for hole cleaning inside the dual drill string. The HOL solution implies the creation of an interface mixing zone between the heavy and the light fluid in the well annulus outside the drill string.

The HOL solution is mainly used in horizontal sections of the well and provides increased buoyancy which reduces torque and drag of the drill string. The solution may also be useful in vertical wells due to the possibility of deeper setting depth for casings. This goal for this work is to investigate the HOL solution in vertical sections of a well through simulations using the COMSOL Multiphysics software and experimental work. For the simulations there were defined several parameters, such as density, plastic viscosity, and well size. The aim of the simulations was to study the effect of these parameters on the HOL mixing zone.

The experiments were performed in vertical cylindrical tubes, using water based mud or oil based mud with various densities and rheology properties. In some of the experiments a pipe inside the tube was rotated to assist the mixing process. Through the experimental work it was found that yield strength (YS) and low shear yield stress (LSYS) has a reducing effect on the development of the mixing zone. Rotation of the inner pipe made the fluids mix more evenly.

The COMSOL simulations indicated that density and well size affect the speed of the development of the mixing zone, while plastic viscosity has no or little effect. COMSOL did not prove to model the mixture process in accordance with the experimental observations. For further work it may be desirable to further investigate the theoretical model and to study the effect of other parameters, such as rheology properties of the fluids, rotational force of an inner pipe and friction from pipe wall.

NOMENCLATURE

ρ = fluid density

m = mass

V = volume

w = specific weight

g = gravitational constant, 9.81 m/s²

F = force

ν = kinematic viscosity

γ = shear rate

σ = shear stress

ρ_{mix} = density of mixed fluid

α_h = heavy fluid fraction

ρ_l = density of light fluid

ρ_h = density of heavy fluid

μ_{mix} = viscosity of mixed fluid

μ_l = viscosity of light fluid

μ_h = viscosity of heavy fluid

D = diffusion coefficient

$J(\text{matter})$ = flux of matter

$\frac{dN}{dz}$ = slope of concentration

ω = angular velocity

r_{dp} = radius of drill pipe

r_w = radius of wellbore

τ_y = yield point

μ_p = plastic viscosity

R_{600} = reading at 600 RPM

R_{300} = reading at 300 RPM

R_6 = reading at 6 RPM

R_3 = reading at 3 RPM

k = consistence index

n = flow behaviour index

$h(t)$ = amplitude of fluid interface

h_0 = initial amplitude

ν = growth rate of the perturbation

V_B = single mode saturated bubble velocity

R = bubble radius

A = Atwood number

α = acceleration rate

c_i = concentration of the species

R_i = reaction rate expression for the species

N = flux vector

p = pressure

u = fluid velocity

ρ_{av} = average density of fluid

ρ_{upper} = density of upper part of fluid column

ρ_{lower} = density of lower part of fluid column

ABBREVIATIONS

BHA – Bottom Hole Assembly
DFV – Dual Float Valve
ECD – Equivalent Circulating Drilling
ERD – Extended Reach Drilling
FCU – Flow Control Unit
HOL – Heavy over Light
HSE – Health, Safety and Environment
LSYS – Low Shear Yield Stress
OBM – Oil Based Mud
PDE- Partial Differential Equation
PV – Plastic Viscosity
RDM – Reelwell Drilling Method
ROP – Rate of Penetration
RPM – Rotations per Minute
RTI – Rayleigh-Taylot Instability
TDA – Top Drive Adapter
WBM – Water Based Mud
WOB – Weight on Bit
XG – Xanthan Gum
YS – Yield Strength

TABLE OF CONTENTS

ACKNOWLEDGEMENT	II
ABSTRACT	III
NOMENCLATURE.....	IV
ABBREVIATIONS	V
TABLE OF CONTENTS	VI
1 INTRODUCTION	1
1.1 Background	1
1.2 Problem Statement.....	3
1.3 Scope and Objective	4
2 REELWELL TECHNOLOGY	5
2.1 Heavy Over Light (HOL)	7
3 THEORETICAL STUDY.....	8
3.1 Density	8
3.2 Gravity.....	9
3.3 Viscosity	9
3.4 Mixture Theory	11
3.5 Convection Theory.....	13
3.6 Diffusion Theory.....	13
3.7 Interfacial Tension.....	14
3.8 Rotational Force.....	14
3.9 Rheology	15
3.9.1 Bingham Plastic Model	15
3.9.2 Power Law	16
3.9.3 Herschel-Bulkley	16
3.10 Rayleigh-Taylor Instability.....	17
3.11 Fluid Transport Governing Equations	19
3.12 Navier-Stokes Equations	20
4 SIMULATION STUDY HEAVY OVER LIGHT.....	22
4.1 Simulation Setup.....	22

4.1.1 Modelling	23
4.1.2 Material data	24
4.1.3 Multiphysics.....	25
4.1.4 Meshing	27
4.1.5 Boundary Conditions	29
4.1.6 Solution.....	30
4.2 Simulation Results.....	30
4.2.1 Results Reference Case.....	32
4.2.2 Effect of Density	44
4.2.3 Effect of Viscosity	67
4.2.4 Effect of Well Size	90
5 EXPERIMENTAL WORK	114
5.1 General Experimental Setup	114
5.2 Experiment #1	117
5.2.1 Description of Fluids	117
5.2.2 Description of Experiment.....	118
5.2.3 Results	119
5.3 Experiment #2	121
5.3.1 Description of Fluids	121
5.3.2 Description of Experiment.....	122
5.3.3 Results	123
5.4 Experiment #3	124
5.4.1 Description of Fluids	124
5.4.2 Description of Experiment.....	126
5.4.3 Results	126
5.5 Experiment #4	129
5.5.1 Description of Fluids	129
5.5.2 Description of Experiment.....	130
5.5.3 Results	130
5.6 Experiment #5	133
5.6.1 Description of Fluids	133
5.6.2 Description of Experiment.....	134
5.6.3 Results	134
5.7 Experiment #6.....	137

5.7.1 Description of Fluids	137
5.7.2 Description of Experiment	138
5.7.3 Results	138
5.8 Experiment #7	142
5.8.1 Description of Fluids	142
5.8.2 Description of Experiment	142
5.8.3 Results	143
5.9 Experiment #8	145
5.9.1 Description of Fluids	145
5.9.2 Description of Experiment	146
5.9.3 Results	147
6 SUMMARY AND DISCUSSION.....	151
6.1 Simulation Study	151
6.1.1 Reference Case	156
6.1.2 Effect of Density	156
6.1.3 Effect of Viscosity	157
6.1.4 Effect of Well Size	158
6.1.5 Summary.....	159
6.2 Experimental Work	160
6.3 Summary.....	166
7 CONCLUSION	168
REFERENCES.....	170
APPENDIX A SIMULATION RESULTS.....	173
APPENDIX B EXPERIMENTS.....	209
APPENDIX C PLUG EXPERIMENT	216
APPENDIX D LIST OF FIGURES	224
APPENDIX E LIST OF TABLES.....	230

1 INTRODUCTION

This thesis presents a numerical simulation and experimental study of the Heavy over Light (HOL) principle. The simulations were done using the COMSOL multiphysics software.

1.1 Background

The oil industry is always looking for new technology and methods to allow them to drill further in the well, especially in horizontal direction. Extended Reach Drilling (ERD) is directional drilling of very long horizontal wells. The purposes of ERD are mainly to reach larger areas from only one drilling location on surface and to maximize productivity and drainage capability by keeping a well in a reservoir for a longer distance. Figure 1 shows the current ERD envelope (Walker & Molloy, 2014) [1]. Until today the longest ERD well exists in Sakhalin Island in Russia and has a measured depth (MD) of 12,700 meters.

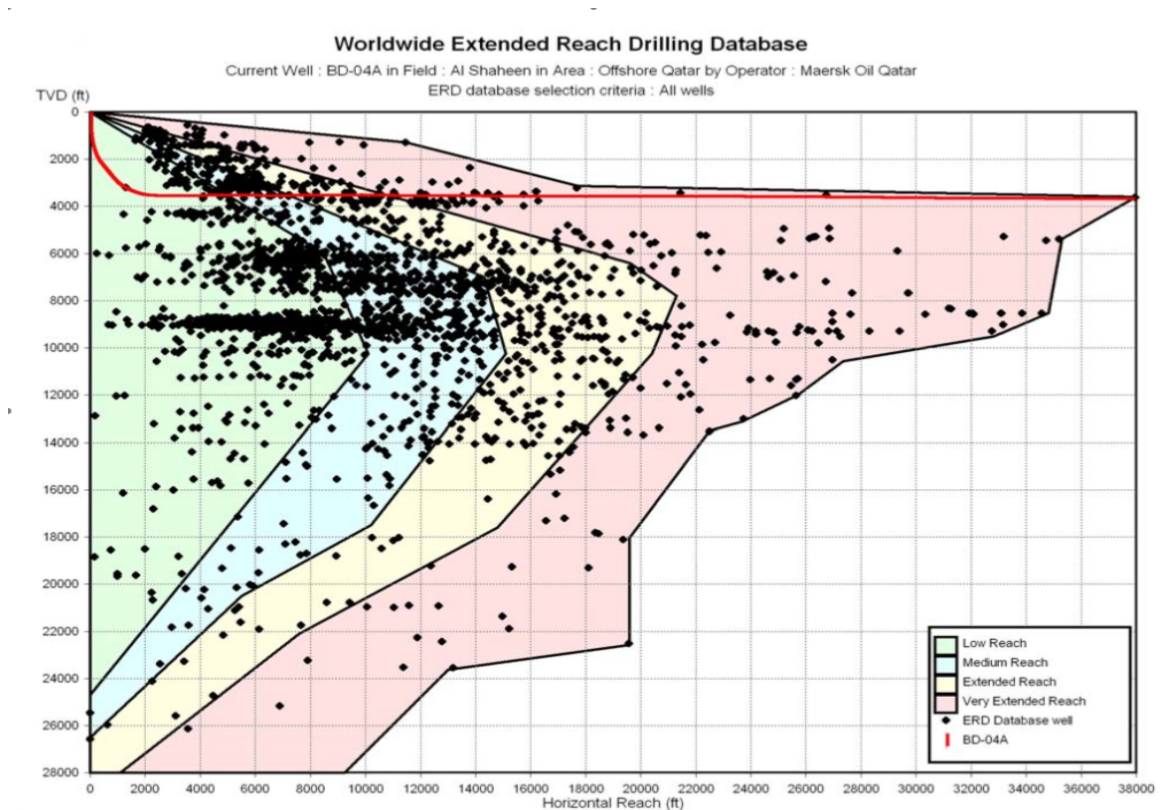


Figure 1: Illustration of an envelope of drilled ERD [1]

Reelwell is a Norwegian company who wants to extend the length of horizontal drilling. They have developed a new drilling method called Reelwell Drilling Method (RDM) which uses a dual drill string with a separate inner pipe. The drilling fluid is pumped down the outer pipe inside the drill string and returned to the surface via the inner pipe along with the cuttings. This can enable drilling beyond the conventional methods [2]. A schematic of the RDM is shown in figure 2.

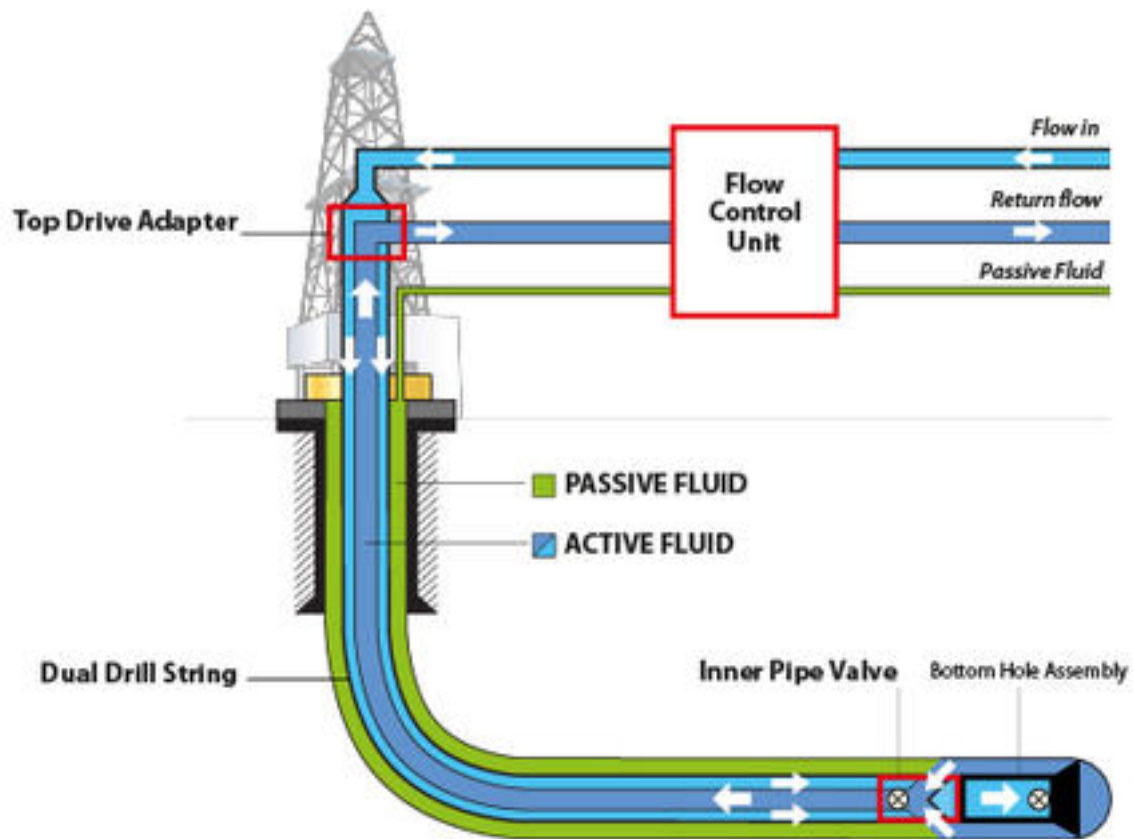


Figure 2: Reelwell Drilling Method [2]

The aim of the RDM is to drill over 20 km MD. One of the technologies to reach this goal is the “Heavy Over Light” (HOL) solution. This enables drilling with a static drilling fluid with high density in the annulus on the outside of the drill string and a drilling fluid with lower density to circulate and transport the cuttings. Due to the density difference between the inside of the drill string and in the annulus, optimum downhole pressure is maintained reducing the torque and drag of the drill string.

The HOL technology is mainly used in horizontal wells where the inclination is larger than 90 degrees. This enables gravity to ensure the position of the two fluids as shown in figure 3.

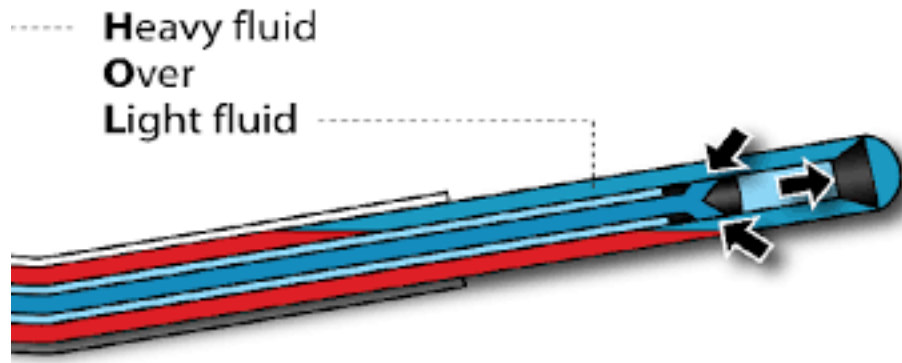


Figure 3: Heavy over Light solution in horizontal section

Former studies of the HOL solution have been carried out in two earlier Master's Thesis. For his Thesis in 2014, Eirik Aasberg Vandvik studied the HOL interface in horizontal sections through experimental work [3]. Magne Hurum investigated weight particle sagging in horizontal sections and conducted an experiment based on the HOL interface in vertical sections [4]. This thesis is going to look at the HOL principle in vertical well sections through numerical simulations in COMSOL and experimental work.

1.2 Problem Statement

The HOL technology is mainly used in horizontal drilling. This thesis will on the other hand investigate the feasibility of using the HOL solution in the vertical section of the well. In this situation the gravity is the main concern as this will force the heavy fluid below the light fluid. For the HOL solution to work, the heavy fluid has to stay on top of the light fluid with a mixing zone between the two fluids. The length of this mixing zone has to stay stable or develop at low speed. This thesis will discuss different models for development of the mixing zone in the vertical section. The main purpose is to prevent the effect of gravity on the two fluids, i.e. to prevent that the heavy fluid flows below the lighter fluid, and instead create a stable mixing zone. It is important to study the effect of

various parameters, such as density, viscosity and well size. The thesis will deal with two methods to achieve this:

- Numerical simulation using the COMSOL Multiphysics software
- Experimental work

1.3 Scope and Objective

The scope of this thesis is limited to numerical simulations and experimental work of the development of the mixing zone between the heavy and the light fluid. The aim is to see which parameters that affect the HOL interface the most.

Summary of research methods of this thesis is presented in figure 4.

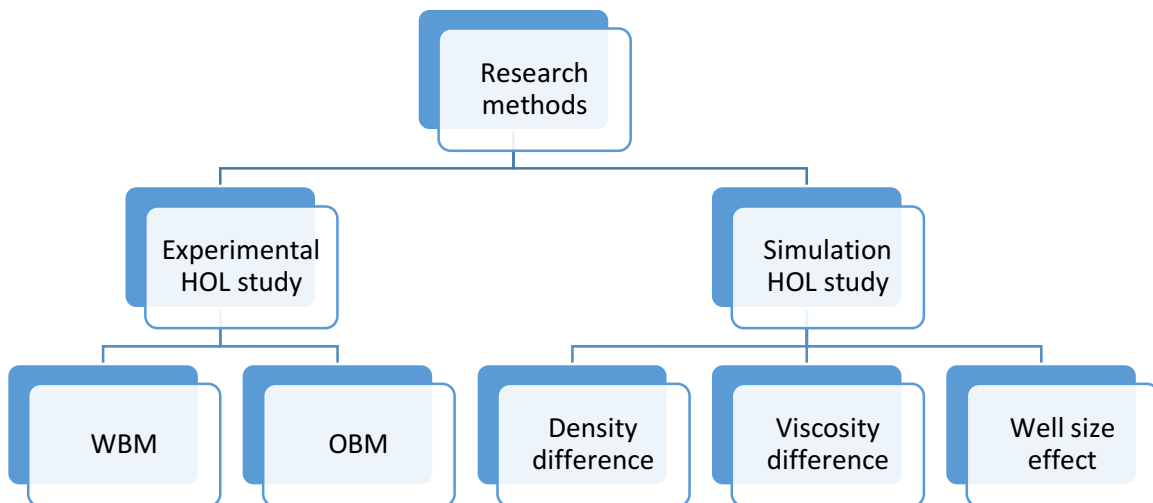


Figure 4: Research methods

2 REELWELL TECHNOLOGY

Reelwell is a drilling technology company which was founded in Stavanger in 2004. The company was established for developing and providing the Reelwell Drilling Method (RDM) which is a solution for drilling exploration and production wells. The method enables drilling of well sections with challenging pressure conditions [5]. RDM is a multi-purpose drilling method based on using a conventional drill string combined with an inner string to form a dual conduit drill string. It has a unique flow arrangement which allows the return fluid together with the drill cuttings, to be transported back to surface through the inside of the drill string [6].

RDM has the ability to increase the envelope for Extended Reach Drilling (ERD) for several reasons [6]:

- Elimination of the dynamic Equivalent Circulating Density (ECD) gradient, since the ECD is screened from the formation.
- Torque and Drag reduction, due to use of a floating technique of the drill string.
- Optional Hydraulic Weight on Bit (WOB), due to a piston type arrangement at the drill string.

The idea for the Reelwell Drilling Method was originally motivated by drilling challenges due to hole cleaning and weight on bit (WOB) control for coiled tubing in drilling operations. After studying this method, it was found that it could also be used to solve several challenges for jointed pipe drilling. The method can be used in managed pressure drilling, liner drilling, deep water drilling and extended reach drilling [7].

RDM is based on the use of a dual drill string which consists of a special solution for a dual wall drill string. The outer channel is used for pumping drilling fluid down the drill string and through the drill bit and the inner channel is used for transporting cuttings back to the surface. In addition, the following tools and arrangements are used: Top Drive Adapter (TDA), Flow Control Unit (FCU), Dual Float Valve (DFV), the active circulating fluid and a Rotary Control Device (RCD). A schematic of the arrangement for the RDM is shown in figure 5 [6].

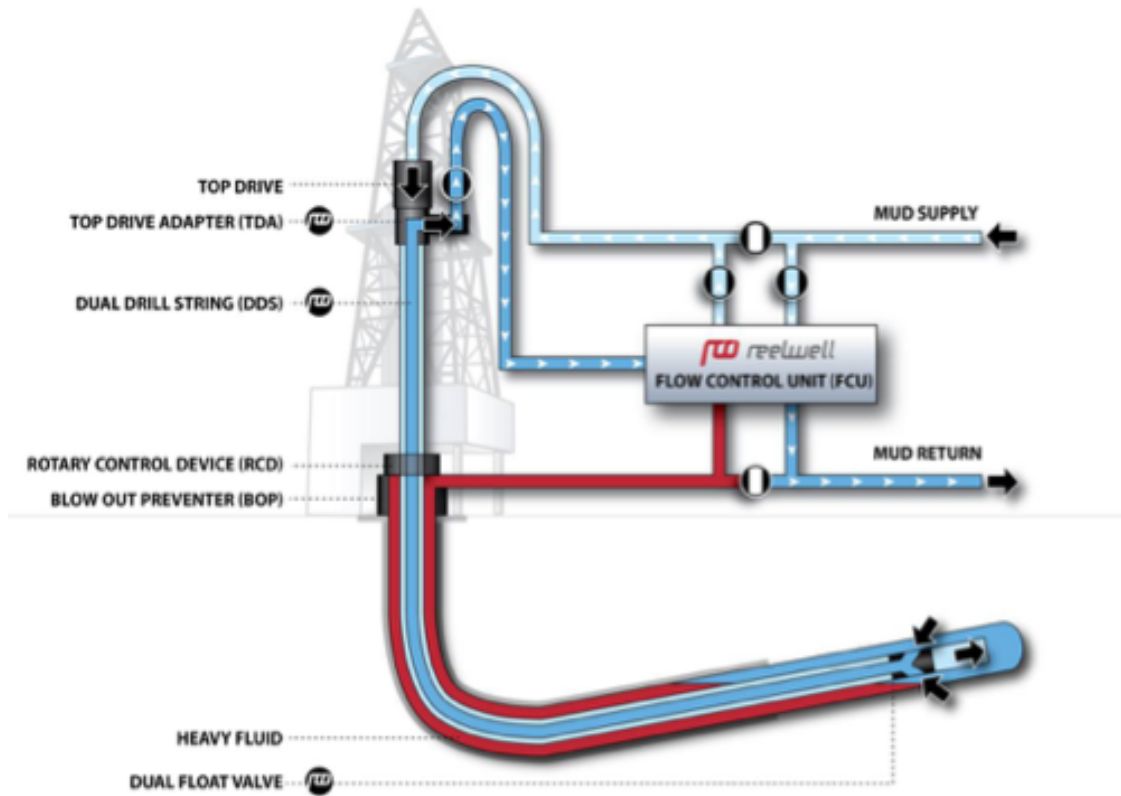


Figure 5: Schematic of the arrangement for the Reelwell Drilling Method

The RDM enables drilling to targets beyond conventional reach and thereby access to significantly larger drainage areas. The formation damage is reduced due to the built-in pressure and flow control system, which increases well productivity. There is less need for additional platforms due to the increase in horizontal reach, making it possible to drill through several reservoirs from one platform. Improved pressure control and use of clean drilling fluids increases safety and reduces environmental damage. RDM is a tool to avoid common drilling problems, improve hole cleaning, reduce circulation time and quick and efficient operations, resulting in reduced non-productive time [5].

In 2011 Reelwell started a large project called “ERD beyond 20 km”. It is a Joint Industry Project supported by Shell, Total, Petrobras and RWE Dea and the Research Council of Norway. The main goal is to drill wells beyond conventional drilling reach in a safe and efficient manner. The project intends to reach this goal due to the following unique features [6]:

- It enables flotation of the drill string, which can reduce torque and drag to a minimum.
- It enables screening out the dynamic ECD gradient.
- It provides means of hydraulic WOB.
- It enables formation evaluation from cuttings – superior to conventional technology.

2.1 Heavy Over Light (HOL)

The Reelwell Drilling Method has some unique ERD functions which are due to “Heavy Over Light” (HOL) operation [6]. The principle of this solution is to keep a high density fluid in the well annulus and a low density fluid inside the drill string. The low density fluid is used to clean the hole and transport cuttings back to surface. The high density fluid is stagnant and provides the required pressure in the well, preventing the formation from fracture or collapse. The HOL solution may be useful in vertical wells due to the possibility of deeper setting depth for casings. This is especially important for drilling in very deep water depths.

To secure that the well pressure is maintained and that the interface between the high density fluid and the low density fluid is correctly positioned as the drilling advances, more heavy drilling fluid is pumped into the annulus. If the well is going to be left open for a longer time without drilling activity, it is preferred to use a mud system with low settling properties [6].

For obtaining highest possible ROP and proper flow rates, the active low density drilling fluid inside the drill string should have as low viscosity as possible. The cuttings are removed from the bottom of the well through ports in the dual drill string at the top of the BHA resulting in good hole cleaning. The downhole pressure for this fluid can be controlled by the flowrate and by choking on the surface [6].

3 THEORETICAL STUDY

This section presents theories that are related to the HOL solution and the simulations in COMSOL Multiphysics.

3.1 Density

Density can be expressed in three different ways, and it is important to distinguish between these [8].

Mass density is defined as the mass of the substance per unit volume. Objects with the same volume, but different mass have thus different densities. The properties of the substance are considered with the substance as a continuum and not with the individual molecules. The mass density at a point is determined by considering the mass of a very small volume surrounding the point. Density is usually represented by ρ and the density of a substance is given by

$$\rho = \frac{m}{V} \quad (3.1)$$

where m is the mass and V is the volume of the substance.

Specific weight is defined as the weight per unit volume. Weight is dependent on the gravitational force and the specific weight will thus vary from point to point, due to the local value of the gravitational acceleration g . According to Newton's second law, the relationship between the mass density ρ and the specific weight w is given by

$$w = \rho \cdot g \quad (3.2)$$

Specific gravity or relative density is defined as the ratio of the mass density of a substance to a specified standard mass density. The usual standard for solids and liquids is water at 4 °C at atmospheric pressure, which is the temperature where water reaches its maximum density. The specific gravity is represented by σ and expressed by

$$\sigma = \frac{\rho_{\text{substance}}}{\rho_{\text{water at } 4^{\circ}\text{C}}} \quad (3.3)$$

3.2 Gravity

One challenge for the Reelwell Drilling Method Heavy over Light solution in vertical wells is to keep a high density fluid to stay above the low density fluid.

Gravity is the attraction of two objects caused by the masses of these objects. According to Isaac Newton the force of gravity acting between one object and any other object is directly proportional to the mass of the first object, directly proportional to the mass of the second object, and inversely proportional to the square of the distance that separates the centre of gravity between the two objects [9].

The gravitational force of any object on Earth is given by

$$F = m \cdot g \quad (3.4)$$

where m is the mass of the object and $g \approx 9.81 \text{ m/s}^2$ is the acceleration of gravity on Earth.

This implies that the fluid with highest density is exposed to greater gravitational force resulting in positioning this fluid beneath the other fluid with lower density.

3.3 Viscosity

The viscosity of a liquid is the measure of the fluid's resistance to flow. Formally, it has been defined as '*the property of a liquid to resist shear deformation increasingly with increasing rate of deformation*'. Viscosity is observed as either the force resulting from the flow of a liquid or as the liquid's response to an applied force. Viscosity can also be referred to as the thickness of the fluid. Fluids with high viscosity are perceived as thick fluids and fluids with low viscosity are perceived as thin fluids [10].

If an object moves inside a fluid, the object will be exposed to a force caused by the viscosity of the fluid. The higher the viscosity, the higher the force on the object. Conversely, if pumping fluids through a pipe at constant pressure the flow rate of the fluid will be lower with higher viscosity.

The unit of viscosity is pascal second with the symbol Pa·s. This unit is directly relatable to the older unit of viscosity which is called the Poise. One Poise is equal to 0.1 pascal second. It is often common to use the unit centi-Poise which is equal to 0.01 Poise and 1 mPa·s (= 0.001 Pa·s). The symbol used for viscosity is the Greek letter η . Kinematic viscosity is defined as viscosity divided by density and is symbolised by ν .

The kind of flow where the liquid can be imagined as layers sliding over one another is called *shear flow*. From this flow the *shear rate* is defined as the velocity gradient, V/h , with unit 1/s or s^{-1} and symbol γ . The force that is produced when the liquid is sheared is called the *shear stress*. This is defined as force per unit area, i.e. N/m^2 or pascal, Pa, and has the symbol σ . The relationship between the shear rate, shear stress and viscosity is defined as

$$\sigma = \eta \cdot \gamma \quad (3.5)$$

For a Newtonian fluid the viscosity is only a function of temperature and pressure, and is not affected by the shear stress and the shear rate. Figure 6 shows the relationship between viscosity, shear stress and shear rate for a Newtonian fluid. For a non-Newtonian fluid, however, the viscosity is also a function of the shear stress and shear rate. A couple of examples of the relationship between viscosity, shear stress and shear rate for a non-Newtonian fluid is illustrated in figure 7.

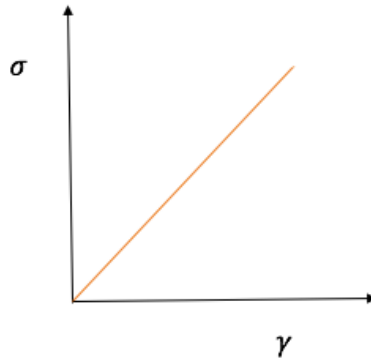


Figure 6: Relationship between viscosity, shear stress and shear rate for a Newtonian fluid

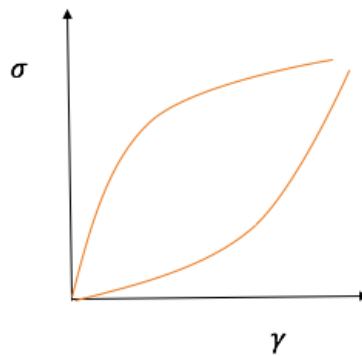


Figure 7: Examples of relationship between viscosity, shear stress and shear rate for a non-Newtonian fluid

3.4 Mixture Theory

The mixture of two miscible drilling fluids results in a new fluid which has different physical and rheological properties. The density and the viscosity of the mixed fluids can be quantified based on the properties and the volume fracture of the mixing fluids.

The density of the mixed fluid of a heavy and a light fluid can be calculated using the formula [11]

$$\rho_{mix} = (1 - \alpha_h)\rho_l + \alpha_h\rho_h \quad (3.6)$$

where α_h is the fraction of heavy fluid, ρ_l is the density of the light fluid and ρ_h is the density of the heavy fluid.

Similarly, the viscosity of the mixed fluid can be calculated as [11]

$$\mu_{mix} = (1 - \alpha_h)\mu_l + \alpha_h\mu_h \quad (3.7)$$

where μ_l is the viscosity of the light fluid and μ_h is the viscosity of the heavy fluid.

Figure 8 illustrates the density of the mixed fluid for volume fraction between 0 and 1. For the volume fraction equal to 0, the fluid system is completely light, i.e. density of 1.10 sg. Similarly, when the volume fraction is equal to 1, the fluid system is completely heavy, i.e. density of 1.65 sg. This phenomenon will be evaluated in chapter 4; Simulation Work, and in chapter 5; Experimental Work.

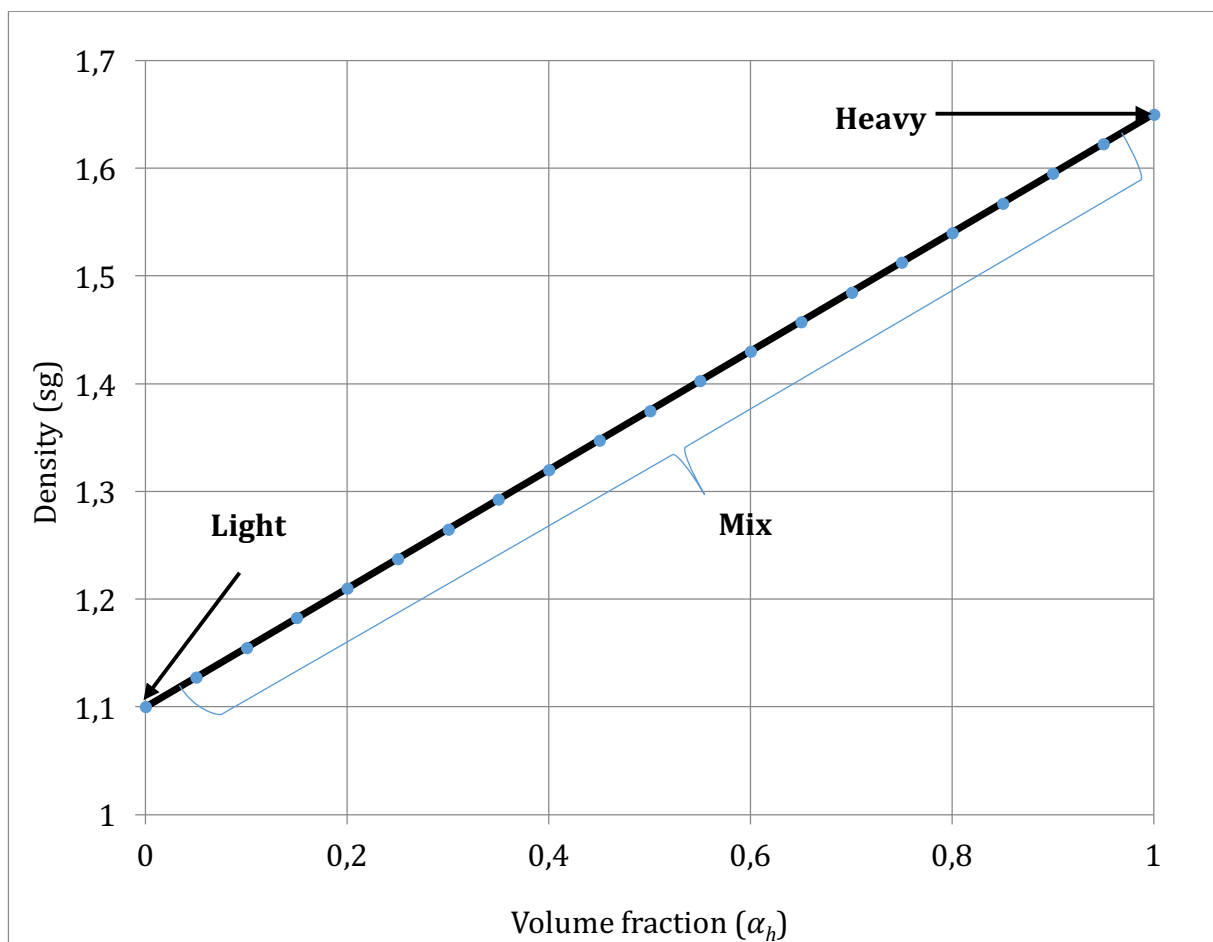


Figure 8: An illustration of density mix as a function of volume fraction

3.5 Convection Theory

Convection is the process where heat is transferred by movement of a heated fluid or gas. Most fluids have the tendency of expanding when heated, which results in natural convection. When the fluid expands due to heating, it will become less dense and rise as a result of the increased buoyancy. Uniform heating of water in a kettle leads to circulation caused by the convection effect. The heated molecules expand and rise as they move in through increased speed against one another. Eventually they cool and come closer again resulting in increase in density and eventually sinking.

Forced convection is the result of movement or transport of the fluid caused by an external force, e.g. a pump, and not by variation in temperature and density [12].

3.6 Diffusion Theory

Diffusion is a mass transfer phenomenon that leads to a more uniform distribution of a chemical species in space as time goes by. Species is in this case described as a chemical dissolved in a solvent or a component in a gas mixture [13].

Molecules are never at rest at temperatures above absolute zero. The driving force for diffusion is the thermal motion of molecules. During their movement the molecules are constantly changing direction and the statistics of this movement cause diffusion to occur.

For describing the statistical process, it is common to use continuous partial differential equations (PDE) when modelling diffusion. The diffusion coefficient, D , has SI units of metres squared per second (m^2/s) and its typical value is relatively small.

Fick's first law of diffusion implies that if the concentration varies steeply with position, diffusion will be fast. If the concentration is uniform, there is no net flux. This flux can be expressed by [14]

$$J(\text{matter}) = -D \frac{dN}{dz} \quad (3.8)$$

where D is the diffusion coefficient and (dN/dz) is the slope of concentration.

3.7 Interfacial Tension

Interfacial or surface tension appears when two phases are present. These phases can consist of gas and oil, oil and water or gas and water. Interfacial tension is the force that makes sure that the surface of a particular phase stays together and is a function of pressure, temperature and the composition of each phase [15].

3.8 Rotational Force

When a drill string is rotated, a rotational force is created by its angular velocity. Deformation of fluid will be greatest at the outer wall of the drill pipe and decreases as the distance to the pipe wall increases. The shear rate created by this situation is given by [16]

$$\gamma = \frac{\omega \cdot r_{dp}}{r_w - r_{dp}} \quad (3.9)$$

where:

ω = angular velocity

r_{dp} = radius of drill pipe

r_w = radius of wellbore

Figure 9 shows a cross section of a rotating drill pipe in a wellbore.

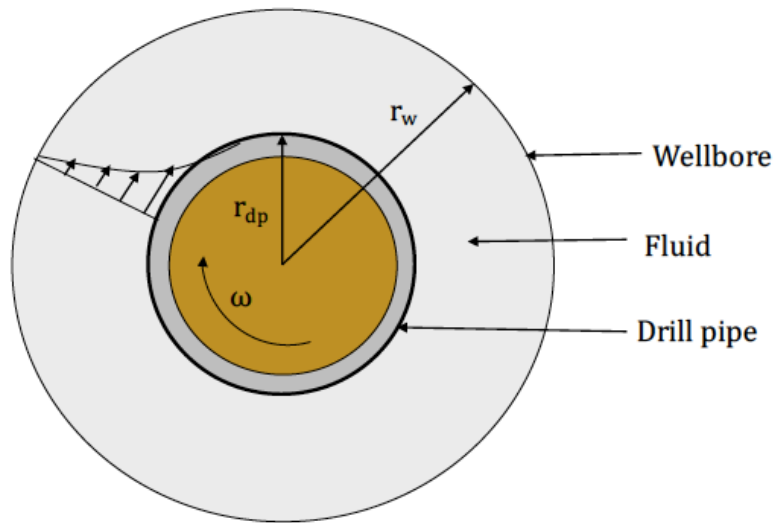


Figure 9: Rotation of drill pipe in wellbore

3.9 Rheology

Rheology means *the study of the deformation and flow of matter*. The term is particularly used for non-Newtonian fluids which is the case for most drilling fluid muds. The viscosity of these fluids decreases as the shear rate increases. Rheometry is the science of reproducing deformation and measuring the consequences on materials of interest [17].

3.9.1 Bingham Plastic Model

The Bingham plastic model is a two-parameter model. However, it is not accurate enough to represent the behaviour of the drilling fluid at very low shear rates in the annulus or at very high shear rates at the bit. The equation of the Bingham Plastic Model is given by [17]

$$\tau = \mu_p \gamma + \tau_y \quad (3.10)$$

where τ_y is the yield point and μ_p is the plastic viscosity. These parameters can be found from a graph or calculated by the following equations

$$\mu_p = R_{600} - R_{300} \quad (3.11)$$

$$\tau_y = R_{300} - \mu_p \quad (3.12)$$

R_{600} and R_{300} represent readings from the viscometer at respectively 600 and 300 rpm.

3.9.2 Power Law

While the Bingham plastic model assumes a linear relationship between shear stress and shear rate, the Power law considers an exponential relationship. This may be a better representation of the behaviour of a drilling fluid. According to Power law the relationship between viscosity and shear rate is represented by [17]

$$\tau = k\gamma^n \quad (3.13)$$

where k is the consistence index and n is the flow behaviour index. By linearizing the equation, n can be determined from the slope and k is the intersection.

$$\log\tau = \log k + n \cdot \log\gamma \quad (3.14)$$

The Power law parameters can also be estimated by the following equations

$$n = 3.32 \cdot \log \frac{R_{600}}{R_{300}} \quad (3.15)$$

$$k = \frac{510 \cdot R_{600}}{511^n} \quad (3.16)$$

3.9.3 Herschel-Bulkley

The Herschel-Bulkley model is a three-parameter model and is mathematically defined by [17]

$$\tau = \tau_0 + k\gamma^n \quad (3.17)$$

$$\log(\tau - \tau_0) = \log k + n \cdot \log\gamma \quad (3.18)$$

where the parameters k and n are the same as in the Power law model. If $\tau > \tau_0$ the material will flow as a Power law fluid, otherwise it will obey the Herschel-Bulkley model.

When adequate experimental data are available, the Herschel-Bulkley equation gives more accurate models of rheological behaviour than the Power law or Bingham plastic model.

3.10 Rayleigh-Taylor Instability

Rayleigh-Taylor instability (RTI) occurs when there exists an interface between two fluids with different densities. The fluid with the highest density is on top of the lighter fluid providing an unstable interface driven by gravity. Only a small perturbation causes the heavy fluid to fall as a spike into the light fluid, and the light fluid will rise as a bubble into the heavy fluid. Figure 10 shows the how forces are affecting the fluids at the interface [18].

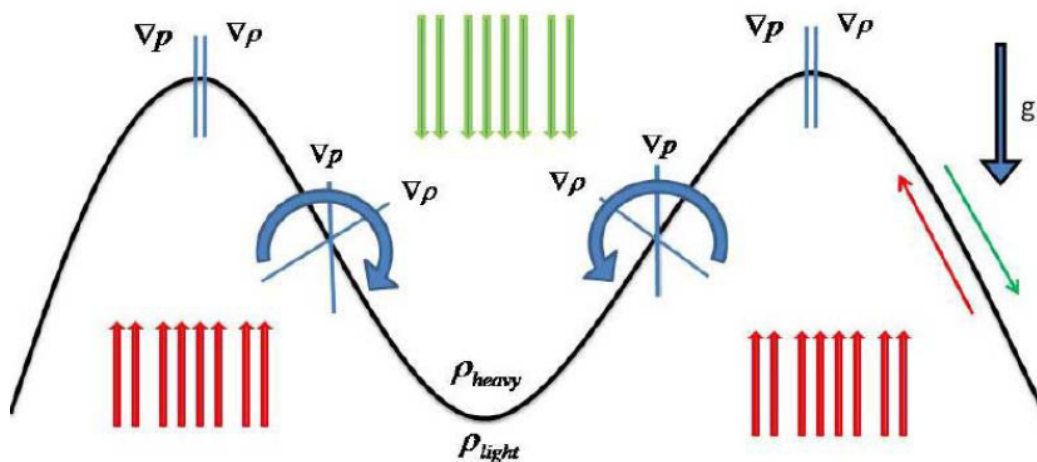


Figure 10: Forces affecting the fluids at the interface

Figure 11 shows hydrodynamics simulation of the Rayleigh-Taylor instability [19].

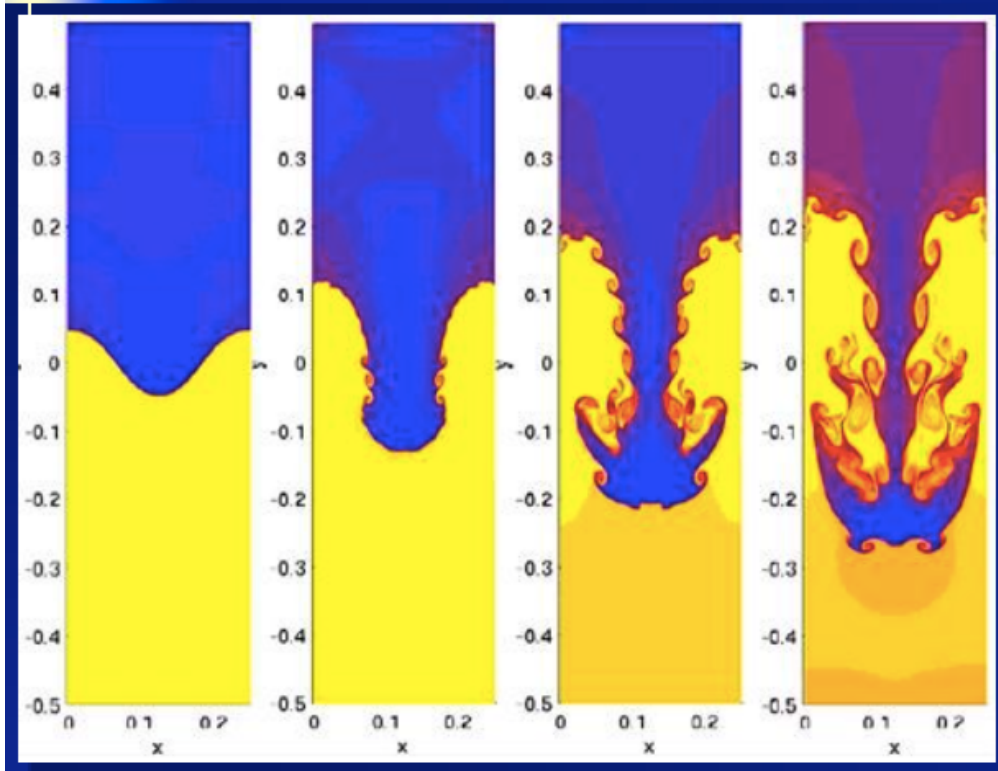


Figure 11: Hydrodynamics simulation of the Rayleigh-Taylor instability

There are three regimes of Rayleigh-Taylor instability. The first regime takes place when the amplitude of perturbation is much smaller than the wavelength. The fluid motion can in this case be analysed using an exponential model. Given a small perturbation of the fluid interface, the amplitude in time, $h(t)$, is expressed by [20]

$$h(t) = h_0 e^{\nu t} \quad (3.19)$$

where h_0 is the initial amplitude and ν is the growth rate of the perturbation. The growth rate is a function of the density ratio, viscosity, surface tension and boundary conditions.

In the second regime the light fluid rises as bubbles while the heavy fluid sinks as spikes. The unstable mode becomes nonlinear and the bubble motion is given by the scaling law [20],

$$V_B = C \sqrt{AgR} \quad (3.20)$$

where V_B is the single mode saturated bubble velocity, g is the gravity constant, R is the bubble radius and A is the Atwood number. The Atwood number is given by [20]

$$A = \frac{\rho_1 - \rho_2}{\rho_1 + \rho_2} \quad (3.21)$$

where ρ_1 is the density of the heavy fluid and ρ_2 is the density of the light fluid. The constant C has been studied both experimentally and analytically. The common values of C for incompressible fluids are 0.32 for a two-dimensional bubble and 0.48 for a three-dimensional bubble.

The third regime is defined by the interaction among bubbles of different sizes resulting in unification, competition and chaotic mixing. The accelerated motion of the bubble front is found from experiment and can be expressed by [20]

$$h = \alpha g A t^2 \quad (3.22)$$

where h is the height of the bubble envelop and t is time. The coefficient, α , is a constant and independent of A . The value of α is measured experimentally and is found to be approximately 0.06. By simulation of the Euler equations in both 2D and 3D, Youngs found the acceleration rate, α , to be approximately 0.04.

3.11 Fluid Transport Governing Equations

Consider the heavy over light phenomenon. Due to physical, rheological, chemical and electrical properties, surface tension and other parameters at the interface, there is a transport phenomenon at the interface. The Transport of Diluted Species interface models chemical species transport governed by several processes. These are through diffusion and convection and solve the mass conservation equation for one or more chemical species, i .

$$\frac{\partial c_i}{\partial t} + \nabla \cdot (-D_i \nabla c_i) + u \cdot \nabla c_i = R_i \quad (3.23)$$

The flux vector N (SI unit: mol/(m²·s)) is associated with the mass balance equation above and used in boundary conditions and flux computations. For the case where the diffusion and convection are the only transport mechanisms, the flux vector is defined as

$$N_i = -D_i \nabla c_i + u c_i \quad (3.24)$$

As shown, Equation 22 includes the transport mechanisms diffusion and convection, where

- c_i is the concentration of the species (SI unit: mol/m³)
- D_i denotes the diffusion coefficient (SI unit: m²/s)
- R_i is a reaction rate expression for the species (SI unit: mol/(m³·s))

The first term on the left side of Equation 22 corresponds to the accumulation (or indeed consumption) of the species. The second term accounts for the diffusive transport, accounting for the interaction between dilute species and the solvent. An input field for the diffusion coefficient is available. Anisotropic diffusion coefficient tensor input is supported. The third term on the left side of Equation 22 describes the convective transport due to a velocity field, u . This field can be expressed analytically or obtained from coupling this physics interface to one that computes fluid flow, such as *Laminar Flow*.

On the right-hand side of the mass-balance equation (Equation 22), R_i represents a source or sink term, typically due to a chemical reaction or desorption on a porous matrix. To specify R_i , another node must be added to the Transport of Diluted Species interface – the Reaction node, which has a field for specifying a reaction equation using the variable names of all participating species.

3.12 Navier-Stokes Equations

The motion of fluid can be described by Momentum Conservation (Navier-Stokes) and mass conservation (continuity equation) [22].

Momentum conservation

Along with the conservation of mass, the HOL motion at the interface can be described by the Navier-Stokes equations. It is documented that the model even describes turbulent flows to agree with real observations. The Navier-Stokes equations are a description of Newton's second law of motion of fluids. The velocity solved from the Navier-Stokes equations is a flow velocity. From the velocity field, pressure or temperature can be determined. The Navier-Stokes equation is given by [22]

$$\rho \left(\frac{\partial u}{\partial t} + u \cdot \nabla u \right) = -\nabla p + \nabla \cdot \left(\mu(\nabla u + (\nabla u)^T) - \frac{2}{3} \mu(\nabla \cdot u)I \right) + F \quad (3.25)$$

where u is the velocity of fluid, p is pressure, ρ is fluid density and μ is the dynamic viscosity.

The first term in Equation 3.25 is the inertial forces, the second term is pressure force, the third term is viscous forces and the fourth term is the external forces applied to the fluid system

For very low Reynolds number, such as the limit $Re \rightarrow 0$ and steady state conditions, the acceleration terms will be insignificant. Equation 3.25 is then reduced to [22]

$$\nabla p = \nabla \cdot \left(\mu(\nabla u + (\nabla u)^T) - \frac{2}{3} \mu(\nabla \cdot u)I \right) + F \quad (3.26)$$

The conservation of mass of fluid can be derived by the equation of continuity. Both momentum and continuity equations are solved simultaneously. The continuity equation is defined as [22]

$$\frac{\partial \rho}{\partial t} + \nabla \cdot (\rho u) = 0 \quad (3.27)$$

For an incompressible fluid, i.e. fluid with constant density, the continuity equation is reduced to

$$\nabla \cdot u = 0 \quad (3.28)$$

4 SIMULATION STUDY HEAVY OVER LIGHT

The purpose of the simulations is to study how various parameters may affect the length and density of the mixing zone between a high density fluid and a low density fluid by varying parameters such as density, viscosity and size of the well bore.

4.1 Simulation Setup

The simulation in this thesis is done using the COMSOL Multiphysics® software, from now on referred to as COMSOL. The data used in the simulation is mainly taken from information given by Reelwell. The author had help from Erlend Kristiansen from COMSOL office in Trondheim for setting up the model. The main menu for the Model Builder in COMSOL is shown in figure 12 [23].

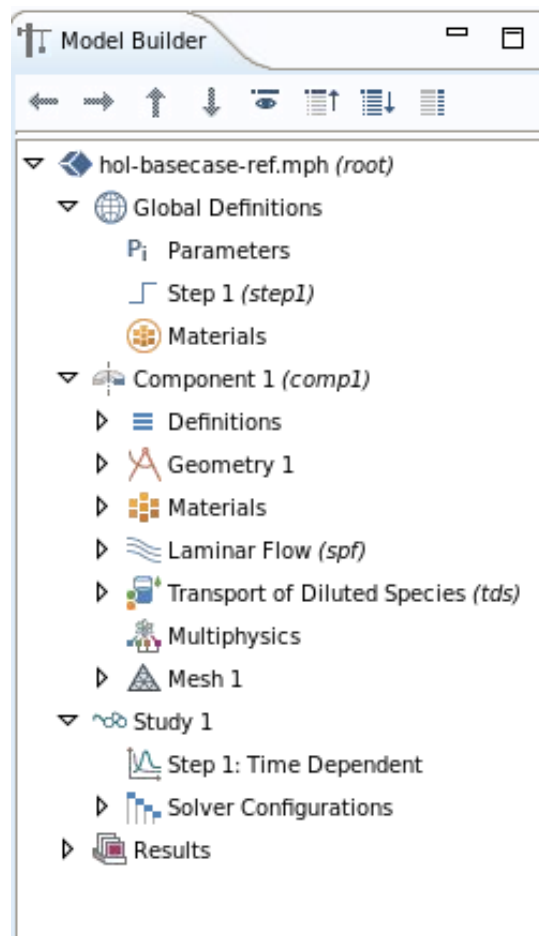


Figure 12: Model Builder in COMSOL

4.1.1 Modelling

When building the model, the geometry has to be defined first. In this case a rectangular shaped model is used to illustrate the inside of the wellbore where the two fluids are located. The height of the rectangle is equal to the height of a selected section of a well with the interface of the two fluids in the middle. The width of the rectangle is equal to the radius of the well. Figure 13 shows how to define the width and the height of the model in COMSOL [23].

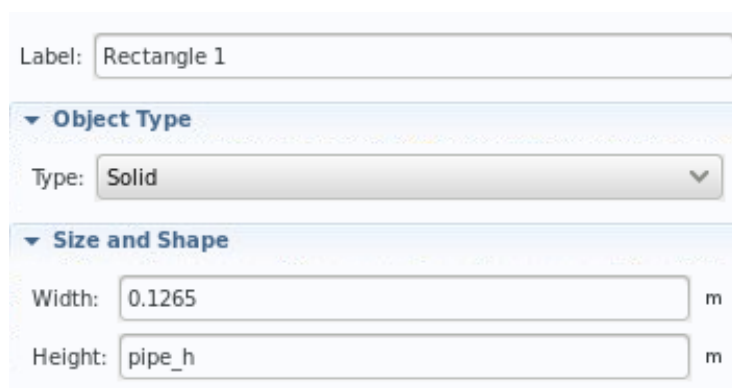


Figure 13: Defining the size of the fluid column in COMSOL

The space dimension used in this simulation is 2D axisymmetric. This implies that only half the pipe is defined in the model and it is turning around its own axis, as shown in figure 14. The picture is taken from the COMSOL software. The radius of the wellbore defined in COMSOL has the length of the blue area in figure 14 [23].

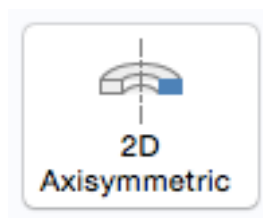
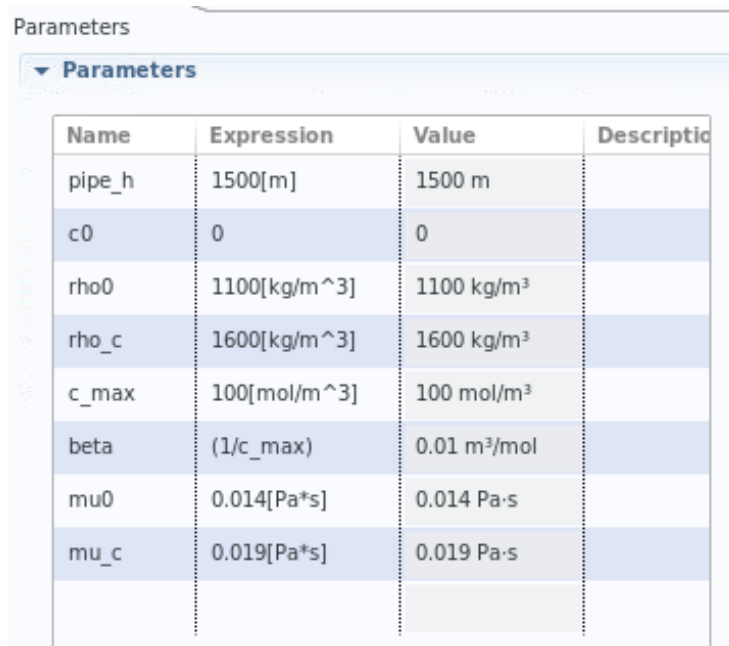


Figure 14: 2D Axisymmetric option in COMSOL Multiphysics®.

To compute the solution of the model, various parameters must be defined. This is done under the parameters section which include among the height of the pipe section and

the densities and viscosities of the fluids. Figure 15 shows the various parameters in COMSOL [23].



Name	Expression	Value	Description
pipe_h	1500[m]	1500 m	
c0	0	0	
rho0	1100[kg/m ³]	1100 kg/m ³	
rho_c	1600[kg/m ³]	1600 kg/m ³	
c_max	100[mol/m ³]	100 mol/m ³	
beta	(1/c_max)	0.01 m ³ /mol	
mu0	0.014[Pa*s]	0.014 Pa-s	
mu_c	0.019[Pa*s]	0.019 Pa-s	

Figure 15: Parameters in COMSOL

In the table in COMSOL pipe_h represents the height of the fluid column, c0 and c_max is the initial concentrations of the light and the heavy fluid, respectively. rho0 and mu0 are the density and viscosity of the light fluid, and rho_c and mu_c are the density and viscosity of the heavy fluid. Beta is a constant for getting the units correct in the equations in COMSOL.

4.1.2 Material data

For material selection, the rectangle is divided into two pieces, one for the heavy fluid and one for the light fluid. The interface between the fluids is located in the middle of the pipe, i.e. the height of the heavy fluid is equal to the height of the light fluid. Figure 16 shows how the rectangle i.e. the fluid column is equally divided at the interface [23].

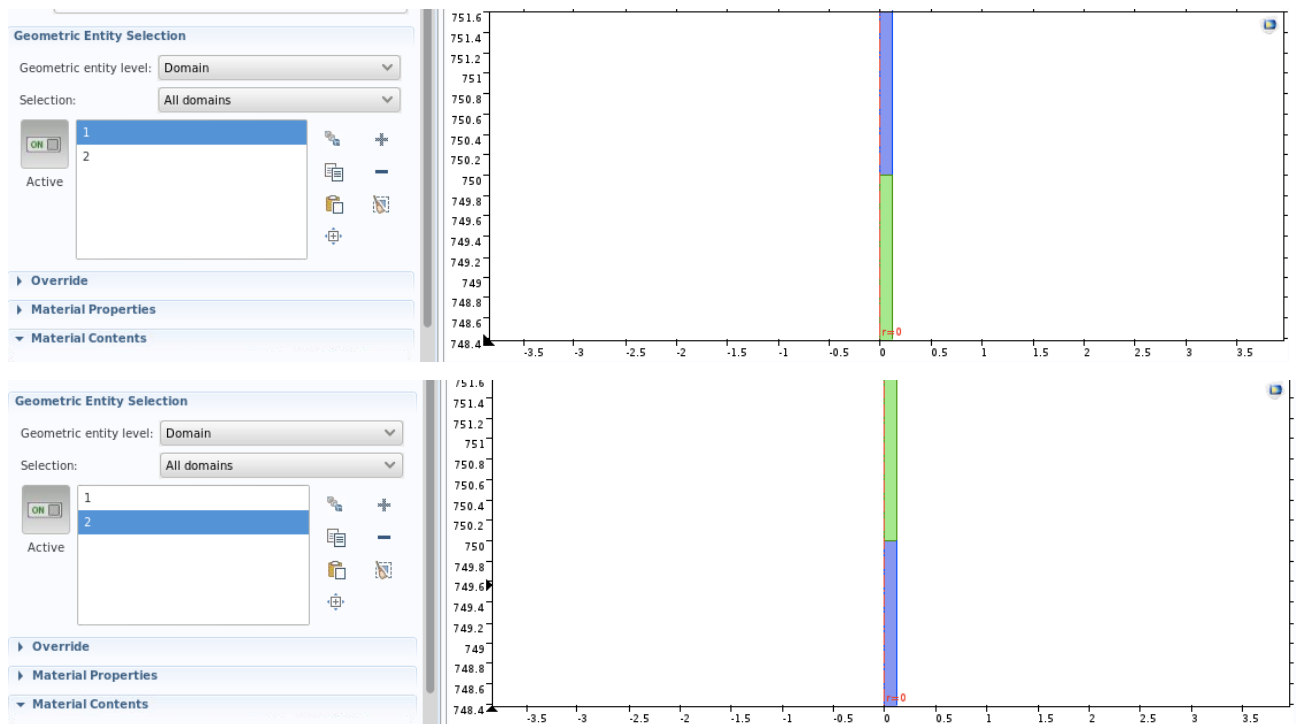


Figure 16: Dividing the rectangle/fluid column into two pieces in COMSOL

4.1.3 Multiphysics

The physics chosen for the multiphysics section are laminar flow and transport of diluted species. In the laminar flow section there are options for fluid properties, initial values, axial symmetry, wall and volume force.

For the fluid properties the density and viscosity for the mixing zone are defined as rho and mu, respectively, and by the following equations. Figure 17 presents the equations for the variables in COMSOL [23].

Variables		
Name	Expression	Unit
rho	$\rho_0 + (\rho_c - \rho_0) \cdot \beta \cdot (c - c_0) \cdot (c > 0) \cdot (c \leq c_{\max}) + (\rho_c - \rho_0) \cdot \beta \cdot (c_{\max} - c_0) \cdot (c > c_{\max})$	kg/m ³
mu	$\mu_0 + (\mu_c - \mu_0) \cdot \beta \cdot (c - c_0) \cdot (c > 0)$	Pa·s

Figure 17: Variables expressions in COMSOL

$$\begin{aligned} \rho = \rho_0 + (\rho_o - \rho_0) \cdot \beta \cdot (c - c_0) \cdot (c > 0) \cdot (c \leq c_{max}) + \\ (\rho_c - \rho_0) \cdot \beta \cdot (c_{max} - c_0) \cdot (c > c_{max}) \end{aligned} \quad (4.1)$$

$$\mu = \mu_0 + (\mu_c - \mu_0) \cdot \beta \cdot (c - c_0) \cdot (c > 0) \quad (4.2)$$

The initial pressure force, P , is defined as the hydrostatic pressure from the fluid columns and acts only in the vertical direction (z -direction). The initial velocity is set to zero and the boundary condition at the wall is set to no slip. The volume force, F , is defined by the hydrostatic weight of the fluid and is given in N/m^3 . The equations for the pressure and the volume force are expressed by Equation 26 and 27 below.

$$F = -\rho \cdot g_{const} \cdot \text{step1}(t[1/s]) \quad (4.3)$$

$$P = \rho_c \cdot g_{const} \cdot \text{pipe}_h/2 + \rho_0 \cdot g_{const} \cdot (\text{pipe}_h/2 - z) \quad (4.4)$$

where ρ is the density of the mixed zone, ρ_c is the initial density of the heavy fluid, ρ_0 is the initial density of the light fluid, g_{const} is the gravitational constant, pipe_h is the height of the fluid column and z is a given height of the fluid column.

For the transport properties the diffusion coefficient is set to $10^{-9} \text{ m}^2/\text{s}$, which is a typical value for aqueous (water) solutions [24].

The initial values in this section are related to the concentrations of the two fluids. Because COMSOL utilizes the concentrations of the fluids and not the densities for computing the solutions, there is need for interpolation for calculating the density of the fluid in the mixed fluid zone. The concentration of the mixed fluid zone at a certain point corresponds to the fraction of the heavy fluid, α_h . This implies that a concentration of $100 \text{ mol}/\text{m}^3$ corresponds to a fraction of 1, and similarly, a concentration of $0 \text{ mol}/\text{m}^3$ corresponds to a fraction equal to 0. By setting the maximum concentration to $100 \text{ mol}/\text{m}^3$ and the minimum concentration to $0 \text{ mol}/\text{m}^3$, the density in the mixed fluid zone at a certain point can be calculated by Equation 6. The range of the fraction, α_h , reaches from 0 to 1. This means that when α_h equals 0 there is no heavy fluid at the certain point and when α_h equals 1 there is only heavy fluid.

4.1.4 Meshing

Meshing the model means to divide the model into several elements and compute the solution for each elements at all time steps. For each element there is a certain number of nodes depending on the type of element that is used and the solution is computed at the node points [25].

The elements can have different shapes given that they are either one-, two- or three-dimensional. The names of the elements depend on the shape and the type of curve or surface bounding that element. One dimensional elements consist of lines and may be either straight or curved. Two dimensional elements are triangles or quadrilaterals. Three-dimensional elements are tetrahedrons, hexahedrons or prisms [25].

For describing the behaviour of a physical system there is need for mathematical models. Engineering sciences use partial differential equations for describing such systems. Finite Element Method (FEM) is one of the most common methods for solving these equations, but it requires intensive use of a computer. It can be used for solving almost every kind of problem which is encountered in practice, for instance, steady state or transient problems in both linear and non-linear regions, and for one-, two- and three-dimensional domains. FEM utilizes simple approximations of unknown variables and transforms partial differential equations into algebraic equations [25].

In COMSOL it is possible to choose how fine or coarse the mesh should be. No matter how coarse the mesh, it is always possible to find a solution, but it may not be as accurate as desired.

There are four different types of elements that can be used for 3-dimensional modelling; tetrahedral, hexahedra, triangular prismatic and pyramid elements. The elements are shown in figure 18. For 2-dimensional modelling triangular and quadrilateral elements are available [26].

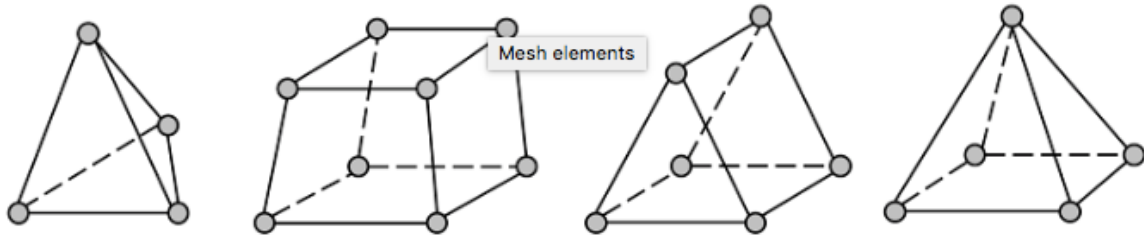


Figure 18: Four different types of elements used for 3D modelling in COMSOL

For meshing the model in this thesis two-dimensional triangular elements are used. These are called Free Triangular elements in COMSOL. The model is divided into three areas where the elements are of various sizes. At the interface the elements are finer distributed and there are thus more elements in this area than further away from the interface. The elements at the boundaries i.e. the pipe wall and at the top and the bottom of the pipe, are coarser distributed. The elements in the rest of the area of the model are even coarser distributed. The critical points of the model are expected at the interface and at the boundaries and smaller elements are used here. Using different size for the elements makes it possible to reduce the total number of elements and thus reduce the solution time.

Figure 19 is from the model in the COMSOL software, showing the meshed model at the interface and at the boundaries [23].

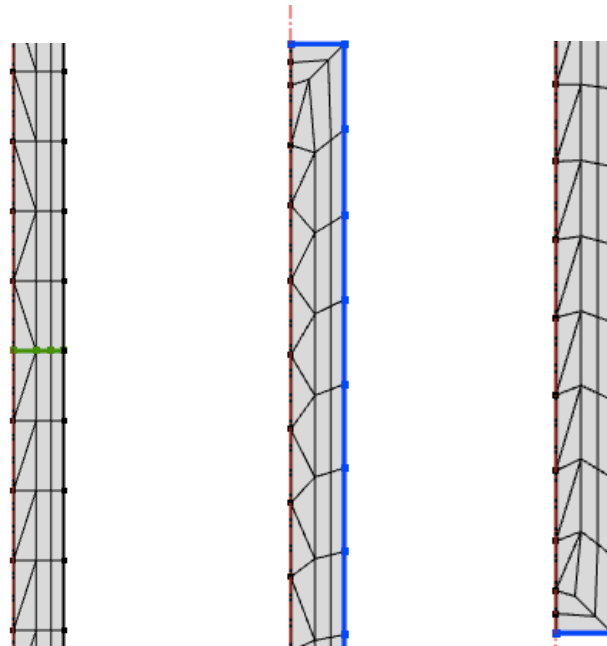


Figure 19: Meshing at the interface (left) and at the boundaries; at the top (in the middle) and at the bottom (to the right), and along the pipe wall

4.1.5 Boundary Conditions

The boundary conditions for the model is set no slip at the wall and the velocity is set to zero at start of simulation. This is shown in figure 20 [23].

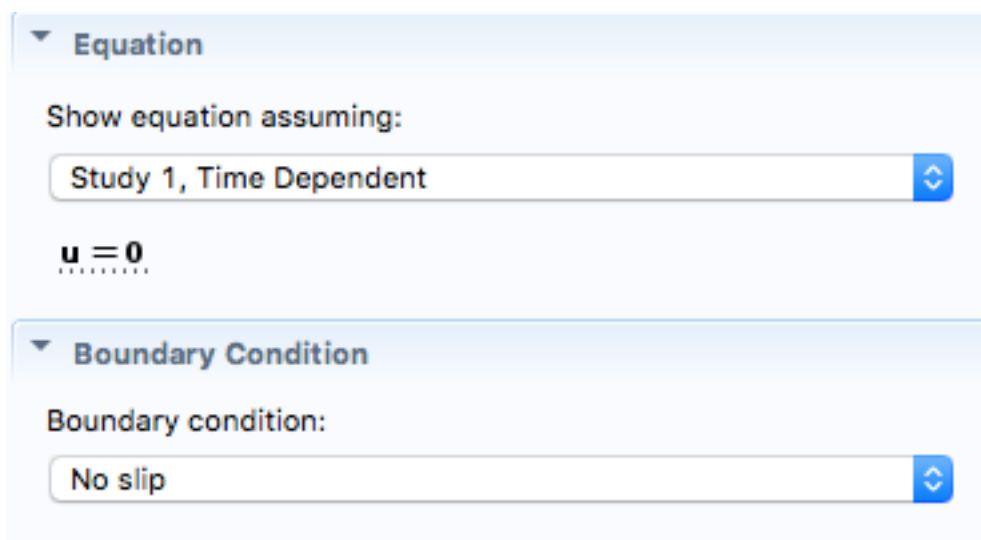


Figure 20: Boundary condition in COMSOL

4.1.6 Solution

The two physics reviewed in section 3.11 and 3.21 are solved at the HOL interface. Figure 21 shows the physics for this model in COMSOL [23]

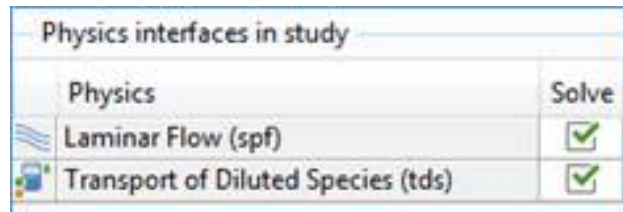


Figure 21: Physics interfaces in COMSOL

4.2 Simulation Results

There were done a total of seven simulations in the COMSOL software for simulating the HOL phenomenon in vertical wells. One simulation was used a reference case and the other simulations were used for studying the effect of density, viscosity and well bore size changes compared to the reference case. Two of the simulations were done for studying the effect of variation in density, two were for studying viscosity changes and the last two the effect of difference in well size were studied. Well size refers the area between the drill pipe and the well bore. When changing one of the parameters, all the others were kept constant. The height of the pipe and the diffusion coefficient were the same in all seven simulations. The height and the diffusion coefficient were set to 1500 m and 10^{-9} m²/s, respectively. All the simulations were simulated for a period of 10 hours.

The parameters for the various simulations are presented in the tables 2, 3 and 4 in the sections below. The parameters that are changed compared to the reference case are written in bold. Table 1 presents the values of the parameters for the reference case.

Table 1: Parameters for the reference case

Case	Heavy fluid		Light fluid		Well bore radius (m)
	Density (sg)	Viscosity (cP)	Density (sg)	Viscosity (cP)	
Reference	1.60	19	1.10	14	0.1265

For all the simulations there were taken screenshots of the main window where it is possible to observe how the surface concentration develops. On the right side of the main window there is placed a colour chart showing the colours that the various concentrations are representing. The screenshots were taken from various time steps during the simulation. The mixing of the two fluids is probably at its most critical state in the beginning of the process. This is the reason for the time steps chosen in the plots, where there are several time steps chosen within the first hour, and fewer between the times one and ten hours.

For each case there are presented four screenshots of the surface concentration; at start, after 1 minute, after 1 hour and after 10 hours. There was also taken screenshots of plots showing line graphs of the concentrations for several time steps. For each case there were made two plots. One for the times 0, 1, 5, 10, 15, 20, 25, 30, 40, 50 and 60 minutes, and another plot for 0, 100, 200, 300, 400, 500 and 600 minutes. For these time steps there were also produced plots showing the velocity profiles of the mixed fluids. For more figures of surface concentration at several time steps and more detailed plots of the line graphs for velocity field, please refer to Appendix A.

Above the main window it is possible to read the time step. As mentioned, all the simulations were done in a time frame of 10 hours. In some of the simulations there appeared a bug in the model which made the time shown above the main window 60 times larger than the actual time step. This means that for an actual time step of for instance 60 minutes, the time above the main window would show a time of 3600 minutes. This also applies for the plots of the concentration and the velocity field. The bug was confirmed by Erlend Kristiansen who works for COMSOL, and may not affect the simulations otherwise. As can be observed from the screenshots, this bug appeared

in the simulations for the reference case, density difference 1 and 2, viscosity difference 2 and well size difference 1.

For each case there were made plots showing how the density develops in the upper and lower part of the fluid column, in addition to the average density in the entire fluid column. The first plot shows the densities during the first hour and the second plot shows the densities during 10 hours. The densities for the upper and lower part of the fluid column are calculated by using Equation 3.6. The fraction of the heavy fluid, α_h , was found from the Line Graph of the concentration in COMSOL, for both the upper part of the fluid column and the lower part. The average density of the fluid was calculated by the following equation.

$$\rho_{av} = \frac{1}{2}(\rho_{upper} + \rho_{lower}) \quad (4.5)$$

where ρ_{upper} is the density of the upper part of the fluid column and ρ_{lower} is the density of the lower part of the fluid column.

There were also produced plots for showing the development of the concentration of the fluid column vs. time. For each case there were produced two plots. One for presenting the concentration development in the upper part of the fluid column, and the other for showing the concentration development in the lower part of the fluid column. Both plots were made for the entire simulation period of 10 hours. The plots are placed below the line graphs of the concentration taken from COMSOL.

4.2.1 Results Reference Case

Screenshots of the surface concentrations at the times 0, 1 minute, 1 hour and 10 hours of the reference case are shown in the figures below.

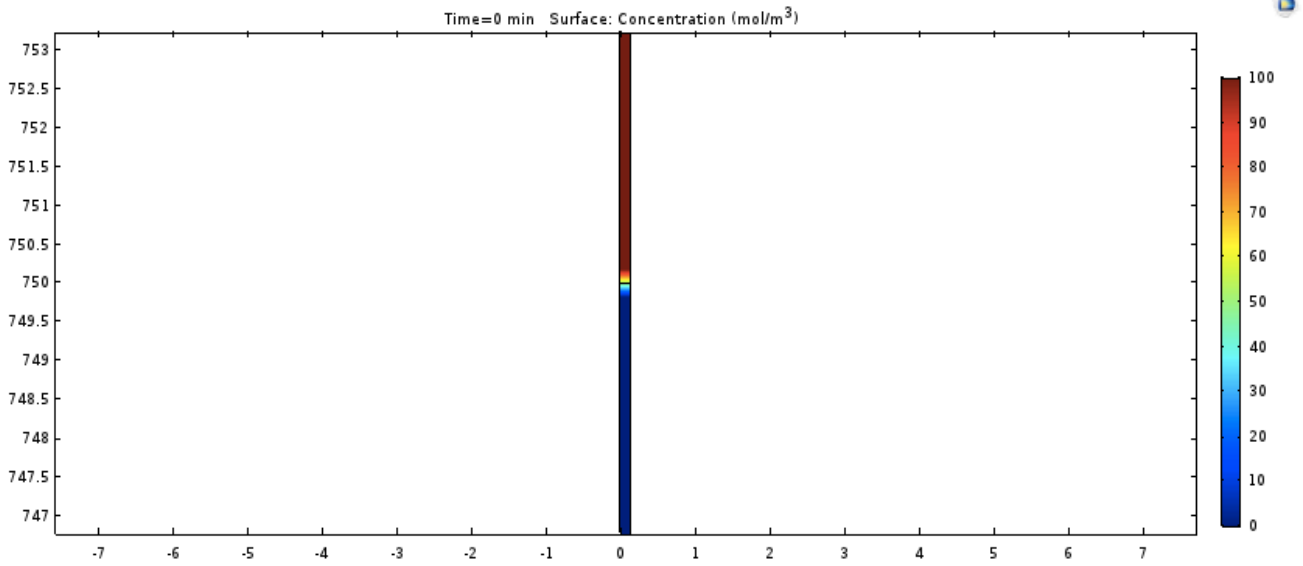


Figure 22: Surface concentration of reference case at start of simulation

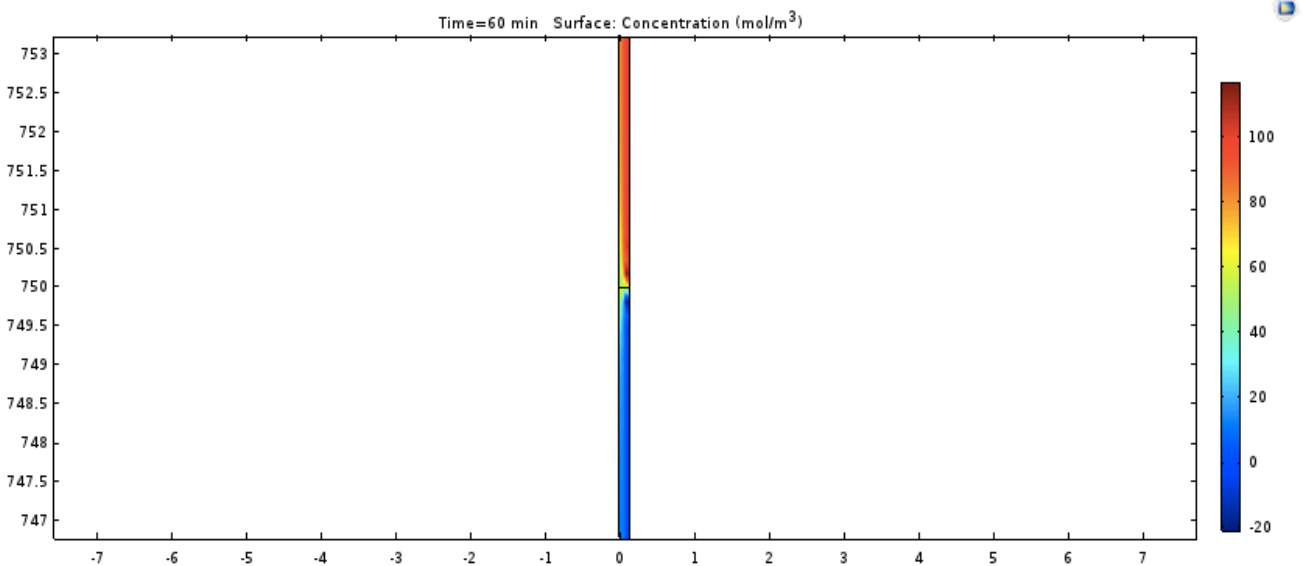


Figure 23: Surface concentration of reference case after 1 minute

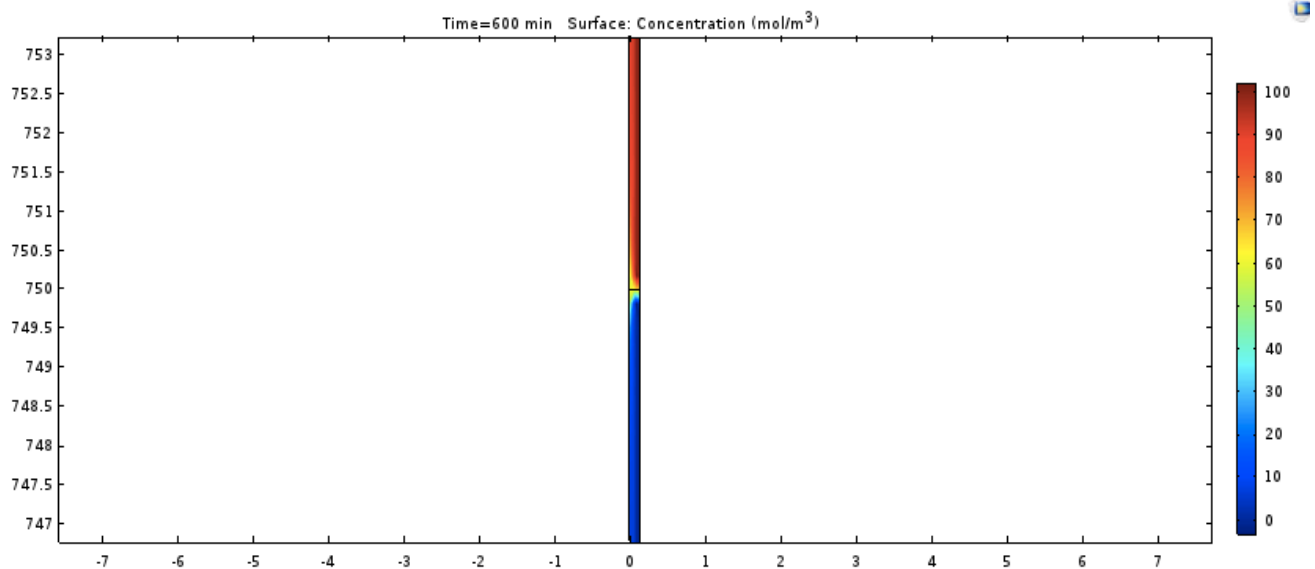


Figure 24: Surface concentration of reference case after 1 hour

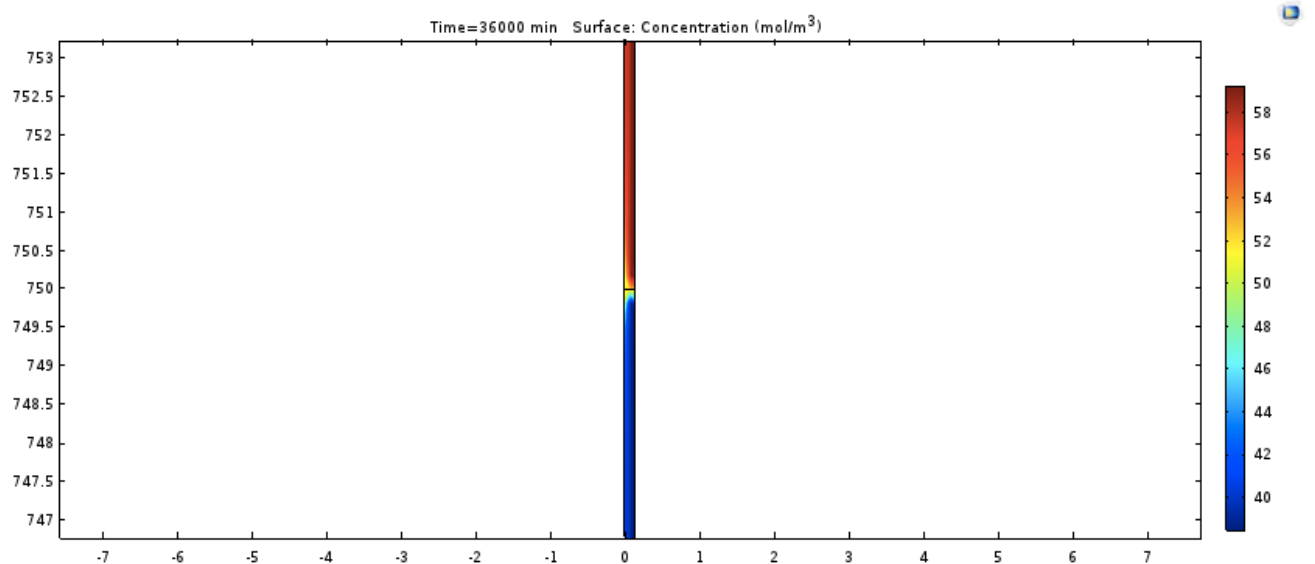


Figure 25: Surface concentration of reference case after 10 hours

At start there is heavy fluid in the upper half of the pipe and light fluid in the lower half of the pipe. At the interface it is possible to observe a slightly mixing of the two fluids. The dark red colour represents a concentration of 100 and the dark blue colour represents a concentration of zero.

After 1 minute it looks like the model is not stabilized yet. The concentration shows values above 100 and below zero, which should not be possible. Otherwise it is clearly

observed that the fluids have started mixing. During the first minute the fluid above the interface has gotten lower density and the fluid below the interface has gotten higher density. The interface stays in the middle of the fluid column.

After 1 hour it is possible to observe that the model is stabilized and the concentration shows values between 0 and 100. The lighter fluid rises towards the top of the fluid column and the heavy fluid sinks towards the bottom of the fluid column. Both fluids penetrate the each other at the left side of the fluid column. The interface continues to stay at a height of 750 meters.

At the end of the simulation, after 10 hours, the concentration surface looks similar to the fluid column after 1 hour. The values for the different colours are changed, though. The dark red colour represents in this case a concentration of approximately 60, while the dark blue colour represents a concentration of just below 40. Thus, the heavy fluid has gone from a concentration of 100 to approximately 60 and the light fluid has gone from a concentration of 0 to just below 40. The interface is still at the middle of the fluid column, at a height of 750 meters.

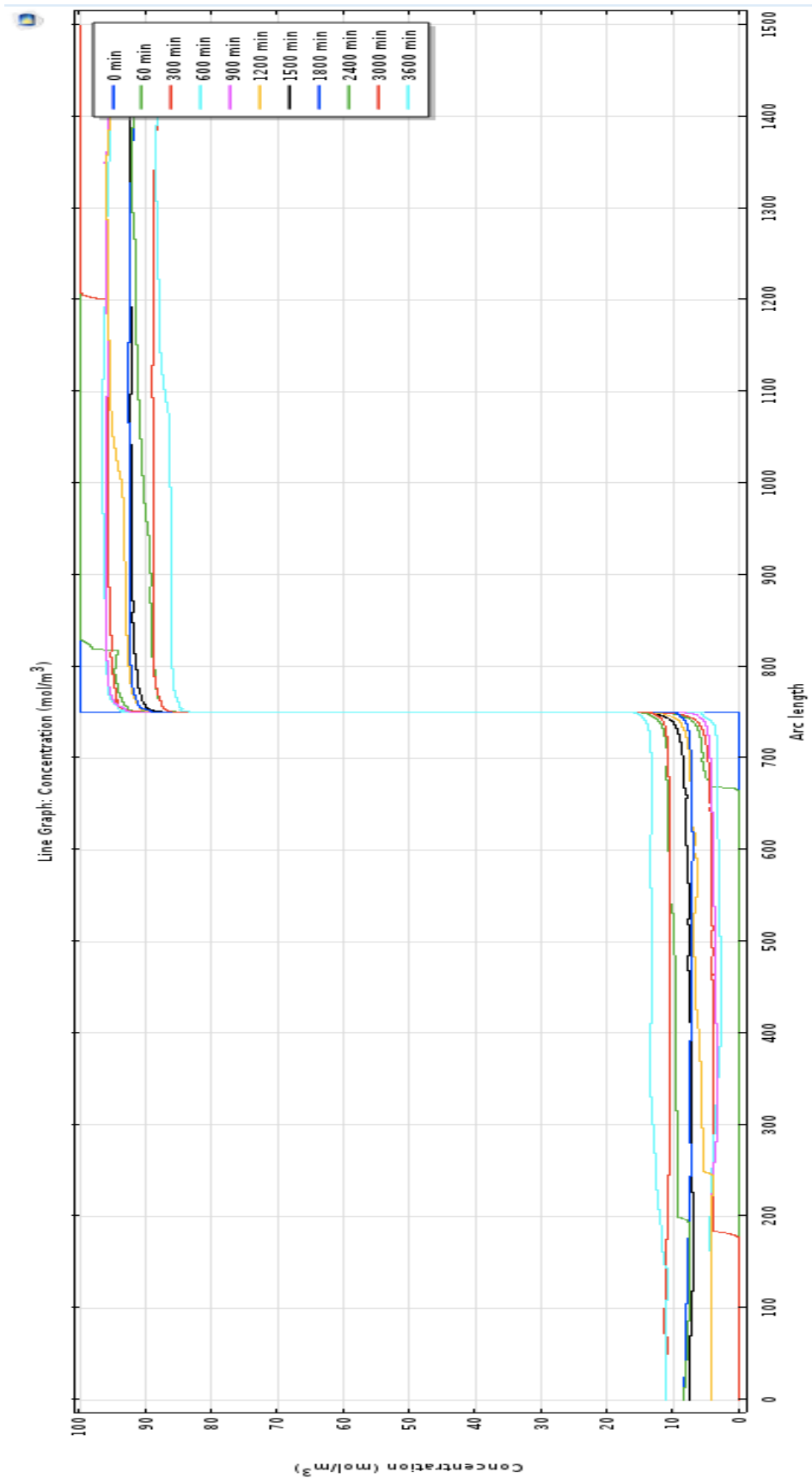


Figure 26: Line Graph Concentration Reference Case after 0, 1, 5, 10, 15, 20, 25, 30, 40, 50 and 60 minutes

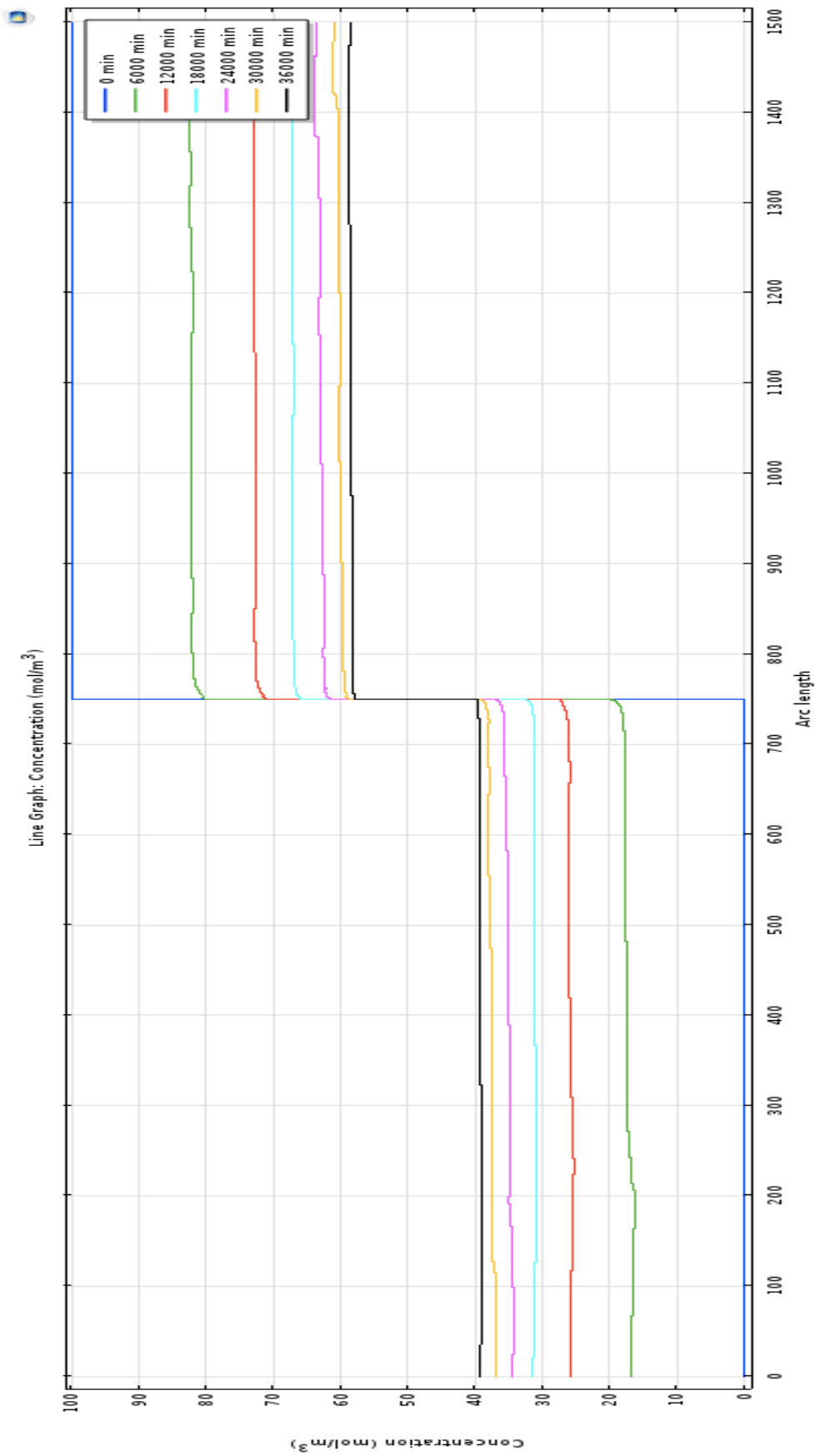


Figure 27: Line Graph Concentration Reference Case after 0, 100, 200, 300, 400, 500 and 600 minutes

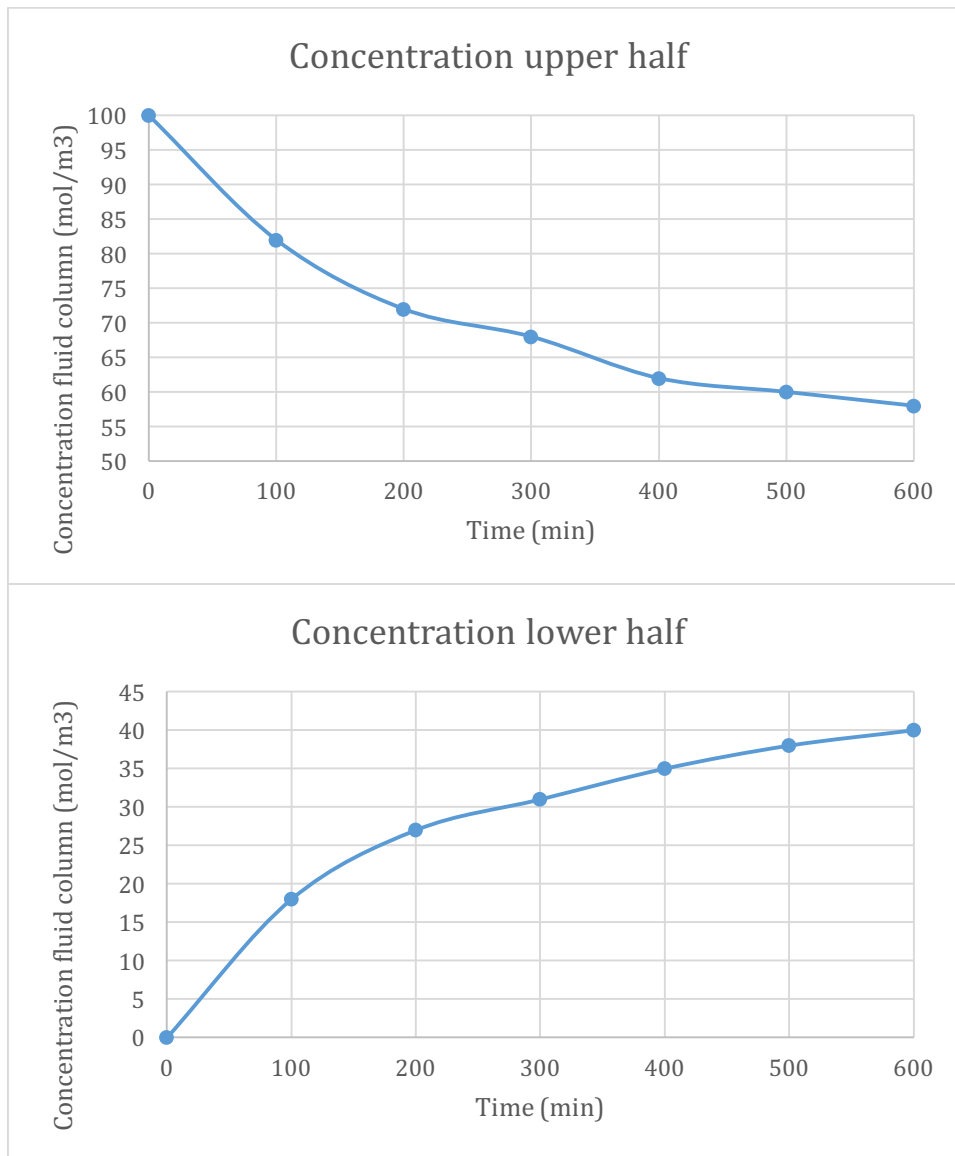


Figure 28: Concentration fluid column, Reference case

Figure 26 shows a line graph of how the surface concentration has developed during the first hour of simulation. At start, the blue line shows that the concentration below 750 meters is 0 and the concentration of the rest of fluid column is 100. As time goes by the concentration of the light fluid is increasing while the concentration of the heavy fluid is decreasing. After 1 and 5 minutes (green and red line) it is possible to define a mixed zone of the two fluids.

After 1 minute the mixed zone is approximately 155 meters (between 670 and 825 meters), and after 5 minutes the mixed zone is approximately 1020 meters (between 180 and 1200 meters). Later the concentrations of the fluids are practically continuously

through the fluid column. During the first hour of simulation the concentration of the light fluid has increased to approximately 12 and the concentration of the heavy fluid has decreased to approximately 86.

Figure 27 shows a plot of the line graph of the concentration for all the 10 hours of the simulation for the reference case and figure 28 shows two plots of the development of the concentration of heavy fluid in both upper and lower part of the fluid column. Clearly, the biggest change in concentration takes place during the first 100 minutes. For all the time steps in the plot the concentrations of the fluids are approximately the same for the entire lower half of the fluid column. This also applies for the upper half.

After 10 hours the concentration have gone to 40 and 58 in the lower and upper part, respectively, of the fluid column. If the case was simulated for a longer time, it is likely to imagine that the concentration of the upper and lower part of the fluid column would be equal. This would also be the concentration of the entire fluid column.

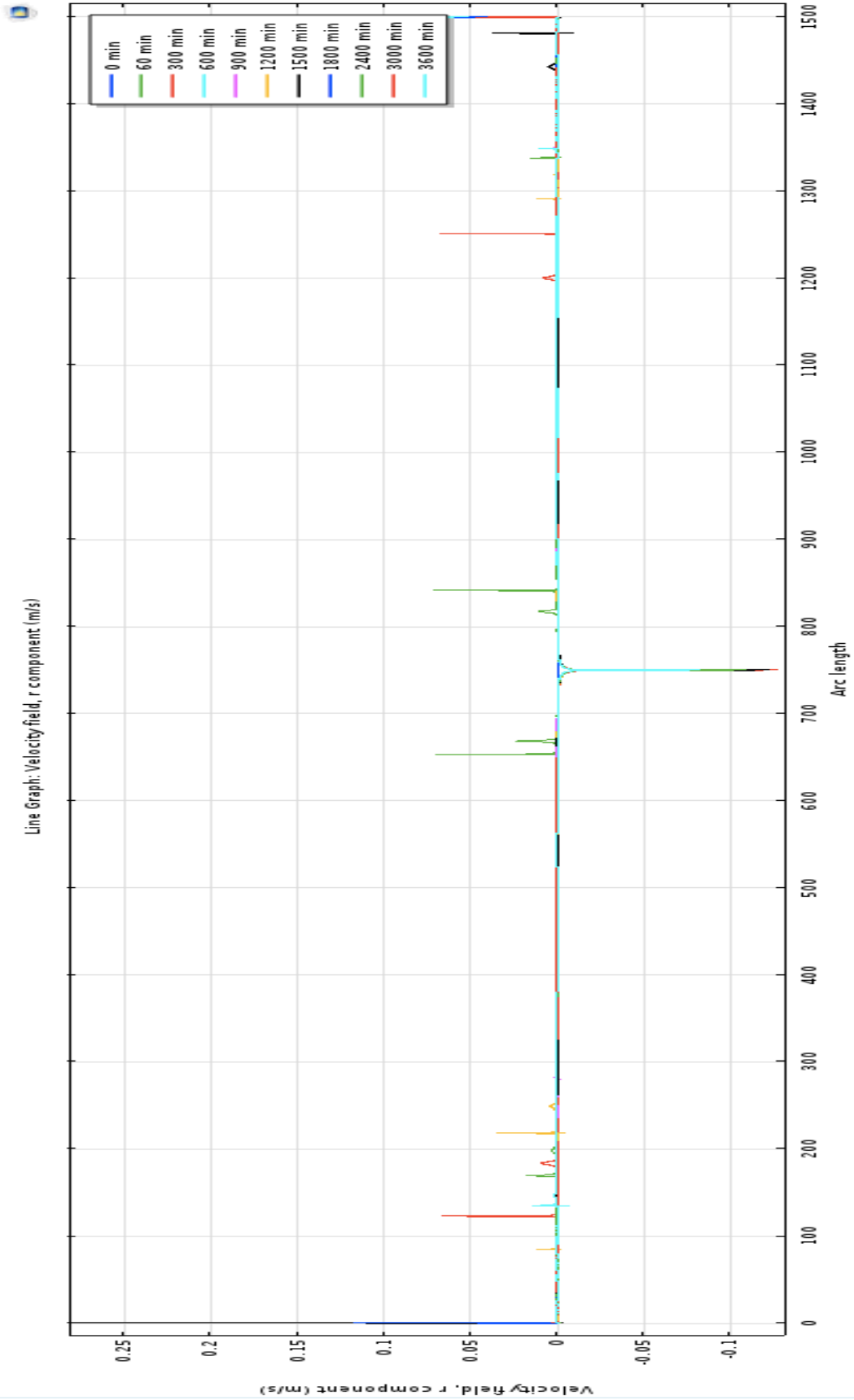


Figure 29: Line Graph Velocity field Reference Case after 0, 1, 5, 10, 15, 20, 25, 30, 40, 50 and 60 minutes

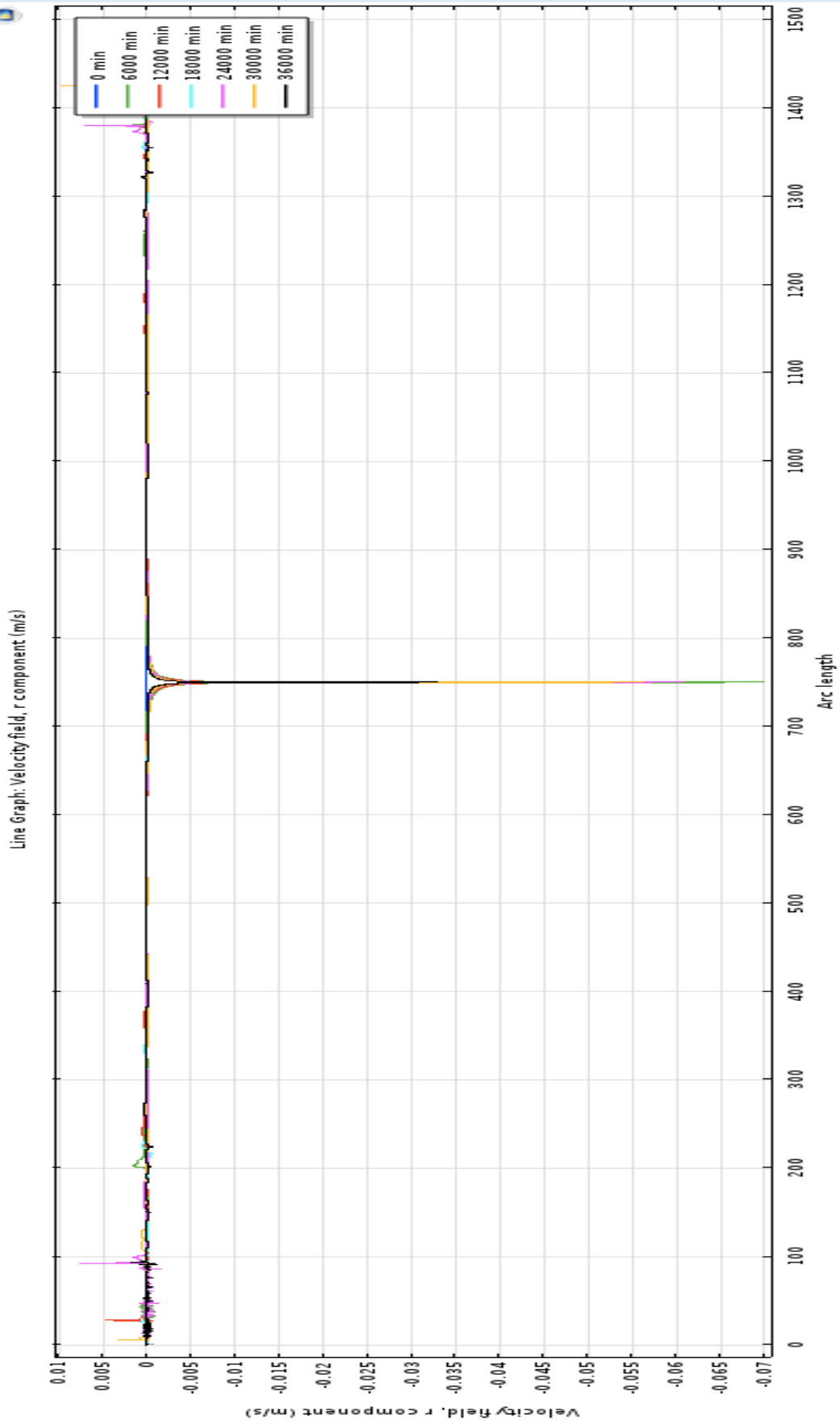


Figure 30: Line Graph Velocity field Reference Case after 0, 100, 200, 300, 400, 500 and 600 minutes

A line graph of the velocity field during the first hour of the reference case is plotted in figure 29 above. The lines show the total velocity of the fluids. A negative velocity implies a fluid flow in upward direction and a positive velocity implies a fluid flow in downward direction. At start the velocity is equal to zero. After 1 minute and/or 40 minutes (green lines), the fluids have a total velocity of around 0.1 m/s in the upward direction at the interface, which means that the light fluid is rising faster than the heavy fluid is sinking. Approximately 100 meters above and below the interface the velocity is about 0.07 m/s in the downward direction.

After 1 hour the velocity at the top of the fluid column has reached a value of almost 0.16 m/s in the downward direction. At the time 30 minutes the total velocity of the bottom of the fluid column is approximately 0.11 in the downward direction.

Figure 30 shows the line graph of the concentration of the reference case for all the 10 hours. As can be seen from the figure the highest velocity is at 100 minutes. The velocity at this time step is 0.07 m/s in the upward direction and takes place at the interface. As time goes by the velocity at the interface decreases. There is some movement of the fluids in the lower 300 meters and the upper 200 meters. The velocities have a maximum value of 0.01 m/s, and the movement of the fluids is mainly in the downward direction.

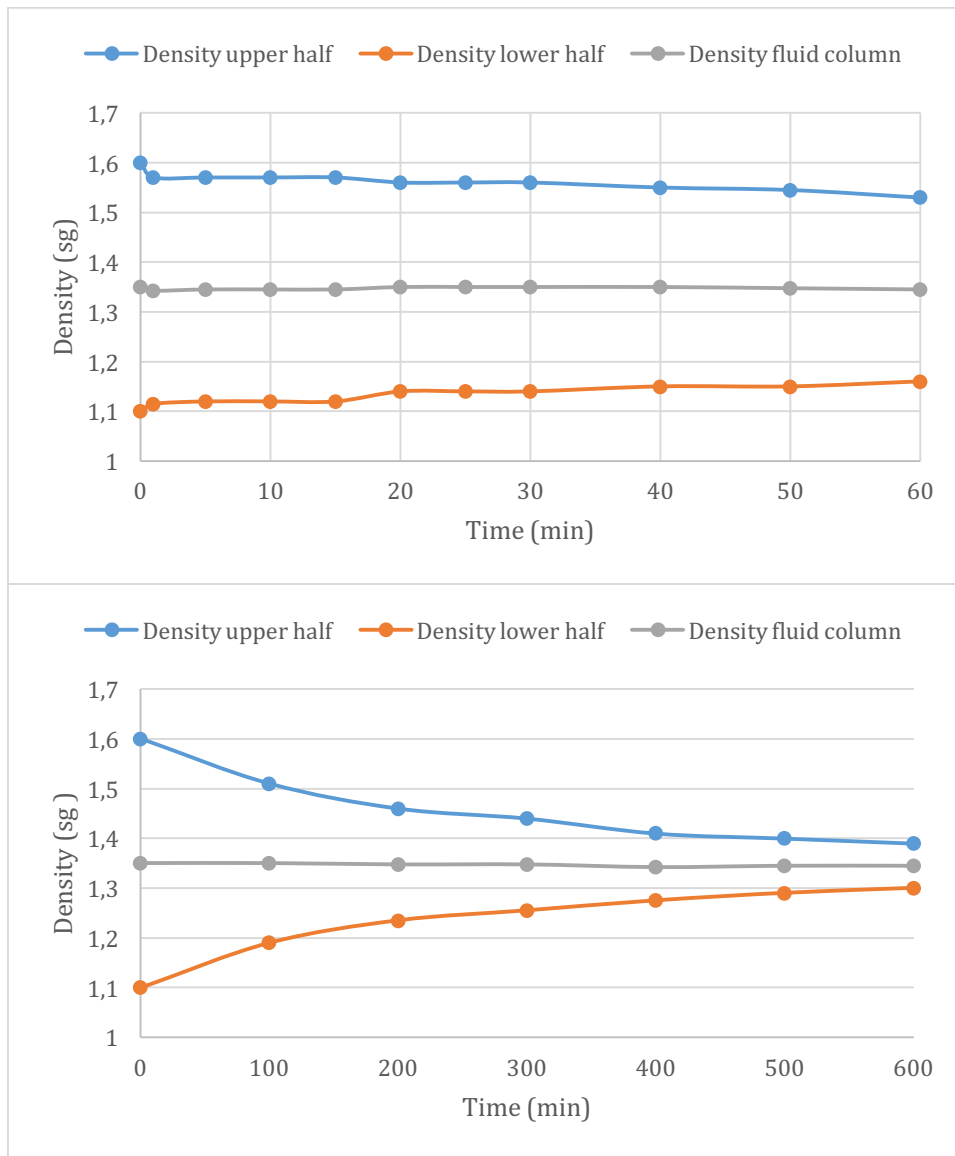


Figure 31: Density fluid column vs. time, Reference Case

The two plots in figure 31 above show how the average densities in both the upper and lower part of the fluid column in addition to the average densities of the entire fluid column, develop in time. During the first hour the density of the light fluid in lower part of the fluid column increases from 1.10 sg to approximately 1.16 sg. The density of the heavy fluid in the upper part of the fluid column decreases from 1.60 sg to roughly 1.53 sg.

During 10 hours the density of the light fluid in the lower part of the fluid column increases to about 1.30 sg and the density of the heavy fluid in the upper part of the fluid column decreases to 1.39 sg.

The average density of the entire fluid column stays almost the same through all 10 hours, and has a density of approximately 1.35 sg.

4.2.2 Effect of Density

The purpose of these simulations is to demonstrate how variation in density may affect the length and density of the mixing zone. There were done two simulations where only the density of the heavy fluid was varied. All the other parameters were kept constant. In the first simulation the density of the heavy fluid was set to 1.45 sg. The density of the heavy fluid in the second simulation was set to 1.30 sg. Thus the density difference is larger in the first simulation than in the second simulation. The parameters for the simulations are presented in table 2.

Table 2: Parameters for simulation of density difference in COMSOL

Case	Heavy fluid		Light fluid		Well bore radius (m)
	Density (sg)	Viscosity (cP)	Density (sg)	Viscosity (cP)	
Density difference 1	1.45	19	1.10	14	0.1265
Density difference 2	1.30	19	1.10	14	0.1265

Density Difference 1

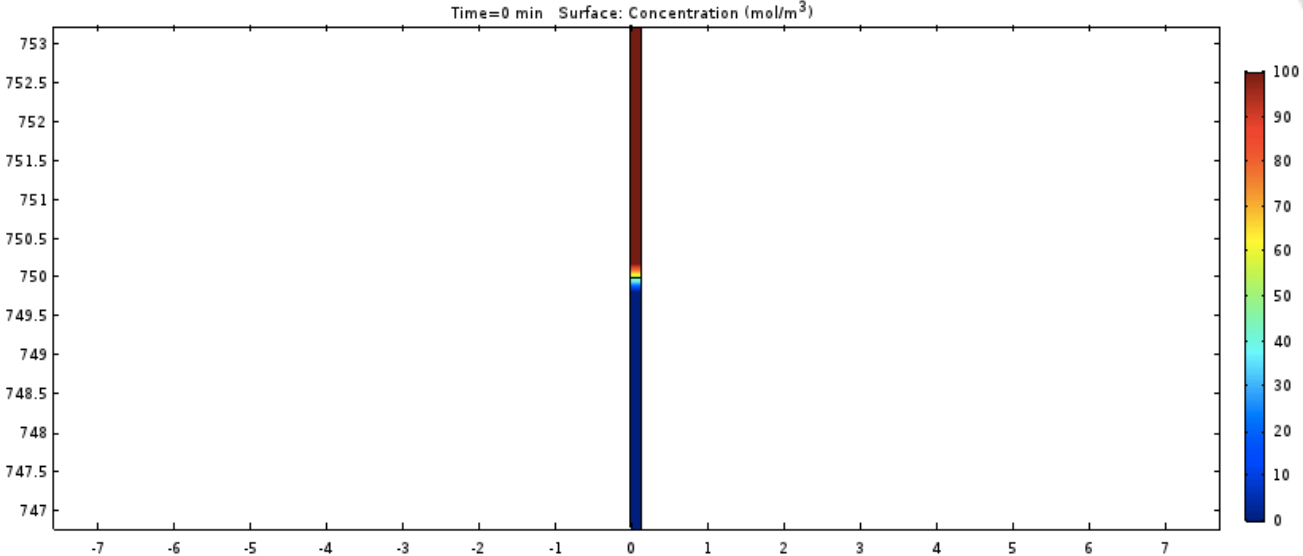


Figure 32: Surface concentration of Density Difference 1 at start

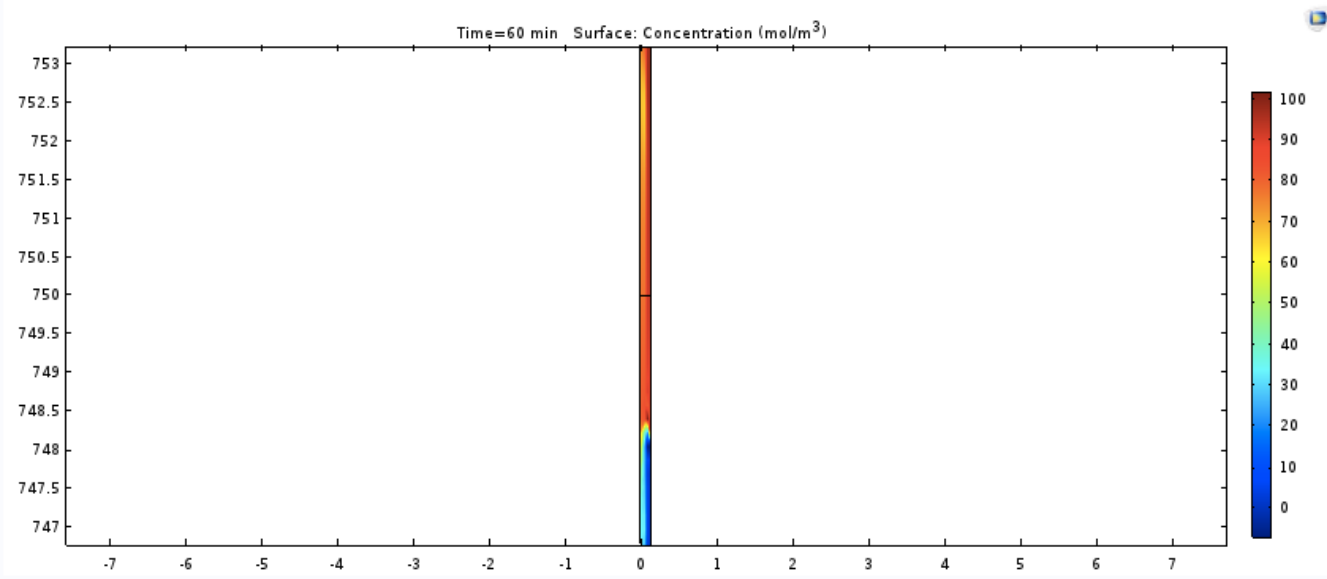


Figure 33: Surface concentration of Density Difference 1 after 1 minute

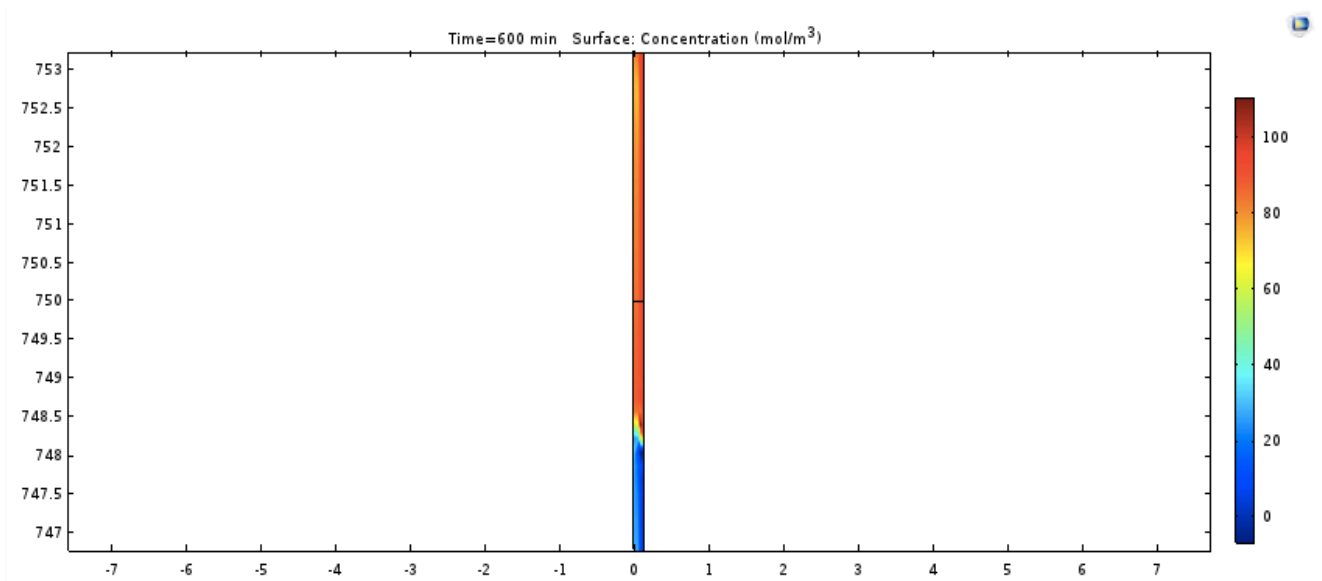


Figure 34: Surface concentration of Density Difference 1 after 1 hour

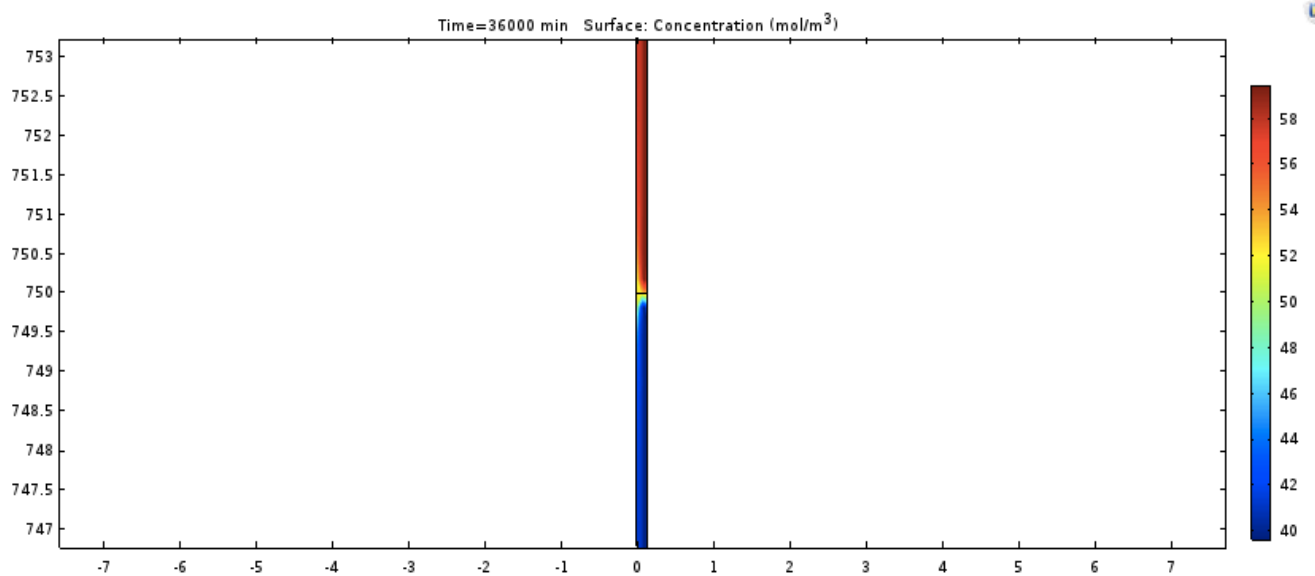


Figure 35: Surface concentration of Density Difference 1 after 10 hours

At start of the simulation the surface concentration is the same as the reference case. After 1 minute the interface has moved from a height of 750 meters and down to a height of approximately 748.5 meters, as shown in figure 33. The concentration of the heavy fluid in the upper part is decreasing, as can be seen from the lighter red colour above the interface. Below the interface there is a slightly lighter blue colour at the right side of the fluid column and at the left side of the fluid column there is an even lighter blue colour. This is where the heavy fluid is penetrating the light fluid.

After 1 hour the interface is still at a height of 748.5 meters. The heavy fluid is roughly the same colour as the previous time step. The values for the concentration at the right side of the main window is slightly different from the previous time step. The range is now from approximately -10 to 110, which should not be possible. This implies that the same red colour represents a higher concentration than at the time step of 1 minute. One should think that it should be the other way around, so it may seem like the model is trying to stabilize, even after simulating 1 hour.

At the end of the simulation, after 10 hours, the maximum concentration of the fluid column is approximately 60 and the minimum concentration is around 40. The interface has moved back up to the middle of the fluid column, at a height of 750 meters.

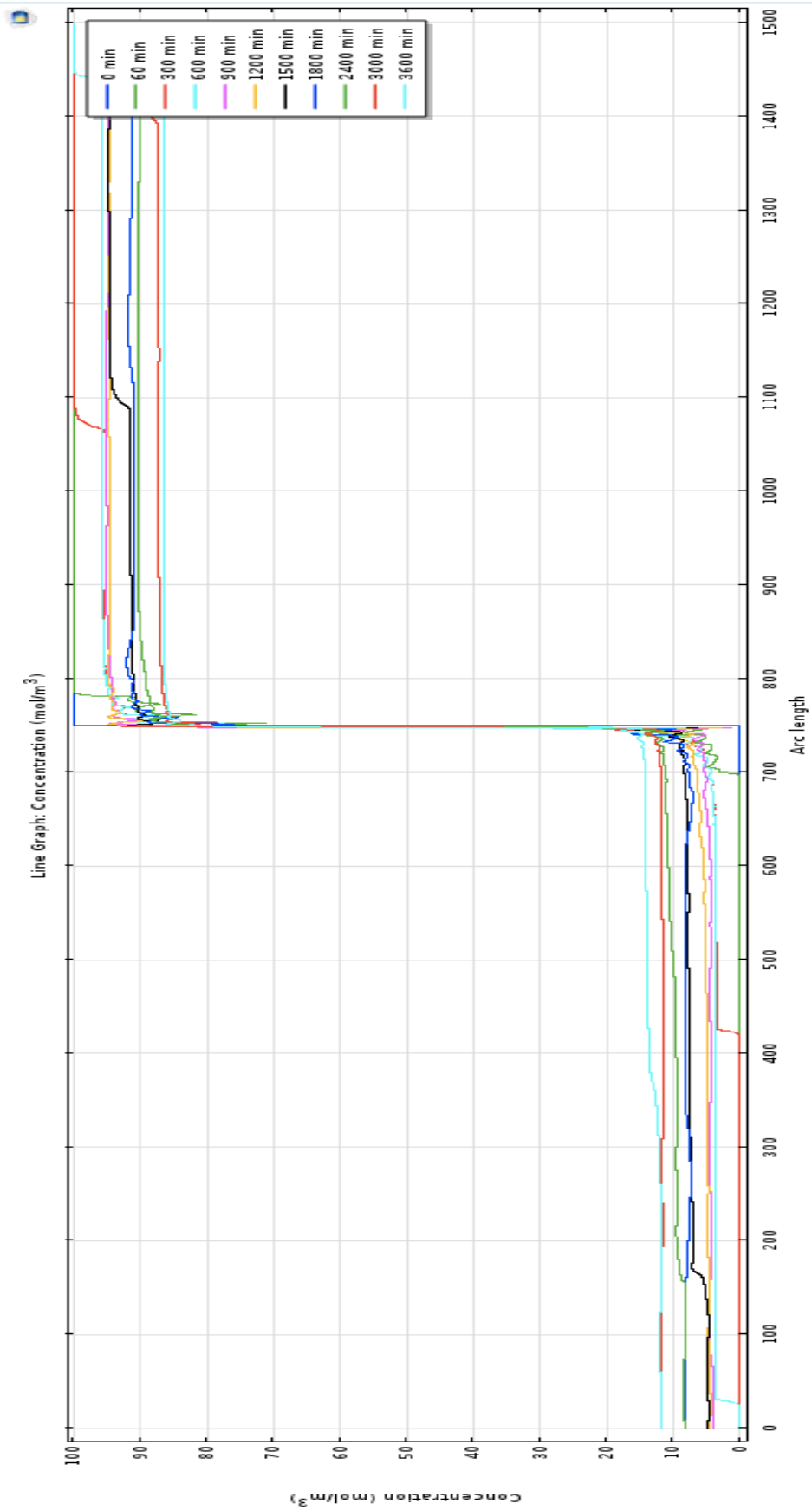


Figure 36: Line Graph Concentration Density Difference 1 after 0, 1, 5, 10, 15, 20, 25, 30, 40, 50 and 60 minutes

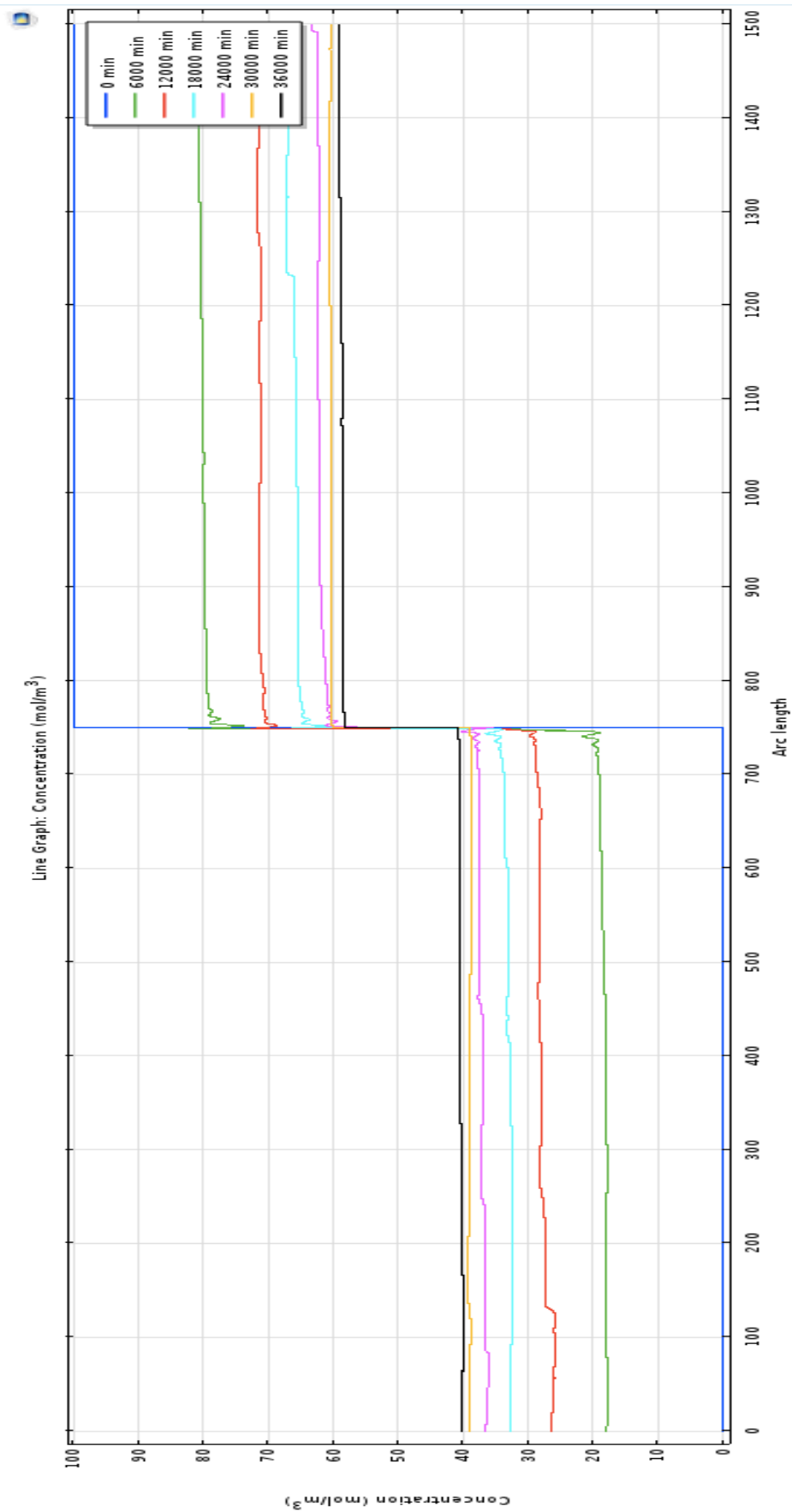


Figure 37: Line Graph Concentration Density Difference 1 after 0, 100, 200, 300, 400, 500 and 600 minutes

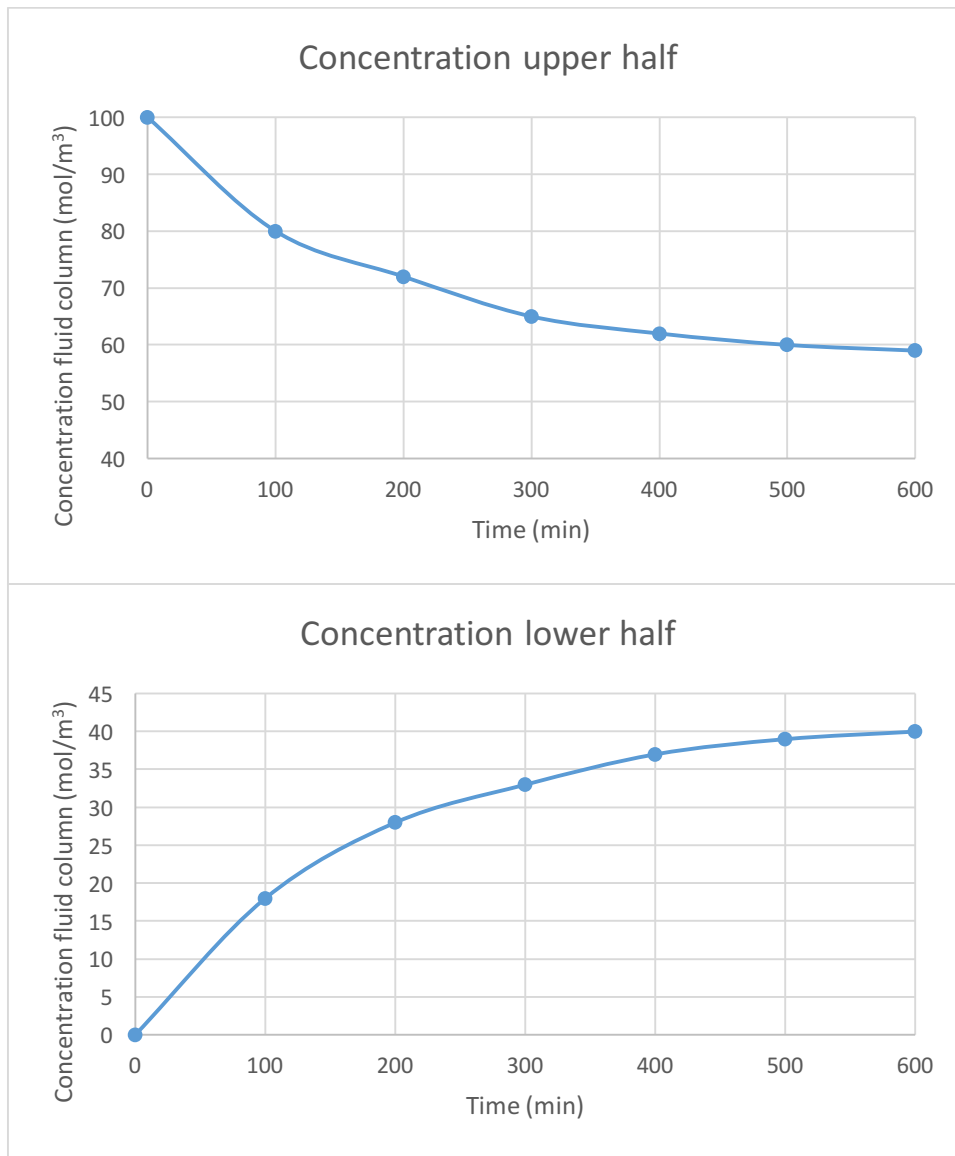


Figure 38: Concentration fluid column, Density Difference case 1

The line graph of the concentration of the density difference case 1 during 1 hour is presented in figure 36. Up to 10 minutes it is possible to define the length of a mixed zone. At 1 minute (green line) the mixed zone has a length of 80 meters (between 700 and 780 meters), at 5 minutes (red line) the mixed zone has a length of 640 meters (between 430 and 1070 meters) and at 10 minutes (light blue line) the mixed zone has a length of 1410 meters (between 30 and 1440 meters).

After 1 hour the concentration of the light fluid in the lower part of the fluid column has increased to approximately 12 and the concentration of the heavy fluid in the upper part of the fluid column has decreased to approximately 87.

Figure 37 presents a line graph of the concentration and figure 38 shows two plots of the development of the concentration for the density difference case 1 for a time period of 10 hours. The difference in concentration is largest during the first 100 minutes. Thereafter the difference in concentration is decreasing by increasing time steps. After 10 hours the concentration of the light fluid in the lower part of the fluid column is approximately 40 and the concentration of the heavy fluid in the upper part of the fluid column is approximately 59.

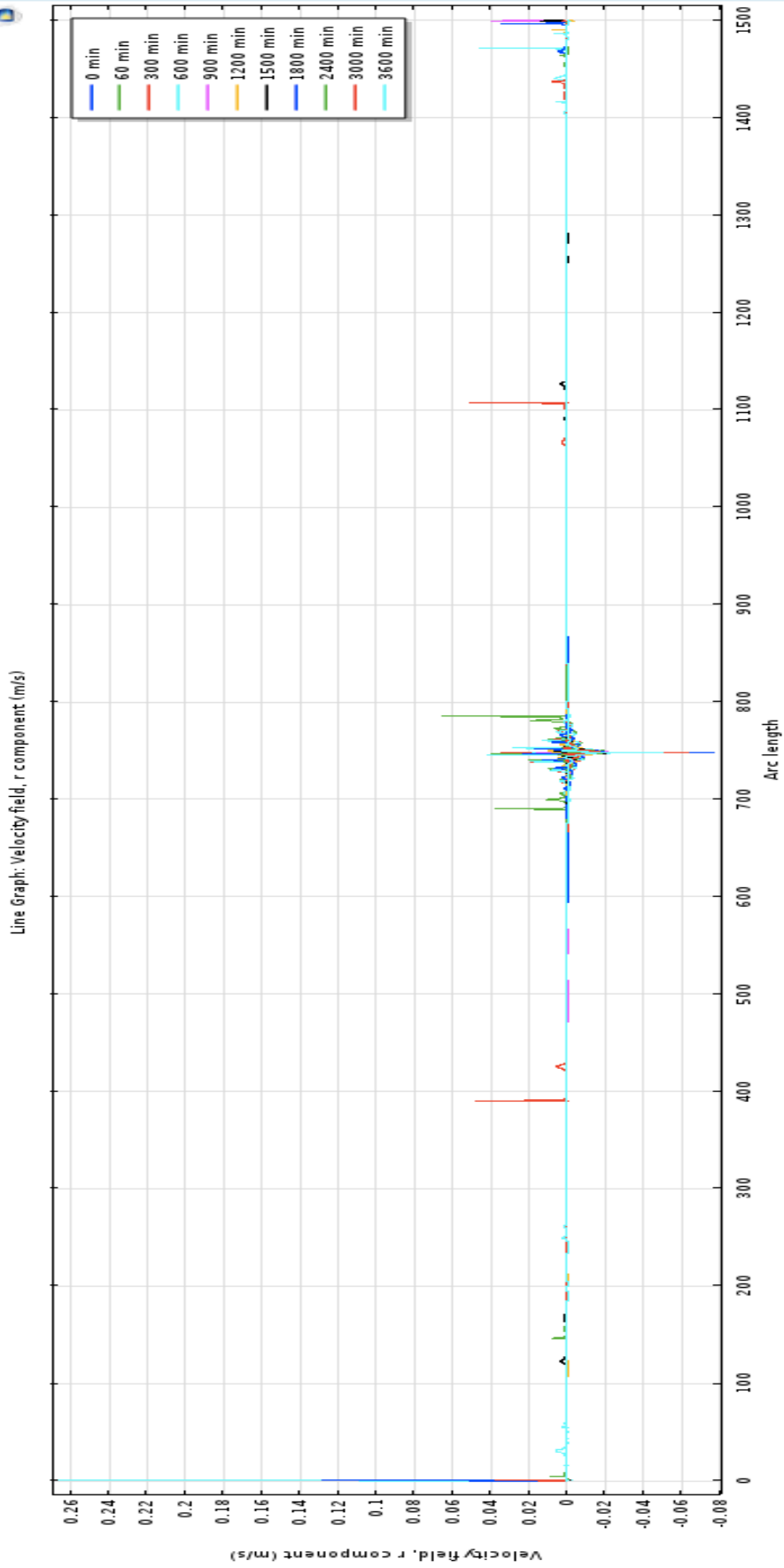


Figure 39: Line Graph Velocity field Density Difference 1 after 0, 1, 5, 10, 15, 20, 25, 30, 40, 50 and 60 minutes

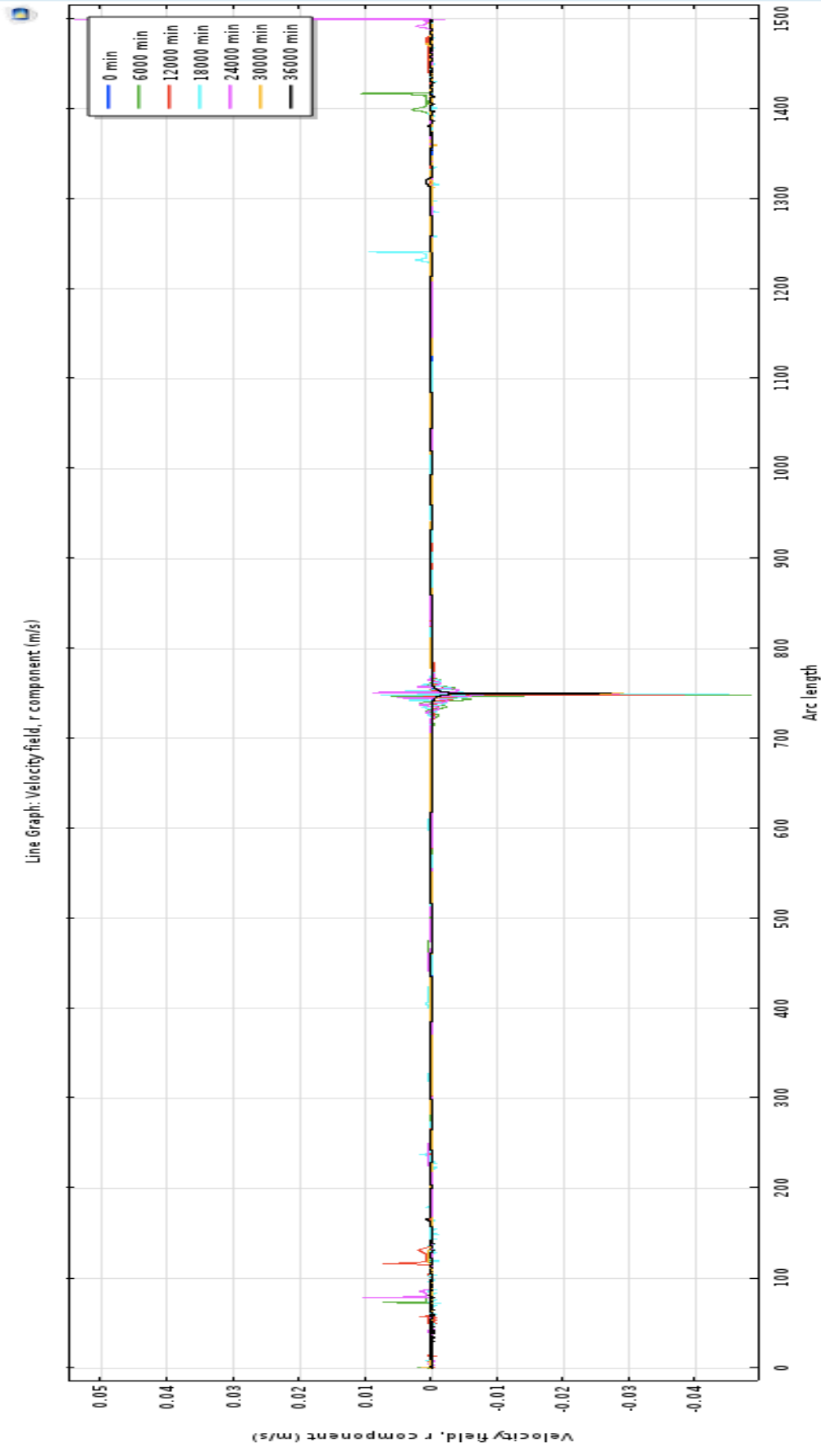


Figure 40: Line Graph Velocity field Density Difference 1 after 0, 100, 200, 300, 400, 500 and 600 minutes

A line graph of the velocity field of the density difference case 1 for the first hour is shown in figure 39 above. There are a lot of velocity variations around the interface. The highest velocity at the interface takes place after 30 minutes with a value of almost 0.08 m/s in the upward direction. The maximum velocity during the first hour is at the bottom of the fluid column after 10 minutes and is roughly 0.27 m/s in the downward direction. The maximum velocity in the downward direction around the interface appears at a height of 785 meters and has a value of approximately 0.065 m/s. At the top of the fluid column there is a maximum velocity in the downward direction of 0.04 m/s after 15 minutes.

Figure 40 shows a line graph of the velocity field for the density difference case 1 during 10 hours. It is clearly observed that the maximum velocity during all the 10 hours of simulation appears at the top of the fluid column after 400 minutes. It has a value of ... in the downward direction.

The maximum velocity in the upward direction at the interface takes place after 100 minutes and has a value of almost 0.05 m/s. The maximum velocity in the downward direction at the interface is approximately 0.009 m/s and appears after 400 minutes.

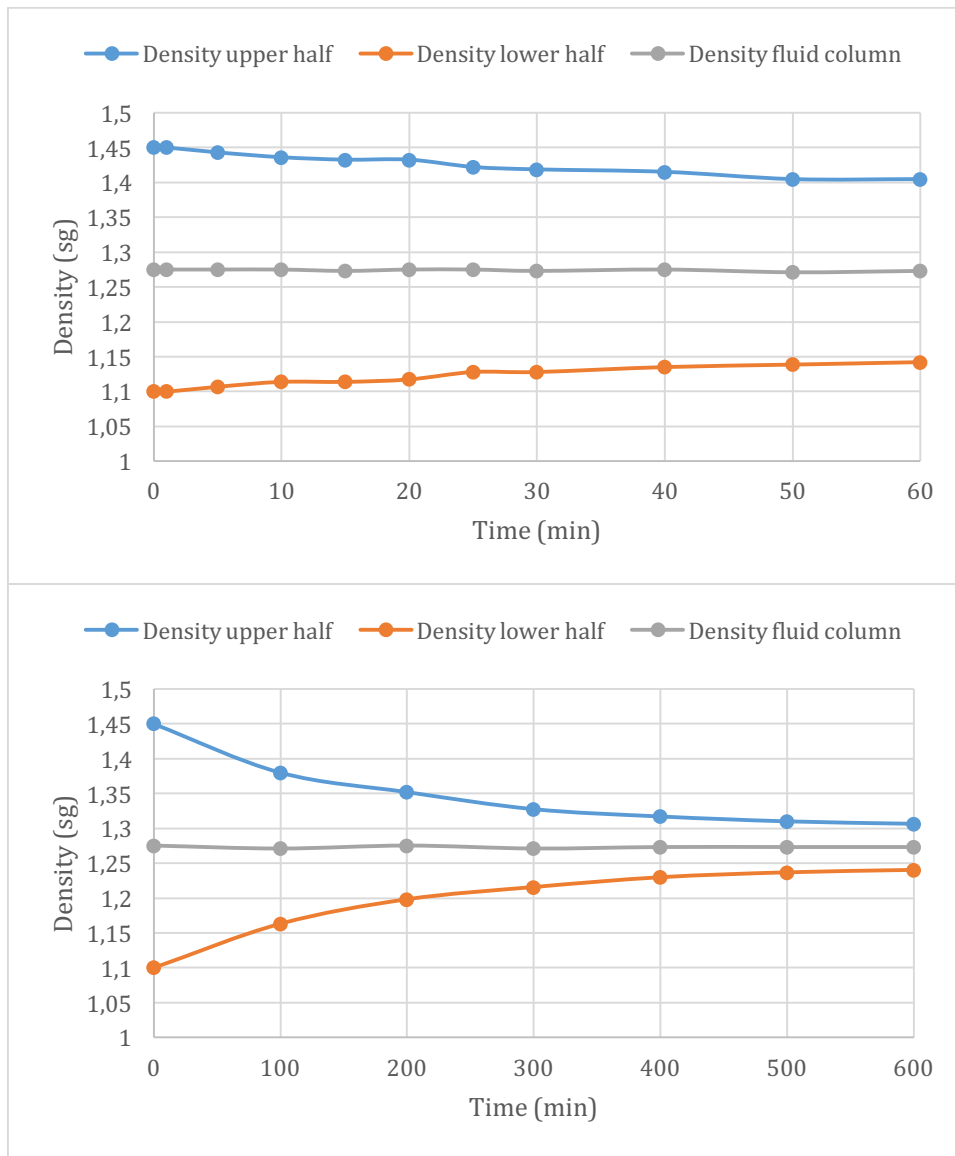


Figure 41: Density fluid column vs. time, Density Difference 1

Figure 41 above presents two plots for the densities in the upper and lower part of the fluid column in addition to the average density in the entire fluid column. The upper plot shows the densities during the first hour while the lower plot shows the densities during all 10 hours of simulation.

During the first hour the density of the heavy fluid in the upper part of the fluid column decreases from 1.45 sg to 1.40 sg, which gives a density difference of 0.05 sg. The density of the light fluid in the lower part of the fluid column is increasing from 1.10 sg to 1.14 sg, which gives a density difference of 0.04 sg. The density difference between the light and the heavy fluid is 0.26 sg.

After 10 hours the density of the heavy fluid has decreased to 1.31 sg and the density of the light fluid has increased to 1.24 sg. This gives a total density difference of 0.14 sg for both the heavy and the light fluid. The average density of the fluid column stays relatively constant throughout the entire simulation period and has a value of approximately 1.275 sg. The density difference between the light and the heavy fluid is 0.07 sg after 10 hours.

Density Difference 2

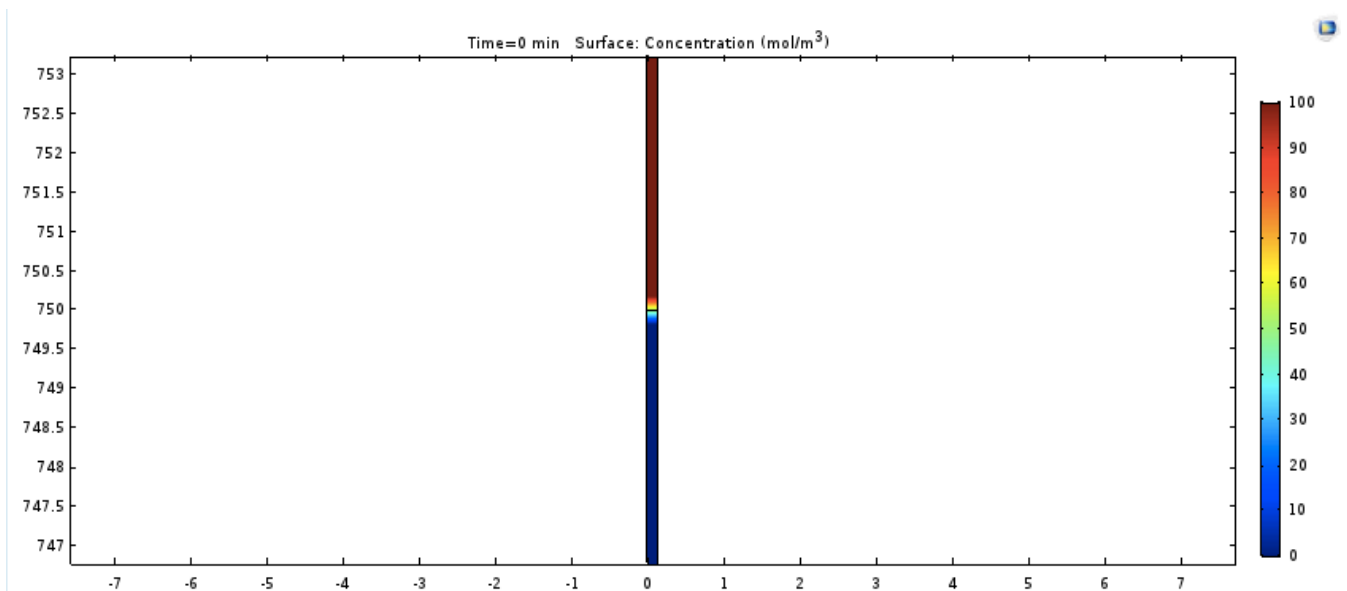


Figure 42: Surface concentration of Density Difference 2 at start

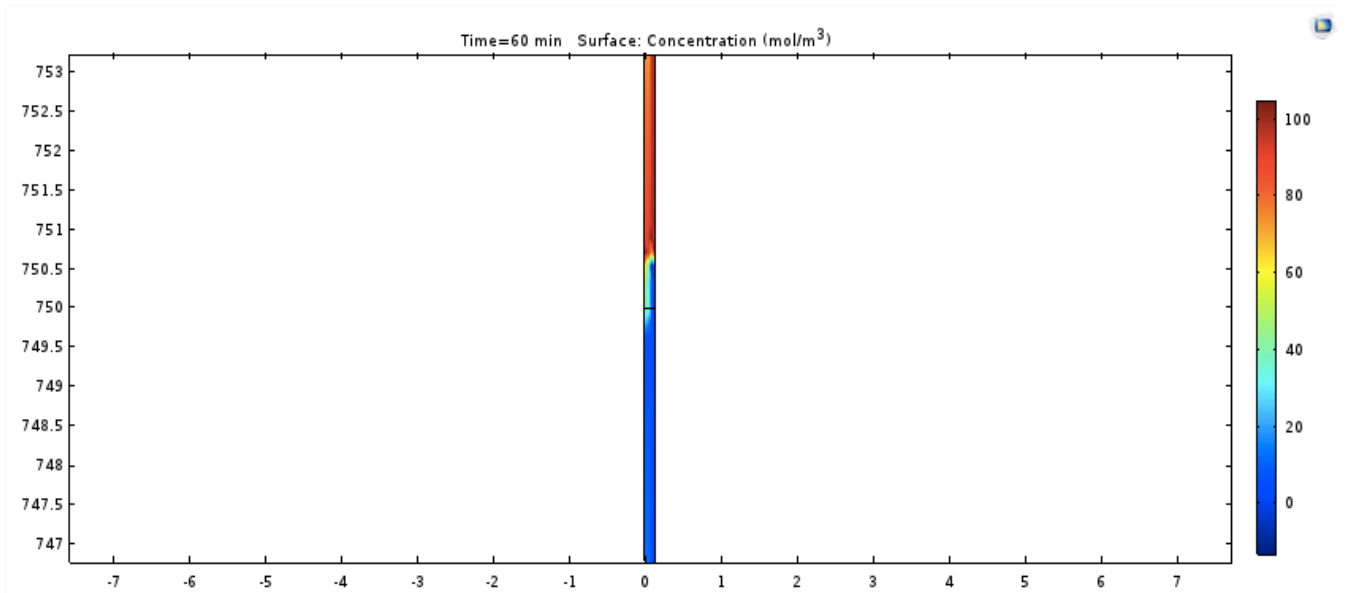


Figure 43: Surface concentration Density Difference 2 after 1 minute

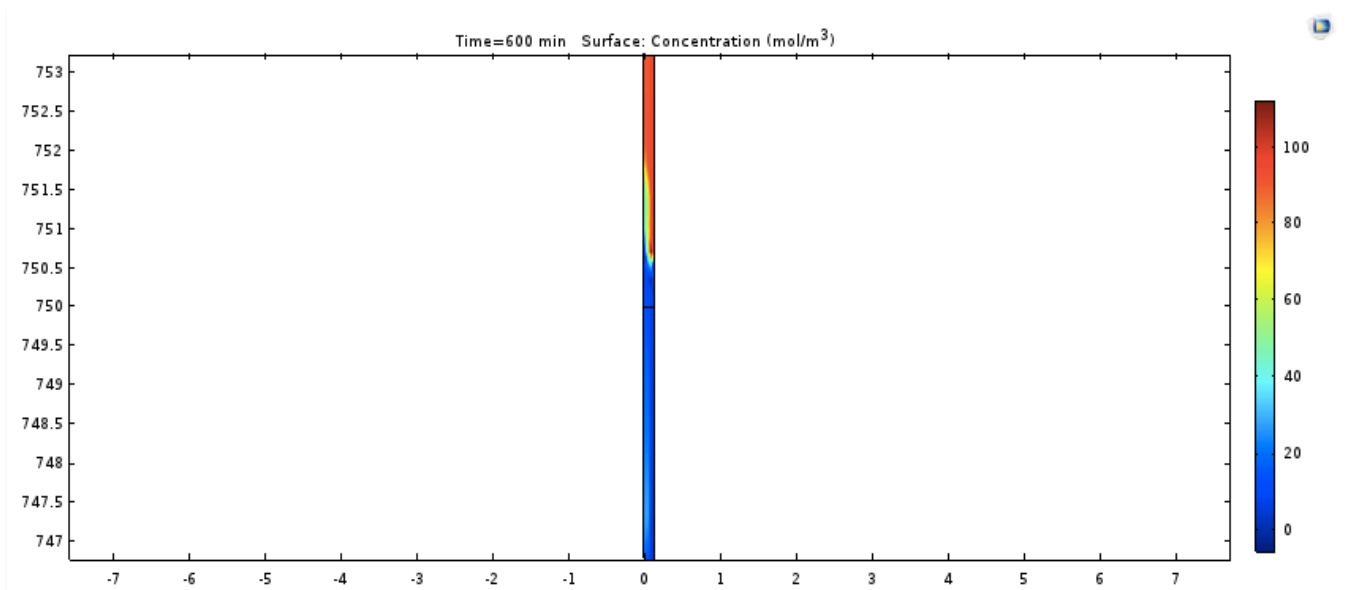


Figure 44: Surface concentration Density Difference 2 after 1 hour

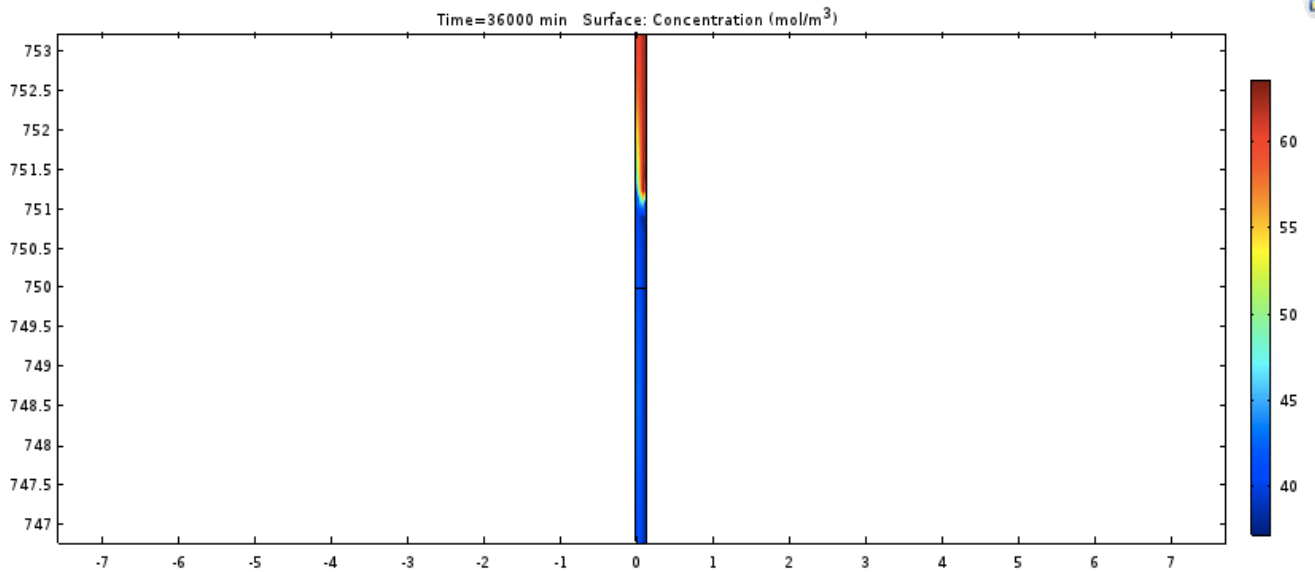


Figure 45: Surface concentration Density Difference 2 after 10 hours

At start of the simulation the interface is in the middle of the fluid column at a height of 750 meters. After 1 minute the interface has moved slightly upwards to a height of 750.5 meters. Both the heavy fluid and the light fluid have gotten a lighter colour which means the concentration of the heavy fluid is lower and the concentration of the light fluid is higher than from the start. At top of the light fluid it is observed a lighter colour on the left side of the fluid column than on the right side. This is where the heavy fluid is infiltrating the light fluid.

After 1 hour the interface is still at a height of 750.5 meters. At this time step it is possible to observe the penetration of the light fluid into the heavy fluid on the left side of the heavy fluid column. The concentrations of the heavy fluid and the light fluid looks about the same as after 1 minute.

After 10 hours the interface has moved even higher up, to a height of 751 meters of the fluid column. It is still possible to see the light fluid penetrating the heavy fluid just above the interface on the left side. The concentration of the heavy fluid is down to a maximum of approximately 64 and the concentration of the light fluid is up to a minimum of approximately 37.

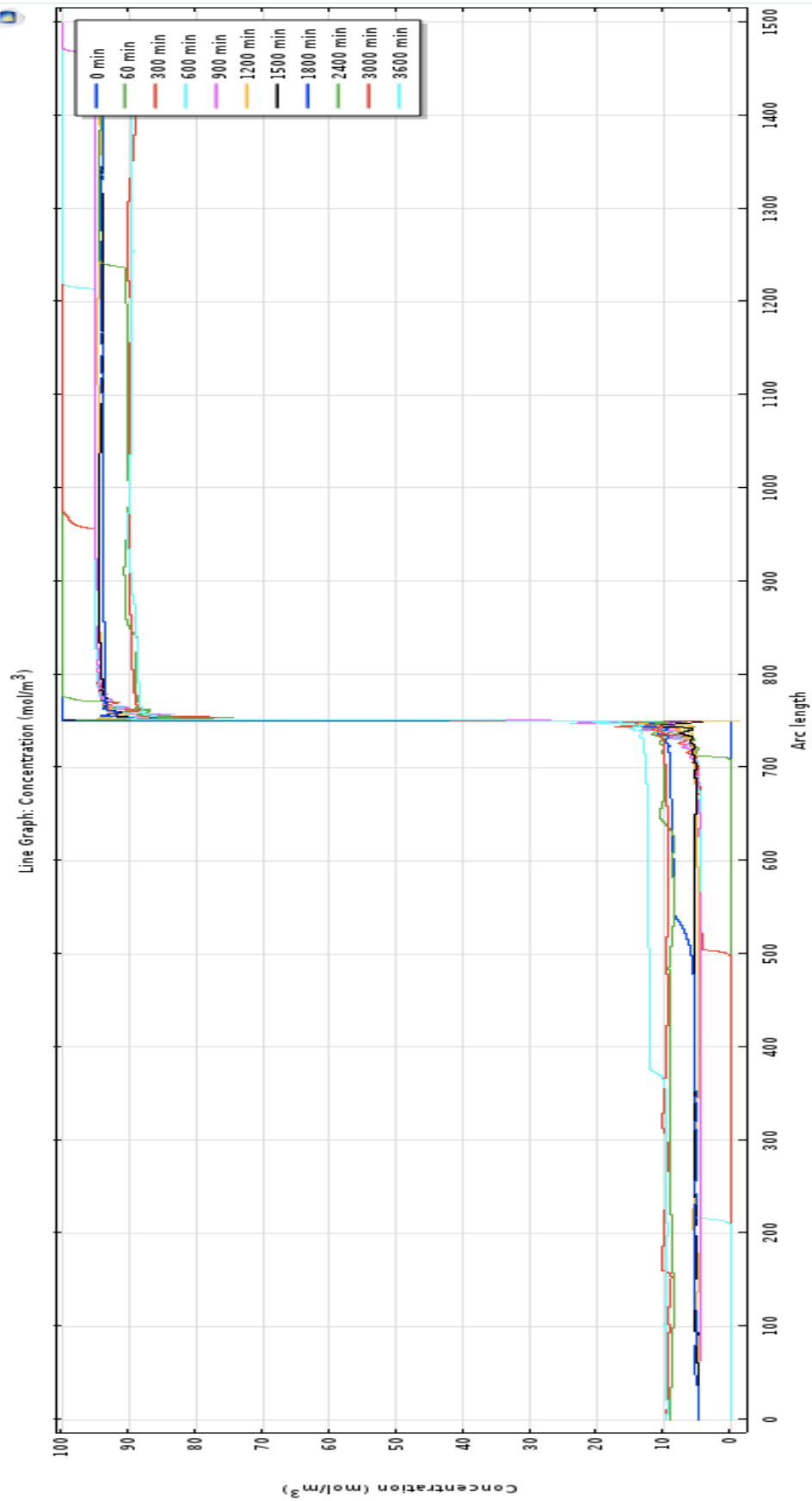


Figure 46: Line Graph Concentration Density Difference 2 after 0, 1, 5, 10, 15, 20, 25, 30, 40, 50 and 60 minutes

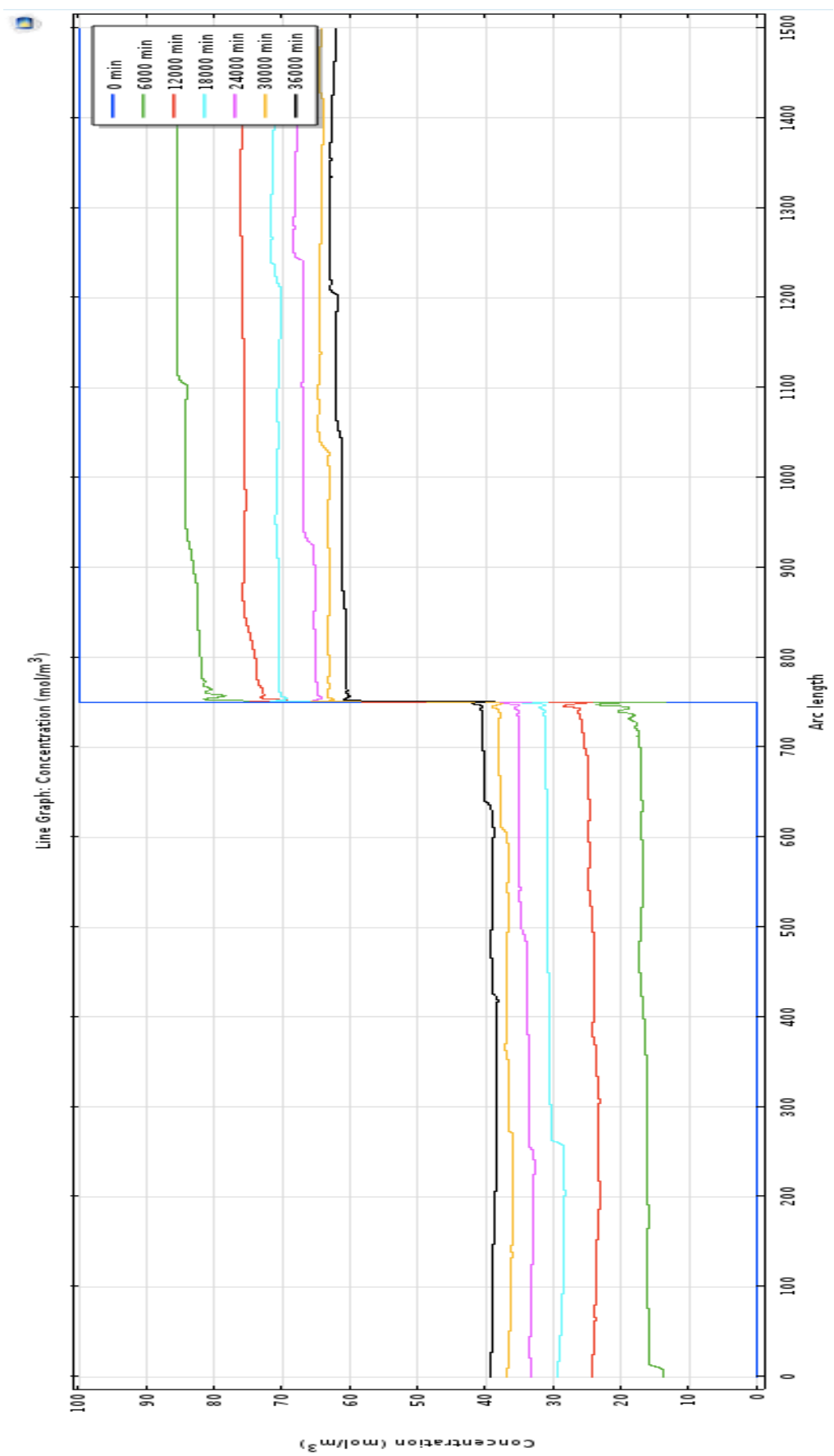


Figure 47: Line Graph Concentration Density Difference 2 after 0, 100, 200, 300, 400, 500 and 600 minutes

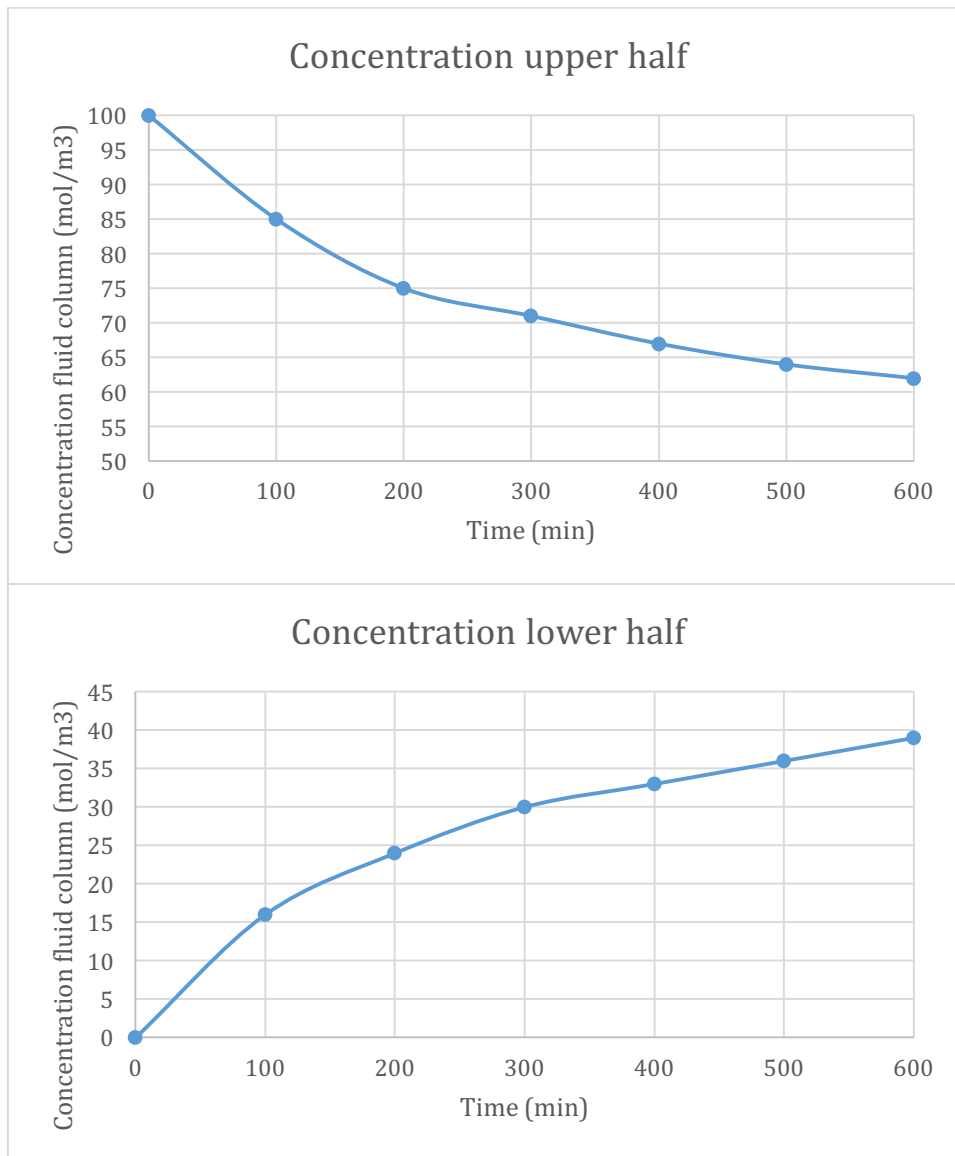


Figure 48: Concentration fluid column, Density Difference case 2

Figure 46 presents a line graph of the concentration for the density difference case 2 during the first hour of simulation. Around the interface there are a lot of variations in the concentration. For the first 10 minutes it is possible to define a mixed zone. After 1 minute the mixed zone has a length of 60 meters (between 710 and 770 meters). After 5 minutes the mixed zone has a length of 460 meters (between 960 and 500 meters). After 10 minutes the length of the mixed zone is equal to 1000 meters (between 220 and 1220 meters). When the time has passed 15 minutes the whole length of the fluid column is a mix between the heavy and the light fluid.

After 1 hour the concentration of the heavy fluid in the upper part of the fluid column has decreased from 100 to approximately 90 and the concentration of the light fluid in the lower part of the fluid column has increased from 0 to approximately 11.

A line graph of the concentration for the density difference case 2 during 10 hours is shown in figure 47. Figure 48 presents two plots showing the development of the concentration of the fluid column. The concentration difference is biggest between 0 and 100 minutes. As time increases the differences in concentration decreases. During 10 hours the concentration of the heavy fluid in the upper part of the fluid column has decreased to roughly 62 and the concentration of the light fluid in the lower part of the fluid column has increased to approximately 39.

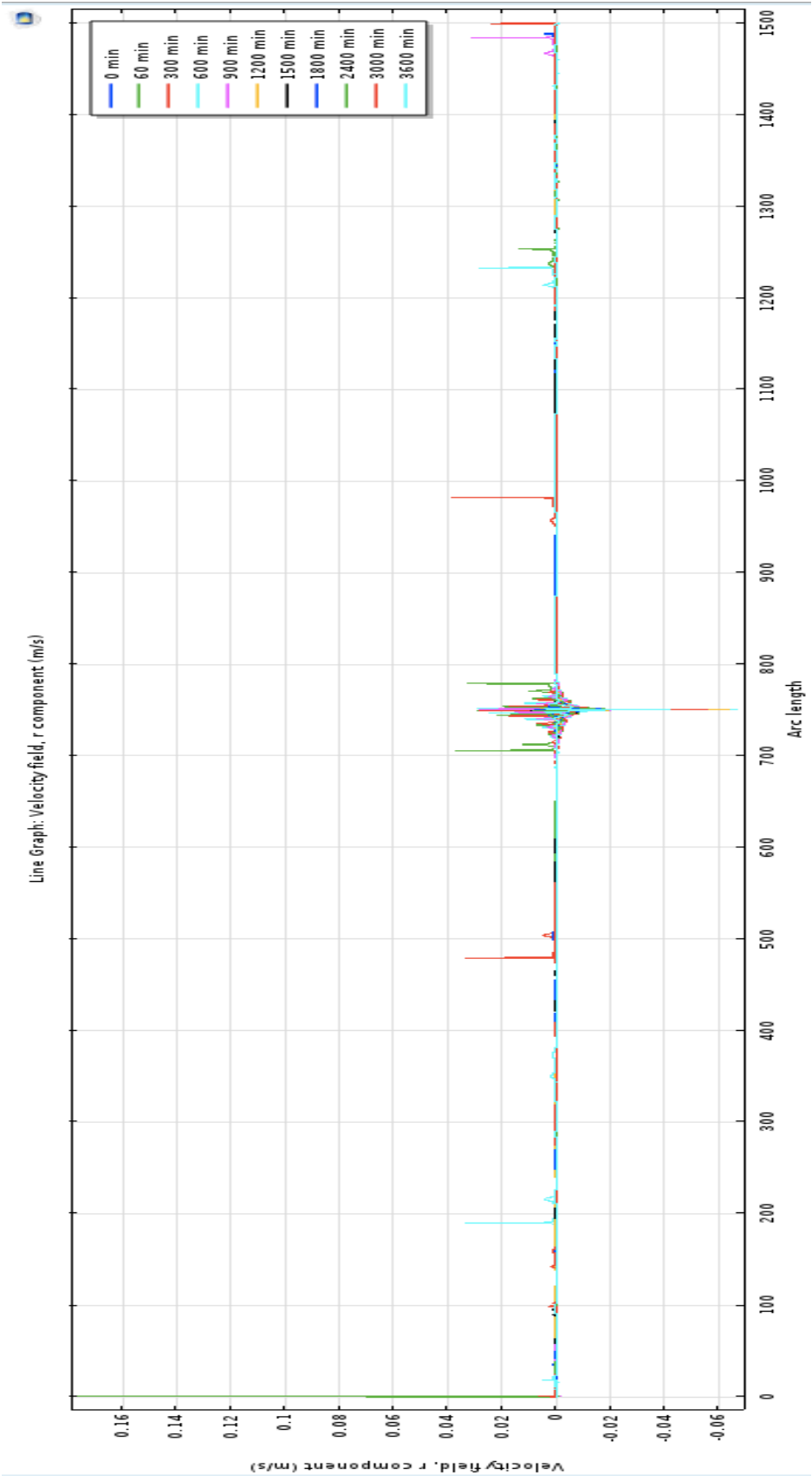


Figure 49: Line Graph Velocity field Density Difference 2 after 0, 1, 5, 10, 15, 20, 25, 30, 40, 50 and 60 minutes

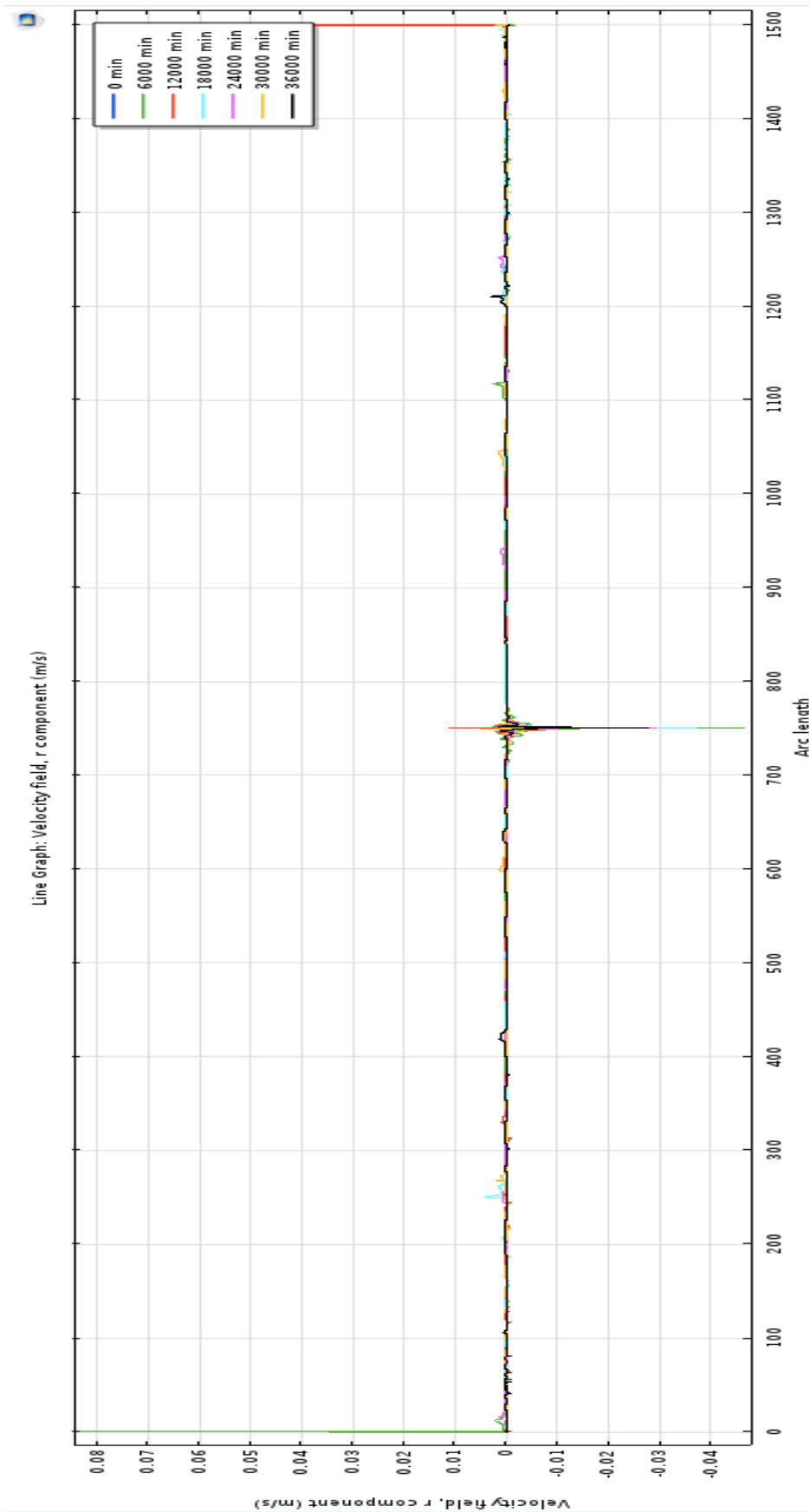


Figure 50: Line Graph Velocity field Density Difference 2 after 0, 100, 200, 300, 400, 500 and 600 minutes

Figure 49 shows a line graph of the velocity field for the density difference case 2 during the first hour of simulation. It is clear that the largest velocity observed is at the bottom of the fluid column. It has a value of almost 0.18 m/s in the downward direction. It is difficult to tell if this velocity appears after 1 or 40 minutes (both green lines), but it is safe to say that this velocity takes place within 40 minutes. The velocity profile seems quite symmetric around the interface.

The highest velocity at the interface appears after 10 minutes and is approximately 0.07 m/s in the upward direction. The highest velocity in the downward direction around the interface is almost 0.04 m/s.

Figure 50 presents a line graph of the velocity field for the density difference case 2 during 10 hours. The highest velocity measured in this time period appears at the bottom of the fluid column after 100 minutes. It has a value of approximately 0.085 m/s in the downward direction. At the interface the highest velocity in the upward direction has a value of approximately 0.04 m/s and appears after 100 minutes. The highest velocity in the downward direction takes place after 200 minutes and has a value of roughly 0.011 m/s. The highest velocity at the top of the fluid column is 0.045 m/s in the downward direction and appears after 200 minutes.

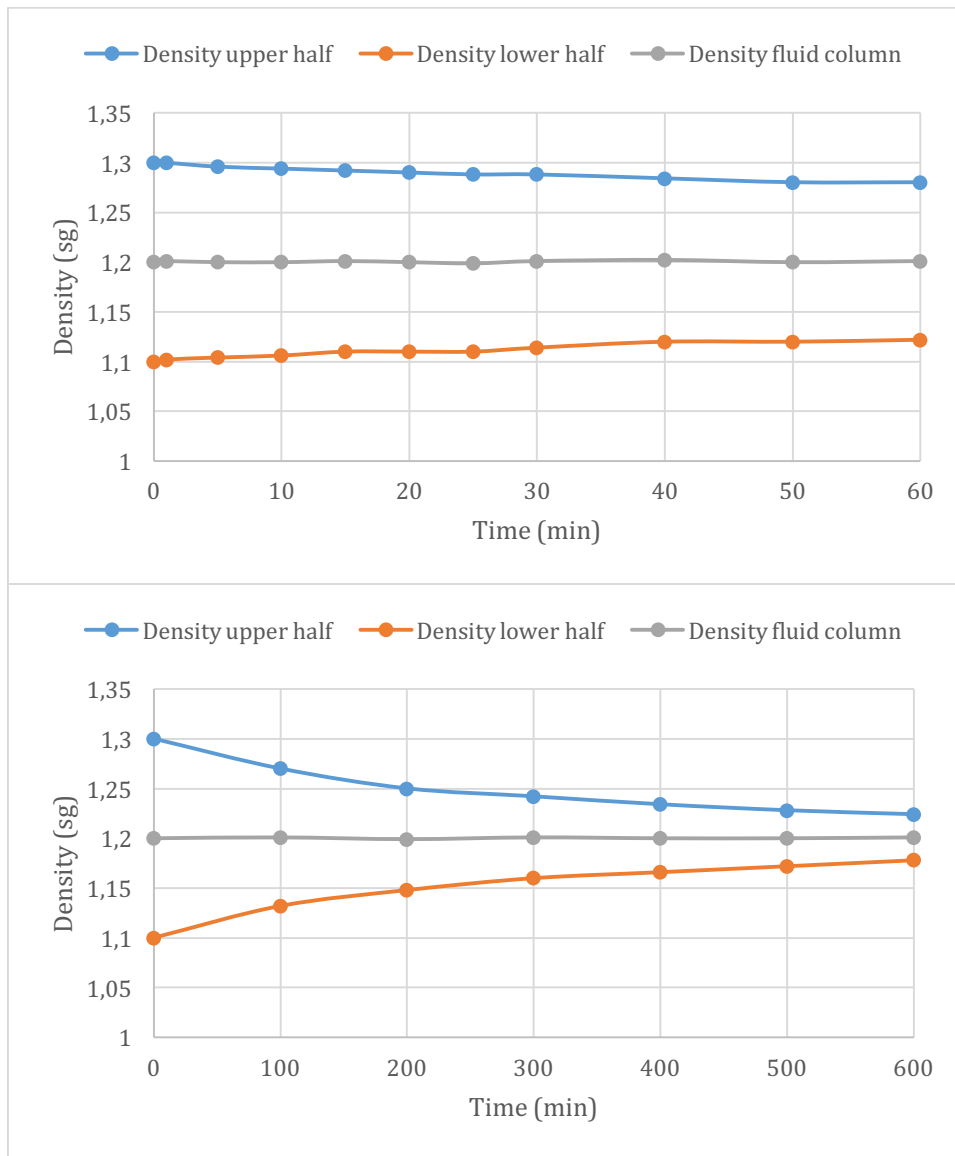


Figure 51: Density fluid column, vs. time, Density Difference 2

The plots in figure 51 show the development of the densities of the light fluid in the lower part of the fluid column and the heavy fluid in the upper part of the fluid column. The upper plot shows the density development during the first hour and the lower plot shows the density development during 10 hours.

After 1 hour the density of the heavy fluid has decreased from 1.30 sg to 1.28 sg and the density of the light fluid has increased from 1.10 sg to 1.12 sg. This equals a density difference of 0.02 sg of both fluids. After 10 hours the density of the heavy fluid has decreased to 1.22 sg and the density of the light fluid has increased to 1.18 sg. The difference between the density of the heavy fluid at start and after 10 hours equals the

difference between the density of the light fluid at start and after 10 hours and has a value of 0.08 sg.

The average density of the entire fluid column remains constant through the 10 hours of simulation and equals approximately 1.20 sg.

4.2.3 Effect of Viscosity

The purpose of these simulations is to demonstrate how change in viscosity may affect the length, density and viscosity of the mixing zone. The viscosity for both the heavy and the light fluid were changed compared to the reference case. In the first simulation the viscosity of the heavy fluid was set to 22 cP and the viscosity of the light fluid was set to 10 cP. The difference between the viscosities are 12 cP. In the second simulation the viscosity for the heavy and light fluid were set to 17 cP and 16 cP, respectively, and the difference between them is reduced to only 1 cP. Table 3 shows the values of the parameters in the simulations.

Table 3: Parameters for simulation of viscosity difference in COMSOL

Case	Heavy fluid		Light fluid		Well bore radius (m)
	Density (sg)	Viscosity (cP)	Density (sg)	Viscosity (cP)	
Viscosity difference 1	1.60	22	1.10	10	0.1265
Viscosity difference 2	1.60	17	1.10	16	0.1265

Viscosity Difference 1

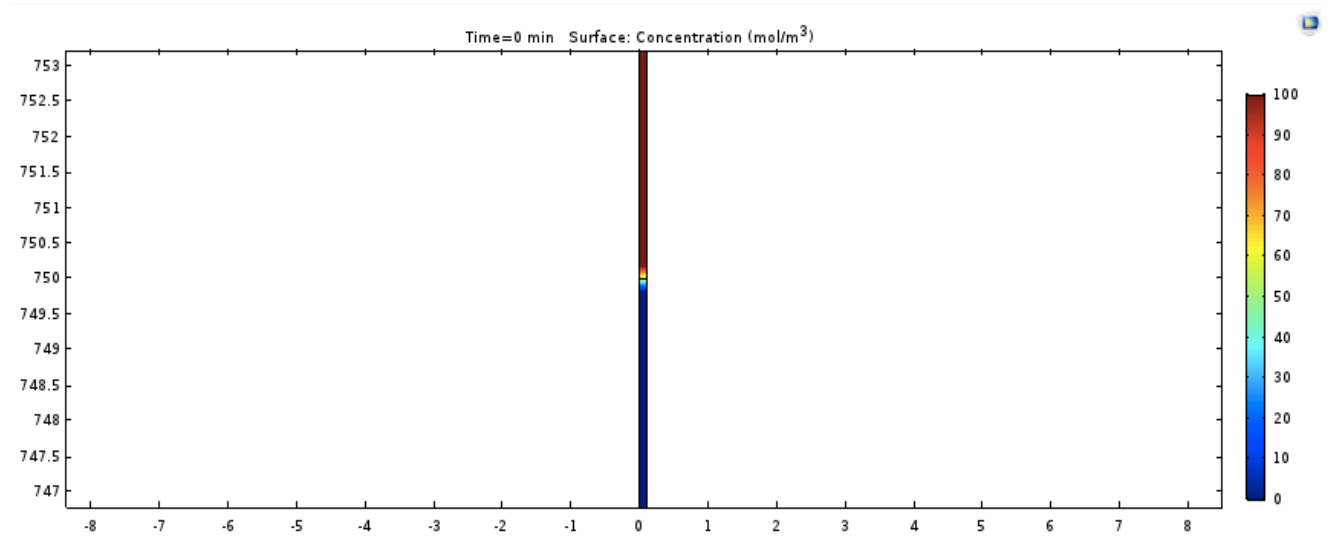


Figure 52: Surface Concentration at start, Viscosity Difference 1

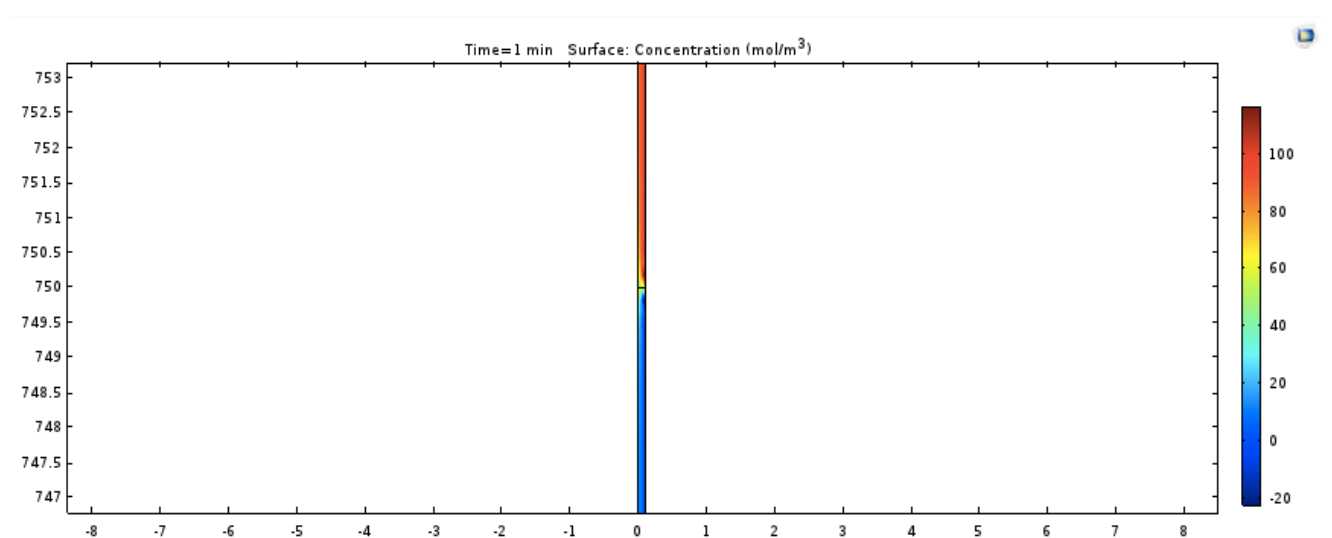


Figure 53: Surface Concentration after 1 minute, Viscosity Difference 1

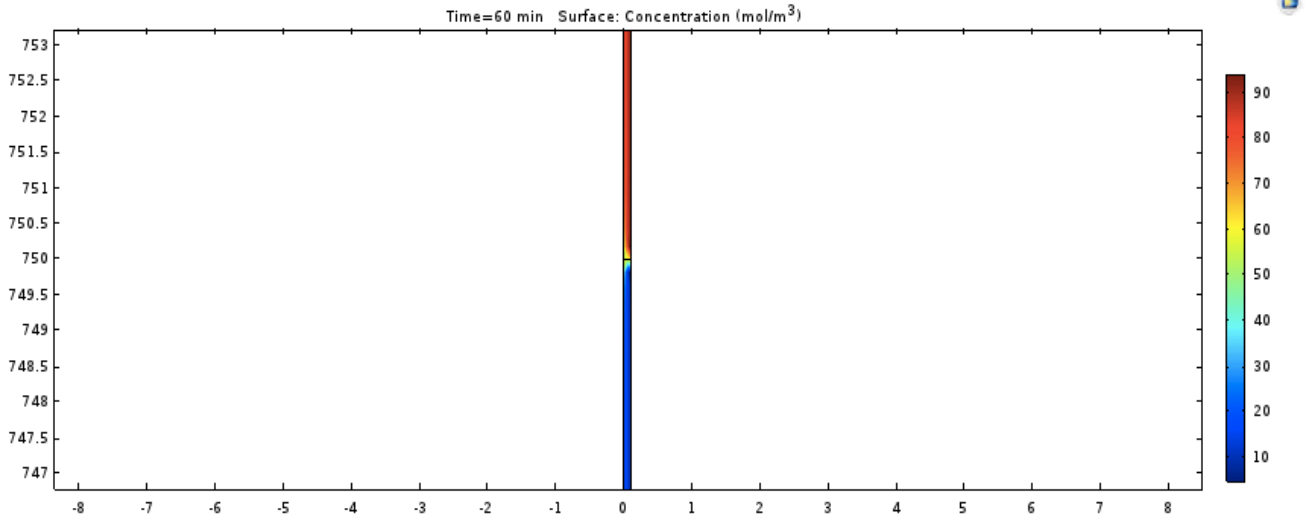


Figure 54: Surface Concentration after 1 hour, Viscosity Difference 1

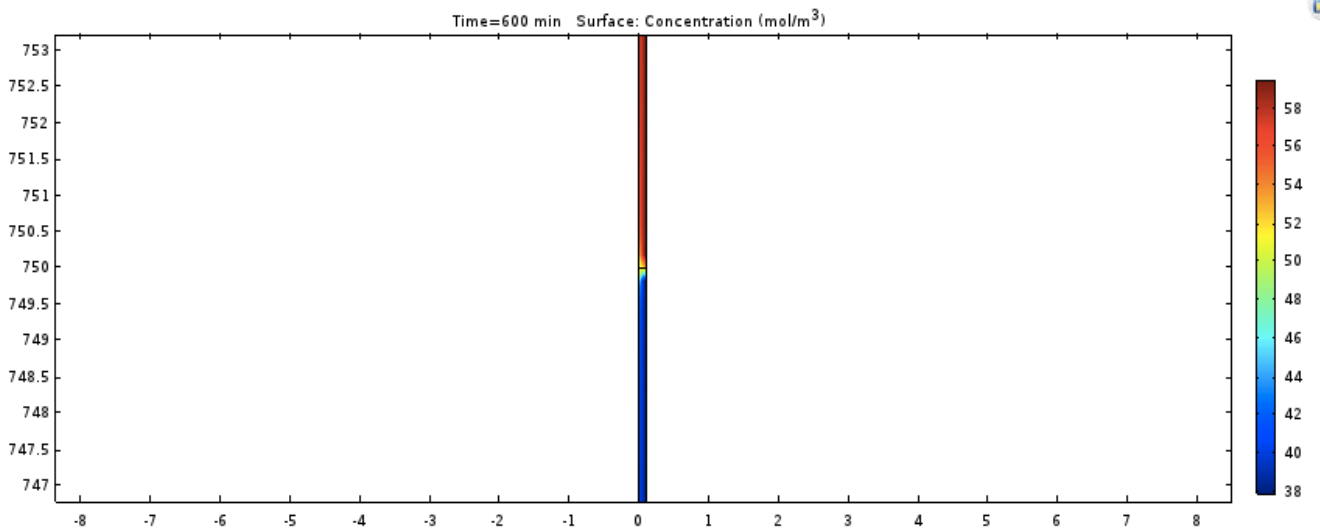


Figure 55: Surface Concentration after 10 hours, Viscosity Difference 1

Figure 52 shows the surface velocity at start of the simulation of the viscosity difference case 1. The interface is in the middle of the fluid column at a height of 750 meters. After 1 minute the interface is still at 750 meters, but the concentrations of the fluids are changed. The concentration of the heavy fluid has decreased while the concentration of the light fluid has increased. The colour chart of the concentration ranges from -20 to above 100, which should not be possible. The model is probably not stabilized yet.

After 1 hour the colour chart is stable and within the desired range. Due to the change in the values of the colour chart it is difficult to distinguish between the concentrations of the heavy and light fluid after 1 minute and after 1 hour. The interface is still at a height of 750 meters.

After 10 hours it is clearly that the concentration of the heavy fluid has decreased and the concentration of the light fluid has increased. The concentration of the heavy fluid has a maximum value of almost 60 and the concentration of the light fluid has a minimum value of 38. As can be seen from all the screenshots from the simulations for this case (please refer to Appendix A), the interface remains in the middle of the fluid column through the whole simulation period of 10 hours.

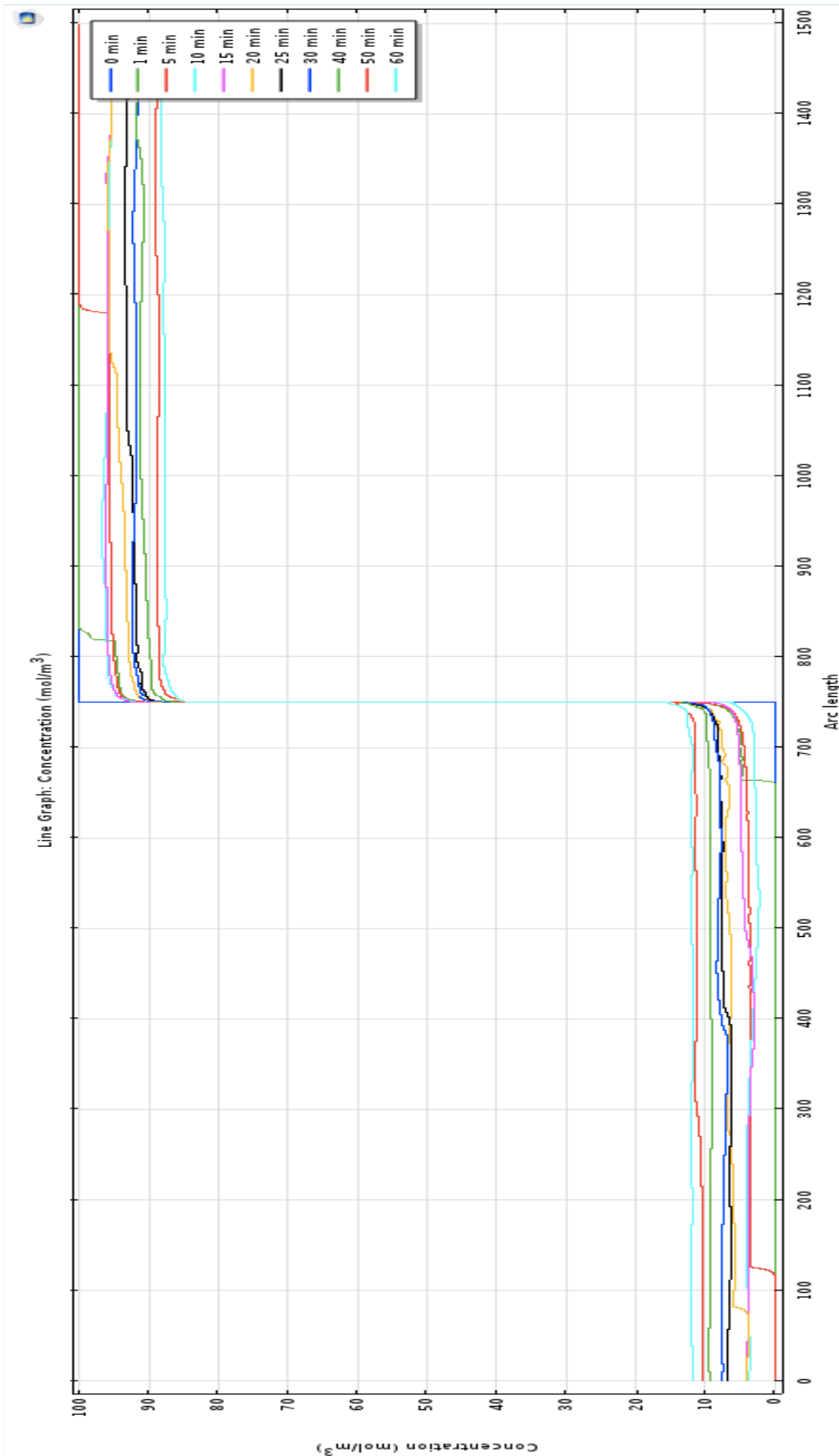


Figure 56: Line Graph Concentration Viscosity Difference 1 after 0, 1, 5, 10, 15, 20, 25, 30, 40, 50 and 60 minutes

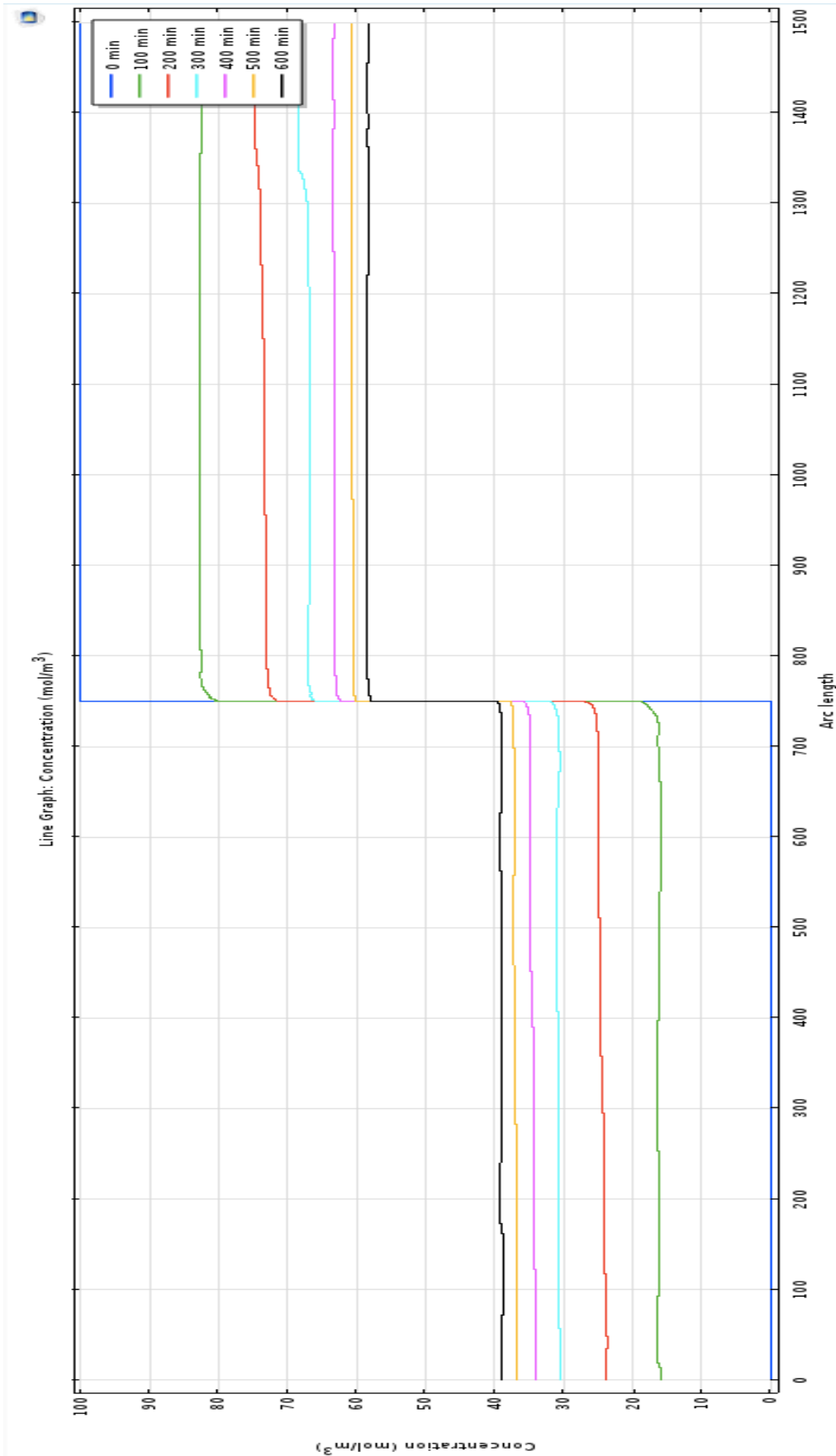


Figure 57: Line Graph Concentration Viscosity Difference 1 after 0, 100, 200, 300, 400, 500 and 600 minutes

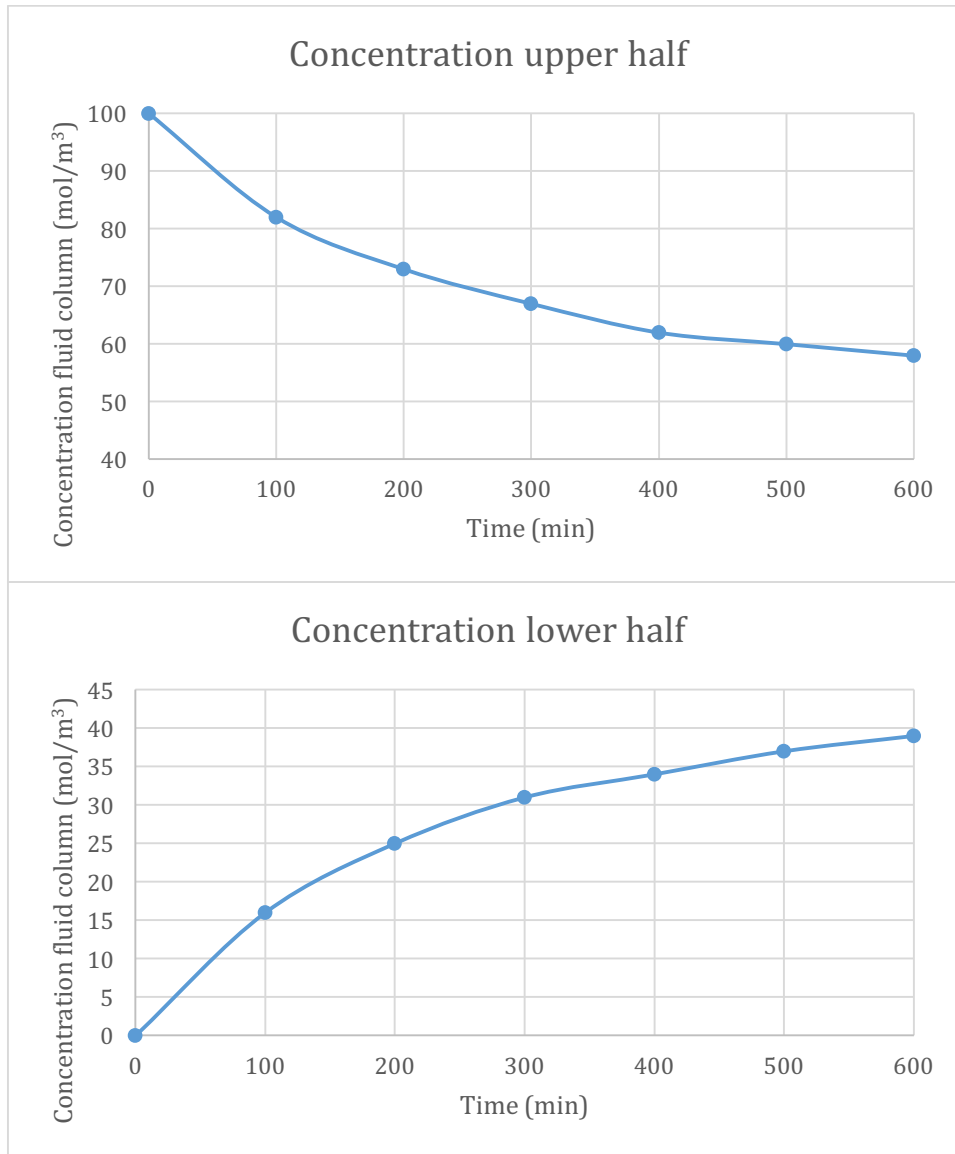


Figure 58: Concentration fluid column, Viscosity Difference case 1

Figure 56 shows a line graph of the concentration for the viscosity difference case 1 during the first hour of simulation. For the first 5 minutes it is possible to define a mixed zone between the fluids. After 1 minute the mixed zone is located between 670 and 820 meters and has a length of 150 meters. After 5 minutes the length of the mixed zone is 1060 meters, between 120 and 1180 meters. The maximum concentration for the light fluid in the lower part of the fluid column during the first hour is 12 and the minimum concentration for the heavy fluid in the upper part of the fluid column is 88. This gives a concentration difference of 12 for both fluids.

Figure 58 presents two plots showing the development of the concentration in the fluid column and figure 57 shows a line graph of the concentration for the viscosity difference case 1, both for a time period of 10 hours. During the first 100 minutes the concentration of the heavy fluid decreases from 100 to 82 and the concentration of the light fluid increases from 0 to 16. After 10 hours the concentration of the heavy fluid has decreased to 58, which gives a difference of 42, and the concentration of the light fluid has increased to 39. The difference between the concentration of the heavy fluid and the concentration of the light fluid is now 19.

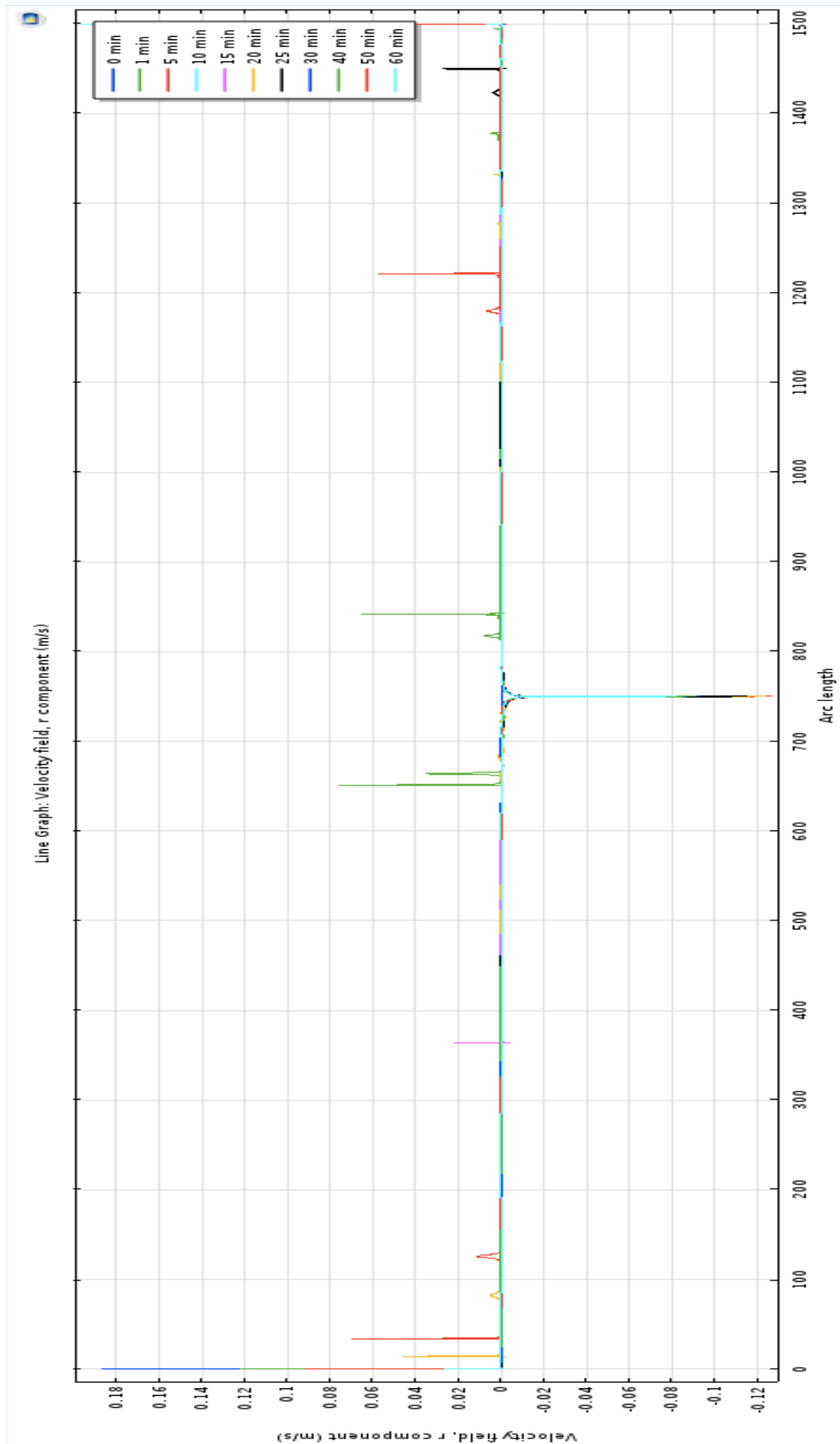


Figure 59: Line Graph Velocity field Viscosity Difference 1 after 0, 1, 5, 10, 15, 20, 25, 30, 40, 50 and 60 minutes

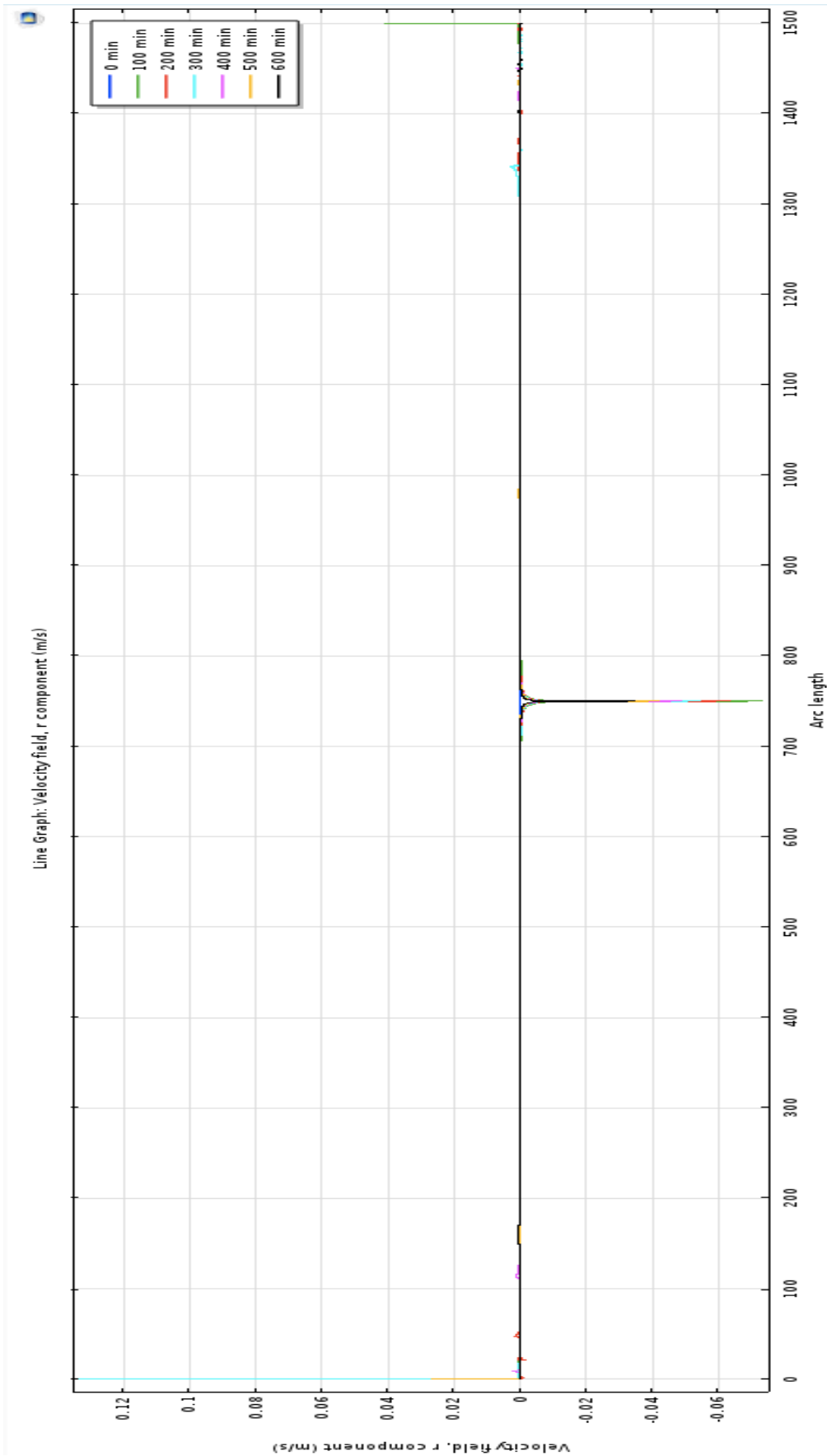


Figure 60: Line Graph Velocity field Viscosity Difference 1 after 0, 100, 200, 300, 400, 500 and 600 minutes

Figure 59 presents a line graph of the velocity field for the viscosity difference case 1 after 1 hour of simulation. The maximum velocity during the first hour is measured to almost 0.2 m/s in the downward direction and is located on the top of the fluid column after 10 minutes. The highest velocity measured on the bottom of the fluid column has a value of approximately 0.185 m/s in the downward direction, and appears after 30 minutes. The maximum velocity at the interface is measured after 5 minutes and has a value of almost 0.13 m/s in the upward direction.

A line graph of the velocity field for the viscosity difference case 2 during 10 hours is shown in figure 60. The maximum velocity measured is located on the bottom of the fluid column and appears after 300 minutes (5 hours). It has a value of roughly 0.135 m/s in the downward direction. On the top of the fluid column there is observed a maximum velocity of 0.041 m/s in the downward direction after 100 minutes. Simultaneously, there is a maximum velocity at the interface. It has a value of approximately 0.075 m/s in the upward direction. Except from the bottom and the top of the fluid column, and at the interface, the total velocity is approximately zero in the fluid column.

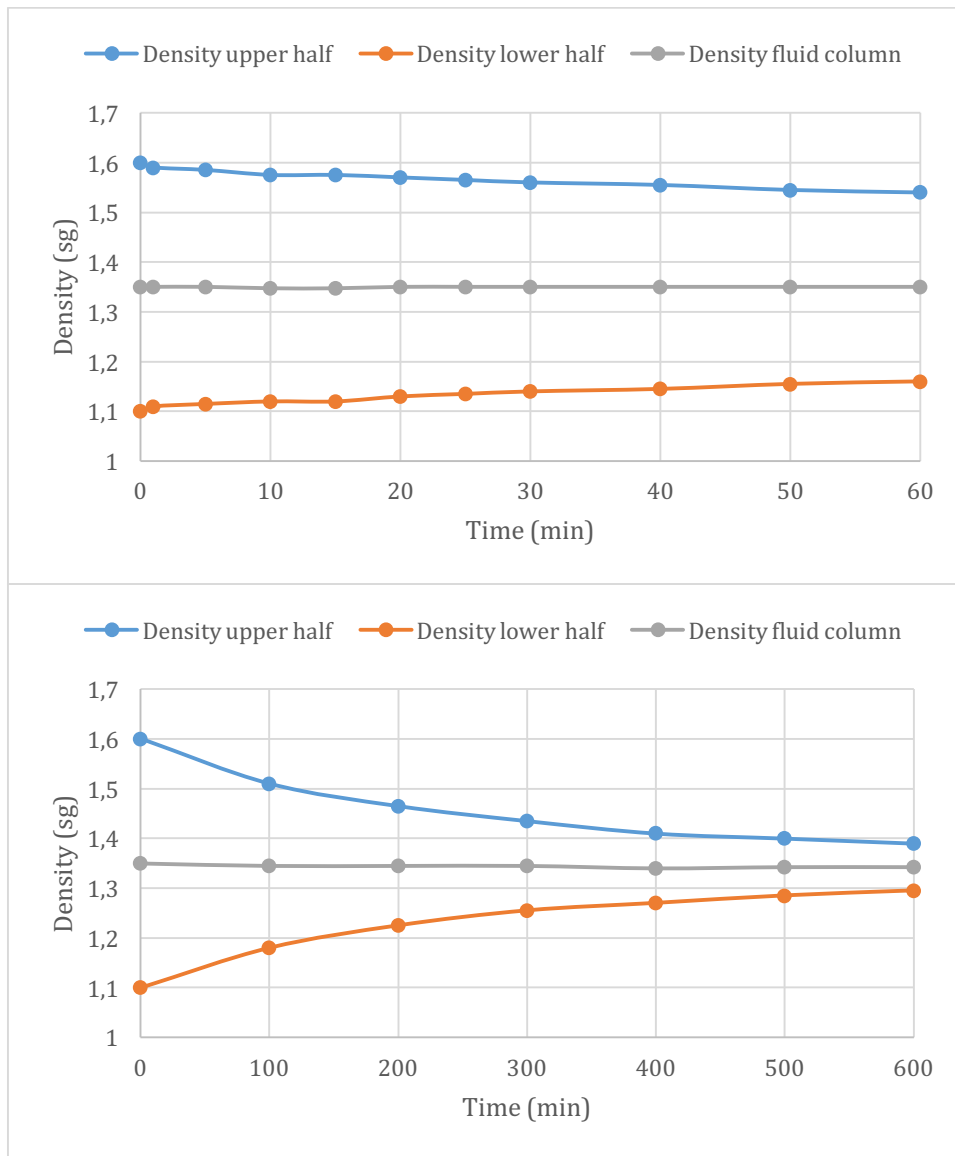


Figure 61: Density fluid column vs. time, Viscosity Difference 1

Figure 61 presents the density development in time for the viscosity difference case 1. The upper plot shows the density development during the first hour of simulation and the lower plot shows the density development during the full simulation period of 10 hours.

After 1 hour the density of the heavy fluid in the upper part of the fluid column has decreased to 1.54 sg and the density of the light fluid in the lower part of the fluid column has increased to 1.16. This gives a density difference of 0.06 sg for both fluids and a difference of 0.38 sg between the densities of the fluids. During 10 hours the density of the heavy fluid decreases to 1.39 sg, which gives a total density difference of

0.21 sg. The density of the light fluid increases to 1.30 sg, which gives a total density difference of 0.20 sg. The density difference between the fluids is now 0.09 sg.

The average density of the entire fluid column remains approximately 1.35 sg throughout the simulation period of 10 hours.

Viscosity Difference 2

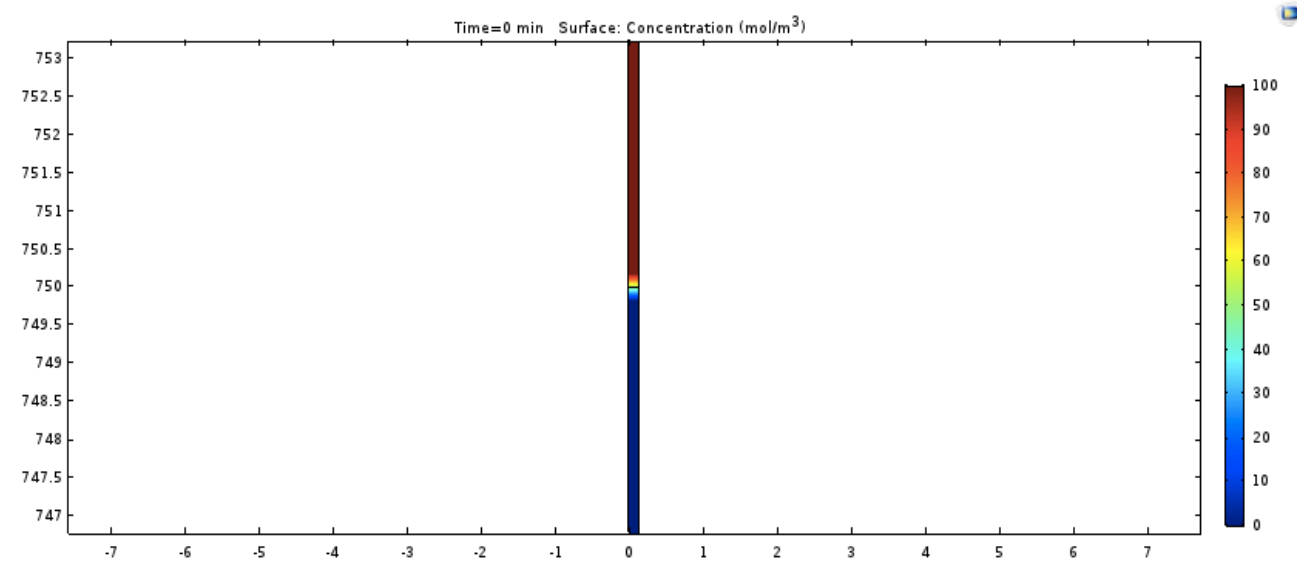


Figure 62: Surface concentration Viscosity Difference 2 at start

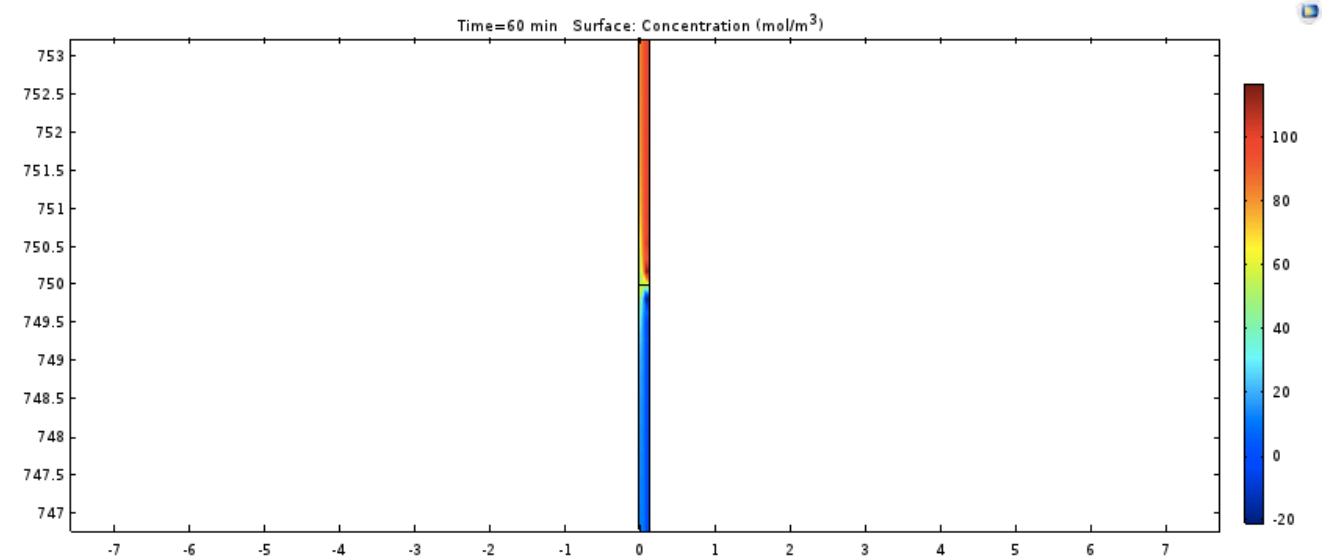


Figure 63: Surface concentration Viscosity Difference 2 after 1 minute

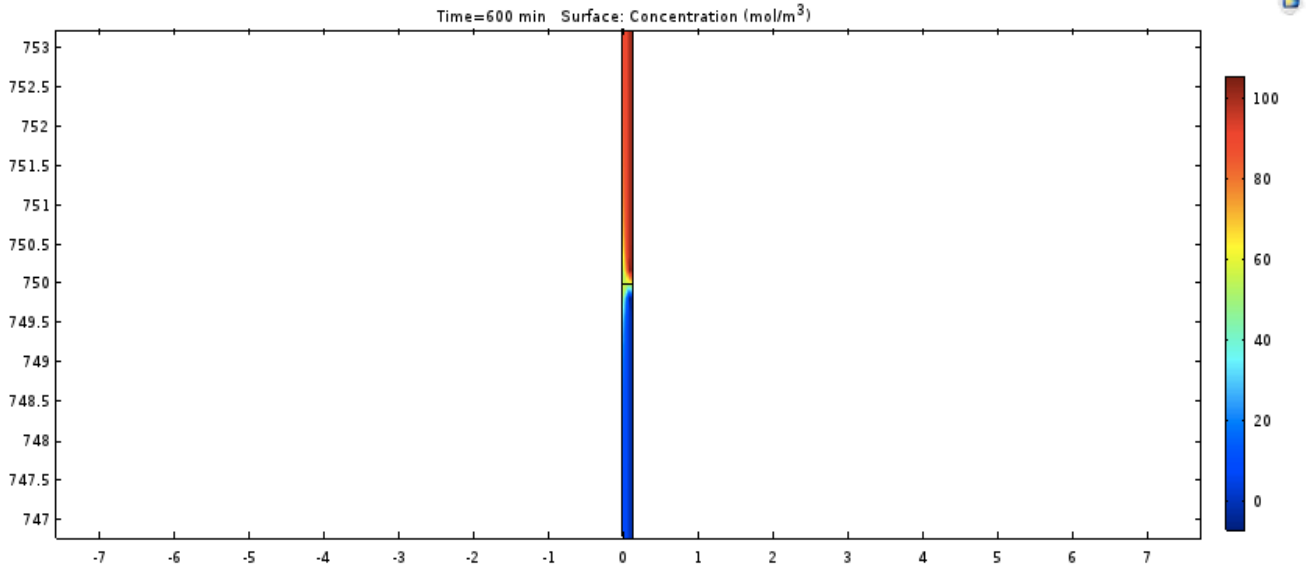


Figure 64: Surface concentration Viscosity Difference 2 after 1 hour

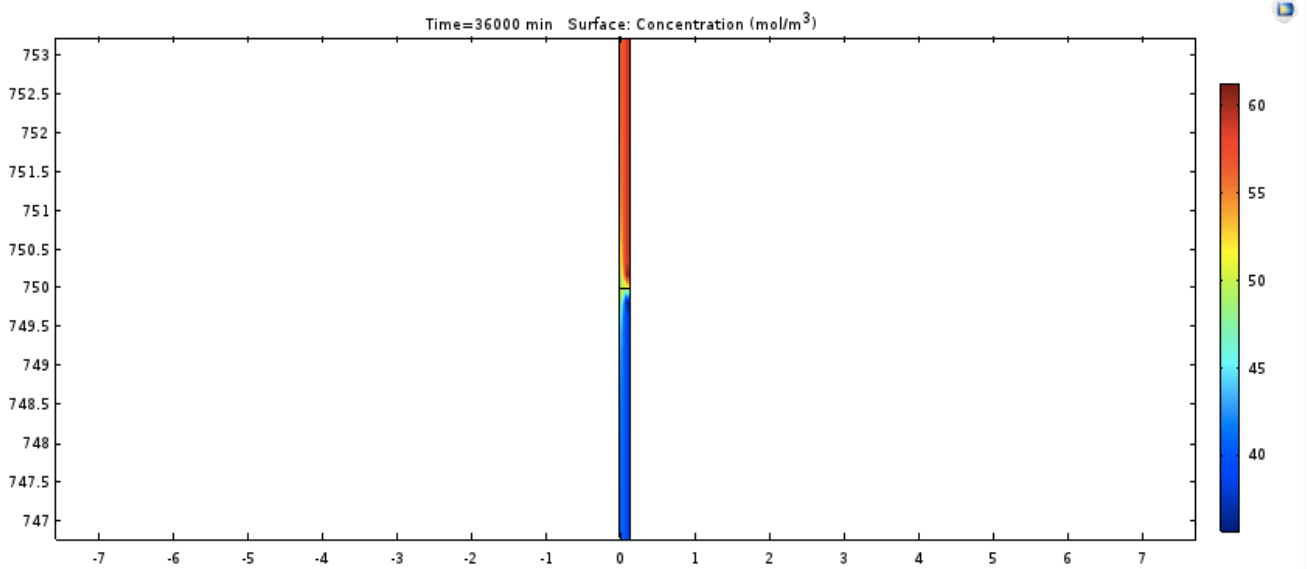


Figure 65: Surface concentration Viscosity Difference 2 after 10 hours

At start of the simulation the interface is in the middle of the fluid column at a height of 750 meters, which can be seen on figure 62. The concentration of the heavy fluid is 100 and the concentration of the light fluid is 0. After 1 minute the colour chart for the concentration shows values that exceed the theoretically possible range, and the model is probably not stabilized yet. The colours of the fluid column show that the concentrations of the heavy and the light fluid have changed.

During the first hour the colour chart is almost within the desired range and the model is practically stabilized by now. The colours of the fluid column are slightly darker which should indicate an increase in concentration for the heavy fluid and a decrease in concentration for the light fluid. However, the values of the colour chart are changed and may show a decrease in concentration for the heavy fluid and an increase in concentration for the light fluid.

After 10 hours there are clearly changes in the concentrations of the fluids. The maximum concentration of the heavy fluid is now limited to approximately 60 and the minimum concentration of the light fluid around 35. The interface remains in the middle of the fluid column at a height of 750 meters during all 10 hour of simulation.

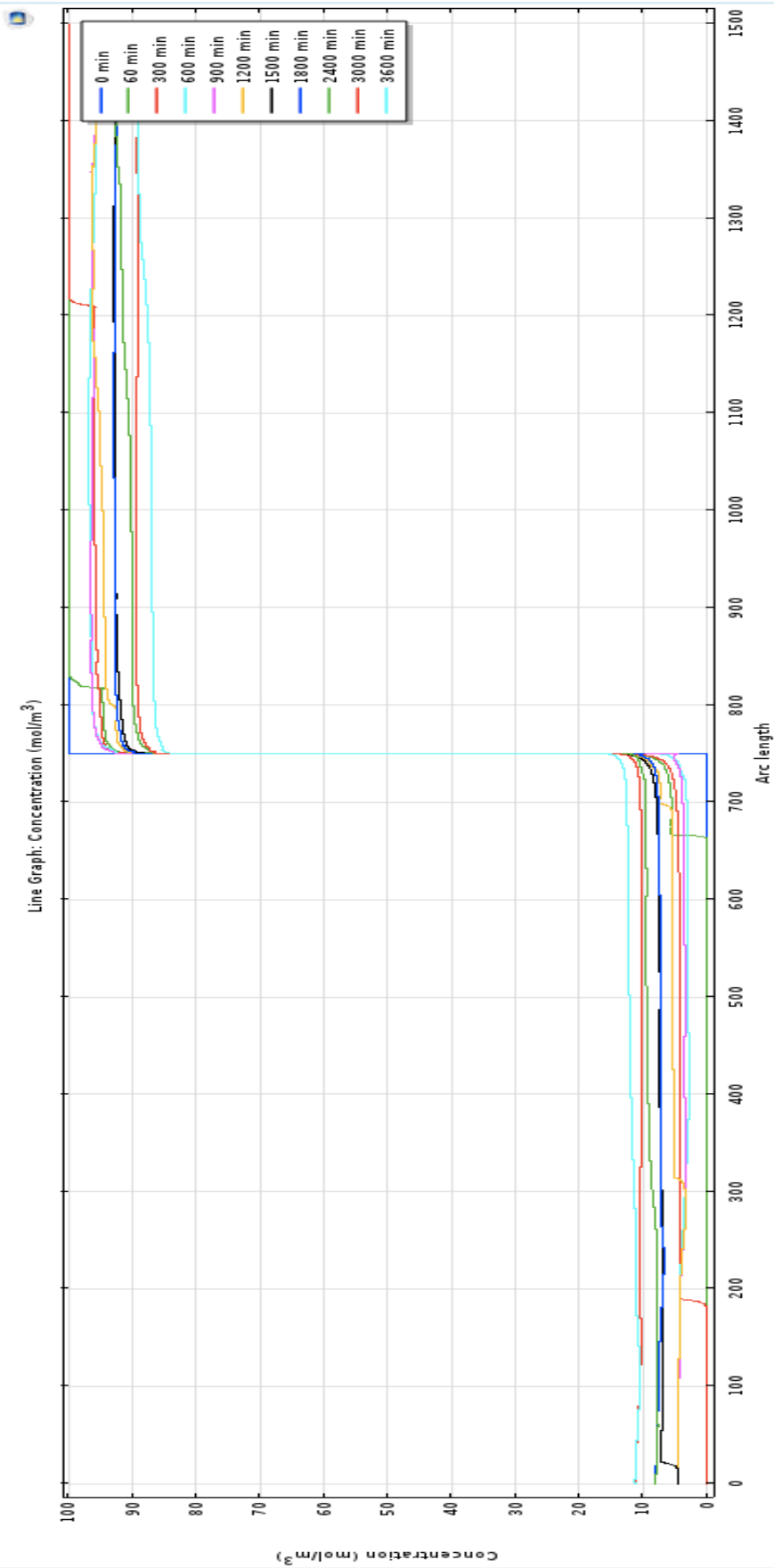


Figure 66: Line Graph Concentration Viscosity Difference 2 after 0, 1, 5, 10, 15, 20, 25, 30, 40, 50 and 60 minutes

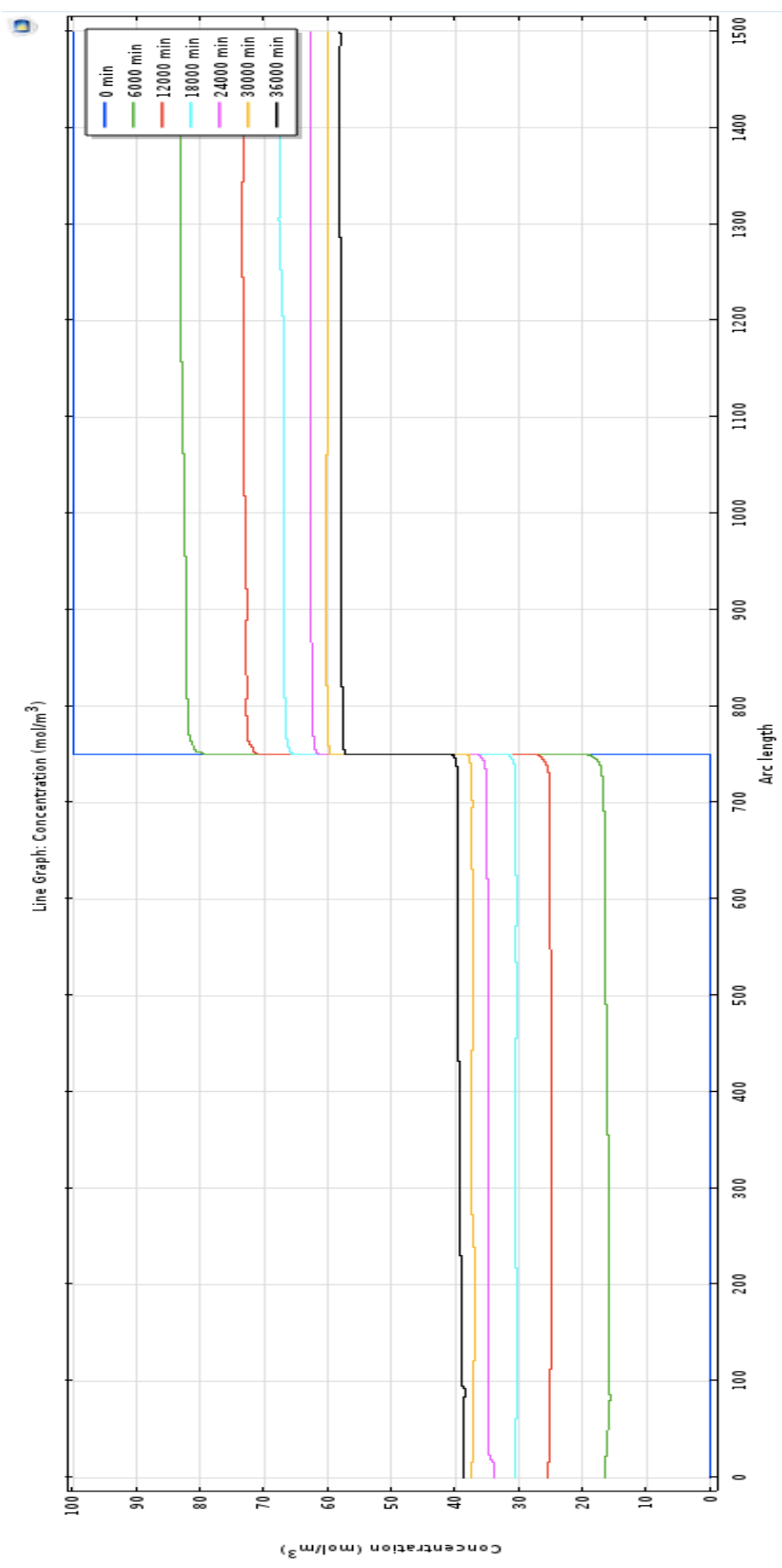


Figure 67: Line Graph Concentration Viscosity Difference 2 after 0, 100, 200, 300, 400, 500 and 600 minutes

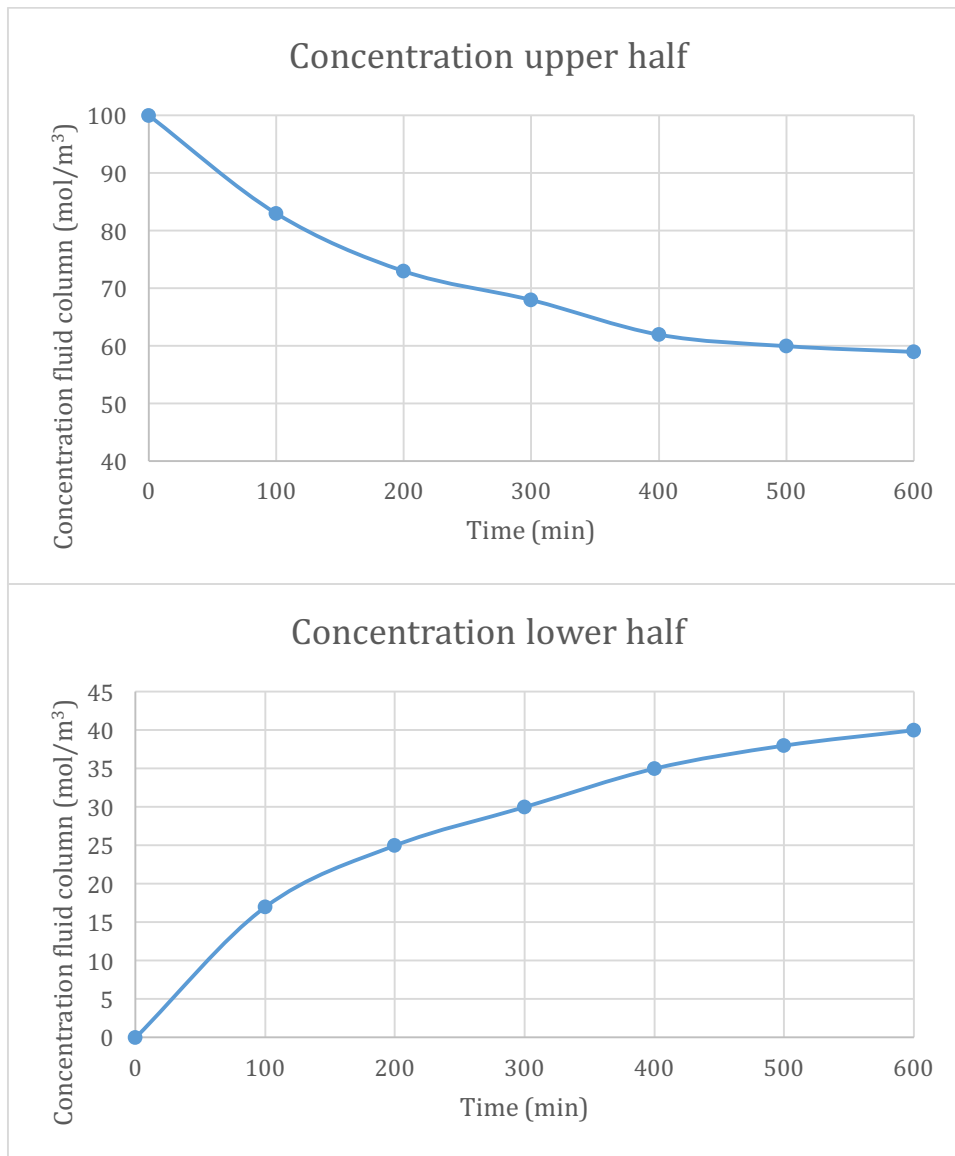


Figure 68: Concentration fluid column, Viscosity Difference case 2

Figure 66 and 67 show a line graph of the concentration for the viscosity case 2 after 1 and 10 hours, respectively. Figure 68 presents two plots showing the development of the concentration of the fluid column. For the first 5 minutes it is possible to define a length of the mixed zone. After 1 minute the mixed zone is located between 670 and 820 meters, which gives a length of 150 meters. After 5 minutes the length of the mixed zone is equal to 1020 meters and is located between 190 and 1210 meters. During the first hour the concentration of the heavy fluid decreases from 100 to 88 and the concentration of the light fluid increases from 0 to 12. The difference between the fluids has decreased from 100 to 76.

After 100 minutes the concentration of the heavy fluid in the upper part of the fluid column has decreased to 83 and the concentration of the light fluid in the lower part of the fluid column has increased to 17. During 10 hours the concentrations of the heavy and the light fluid have changed to respectively 59 and 40. The concentration difference for the heavy fluid is 41, and 40 for the light fluid. After 10 hours the concentration difference between the fluids has decreased from 100 to 19.

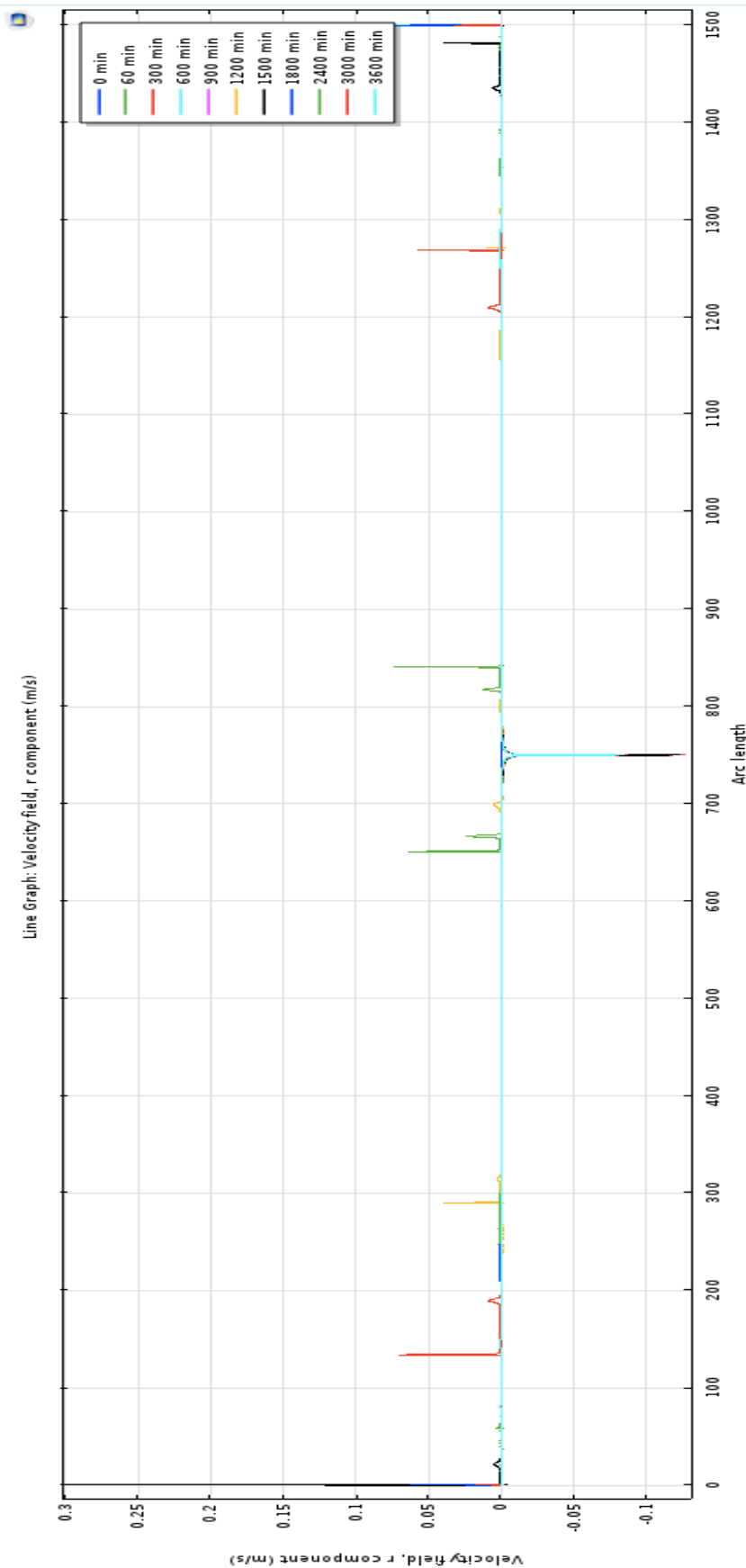


Figure 69: Line Graph Velocity field Viscosity Difference 2 after 0, 1, 5, 10, 15, 20, 25, 30, 40, 50 and 60 minutes

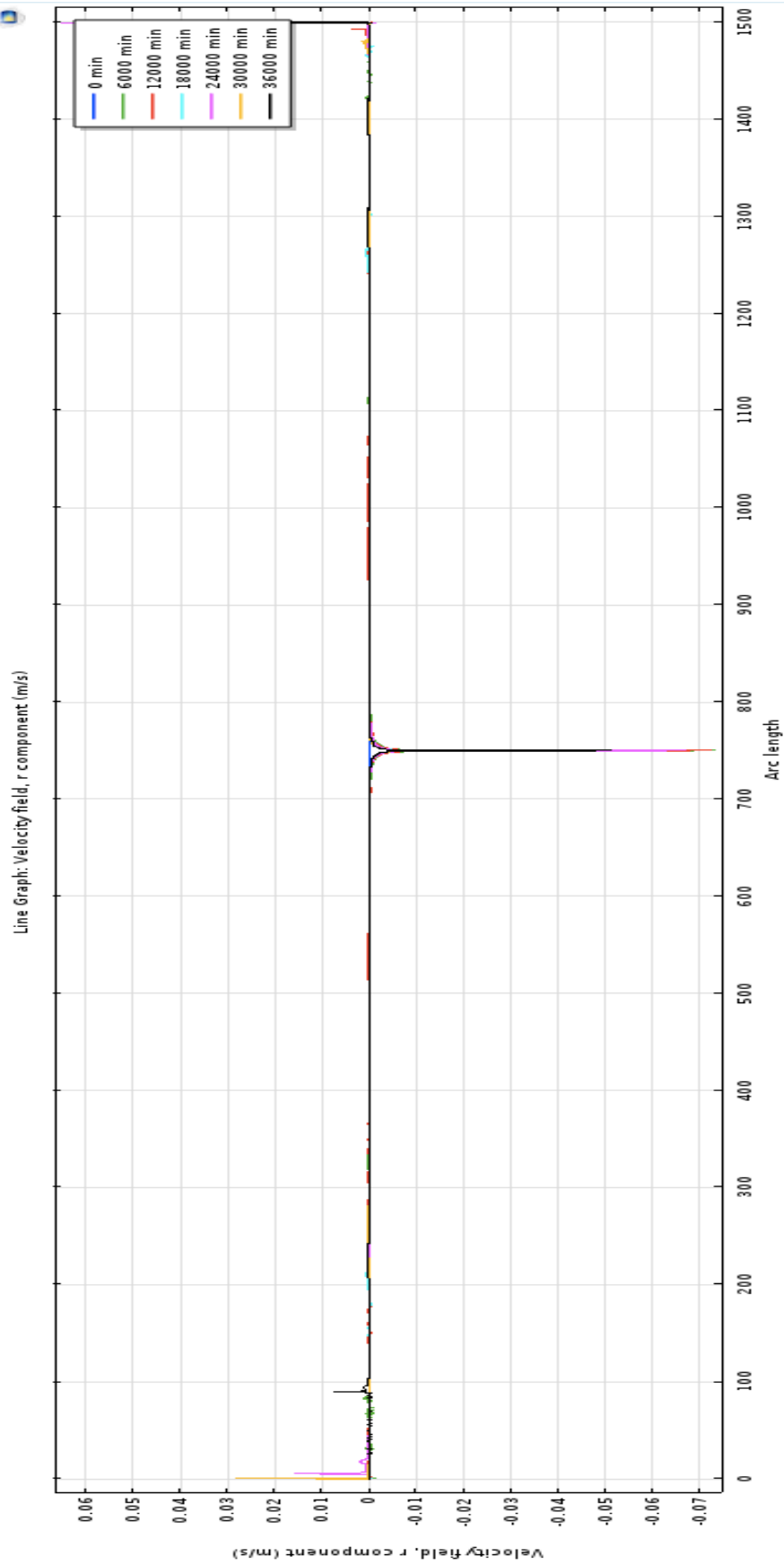


Figure 70: Line Graph Velocity field Viscosity Difference 2 after 0, 100, 200, 300, 400, 500 and 600 minutes

A line graph of the velocity field for the viscosity difference case 2 is presented in Figure 69 and 70. Figure 69 shows line graphs for the first hour of simulation while figure 70 shows line graphs for the entire simulation period of 10 hours. During the first hour there is observed a maximum velocity located on the bottom of the fluid column. It has a value of approximately 0.30 m/s in the downward direction, and takes place after 25 minutes. After 10 minutes the maximum velocity on the top of the fluid column was measured to 0.21 m/s in the downward direction. The maximum velocity measured at the interface had a value of approximately 0.13 m/s in the upward direction and was observed after 5 minutes. After 10 minutes the maximum velocity on the top of the fluid column was measured to 0.21 m/s. A total velocity in the upward direction could only be observed at the interface. All other velocities measured had a total value in the downward direction.

The maximum velocity during 10 hours was detected at the interface after 100 minutes. It had a value of approximately 0.073 m/s in the upward direction. A velocity of roughly 0.072 m/s in the upward direction was measured at the interface after 200 minutes, implying that the highest velocities at the interface appears in the first half time period of the simulation. The maximum velocity measured on the top of the pipe was found after 400 minutes and had a value of 0.065 m/s in the downward direction. After 500 minutes the maximum velocity on the bottom of the fluid column was observed. It was measured to 0.027 m/s in the downward direction. This implies that the velocity at the interface is high in the beginning of the simulation, and as time goes by, the high velocities eventually reach the top and the bottom of the fluid column.

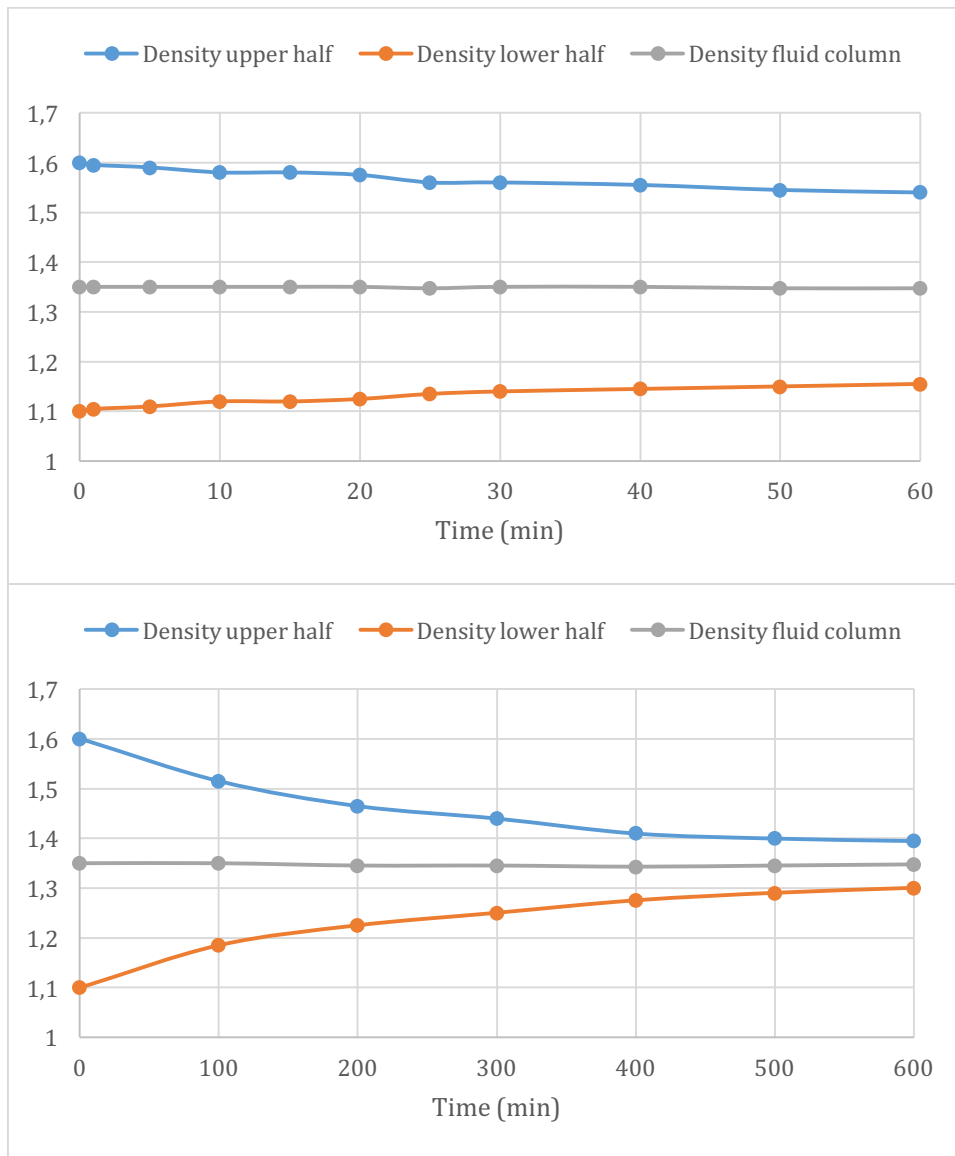


Figure 71: Density fluid column vs. time, Viscosity Difference 2

Figure 71 presents two plots showing the density development of the heavy and light fluid. The upper plot shows the density development during 1 hour and the lower plot shows the density development during 10 hours. During the first hour the density of the heavy fluid in the upper part of the fluid column decreases to 1.54 sg and the density of the light fluid in the lower part of the fluid column has increases to 1.16 sg. Both of the fluids experience a density difference of 0.06 sg during the first hour. The density difference between the fluids is decreased to 0.38 sg.

After 10 hours the density of the heavy fluid had decreased to 1.40 sg and the density of the light fluid has increased to 1.30 sg. The density difference between the fluids are

now decreased to 0.10 sg. Both the heavy and the light fluid had a total variation in density of 0.20 sg. Due to the simultaneous decrease and increase of the heavy and the light fluid, respectively, the average density of the entire fluid column remains constant during a time period of 10 hours, and has a value of approximately 1.35 sg.

4.2.4 Effect of Well Size

The purpose of these simulations is to demonstrate the effect of changing the well size, i.e. change the diameter of the fluid column of the heavy, light and mixed fluid, which all have the same diameter. In COMSOL it is the radius of this fluid column that represents the size of the well. These simulations are for investigating if different well sizes affect the length and the density of the mixed zone. The radius of the well in the first simulation is set to 0.2 meters, which corresponds to a diameter of 0.4 meters. In the second simulation the radius of the well is set to 0.075 meters, i.e. a well diameter of 1.5 meters. The radius of the well for the reference case was set to 0.1265 meters, which gives a difference of 0.0735 meters and 0.0515 meters for the first and second simulation, respectively.

Table 4: Parameters for simulation of well size difference in COMSOL

Case	Heavy fluid		Light fluid		Well radius (m)
	Density (sg)	Viscosity (cP)	Density (sg)	Viscosity (cP)	
Well size difference 1	1.60	19	1.10	14	0.2000
Well size difference 2	1.60	19	1.10	14	0.0750

Well Size Difference 1

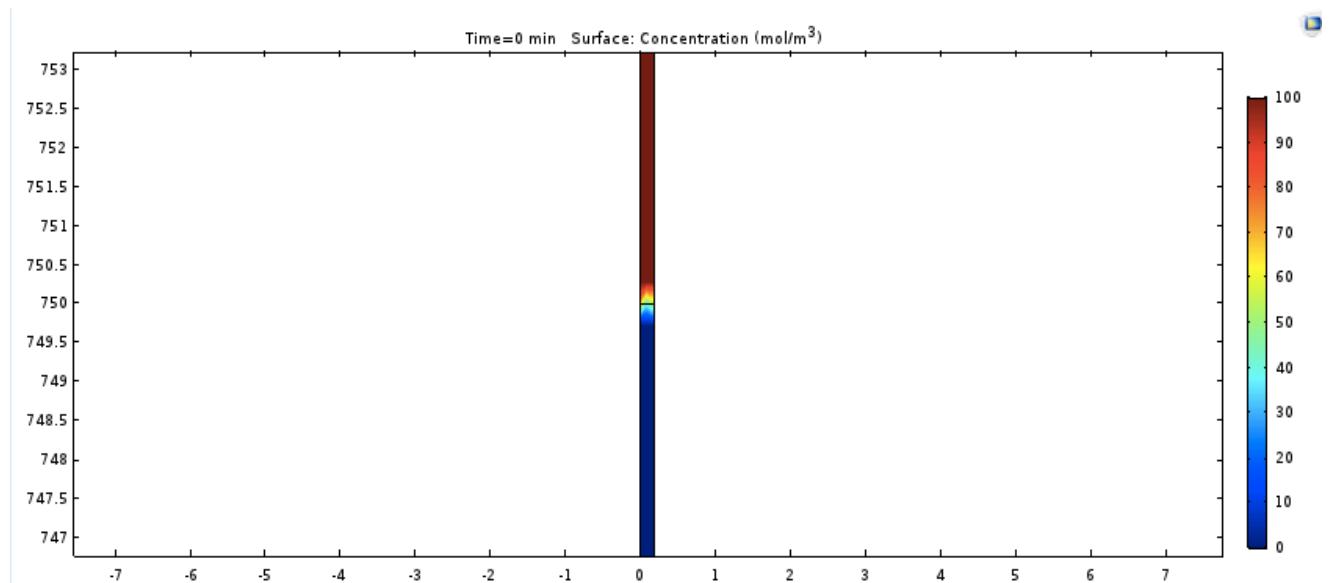


Figure 72: Surface concentration Well Size Difference 1 at start

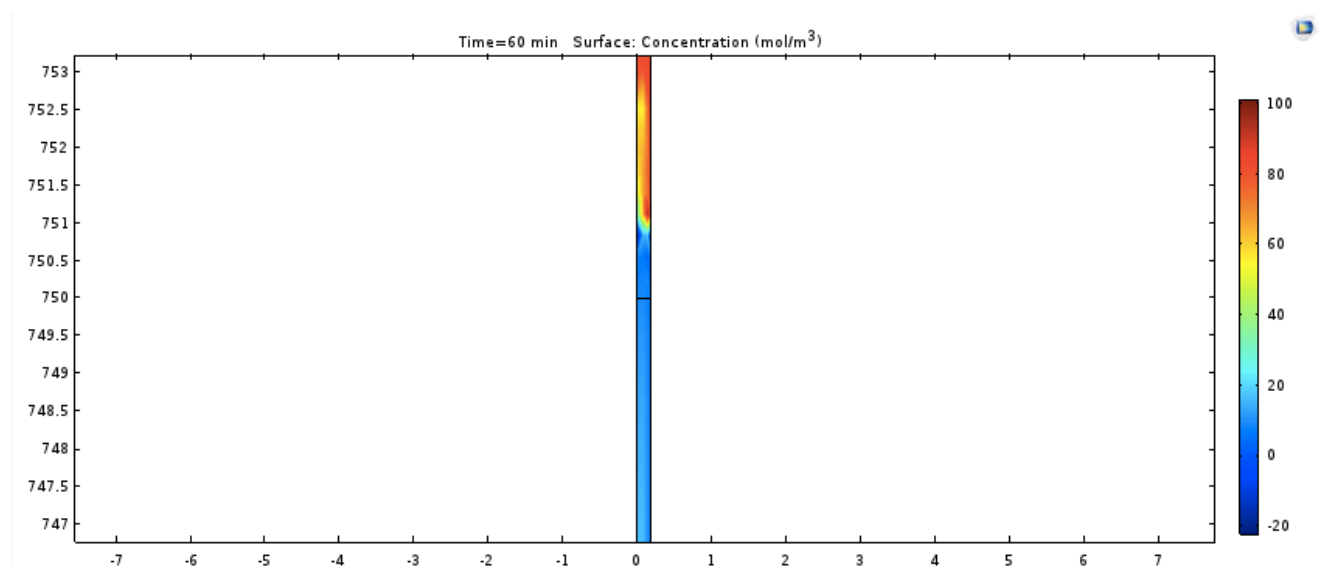


Figure 73: Surface concentration Well Size Difference 1 after 1 minute

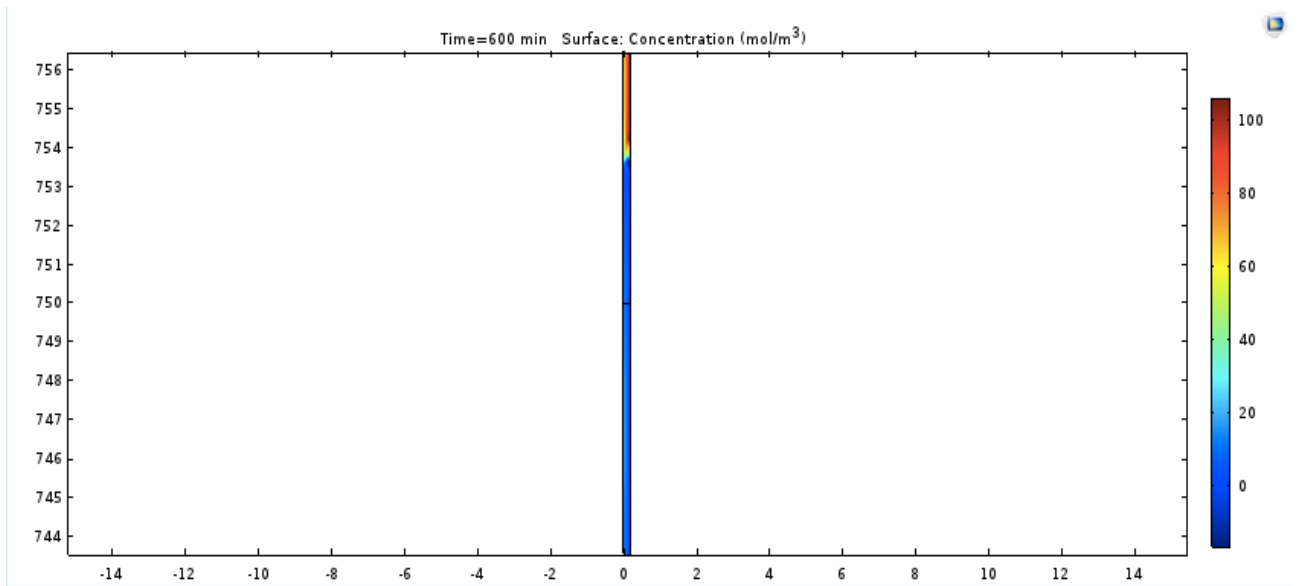


Figure 74: Surface concentration Well Size Difference 1 after 1 hour

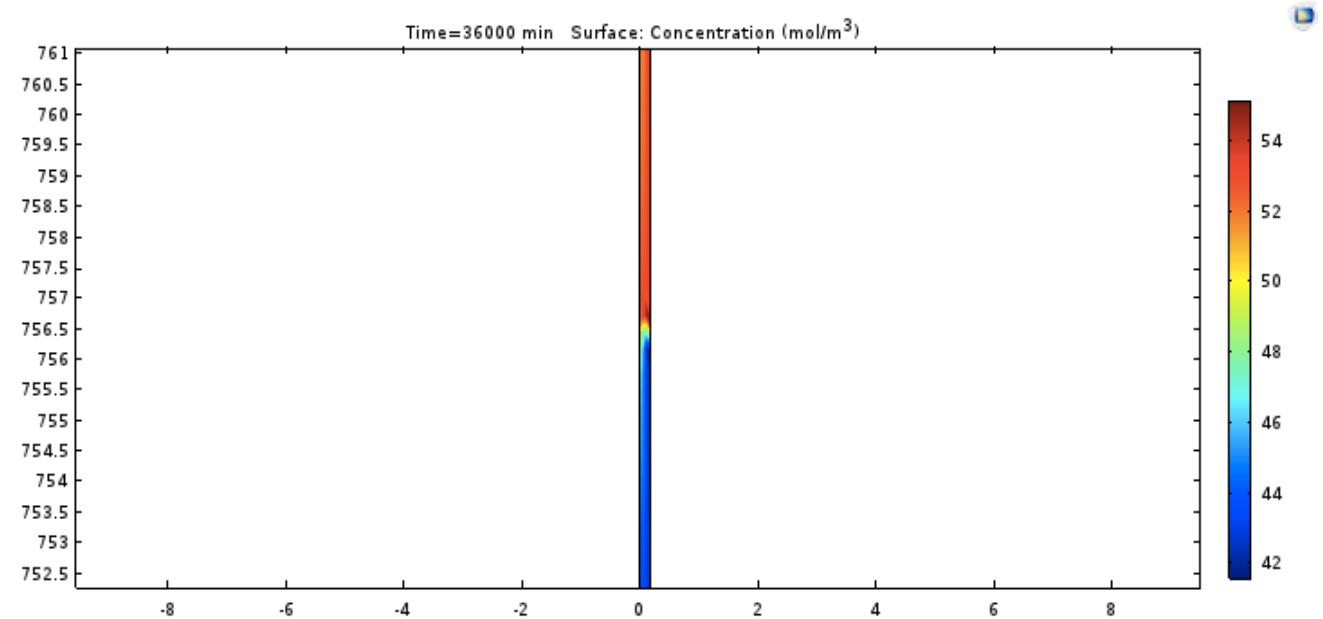


Figure 75: Surface concentration Well Size Difference 1 after 10 hours

At start of the simulation the heavy fluid is located in the upper part of the fluid column, the light fluid is located in the lower part of the fluid column and the interface is located in the middle of the fluid column at a height of 750 meters. After 1 minute the interface has changed position to a height of approximately 751 meters. The colours of the fluid column have gotten slightly lighter, implying that the concentration of heavy fluid just

above the interface has decreased while the concentration of the light fluid just below the interface has increased. The concentration of the interface has a value of around 50.

During the first hour of simulation the interface has risen to a height of approximately 753.5 meters. After 10 hours the interface had risen even more to a height of roughly 756.5 meters. The concentration of the heavy fluid had a maximum value of around 53 and the minimum value of the concentration of the light fluid was 42.

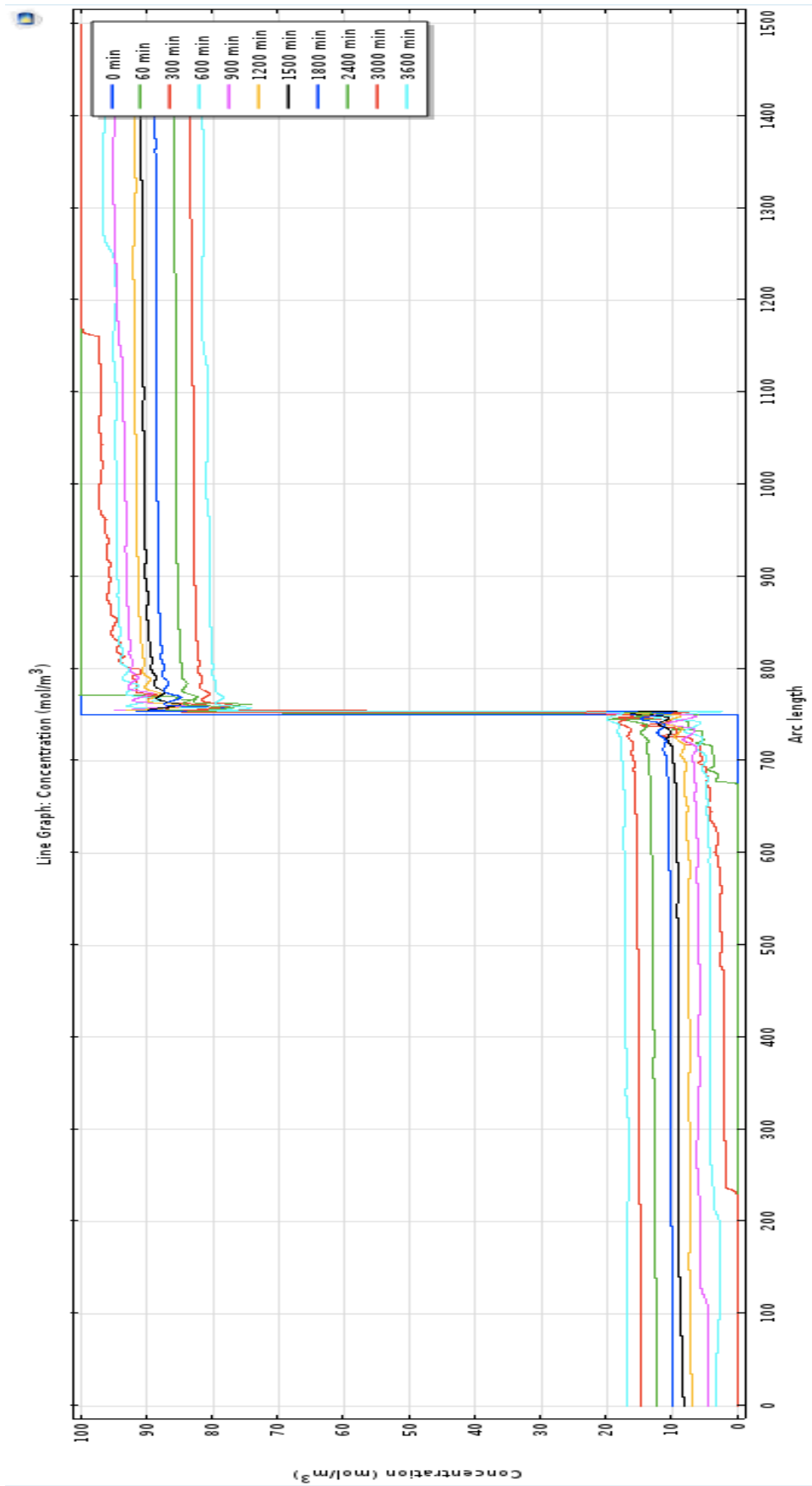


Figure 76: Line Graph Concentration Well Size Difference 1 after 0, 1, 5, 10, 15, 20, 25, 30, 40, 50 and 60 minutes

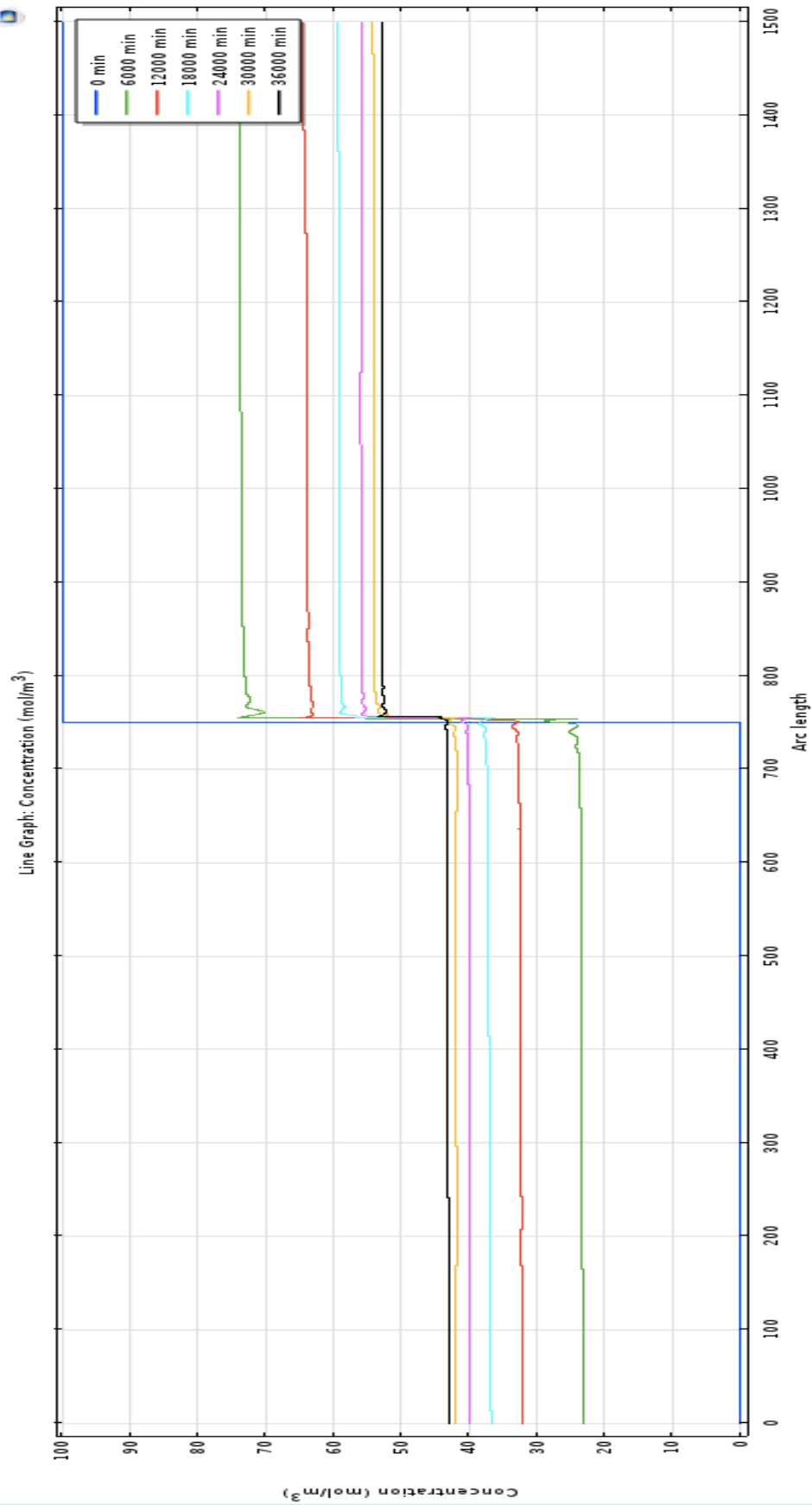


Figure 77: Line Graph Concentration Well Size Difference 1 after 0, 100, 200, 300, 400, 500 and 600 minutes

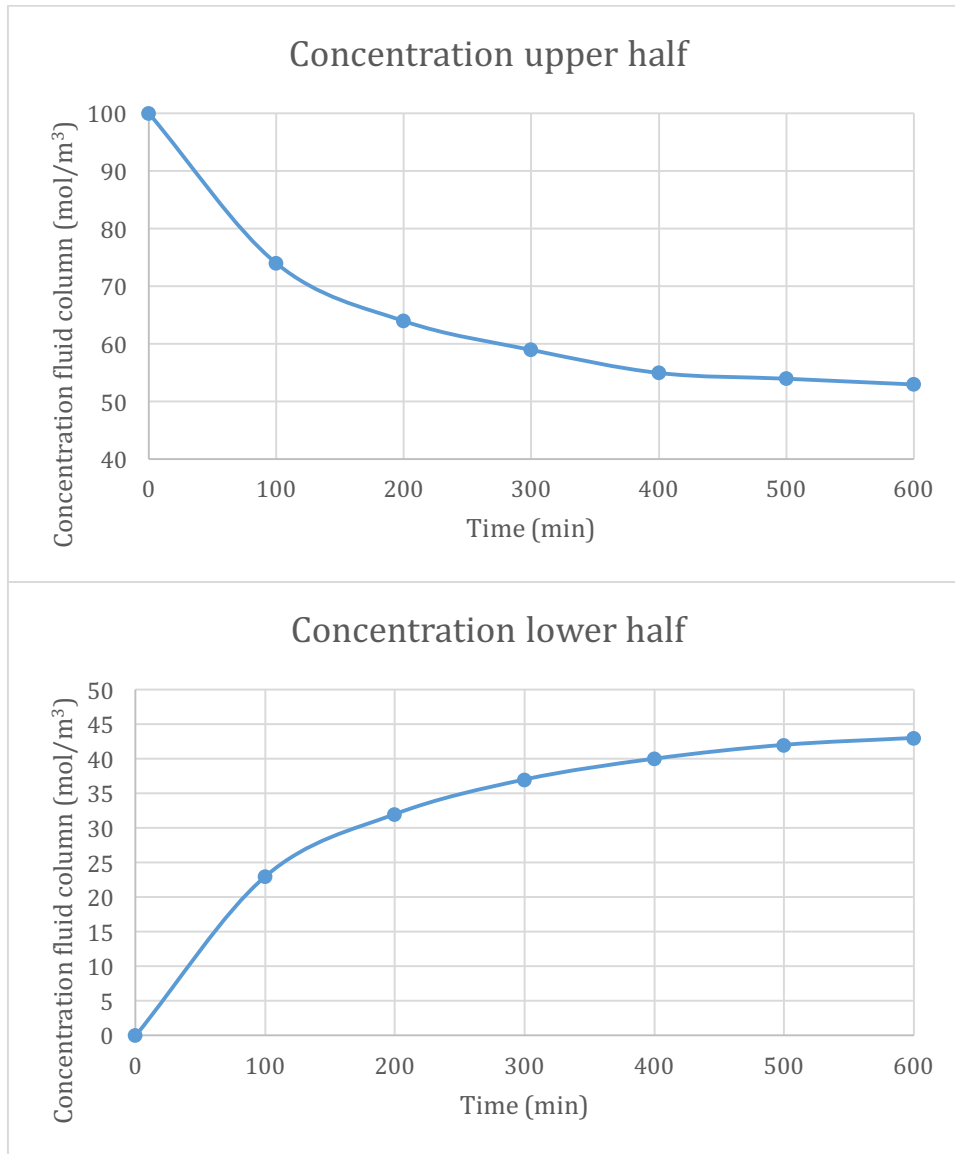


Figure 78: Concentration fluid column, Well Size Difference case 1

A line graph of the concentration for the well size difference case 1 after 1 and 10 hours is presented in figure 76 and 77, respectively. Figure 78 presents two plots showing the development of the concentration of the fluid column. During 1 hour the concentration of the heavy fluid decreases from 100 to approximately 81 and the concentration of the light fluid increases from 0 to 17. For the time steps 1 and 5 minutes it is possible to define the length of a mixed fluid zone. After 1 minute the mixed zone is located between a height of 680 and 780 meters and has a length of 100 meters. After 5 minutes the mixed zone has grown to a length of 940 meters and is located between a height of 230 and 1170 meters. The concentrations are slightly varying around the interface.

During 10 hours the concentration of the heavy fluid decreases to 53 and the concentration of the light fluid increases to 43. The change in concentrations is largest in during the first 100 minutes. During this time period the concentration of the heavy fluid decreases to 74 and the concentration of the light fluid increases to 23. This is more than half of the total concentration difference for both fluids. Since the interface moved upwards the fluid column, it makes sense that the concentration of the heavy fluid has the highest variation.

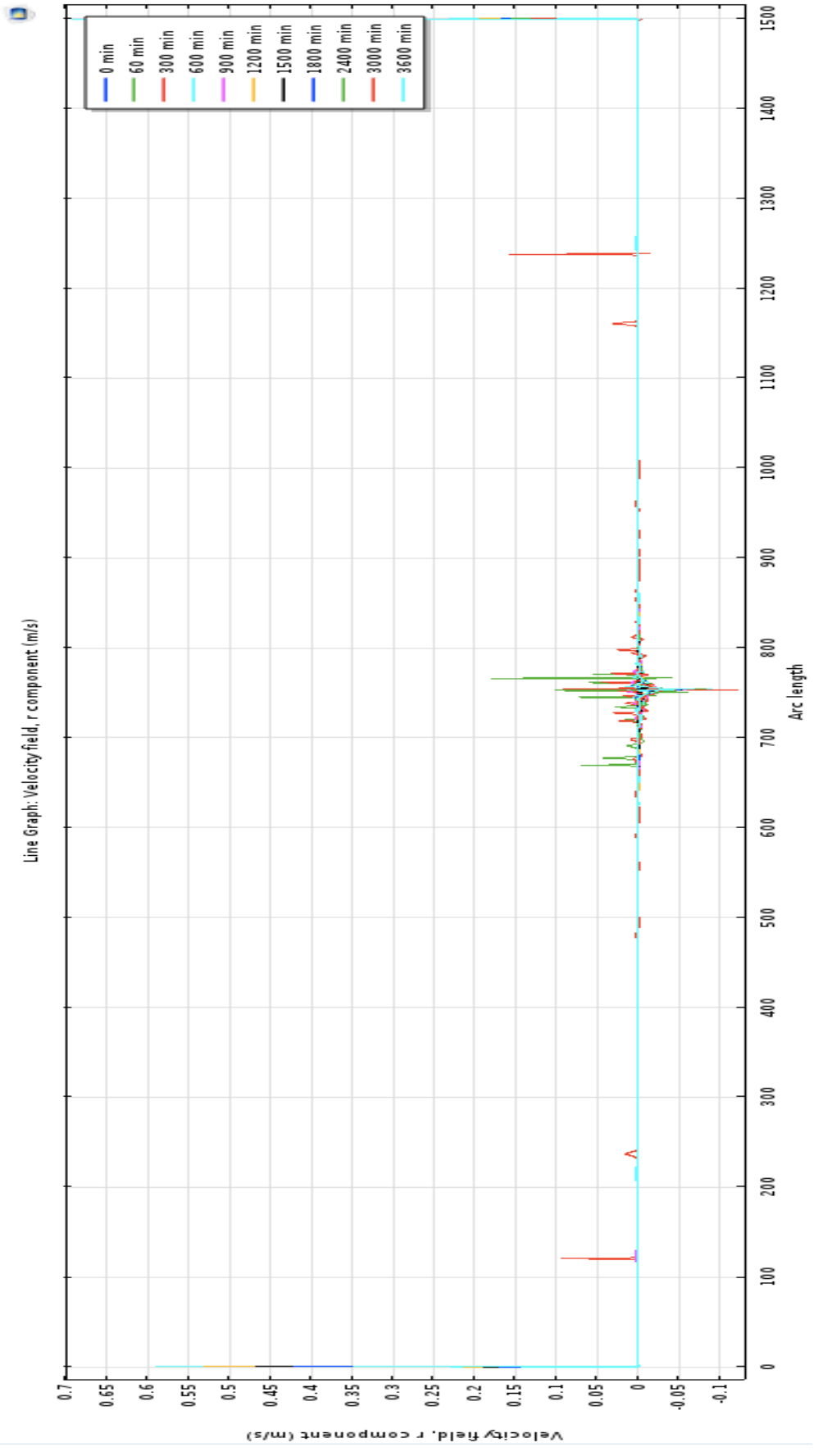


Figure 79: Line Graph Velocity field Well Size Difference 1 after 0, 1, 5, 10, 15, 20, 25, 30, 40, 50 and 60 minutes

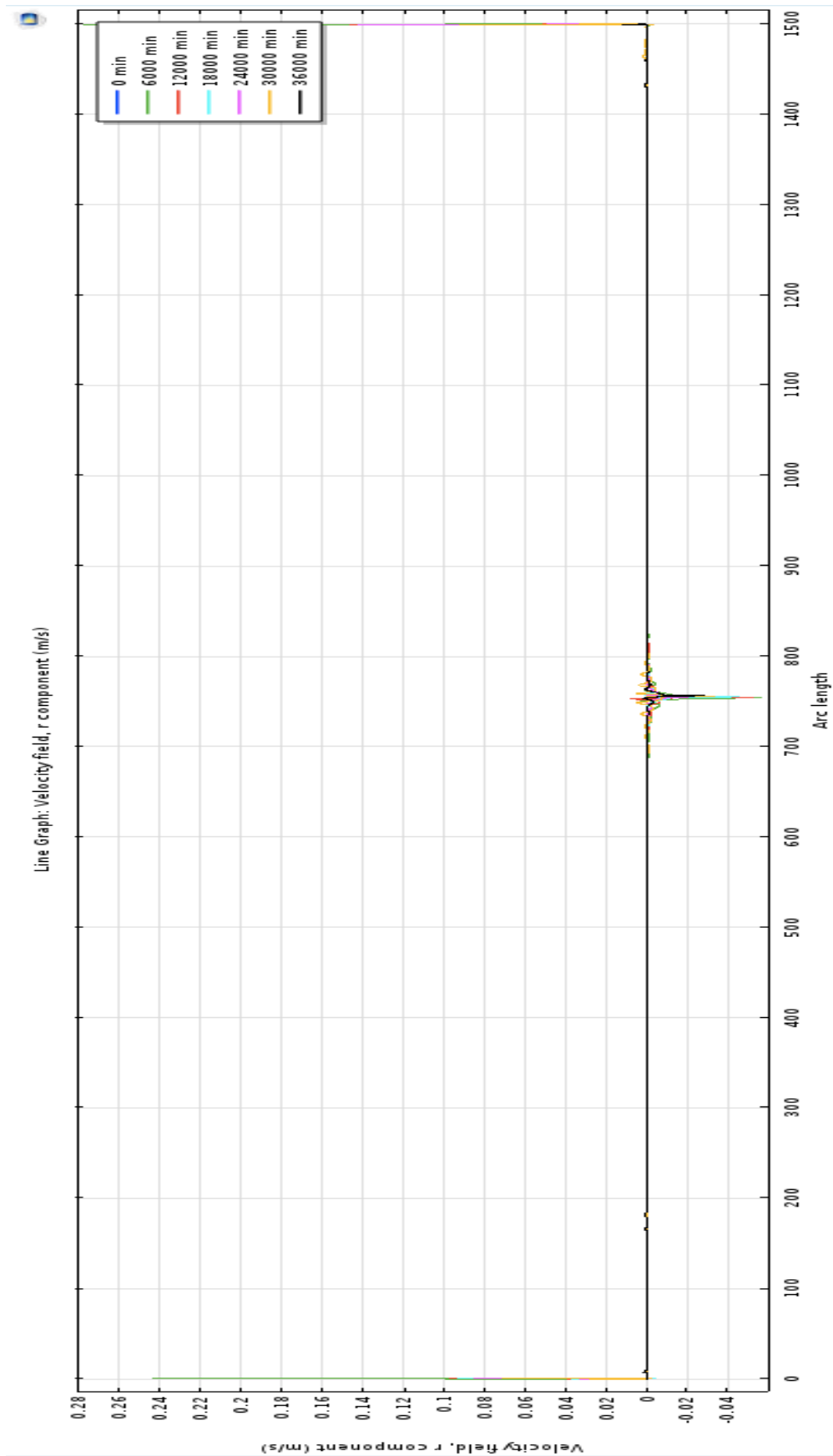


Figure 80: Line Graph Velocity field Well Size Difference 1 after 0, 100, 200, 300, 400, 500 and 600 minutes

Figure 79 and 80 show line graphs of the velocity field for the well size difference case 1, for the time periods 1 hour and 10 hours, respectively. During the first hour there is a lot of velocity variations around the interface. The highest velocity in this area is measured to 0.18 m/s in the downward direction. The highest velocity in the upward direction around the interface was found to be 0.12 m/s. The maximum velocity observed during the first hour is located at the top of the fluid column and is measured to almost 0.70 m/s in the downward direction. The maximum velocity observed at the bottom of the pipe had a value of almost 0.60 m/s.

The highest velocity observed during 10 hours is located on the top of the fluid column with a velocity of almost 0.28 m/s in the downward direction. The maximum velocity located on the bottom of the fluid column was measured to approximately 0.24 m/s in the downward direction. At the interface it was measured a maximum velocity of roughly 0.056 m/s in the upward direction.

When studying the close-up screenshots of the velocity field at the interface and on the top and on the bottom of the fluid column (please refer to figures A-85 – A-90 in Appendix A), it was observed that the velocities are highest after the first 100 minutes and then decreasing.

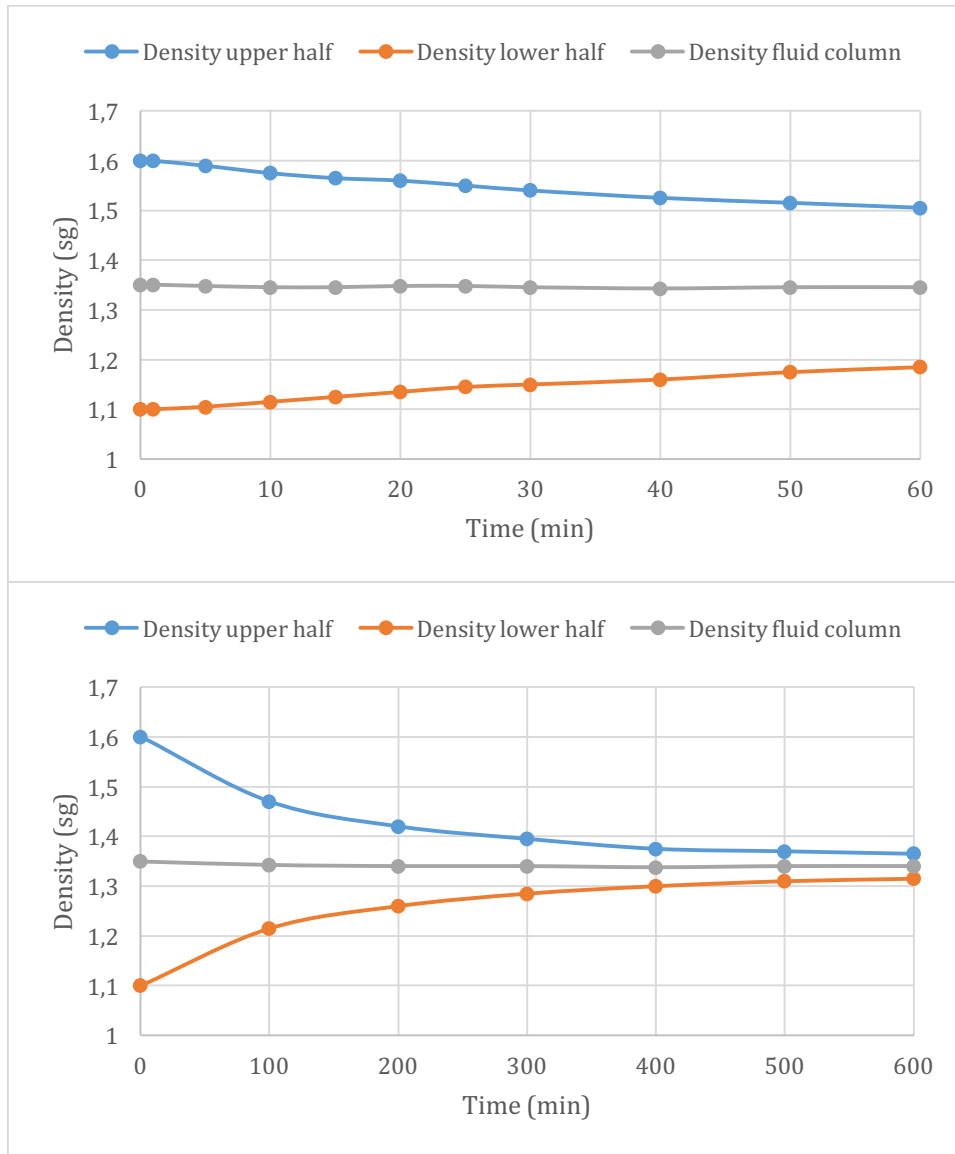


Figure 81: Density fluid column vs. time, Well Size Difference 1

Figure 81 shows a presentation of the density development in time of the fluid column for well size difference case 1. The upper plot presents the density development during the first hour and the lower plot after 10 hours of simulation. During 1 hour the density has an approximately linear development. The density of the heavy fluid in the upper part of the fluid column has decreased to 1.51 sg and the density of the light fluid in the lower part of the fluid column has increased to 1.19. Both fluids have a change in density of 0.09 sg. The density difference between the fluids has decreased from 0.50 sg to 0.32 sg.

During 10 hours the density shows a more logarithm/inverse exponential development. After 10 hours the density of the heavy fluid has decreased to 1.37 sg and the density of the light fluid has increased to 1.32 sg. This gives a density difference between the fluids of only 0.05 sg. The average density of the entire fluid column is approximately 1.35 sg during the first hour. After 100 minutes the average density decreases to approximately 1.34 sg and remains 1.34 sg during the rest of the simulation period.

Well Size Difference 2

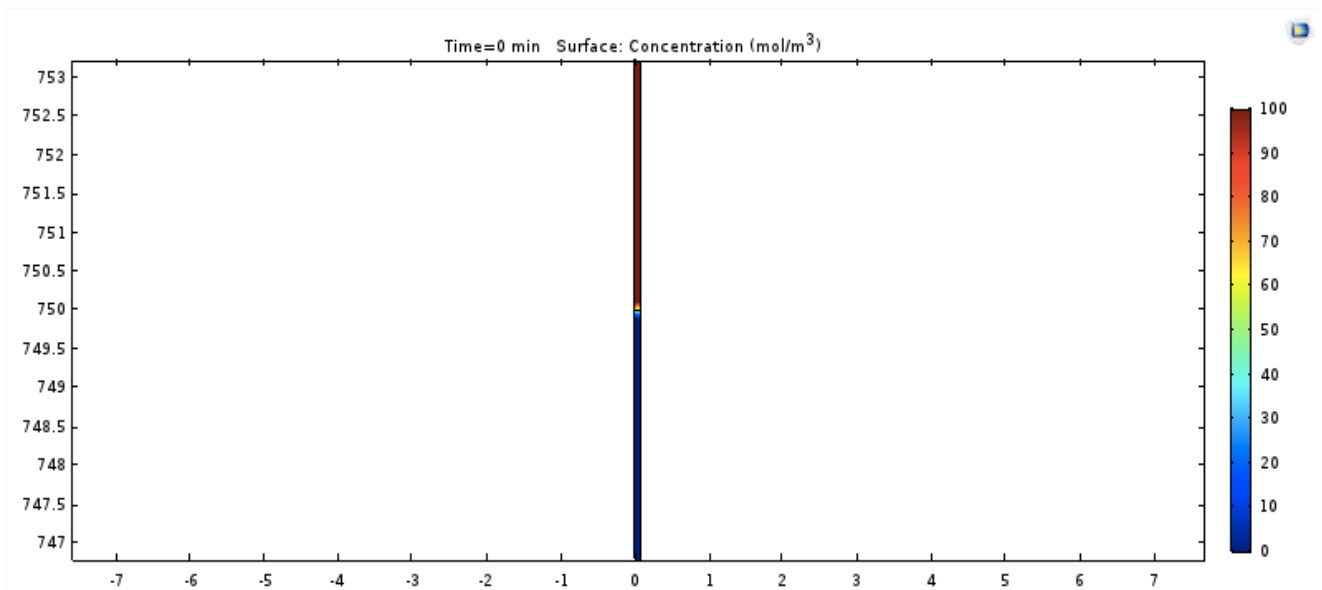


Figure 82: Surface Concentration Well Size Different 2 at start

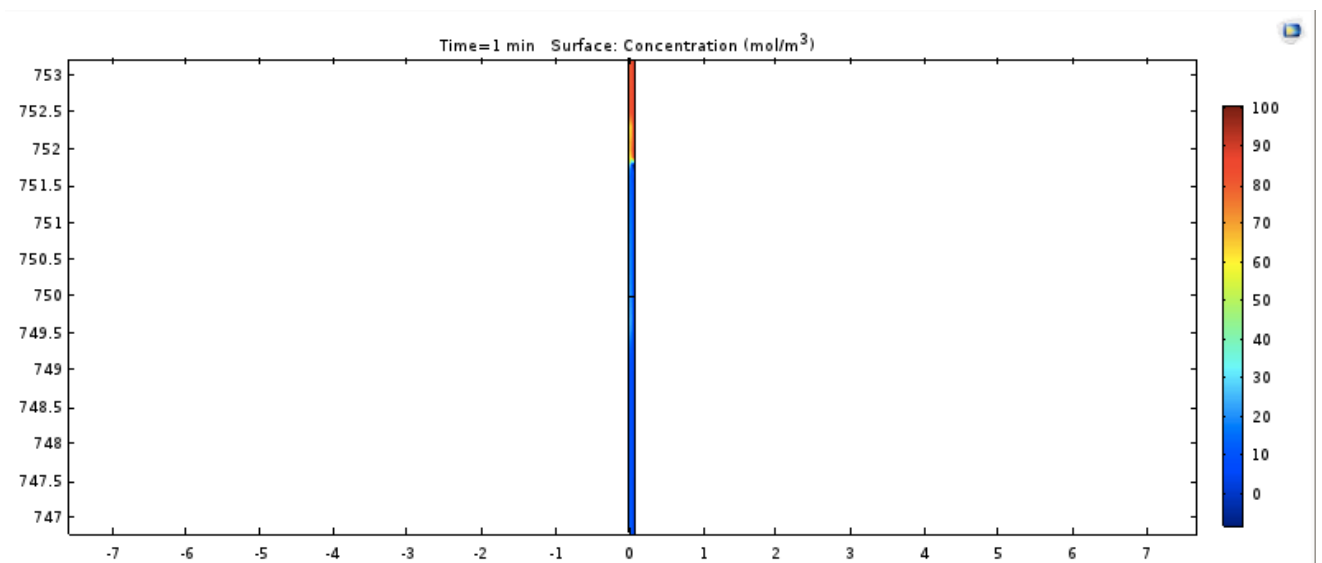


Figure 83: Surface Concentration Well Size Different 2 after 1 minute

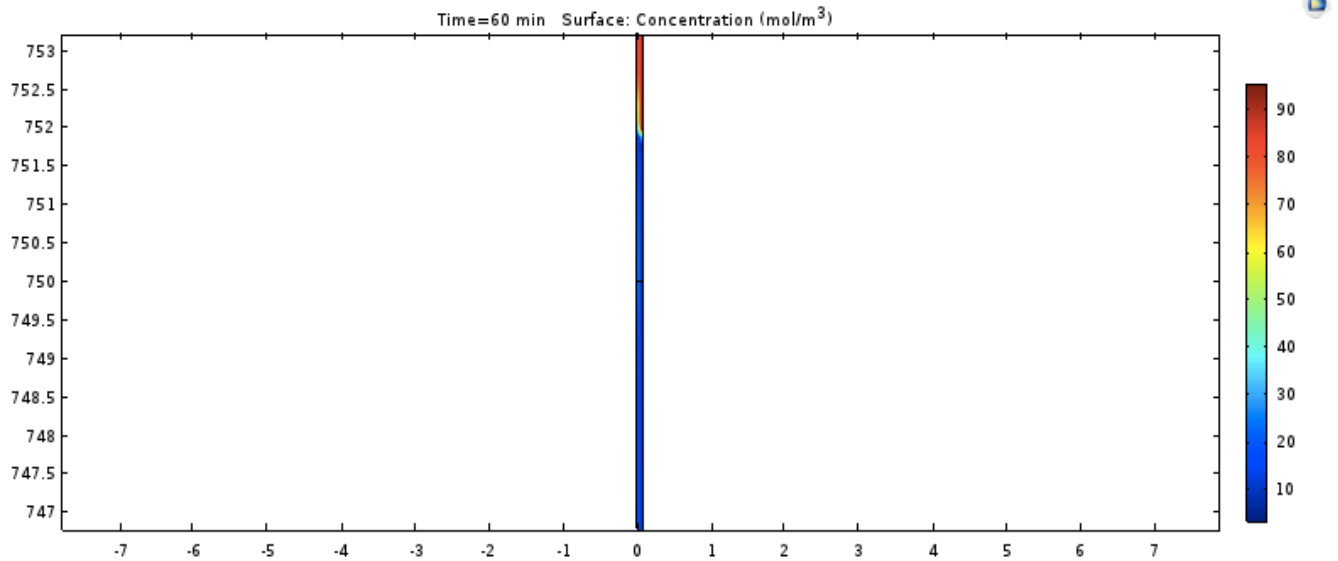


Figure 84: Surface Concentration Well Size Different 2 after 1 hour

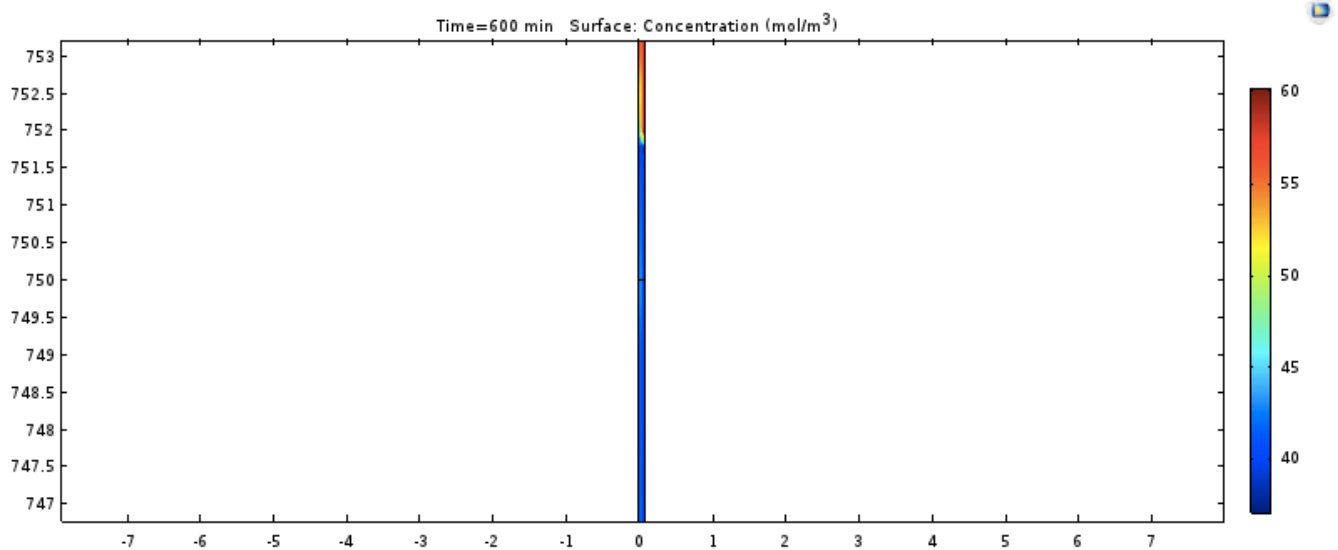


Figure 85: Surface Concentration Well Size Different 2 after 10 hours

At start of the simulation the interface is located in the middle of the fluid column at a height of 750 meters. The concentration of the heavy fluid in the upper part of the fluid is equal to 100 and the light fluid in the lower part of the fluid column has a concentration of 0. After 1 minute the interface has moved upwards in the fluid column and was located at a height of approximately 752 meters. As can be observed by the colours of the fluid column around the interface, the concentration of the heavy fluid has decreased while the concentration of the light fluid has increased.

After 1 hour the interface is still at a height of approximately 752 meters. The colours of the fluid column are practically identical to the colours after 1 minute. The values of the colours are different, though, and imply a lower concentration of the heavy fluid and a higher concentration of the light fluid. The same principle applies to the fluid column after 10 hours. The values of the colour chart have decreased and so has the concentration of the heavy fluid. The concentration of the light fluid has increased. The maximum concentration of the heavy fluid is equal to 60 and the minimum concentration of the light fluid is equal to approximately 38.

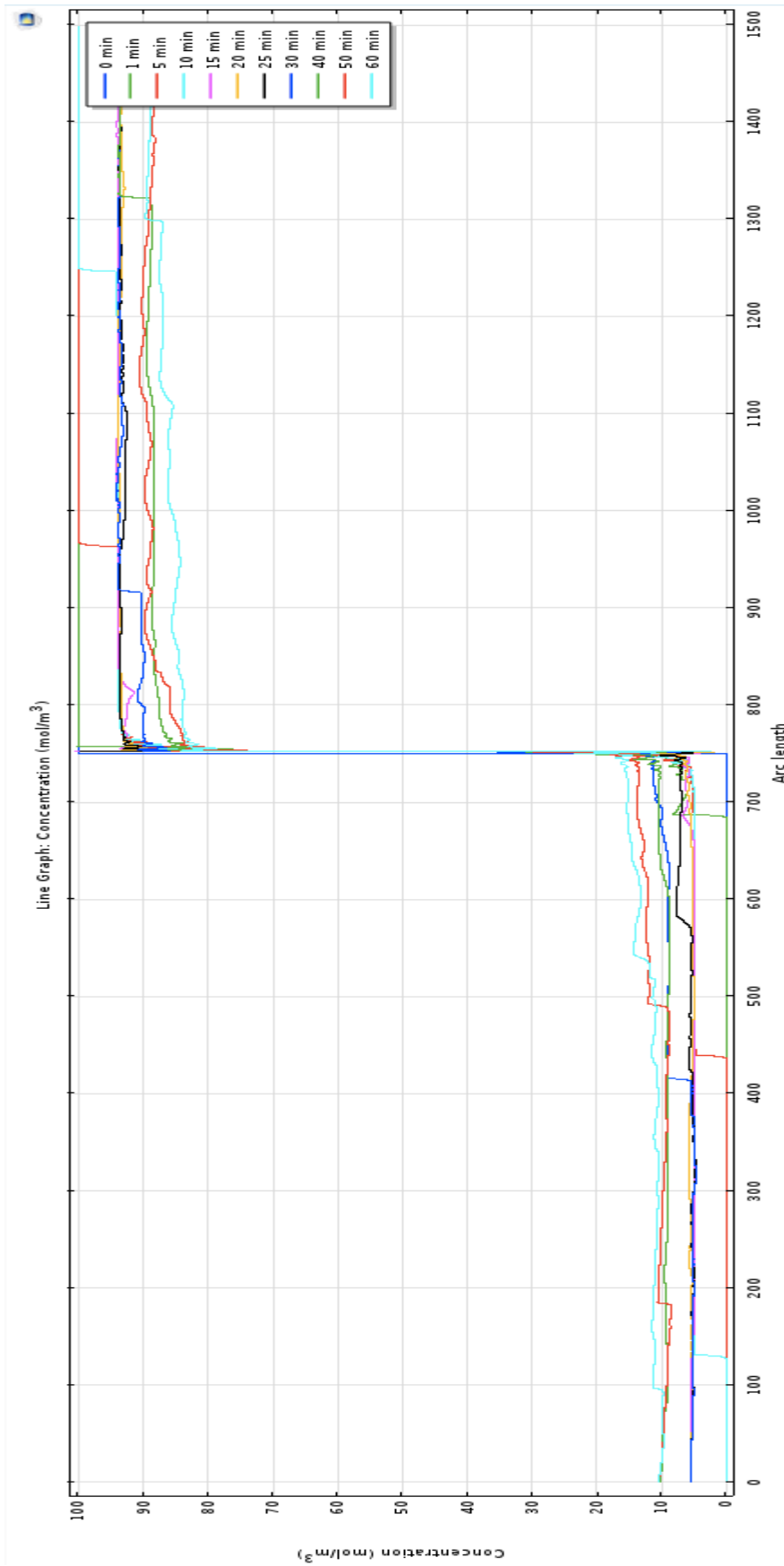


Figure 86: Line Graph Concentration Well Size Difference 2 after 0, 1, 5, 10, 15, 20, 25, 30, 40, 50 and 60 minutes

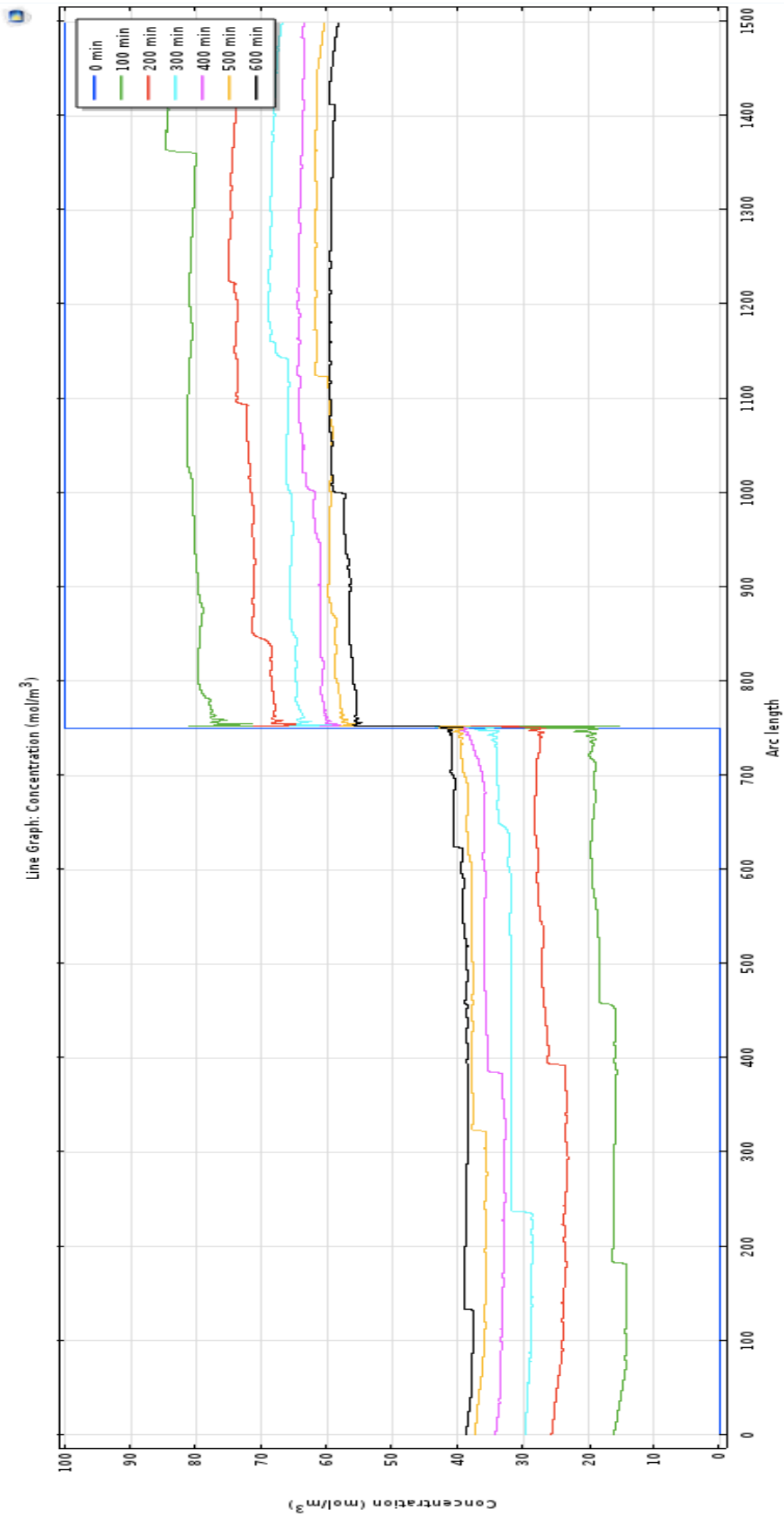


Figure 87: Line Graph Concentration Well Size Difference 2 after 0, 100, 200, 300, 400, 500 and 600 minutes

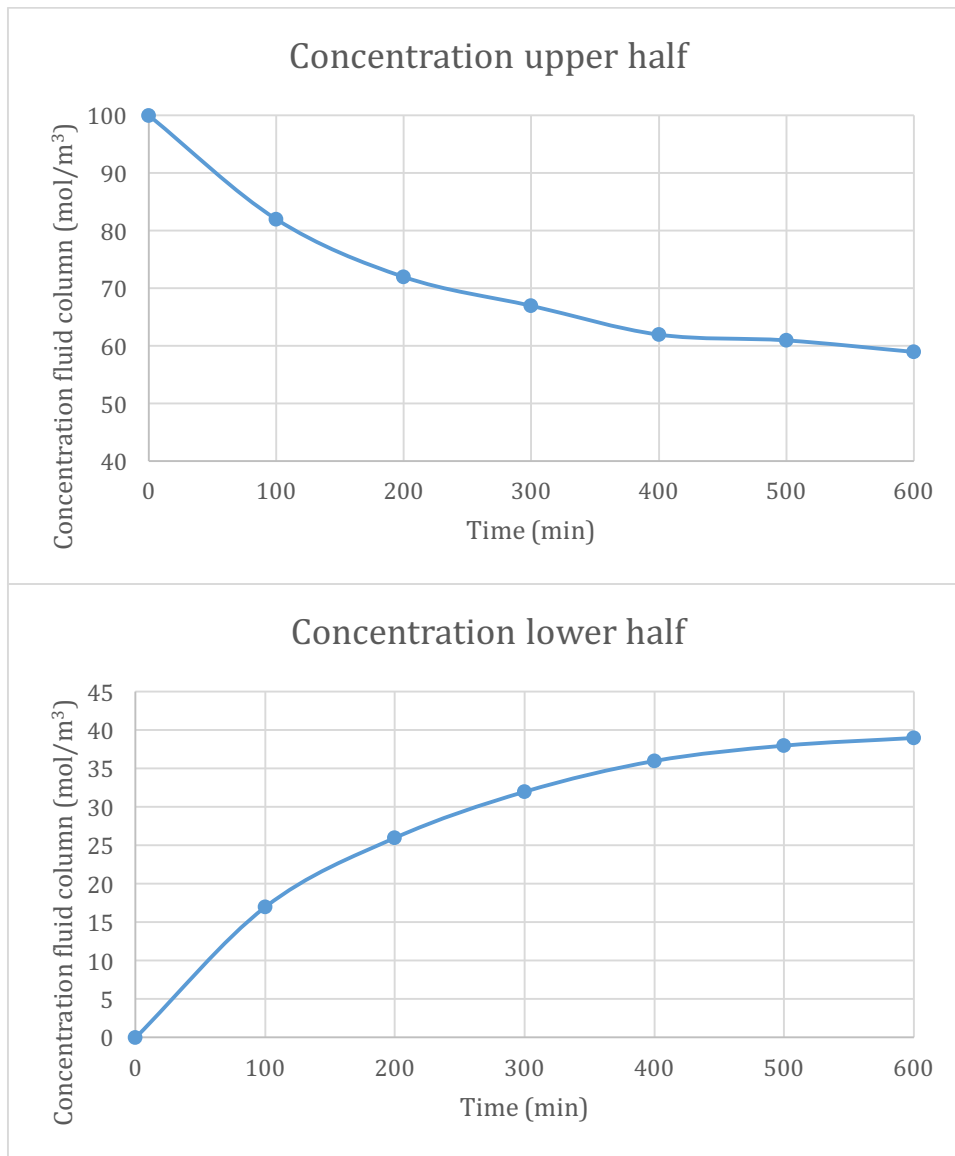


Figure 88: Concentration fluid column, Well Size Difference case 2

Figure 86 and 87 present line graphs of the concentrations for the well size difference case 2 after 1 and 10 hours, respectively. Figure 88 presents two plots showing the development of the concentration of the fluid column. By using figure 86 it is possible to define the length of a mixed zone between the fluids for the first 10 minutes. After 1 minute the mixed zone is located between 680 and 760 meters and has a length of 80 meters. After 5 minutes the mixed zone has a length of 520 meters and is located between 440 and 960 meters, and after 10 minutes the mixed zone is located between 130 and 1250 meters and has a length of 1120 meters. During 1 hour the concentration of the heavy fluid has decreased to approximately 87 while the concentration of the light fluid has increased to roughly 12. Both fluids have almost equal variation in

concentration after 1 hour. The difference between the concentration of the fluids after 1 hour has decreased from 100 to 75.

During 10 hours the concentration of the heavy fluid has decreased to approximately 59 which gives a concentration difference of 41. The concentration of the light fluid has decreased to approximately 40 which implies a concentration variation of 40. The difference in concentration for the fluids is equal to 9. The variation in concentration is highest during the first 100 minutes and then it decreases as time escalates.

Due to the variation of the line graphs of the concentration through the fluid column, it may be difficult to read the values for the various time steps.

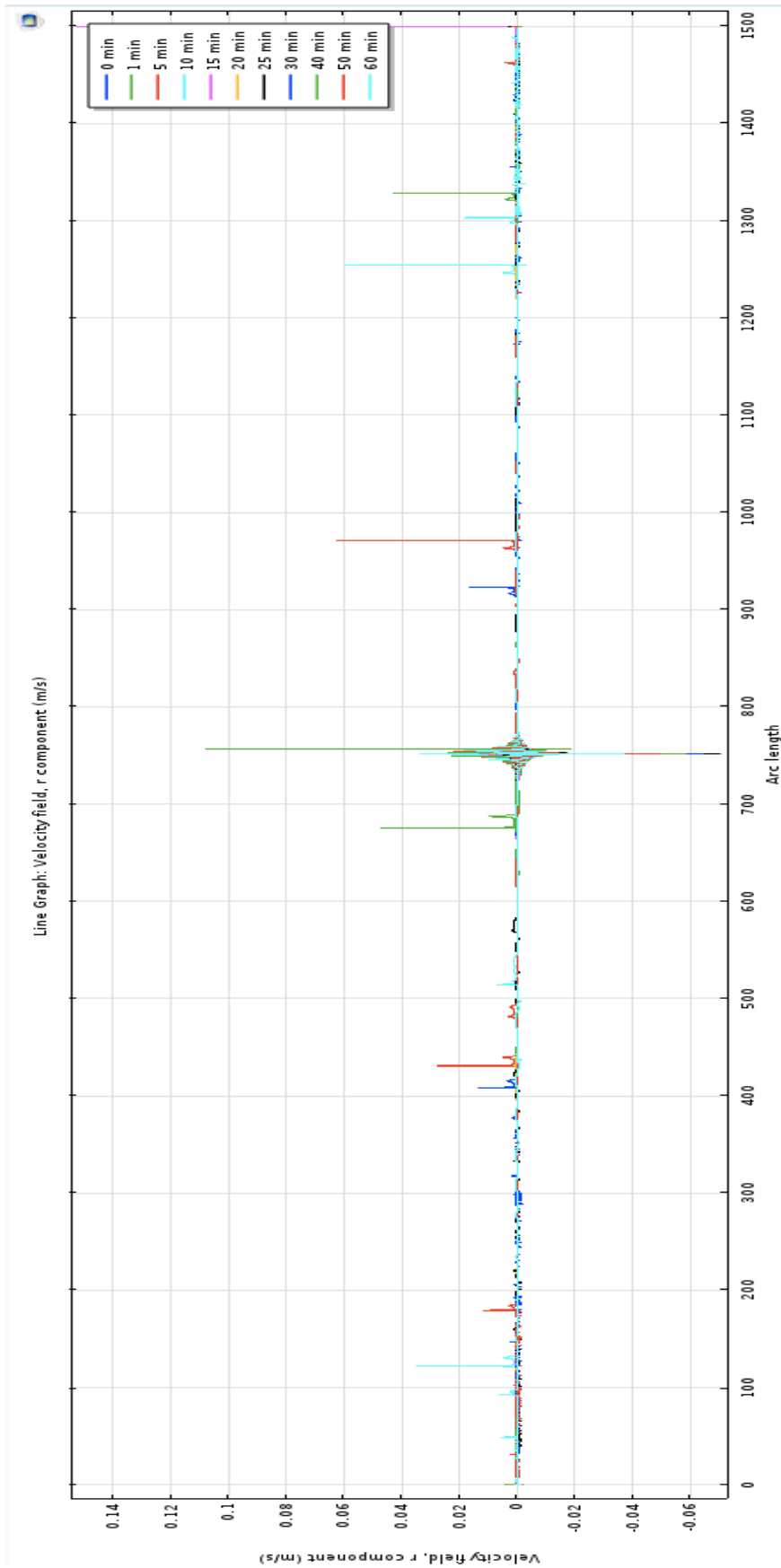


Figure 89: Line Graph Velocity field Well Size Difference 2 after 0, 1, 5, 10, 15, 20, 25, 30, 40, 50 and 60 minutes

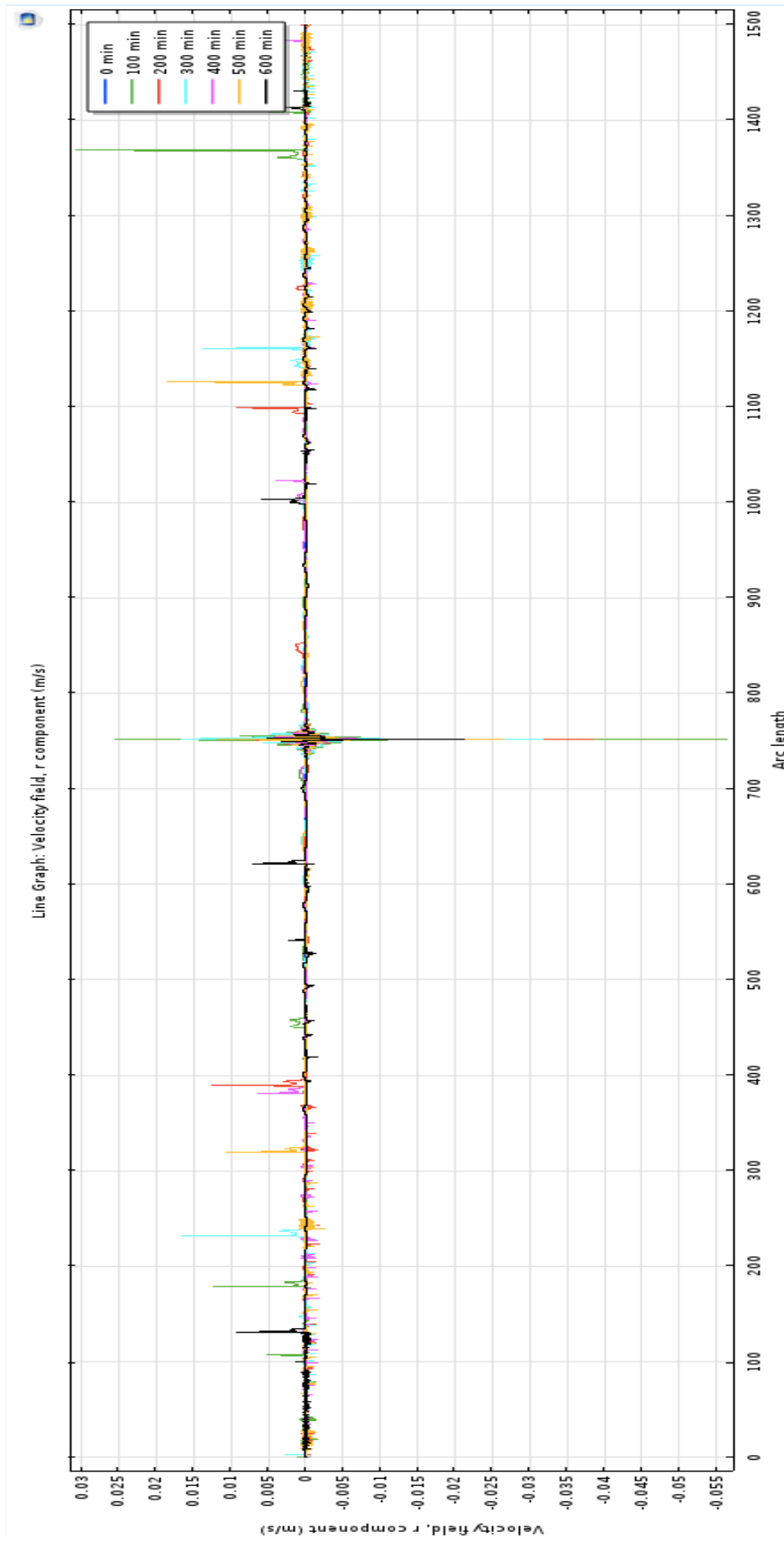


Figure 90: Line Graph Velocity field Well Size Difference 2 after 0, 100, 200, 300, 400, 500 and 600 minutes

Line graphs of the velocity field for well size difference case 2 are presented in Figure 89 and 90 after respectively 1 hour and 10 hours. The maximum velocity measured after 1 hour is located on the top of the fluid column and has a value of roughly 0.152 m/s in the downward direction. The highest velocity measured around the interface is equal to approximately 0.109 m/s in the downward direction. The maximum velocity around the interface in the upward direction was measured to roughly 0.07 m/s. On the bottom of the fluid column the total velocity of the fluid is approximately equal to zero.

The maximum velocity observed during 10 hours is located at the interface and was measured to approximately 0.057 m/s in the upward direction. The maximum velocity in the downward direction at the interface was found to be approximately 0.025 m/s. The highest velocity in the upper part of the fluid column was measured to approximately 0.031 m/s in the downward direction and was located at a height of around 1370 meters. The maximum velocity in the lower part of the fluid column was located at a height of approximately 230 meters and had a value of roughly 0.0165 m/s in the downward direction.

On both the top and the bottom of the fluid column the total velocity is practically equal to zero through the simulation period of 10 hours. During the same time period there are a lot of velocity variations through the entire fluid column.

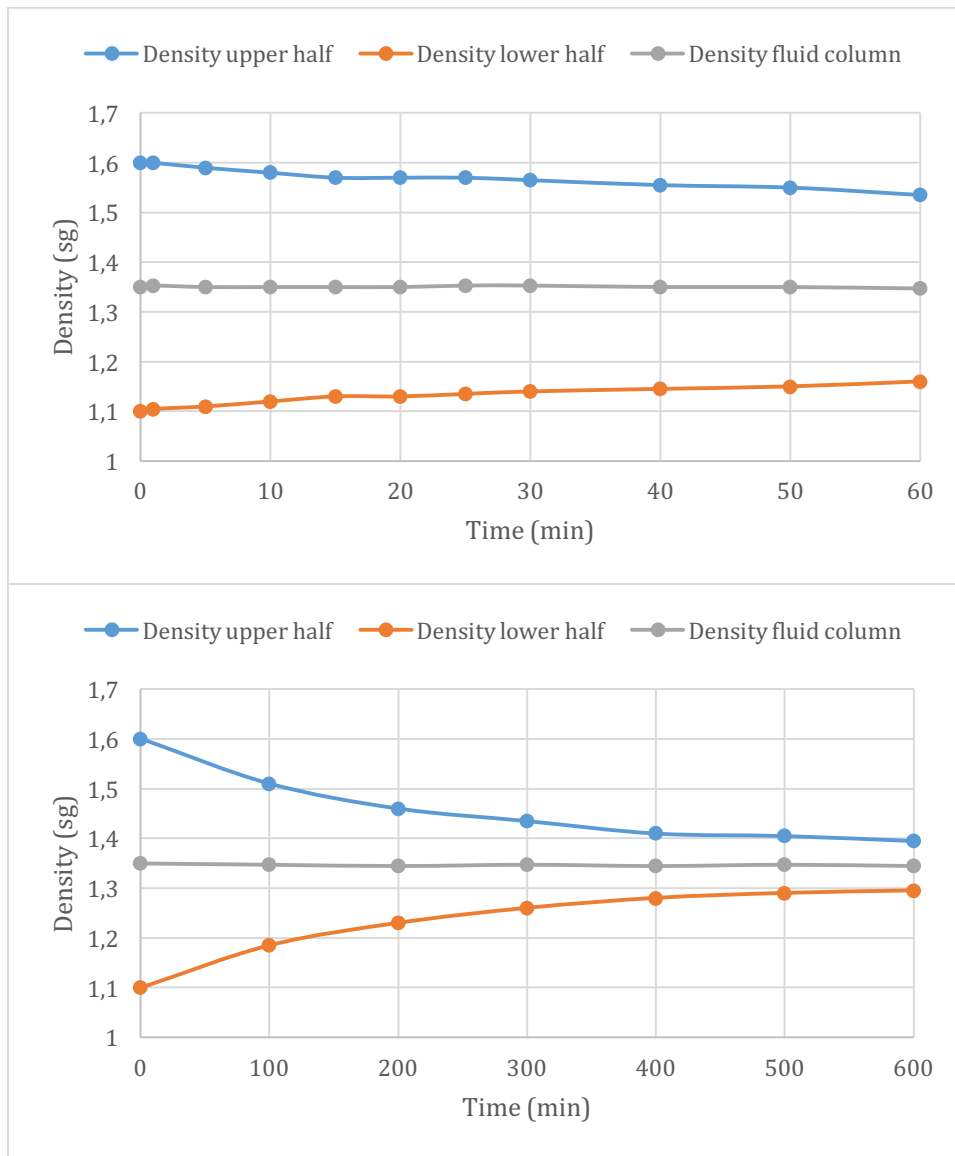


Figure 91: Density fluid column vs. time, Well Size Difference 2

Figure 91 presents two plots showing the density development in time. The upper plot shows the development during 1 hour and the lower plot shows the development during 10 hours. After 1 hour the density of the heavy fluid in the upper part of the fluid column has decreased to 1.54 sg and the density of the light fluid has increased to 1.16, constituting a density difference of 0.06 sg for both fluids. The density difference between the fluids after 1 hour is equal to 0.38 sg.

During 10 hours the density of the heavy fluid decreases to 1.40 sg and the density of the light fluid increases to 1.30, creating a density difference between the fluids of 0.10 sg after 10 hours. The density difference for the heavy fluid equals the density difference

for the light fluid and is equal to 0.20 sg. The average density of the fluid column is measured to approximately 1.35 sg throughout the entire simulation period of 10 hours.

5 EXPERIMENTAL WORK

The experimental work aims to demonstrate the HOL principle in vertical pipes. The experiments were executed conforming to the HSE agreements of the University of Stavanger and the Department of Petroleum Engineering.

5.1 General Experimental Setup

This section describes fluid properties, experimental setup, the execution of the experiments, and presents the results. All the pipes used in the experiments are of the same length of approximately 2 meters, but the outer pipe to inner pipe ratio is different. The outer pipe was strapped to a metal pole using strips made of plastic or metal to keep the pipe vertical and preventing it from moving or falling. Figure 92 presents the general experimental setup. The outer pipe is filled with light fluid in the lower half of the pipe and heavy fluid in the upper half.

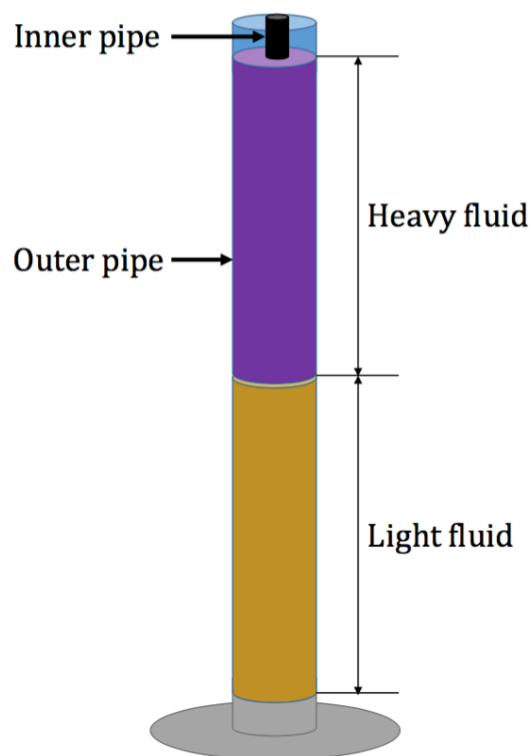


Figure 92: General experimental setup

The length of the mixing zone was measured by observation and visual interpretation. The mixing zone was defined where there was a clear difference between the heavy and the light fluid and channels of fluids were also defined as part of the mixing zone.

There are two types of drilling fluids: water based muds (WBMs) and oil based muds (OBMs). The fluids used in the experiments were simple WBMs and OBMs. WBMs consist of typical water as the liquid phase, bentonite, barite for increasing density and polymers for increasing viscosity and gel properties. Good gel properties are important for good hole cleaning and stability of wellbore. OBMs consist normally of a type of oil as the liquid phase, and other additives for decreasing density and viscosity. OBMs do not possess the same gel properties as WBMs.

Both newly formulated and commercial oil/water based fluids were used for the experimental investigation. A total of eight experiments are presented below. In some of the experiments there are used an inner, smaller pipe in addition to a drill at the top for rotating the inner pipe. This is for simulating a drilling scenario where the inner pipe represents the drill string and the outer pipe represents the wellbore.

For filling the pipe with the light fluid there was used a funnel attached to a smaller pipe which was placed inside the outer pipe. The smaller pipe had a length of approximately half of the length of the outer pipe. This was done to prevent the light fluid from sticking to the inner pipe wall of the upper half of the pipe. If this situation occurs, it would make it difficult to distinguish between the heavy and the light fluid and thus determine the length of the mixing zone. The heavy fluid was poured into the outer pipe through the funnel, here the small pipe had a length of approximately 10 cm.

The density of the fluids was measured by weighing 10 ml of fluid and dividing the weight on the volume. A syringe was used for measuring 10 ml of fluid and a digital scale was used for weighing the fluid. The equipment is shown in figure 93 and 94.



Figure 93: Syringe for measuring 10 ml of fluid



Figure 94: Digital scale for weighing fluid

In addition to the density, there were also measured the rheology properties of the fluids. Plastic viscosity (PV), yield strength (YS) and low shear yield stress (LSYS) were calculated from the rheology measurements. PV and YS were calculated respectively by Equation 3.11 and Equation 3.12 from section 3.9.1. LSYS was calculated by

$$YS = 2R_3 - R_6 \quad (5.1)$$

where R_3 is the reading at 3 RPM and R_6 is the reading at 6 RPM from the viscometer.

Table 5 presents an overview of most of the parameters in the experiments. $\Delta\rho$ represents the density difference and $\Delta\mu$ represents the plastic viscosity (PV) difference between the heavy and light fluid.

Table 5: Parameters in the experiments

Exp. #	Inner diameter outer pipe	Outer diameter inner pipe	Cross sectional area of fluid column	Time	RPM	WBM/OBM	$\Delta\rho$	$\Delta\mu$
1	11.6 mm	-	105.7 mm ²	40 min	-	WBM	0.32 sg	-
2	10.0 mm	-	78.5 mm ²	24 hours	-	WBM	0.19 sg	11 cP
3	31.1 mm	19.6 mm	457.9 mm ²	2 hours, 15 min	86	WBM	0.39 sg	11 cP
4	10.0 mm	3.0 mm	71.5 mm ²	2 hours	60	WBM	0.48 sg	0 cP
5	31.1 mm	19.6 mm	457.9 mm ²	4 hours	60-70	WBM	0.50 sg	7 cP
6	10.0 mm	3.0 mm	71.5 mm ²	4.5 hours	120	OBM	0.48 sg	63 cP
7	10.0 mm	3.0 mm	71.5 mm ²	3 hours	120	OBM	0.44 sg	-
8	10.0 mm	3.0 mm	71.5 mm ²	1 hour, 5 min	120	OBM	0.31 sg	-

5.2 Experiment #1

The purpose of this experiment is to demonstrate the HOL principle using two water based muds with different densities. There was used an outer pipe and no inner pipe.

5.2.1 Description of Fluids

The heavy fluid and the light fluid in the first experiment had densities of respectively 1.34 sg and 1.02 sg. The heavy fluid had was the same as one of the fluids used in the

Master Thesis of Eirik Vandvik [3] and was made of water and syrup of which the syrup provides a high viscosity. The light fluid contains mostly water. Both the heavy and the light fluid were prepared the same day as the execution of the experiment. For distinguishing the fluids there was added some dark colour to the heavy fluid. The properties of the fluids are presented in figure 95 and table 6.

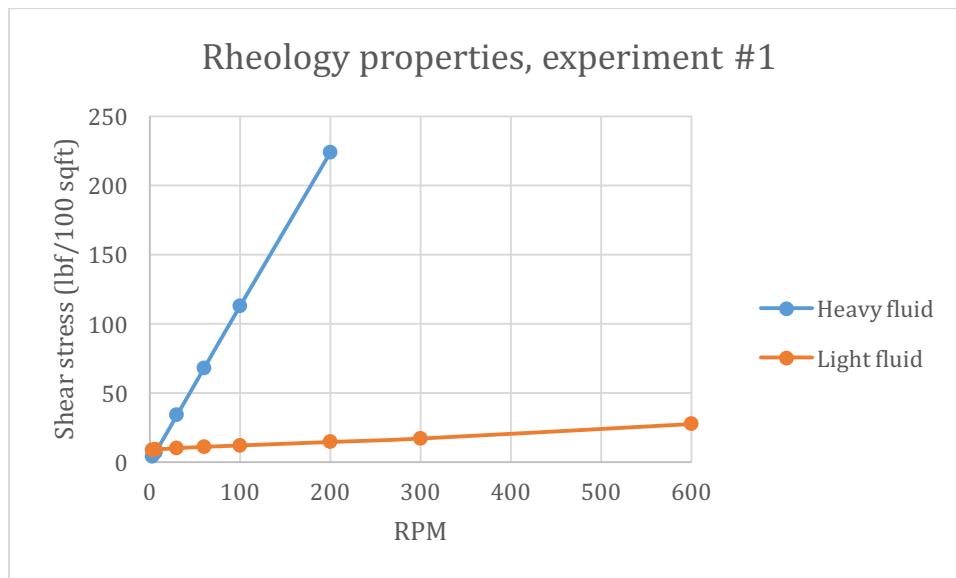


Figure 95: Rheology properties, experiment #1

Table 6: Fluid parameters, experiment #1

Fluid parameters	Heavy fluid	Light fluid
Density (sg)	1.34	1.02
PV (cP)	-	10.5
YS (lbf/100sqft)	-	6.5
LSYS (lbf/100sqft)	1	8

As can be seen from the table above, the plastic viscosity and the yield strength of the heavy fluid cannot be found from these values.

5.2.2 Description of Experiment

The pipe used in this experiment had an inner diameter of 11.6 mm. There was not used an inner pipe in this experiment.

First 87 cm of the pipe was filled with the light fluid and the top of the light fluid column was marked on the pipe by using a white metal strap. Then 100 cm of the length of the pipe was filled with the heavy fluid. The fluids were at rest the entire experiment and the length of the mixing zone was measured every third minute for 40 minutes.

5.2.3 Results

The fluids started mixing right after the pipe had been filled with heavy fluid. The length of the mixing zone grew gradually. After approximately 15 minutes it was observed heavy fluid accumulating and forming several clusters in the light fluid, as can be seen from the pictures in figure 97. The heavy fluid was observed at the bottom of the pipe after approximately 26-27 minutes. When time had reached 40 minutes, the length of the mixing zone was measured to approximately 116.3 cm. A sample of the fluid was taken from the interface and the density was measured to 1.297 sg. The development of the length of the mixing zone in time is presented in figure 96.

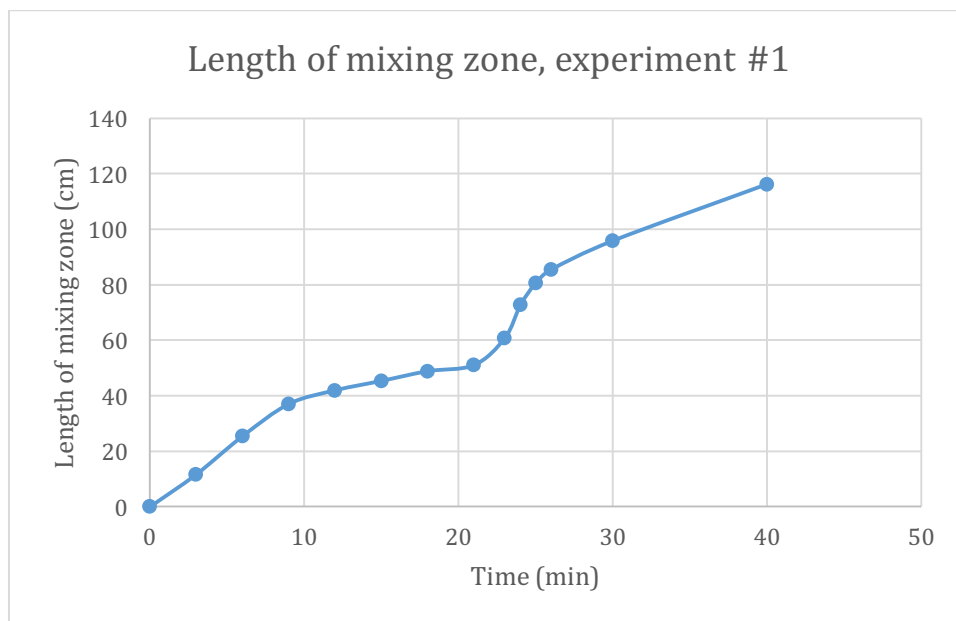


Figure 96: Length of mixing zone, experiment #1

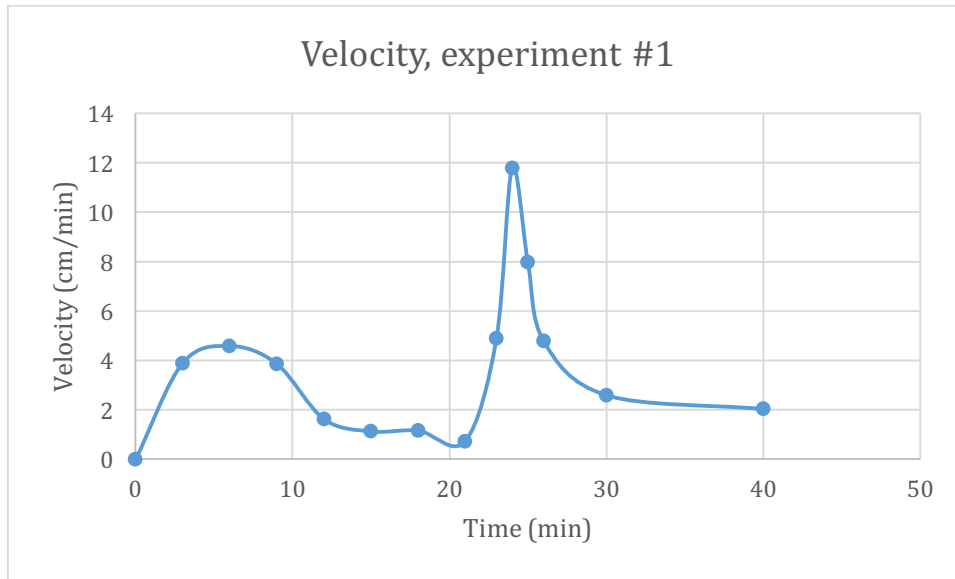


Figure 97: Speed of mixing zone, experiment #1

Figure 96 shows a smooth mixing length development between 0 and 10 minutes and between 10 and 20 minutes of the experiment period. After 20 minutes there is a step up increase in the mixing zone until 26 minutes, as shown on the figure. The dynamics of the speed of the mixing zone have been calculated and shown on figure 97. The result shows that the speed after 24 minutes in the transition zone was found to approximately 12 cm/min.

Figure 98 shows pictures of the fluids in the pipe at start, after 20 minutes and after 30 minutes.



Figure 98: Pictures experiment #1 after 0, 20 and 30 minutes

5.3 Experiment #2

For this experiment there were used two water based muds with almost equal densities as the previous experiment. The outer pipe had a slightly smaller diameter than in experiment #1 and there was not used an inner pipe.

5.3.1 Description of Fluids

For the second experiment the heavy and the light fluid had densities of respectively 1.32 sg and 1.13 sg. For making the fluids there were used water, bentonite, barite and Xanthan Gum XG. Barite is used for adding weight to the fluids and XG is used for higher viscosity. Table 7 shows the additives of the fluids.

Table 7: Additives of the fluids in experiment #2

	Water	Bentonite	Barite	XG
Light fluid	500 ml	25 g	60 g	1.1 g
Heavy fluid	500 ml	25 g	490 g	0.5 g

It is important to distinguish between the heavy fluid and the light fluid during the experiment. There were added methylene blue and a little bit of tin to the heavy fluid to change the colour. Due to these additives the viscosity increased drastically and water was added to decrease the viscosity. Originally it was attempted to make a heavy fluid with density of 1.60 sg, but because of the extra water added, the density decreased. The properties of the fluids are shown in figure 99 and table 8.

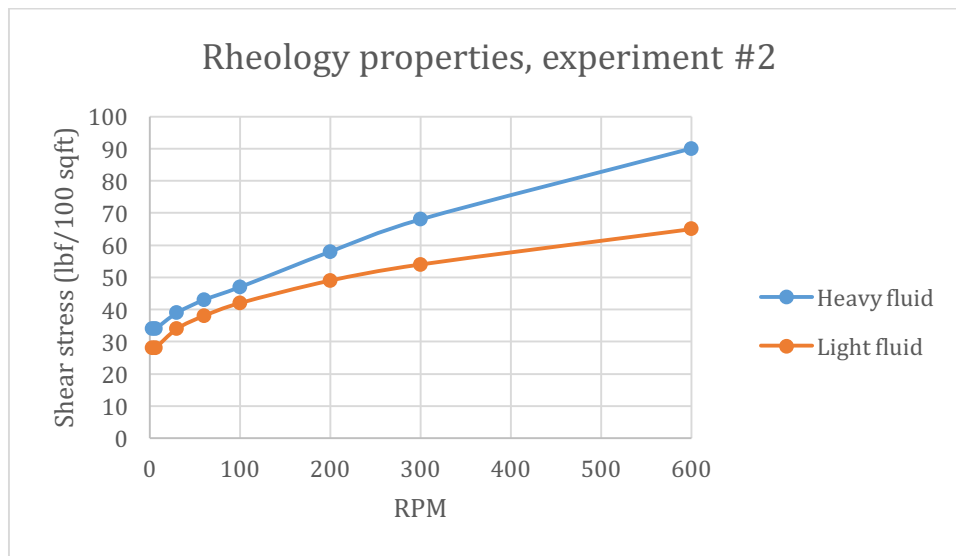


Figure 99: Rheology properties, experiment #2

Table 8: Fluid parameters, experiment #2

Fluid parameters	Heavy fluid	Light fluid
Density (sg)	1.32	1.13
PV (cP)	22	11
YS (lbf/100sqft)	46	43
LSYS (lbf/100sqft)	34	28

5.3.2 Description of Experiment

For this experiment there was used an outer pipe with inner diameter of 10.0 mm and no inner pipe.

There was also used a test glass of 100 ml with inner diameter of 25.4 mm to demonstrate the HOL principle with these fluids with a larger diameter of the pipe.

The light fluid was poured into the pipe through a funnel attached to a smaller pipe which was placed inside the 10.0 mm pipe. This was done to prevent the light fluid from sticking to the inner pipe wall which makes it difficult to distinguish between the heavy and the light fluid and determine the length of the mixing zone. The heavy fluid was then placed above the light fluid and the length of the mixing zone was measured every third minute. The fluids were static through the entire experiment.

The test glass was filled with approximately equal volumes of light fluid and heavy fluid. The mixing zone was not constantly monitored, but measured after 24 hours.

5.3.3 Results

The fluids in this experiment did not mix at all. There was no mixing zone, not even after 24 hours. Figure 100 shows the fluids at the interface. As can be seen from the pictures the fluids have not moved at all during 24 hours.

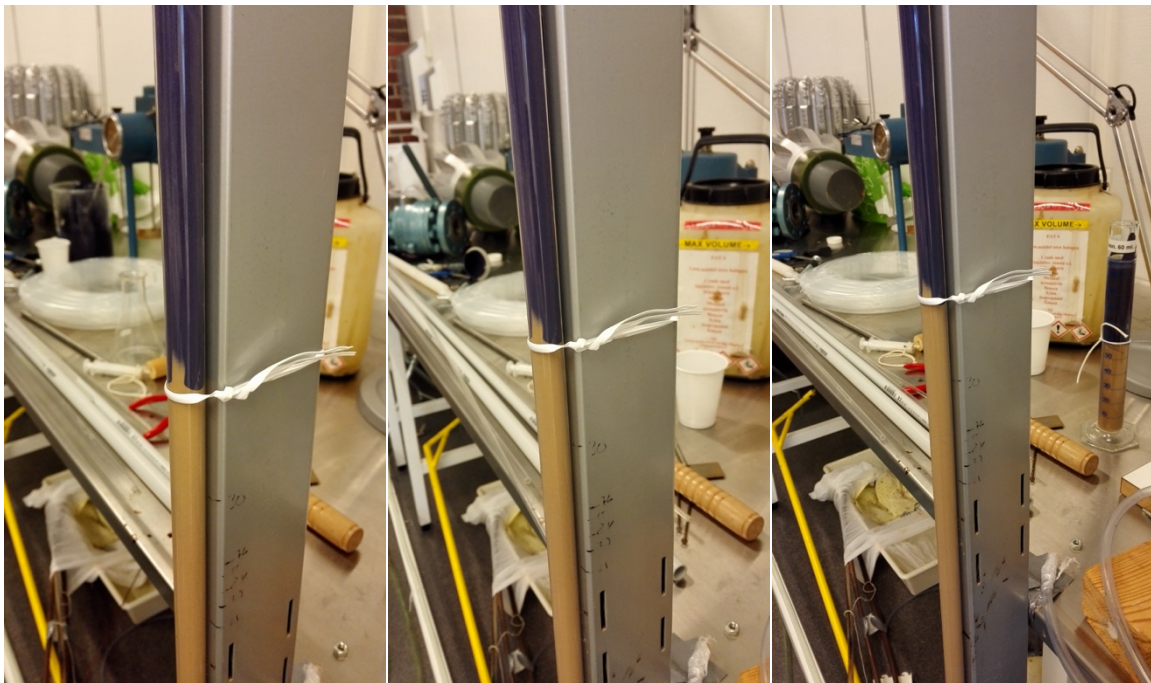


Figure 100: Pictures experiment #2 at start, after 1 hour and after 24 hours

Figure 101 shows the fluids in the test glass at start and after 24 hours. As shown on the pictures, the fluids in the test glass were stable after 24 hours and no mixing zone was observed.

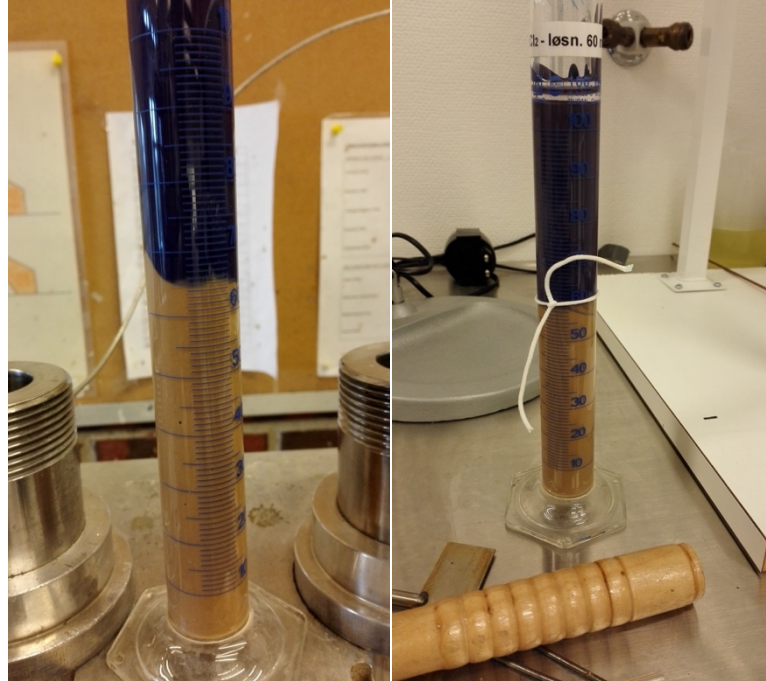


Figure 101: Experiment #2, fluids in test glass at start and after 24 hours

5.4 Experiment #3

In this experiment there were used water based muds, and both an outer and an inner pipe for demonstrating the HOL principle in vertical pipe. There was prepared twice as much fluid compared to the previous experiments due to larger diameter of the outer pipe.

5.4.1 Description of Fluids

The fluids in experiment #3 were made with the same additives as in experiment #2. The only difference was that there was used 1000 ml water in each fluid instead of 500 ml. The amount of additives was thus doubled as well. Like the previous experiment there were added some methylene blue to the heavy fluid for changing the colour. The

light fluid had density of 1.10 sg and the heavy fluid had density of 1.49 sg. The additives of the fluids are presented in table 9 below.

Table 9: Additives of the fluids in experiment #3

	Water	Bentonite	Barite	XG
Light fluid	1000 ml	50 g	112 g	2.2 g
Heavy fluid	1000 ml	50 g	965 g	1.0 g

The rheology properties of the fluids were measured and are presented in figure 102. Fluid parameters are presented in table 10.

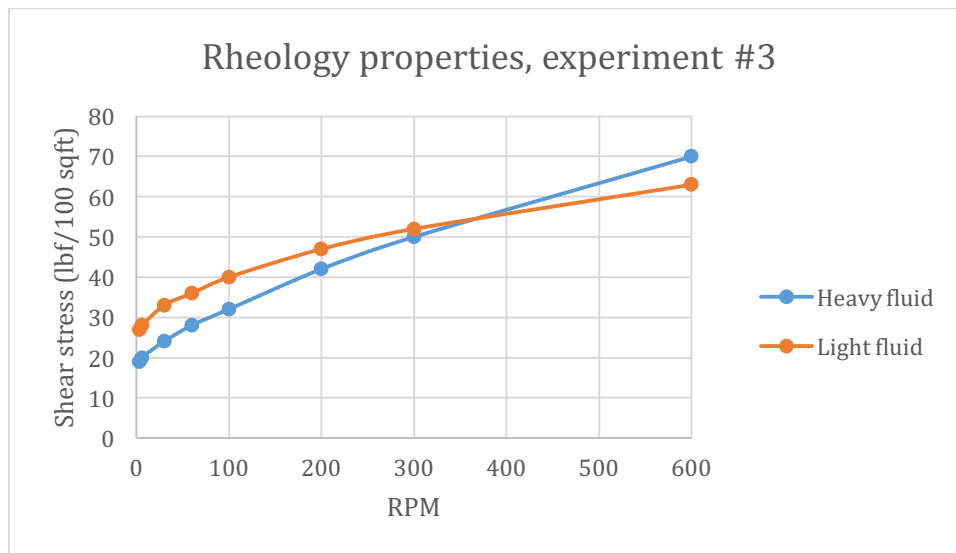


Figure 102: Rheology properties, experiment #3

Table 10: Fluid parameters, experiment #3

Fluid parameters	Heavy fluid	Light fluid
Density (sg)	1.49	1.10
PV (cP)	20	11
YS (lbf/100sqft)	30	41
LSYS (lbf/100sqft)	18	26

5.4.2 Description of Experiment

For this experiment there was used a larger acrylic pipe than the previous experiments. The inner diameter was 31.1 mm. There was also placed a smaller aluminium pipe inside the acrylic pipe which had an outer diameter of 19.6 mm. This gives a well bore ratio (inner diameter/outer diameter) of 1.59, which is also the given well bore ratio from Reelwell. Thus, this makes a realistic scaling of the pipes.

The purpose of the inner pipe is the ability of rotation. Placing a drill on top of the pipe gives the opportunity to attach it to the inner pipe and rotate it with a desirable RPM (rotations per minute).

The pipe was filled with light fluid in the lower part of the pipe and with heavy fluid in the upper part of the pipe. The fluids were static (no rotation) during the first 2 hours. The length of the mixing zone was measured every 5 minutes.

After 2 hours the inner pipe was rotated with a RPM of approximately 86. The length of the mixing zone was measured every 5 minutes.

5.4.3 Results

During the first 2 hours where there was no rotation of the inner pipe, there was not observed any mixing zone. 10 minutes after starting rotation of the inner pipe, there was measured a mixing zone of approximately 2 cm. After 15 minutes the mixing zone had increased to a length of approximately 3 cm. The battery of the drill ran out of power after 27 minutes of rotation, and the fluids were static until 45 minutes. During these minutes the length of the mixing zone did not grow any further.

The battery was charged and the inner pipe was rotated with an RPM of 150. The high rotation speed made the mixing zone grow to a length of approximately 10 cm after 5 minutes of rotation. After 30 minutes the mixing zone reached a length of approximately 60 cm. The battery ran out of power after 32 minutes of rotation. The development of the length of the mixing zone during 75 minutes of rotation with an RPM of 86, no

rotation and rotation with an RPM of 150 is presented in Figure 103. The speed of the mixing zone is shown in figure 104.

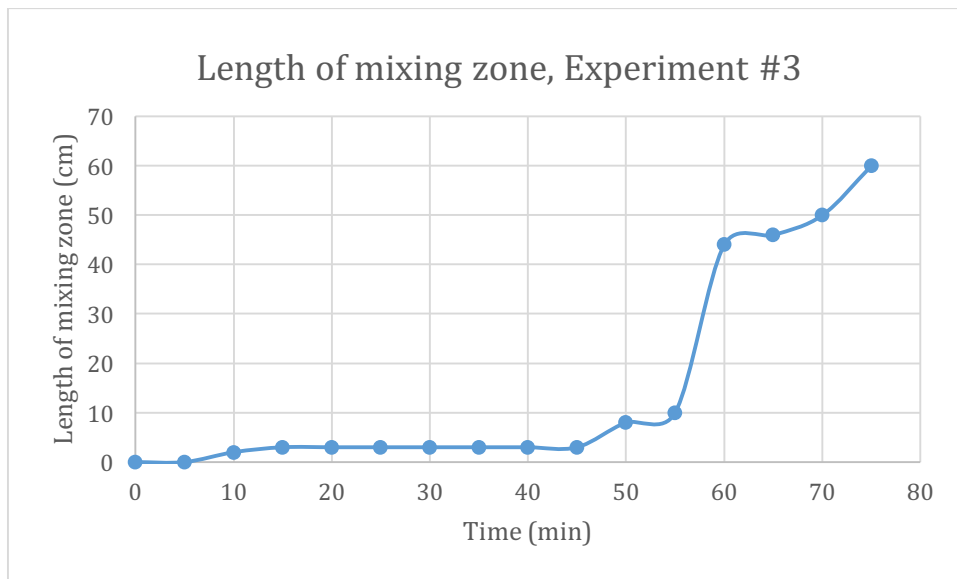


Figure 103: Length of mixing zone, experiment #3

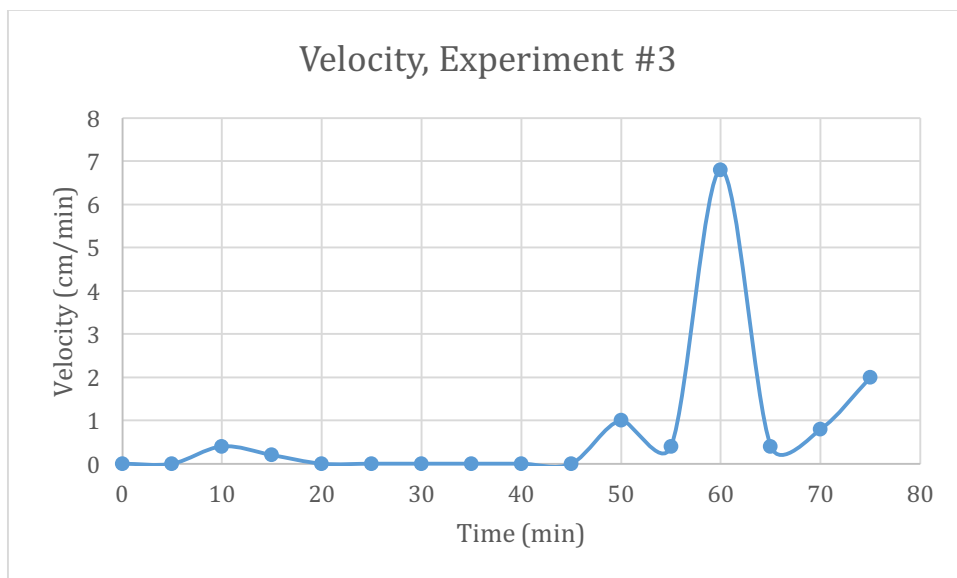


Figure 104: Speed of mixing length, experiment #3

Figure 105 and 106 show pictures of the fluids at start of the experiment, after 2 hours, at start of rotation of the inner pipe and after 30 minutes of rotation.

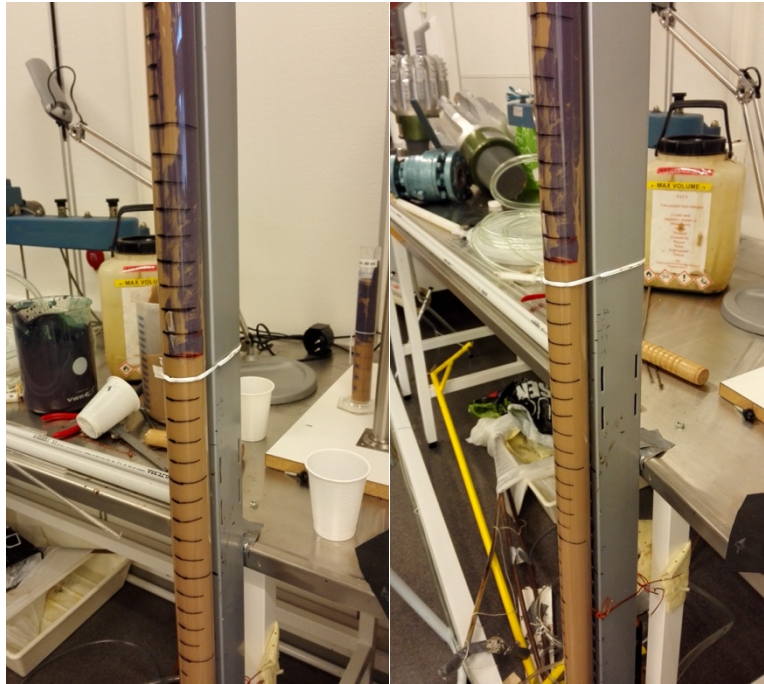


Figure 105: Pictures, experiment #3, at start and after 2 hours



Figure 106: Pictures, experiment #3, with rotation at start and after 30 minutes

5.5 Experiment #4

The fluids used in this experiment had relatively high density difference and there was used a smaller outer pipe compared to the previous experiments. There was also used an inner pipe and a drill for rotation of the inner pipe.

5.5.1 Description of Fluids

For this experiment there were used a heavy fluid with density of 1.59 sg and a light fluid with density of 1.11 sg. The fluids were made with the same additives as experiment #2, but with more XG in both fluids. This was done to increase the viscosity even more. Methylene blue was added to the heavy fluid for changing the colour of the fluid. Table 11 shows the additives of the fluids in experiment #4.

Table 11: Additives of the fluids in experiment #4

	Water	Bentonite	Barite	XG
Light fluid	500 ml	25 g	60 g	1.925 g
Heavy fluid	500 ml + methylene blue	25 g	490 g	0.95 g

The rheology properties of the fluids are presented in figure 107.

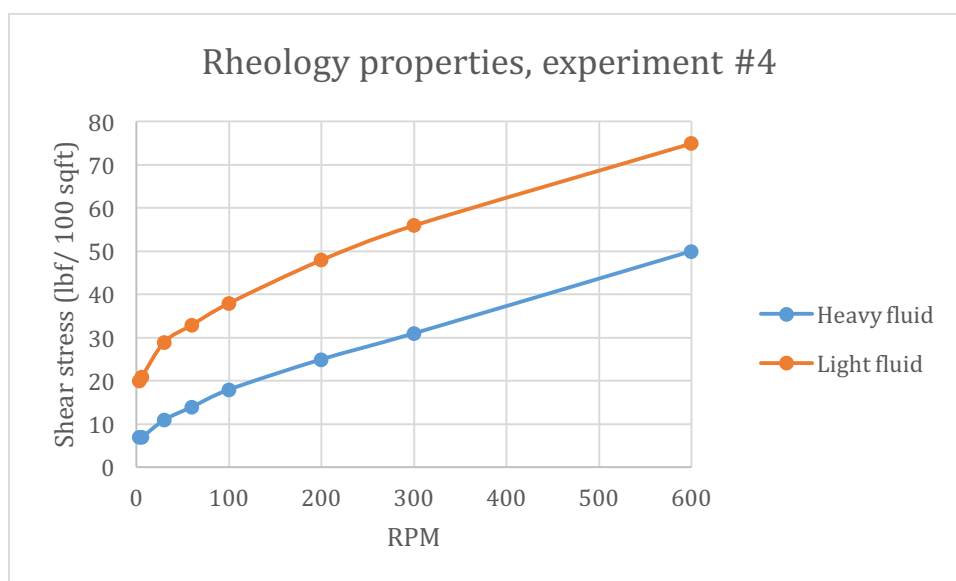


Figure 107: Rheology properties, experiment #4

The fluid parameters are presented in table 12.

Table 12: Fluid parameters, experiment #4

Fluid parameters	Heavy fluid	Light fluid
Density (sg)	1.59	1.11
PV (cP)	19	19
YS (lbf/100sqft)	12	37
LSYS (lbf/100sqft)	7	19

5.5.2 Description of Experiment

The outer pipe in this experiment was an acrylic pipe with inner diameter of 10.0 mm. For this experiment there was also used a metal string with outer diameter of 3.0 mm as the inner pipe. The drill was placed on top of the pipes, giving the opportunity of rotating the metal string.

The lower part of the pipe was filled with light fluid and the upper part of the pipe was filled with heavy fluid. The length of the mixing zone was measured every 5 minutes. After 1 hour the inner metal string was rotated with a RPM of 60. The length of the mixing zone was measured every 5 minutes.

5.5.3 Results

During the first hour of the experiment there was not observed any mixing zone. When the inner metal string was rotated the fluids started to mix and it was possible to measure the length of a mixing zone. After 10 minutes the length of the mixing zone was found to be 4 cm, and after 2 hours of rotating the mixing zone had grown to a length of 24 cm. The development of the length of the mixing zone is shown in figure 108 and the speed of the mixing zone is shown in figure 109. As can be seen from the figures the increase of the length of the mixing zone was highest in the beginning after starting rotation of the inner pipe. During the last 15 minutes there was observed a length of the mixing zone of 24 cm. Pictures taken during the experiment are presented in Figure 110 and 111. It is clear that the fluids did not move during the first hour. After 1 hour of rotation it is possible to observe the mixing zone.

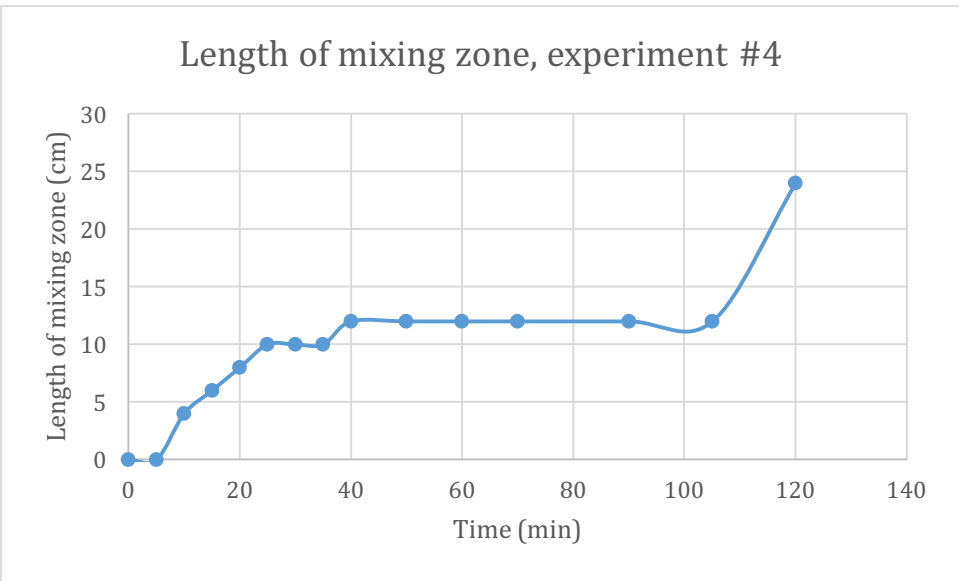


Figure 108: Length of mixing zone, experiment #4

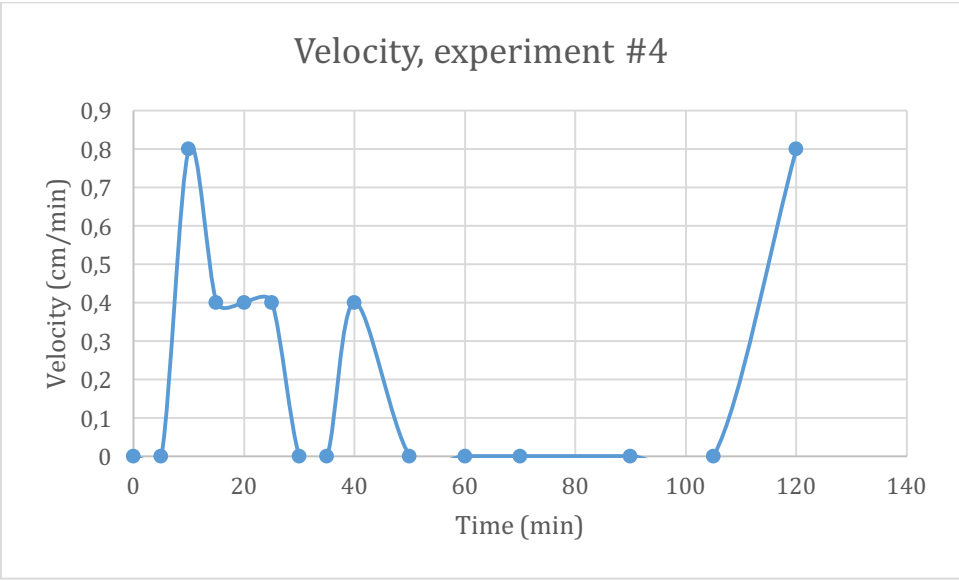


Figure 109: Speed of mixing zone, experiment #4



Figure 110: Pictures, experiment #4, at start and after 1 hour



Figure 111: Pictures, experiment #4, after 1 hour of rotation

5.6 Experiment #5

The density difference between the heavy and the light fluid was approximately the same as in the previous experiment. The fluids were water based muds and the pipes were of the same size dimensions as experiment #4.

5.6.1 Description of Fluids

For this experiment there were prepared a heavy fluid and a light fluid with densities of respectively 1.60 sg and 1.10 sg. The heavy fluid was added some methylene blue for changing the colour. The additives of the fluids are presented in table 13 below.

Table 13: Additives of the fluids in experiment #5

	Water	Bentonite	Barite	XG
Light fluid	500 ml	25 g	60 g	0.70 g
Heavy fluid	500 ml + methylene blue	25 g	490 g	0.20 g

The rheology properties of the fluids were measured and are presented in figure 112 and the fluid parameters are presented in table 14.

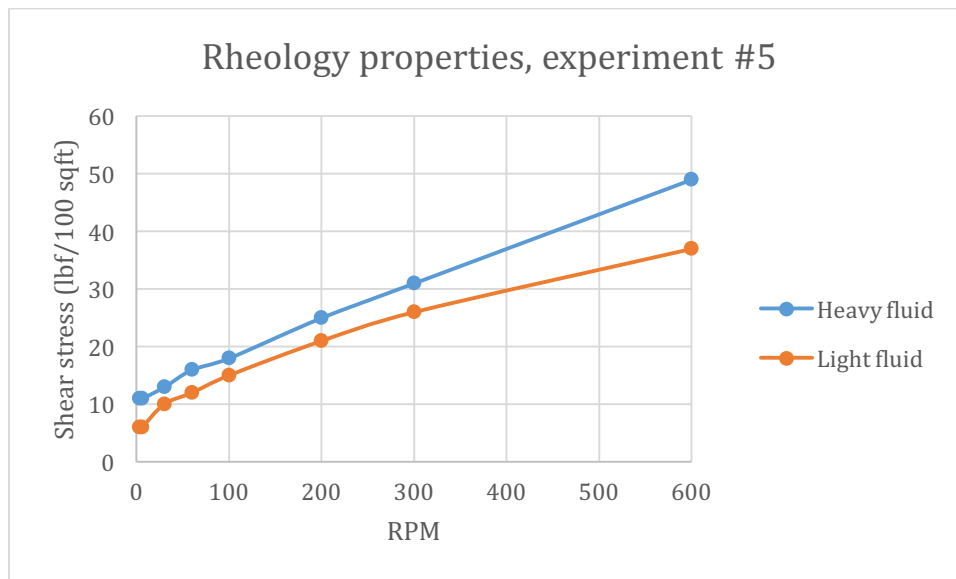


Figure 112: Rheology properties, experiment #5

Table 14: Fluid parameters, experiment #5

Fluid parameters	Heavy fluid	Light fluid
Density (sg)	1.60	1.10
PV (cP)	18	11
YS (lbf/100sqft)	13	15
LSYS (lbf/100sqft)	11	6

5.6.2 Description of Experiment

For this experiment there were used an outer acrylic pipe and an inner aluminium pipe. Like the previous experiment, the outer pipe had an inner diameter of 31.1 mm and the inner pipe had an outer pipe of 19.6 mm. A drill was placed at top of the pipes and attached to the inner pipe.

84 cm of the lower part of the outer pipe was filled with light fluid. Then the rest of the pipe was filled with heavy fluid. The length of the mixing zone was measured every 5 minutes. After 35 minutes the inner pipe was rotated with a speed of 60-70 RPM. The length of the mixing zone was still measured every 5 minutes. The rotation of the inner pipe was stopped after 180 minutes (3 hours) and the experiment proceeded without rotation of the inner pipe until 240 minutes (4 hours).

5.6.3 Results

From the point where heavy fluid was put on top of the light fluid, a mixing zone with length of 22 cm occurred. The mixing zone was static until it increased to 24 cm after 20 minutes. At 35 minutes the inner pipe was rotated, and after 50 minutes the length of the mixing zone was measured to 30 cm. After 1 hour and 50 minutes the mixing zone increased remarkably from a length of 44 cm to a length of 110 cm. This was the time step where the heavy fluid was first observed on the bottom of the pipe, which can be seen in figure 115. The mixing zone was stabilized after 2,5 hours at a length of 120 cm. After 3 hours there was no rotation of the pipe, and the length of the mixing zone was stable the next hour, until the experimental time period had reached 4 hours. The development of the length of the mixing zone and the speed of the mixing zone are

presented in figure 113 and 114, respectively. Pictures taken during the experiment are shown in figure 115 and 116.

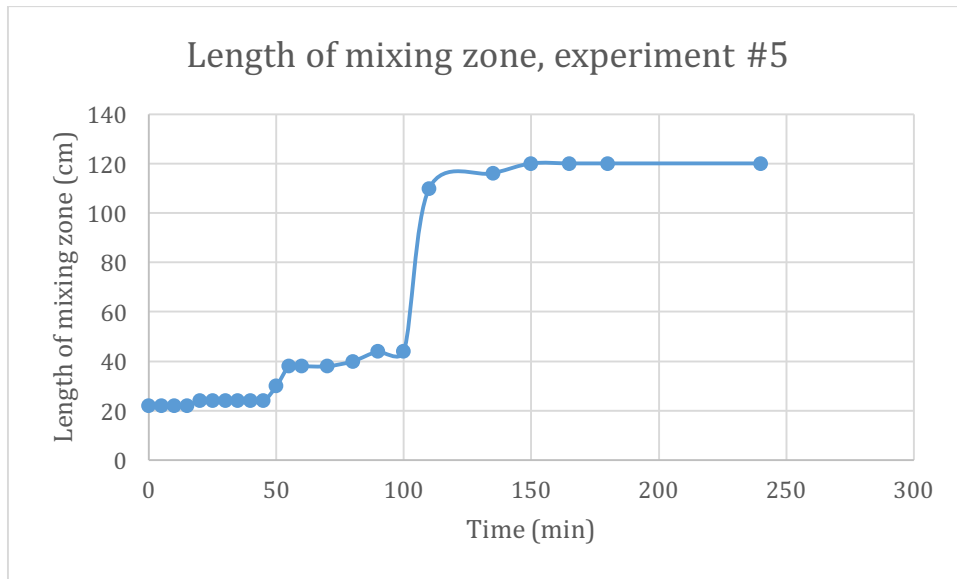


Figure 113: Length of mixing zone, experiment #5

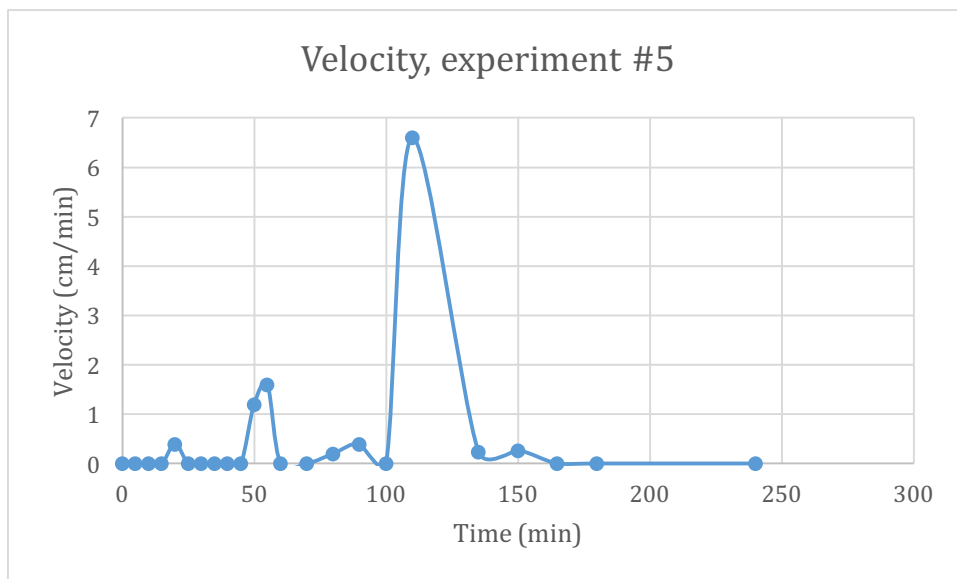


Figure 114: Speed of mixing zone, experiment #5



Figure 115: Pictures, experiment #5, at start and after 35 minutes



Figure 116: Pictures, experiment #5, after 1 hour and 50 minutes

5.7 Experiment #6

The fluids in this experiment had relatively high density differences. There were used both an outer and an inner pipe with smaller diameters than in the two previous experiments.

5.7.1 Description of Fluids

For this experiment there were used oil based muds (OBMs). The heavy fluid had a density of 1.63 sg and was already prepared by Magne Hurum for his Master Thesis in 2015 [4]. The light fluid consisted of oil with density 0.83 sg, barite, viscosifier and 60/40 oil-water mixture. The viscosifier used was Bentone 128. The density of the light oil was measured to 1.15 sg. The amounts of the additives of the light fluid are presented in table 15. The heavy fluid had a natural light colour while the light fluid had a dark brown colour, so there was no need for a colour changing additive.

Table 15: Additives of the light fluid in experiment #6

	Oil	Barite	Bentone 128	60/40 oil-water
Light fluid	300 g	133 g	4.0 g	2 spoons

The rheology properties for the fluids are shown in figure 117 below.

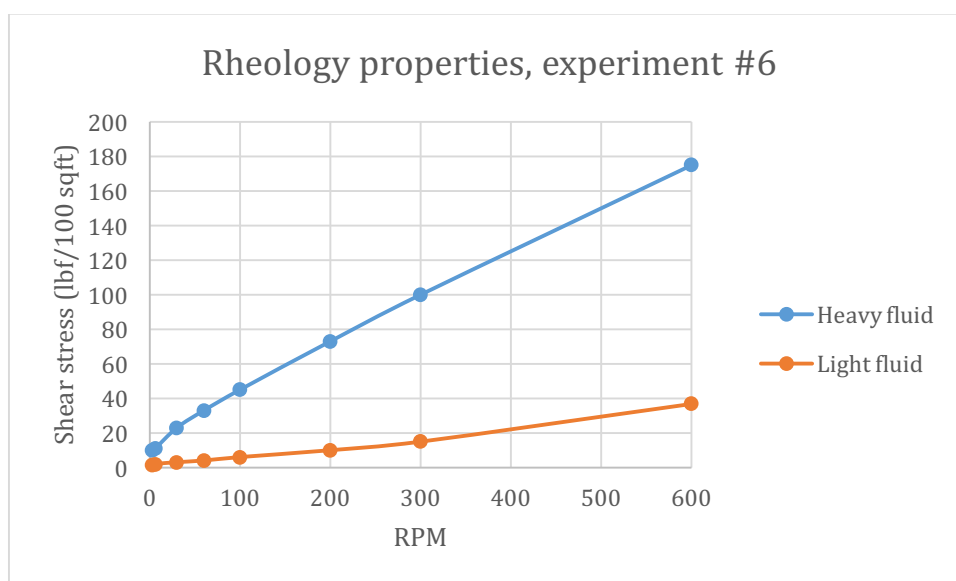


Figure 117: Rheology properties, experiment #6

The fluid parameters are presented in table 16.

Table 16: Fluid parameters, experiment #6

Fluid parameters	Heavy fluid	Light fluid
Density (sg)	1.63	1.15
PV (cP)	75	12
YS (lbf/100sqft)	25	3
LSYS (lbf/100sqft)	9	1

5.7.2 Description of Experiment

For this experiment there was used an acrylic pipe with inner diameter of 10.0 mm. A metal string with outer diameter of 3.0 mm was placed inside the acrylic pipe.

The light fluid was poured into the pipe through a funnel until the pipe was approximately half full. The pipe was then filled with heavy fluid at top of the light fluid. The fluids were at rest and the length of the mixing zone was measured every 5 minutes. After 210 minutes (3.5 hours) the inner metal string was rotated with a RPM of 120. The inner pipe was rotated until 270 minutes (4.5 hours) and the length of the mixing zone was measured every 5 minutes. After 270 minutes the density of the fluid at top of the fluid column was measured.

5.7.3 Results

The fluids were mixed from the beginning of the experiment with a mixing length of 53 cm. The length was stable until 30 minutes where the length of the mixing zone was measured to 106 cm. 5 minutes later the length was found to be 116 cm which it remained until 1 hour and 15 minutes. It increased to 130 cm and 5 minutes later it increased further to 158 cm. When the inner pipe was rotated after 3,5 hours the length of the mixing zone immediately increased to the length of the pipe. The inner pipe was rotated for 1 hour and the fluids were practically evenly mixed.

Figure 118 and 119 present the development of the length of the mixing zone and the speed of the mixing zone, respectively. Figure 120, 121, and 122 show pictures taken

during the experiment at start, after 30 minutes, after 90 minutes, at start of rotation and at the end of experiment. In Figure 120 the mixing zone is clearly visible. It is possible to observe that the reason for the remarkable increase in the length of the mixing zone after 30 minutes is the appearance of heavy fluid on the bottom of the pipe. The growth of the mixing zone between 60 and 90 minutes is due to light fluid rising through the heavy fluid.

When starting rotation of the inner pipe, the fluids mixed quite fast. As shown in figure 121 and 122 the fluid column looks relatively similar which may indicate that the mixing of the fluids happens rather rapidly. The light fluid may already have reached the top of the pipe before starting rotation, but was not visible through the outer pipe wall. After 1 hour of rotating the inner pipe, and a total time period of 4,5 hours, the density of a fluid sample from the top of the fluid column was measured. It was found to be 1.37 sg, close to the average density of the heavy and light fluid which is calculated to 1.39 sg. This may imply that the two fluids were almost completely mixed at the top of the fluid column.

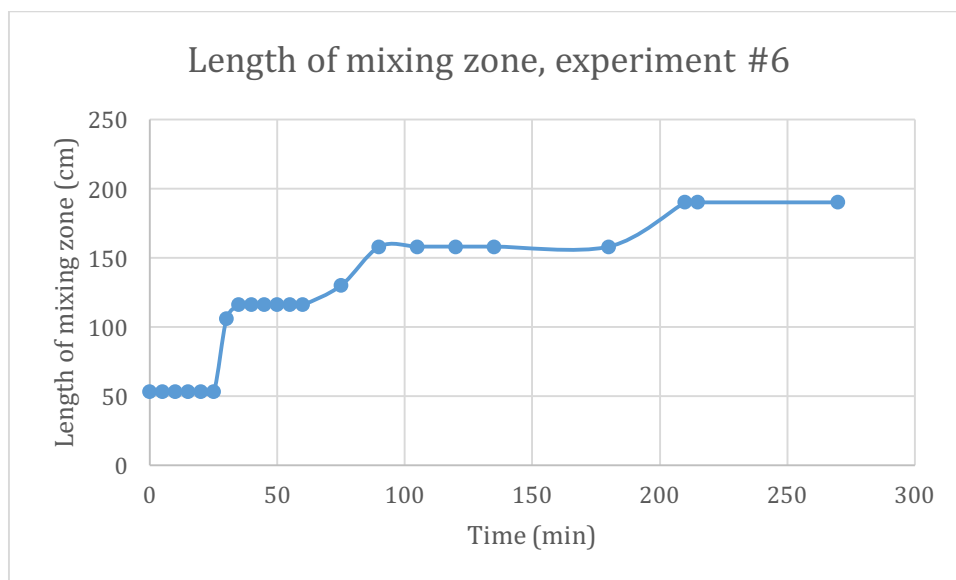


Figure 118: Length of mixing zone, experiment #6

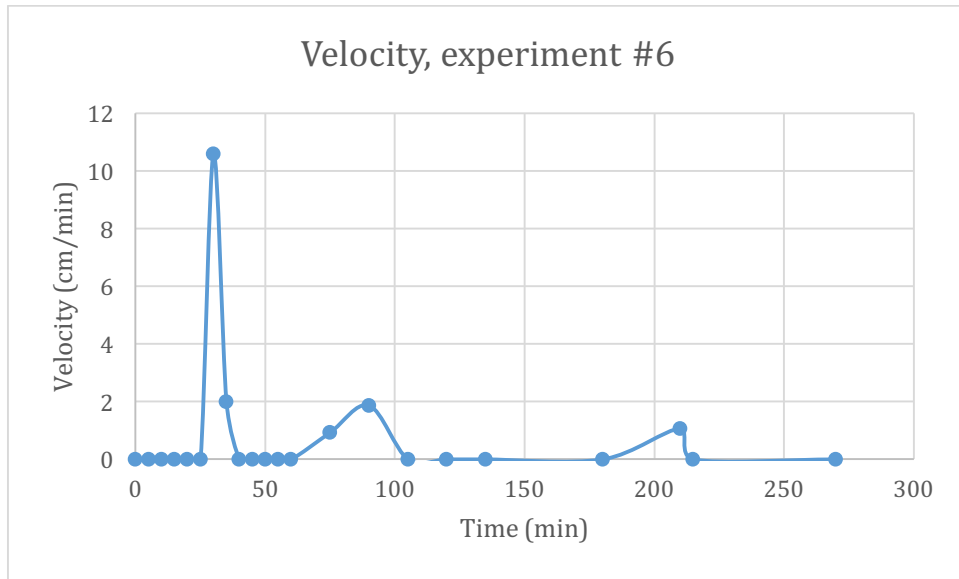


Figure 119: Speed of mixing zone, experiment #6

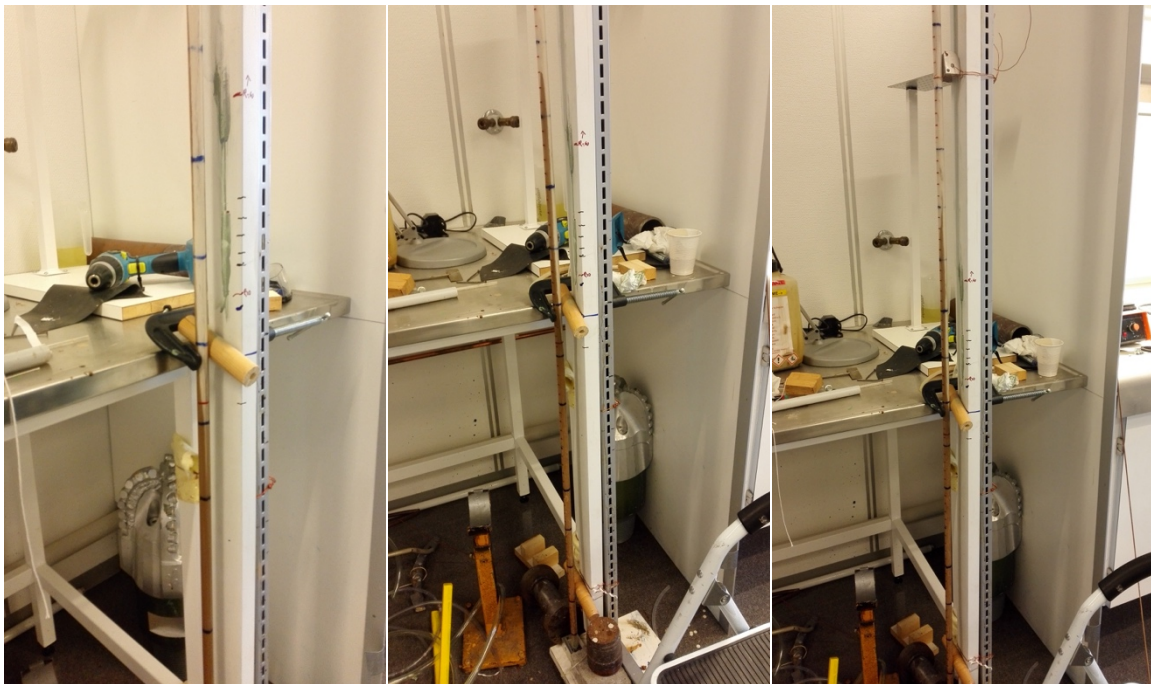


Figure 120: Pictures, experiment #6, at start, after 30 minutes and after 90 minutes



Figure 121: Pictures, experiment #6, at start of rotation



Figure 122: Pictures, experiment #6, after 1 hour of rotation (4,5 hours of experiment)

5.8 Experiment #7

The fluids in this experiments were oil based muds and the pipes used were of the same sizes as in the previous experiment.

5.8.1 Description of Fluids

The heavy fluid was made of two of the fluids that Magne Hurum had prepared for his Master Thesis in 2015 [4]. These were mixed together and added some EDC 95/11 oil in addition to 4.2 grams of XG for increasing viscosity. The density of the heavy fluid was measured to 1.59 sg.

The light fluid was the same as in the previous experiment, with density of 1.15 sg and the same rheology properties. The rheology properties for the heavy fluid were not measured. The fluid parameters are presented in table 17.

Table 17: Fluid parameters, experiment #7

Fluid parameters	Heavy fluid	Light fluid
Density (sg)	1.59	1.15
PV (cP)	-	12
YS (lbf/100sqft)	-	3
LSYS (lbf/100sqft)	-	1

5.8.2 Description of Experiment

The pipes used in this experiment were the same as in the previous experiment; the outer pipe was an acrylic pipe with diameter of 10.0 mm and the inner pipe was a metal string with diameter of 3.0 mm.

The outer acrylic pipe was filled with the fluids without having the inner metal string in place. The total height of the fluid column was measured to 190 cm. The light fluid reached a height of 104.5 cm and the heavy fluid was filled up to 190 cm of the pipe, giving a height of 85.5 cm of the heavy fluid column.

The fluids were static the first 60 minutes and the length of the mixing zone was measured every 5 minutes. After 60 minutes the metal string was placed inside the acrylic pipe and started rotating with a RPM of 120. The length of the mixing zone was measured every 5 minutes. The experiment was stopped after 2 hours of rotating the inner metal string, giving a total time of 3 hours.

5.8.3 Results

At start there was developed a mixing zone with length of 24 cm. It remained relatively constant until 15 minutes where it increased to 56 cm. There was observed heavy fluid on the bottom of the pipe but that was not considered as part of the mixing zone. Figure 123 shows the heavy fluid on the bottom of the pipe after 15 minutes.



Figure 123: Heavy fluid on the bottom of the pipe, experiment #7

After 30 minutes the mixing zone had a length of 60 cm which it remained until 60 minutes when the inner pipe was rotated. The inner pipe was set after 60 minutes and it was observed light fluid on the top of the fluid column. After 5 minutes of rotation the length of the mixing zone was equal to the length of the pipe. Figure 126 shows pictures taken during the experiment at start after 1 hour and after 5 minutes of rotation of the

inner pipe. Figure 124 shows the development of the length of the mixing zone and figure 125 shows the speed of the mixing zone.

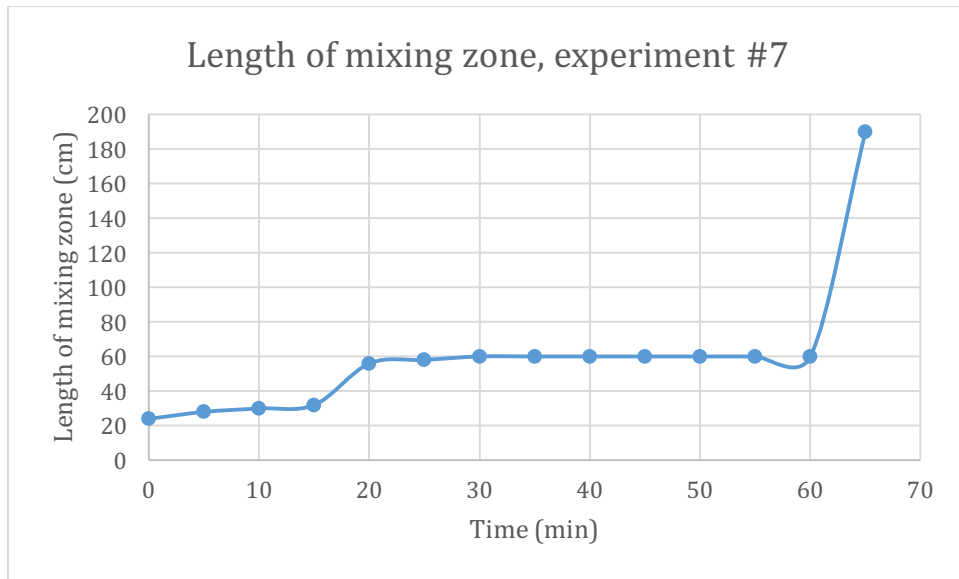


Figure 124: Length of mixing zone, experiment #7

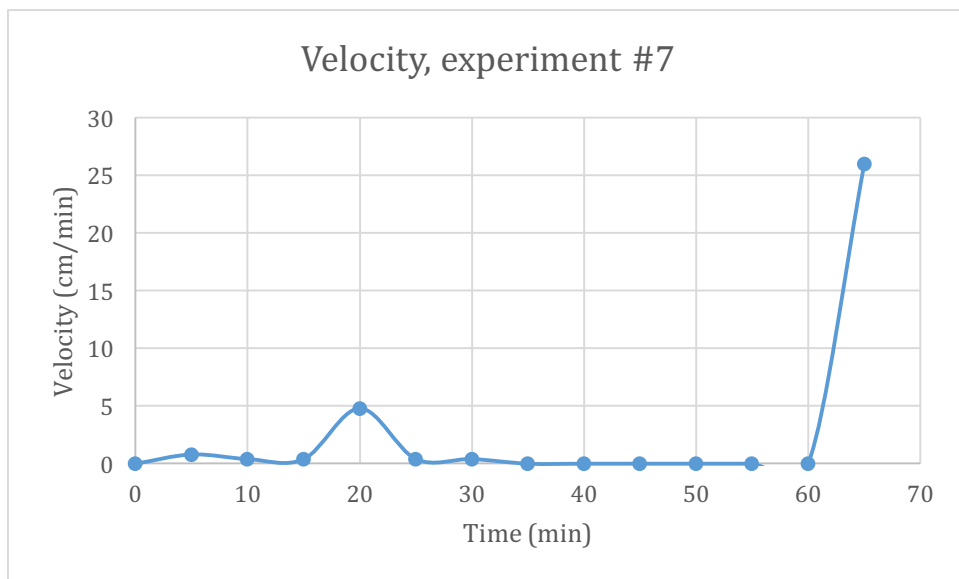


Figure 125: Speed of mixing zone, experiment #7



Figure 126: Pictures, experiment #7, at start, after 1 hour and after 5 minutes of rotation

5.9 Experiment #8

Like the two previous experiments, there were used oil based muds for this experiment. For the heavy fluid it was used chalk as weight material and the light fluid was almost the same as experiment #6. There were used both an inner and an outer pipe in addition to a drill for rotating the inner pipe.

5.9.1 Description of Fluids

For this experiment it was attempted to prepare a new sort of an oil based mud system by using chalk as weight material for the heavy fluid. For achieving the desired density of 1.60 sg it was calculated that there had to be added a total of 685 grams of chalk to 300 grams of diesel oil. It was chosen to add 419 grams of chalk and 266 grams of Calcium Carbonate (CaCO_3). There was also added 40 ml of EDC 95/11 oil and Zalo for decreasing viscosity. The amount of Zalo was not measured. For making the fluid even less viscous there was need for a few drops of OneMul which is an emulsifier. Due to these additional additives for decreasing the viscosity, there was also a decrease in

density. The density of the heavy fluid was measured to 1.51 sg, and not 1.60 sg, which was the intended density for the heavy fluid. The additives of the heavy fluid are shown in table 18 below.

Table 18: : Additives of the heavy fluid in experiment #8

	Diesel oil	EDC 95/11 oil	Chalk (Ca)	Calcium Carbonate (CaCO₃)	Zalo and emulsifier
Heavy fluid	300 g	40 ml	419 g	266 g	Did not measure exact amount added.

The rheology properties of the heavy were measured and are presented in table 19 along with the densities of the fluids. The light fluid was the same as in experiment #6. For this experiment there was also added 1.0 grams of Bentone 128 to the light fluid for increasing viscosity. The density of the light fluid was measured to 1.20 sg. The other fluid properties were not measured.

Table 19: Fluid properties, experiment #8

Fluid properties	Heavy fluid	Light fluid
Density (sg)	1.51	1.20
PV (cP)	36.5	-
YS (lbf/100sqft)	3	-
LSYS (lbf/100sqft)	1	-

5.9.2 Description of Experiment

The outer pipe used in this experiment was an acrylic pipe with inner diameter of 10.0 mm. The inner pipe was a metal string with outer diameter of 3.0 mm. There was also used a drill for rotating the inner pipe.

The outer pipe was filled the fluids without having the inner pipe in place. The light fluid column had a height of 96.5 cm while the heavy fluid column was 74.5 cm high. The heavy fluid was on top of the light fluid. The fluids were static with no inner pipe. The length of the mixing zone was measured every 5 minutes.

After 60 minutes the metal string was placed inside the acrylic pipe and was rotated with a RPM of approximately 120. The length of the mixing zone was measured every 5 minutes and the experiment kept going until the length of the mixing zone was equal to the length of the pipes.

The fluid column in the pipe was then divided into four almost equal parts, as shown in figure 127, and the density of each part was measured and compared to the average density of the light and the heavy fluid.



Figure 127: Dividing fluid column in 4 parts

5.9.3 Results

The fluids started mixing from the start and after 5 minutes the length of the mixing zone was measured to 28 cm. Until 20 minutes the mixing zone had a relatively smooth increase. From 20 minutes the length of the mixing zone was practically constant until 60 minutes when the inner pipe was rotated. Immediately after rotation had started

there was observed heavy fluid on the bottom of the pipe and light fluid on the top of the pipe, i.e. the length of the mixing zone was equal to the length of the pipe. Rotation of the inner pipe made the fluids mix more evenly. The development of the length of the mixing zone is presented in figure 128. Figure 129 shows the velocity profile of the mixing zone and figure 130 and 131 show pictures taken during the experiment, both without and with rotation of the inner pipe.

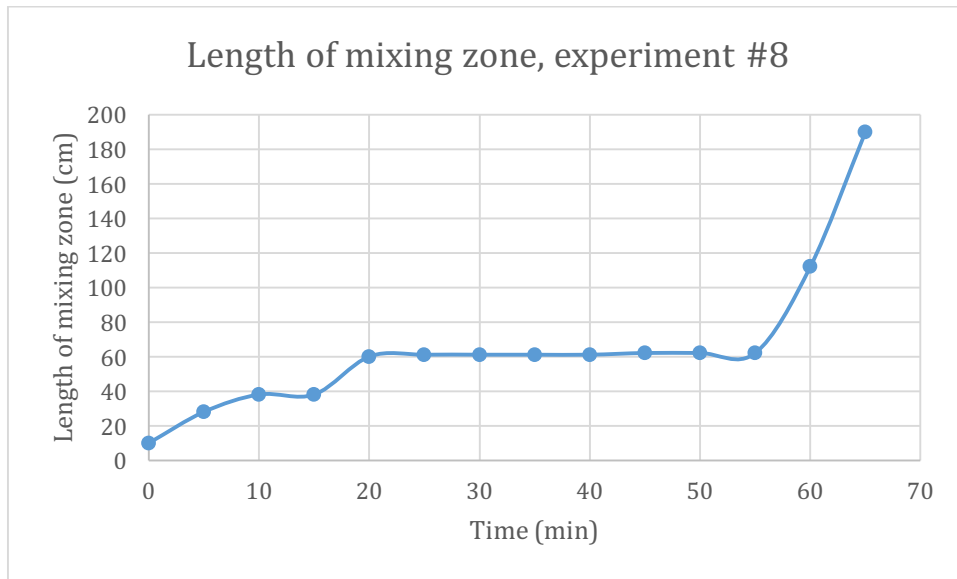


Figure 128: Length of mixing zone, experiment #8

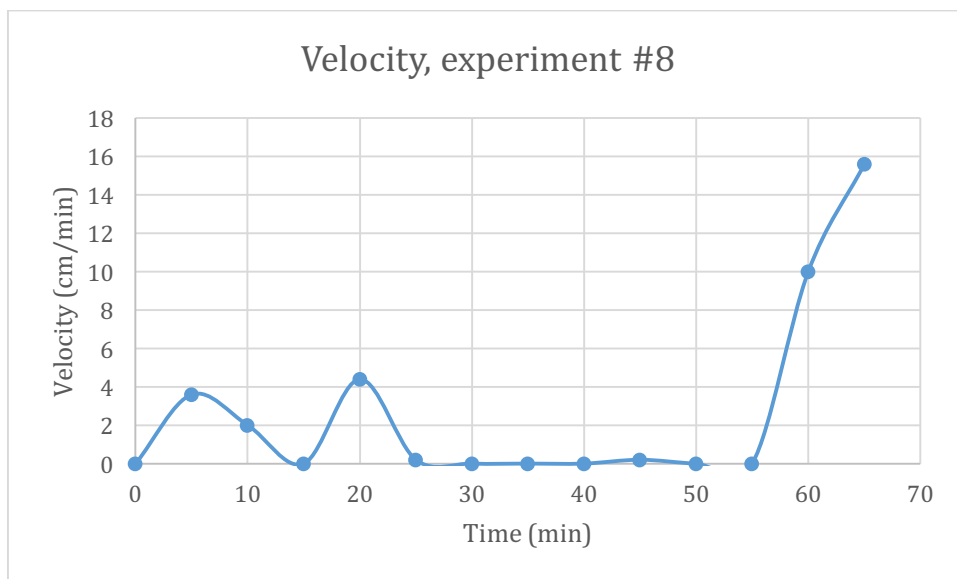


Figure 129: Velocity of mixing zone, experiment #8



Figure 130: Pictures, experiment #8, at start



Figure 131: Pictures, experiment #8, at start of rotation and 5 minutes after rotation

The heights of the fluid column of the four parts were measured to 53 cm, 48 cm, 56 cm and 30 cm, and the densities were measured to 1.36 sg, 1.37 sg, 1.26 sg and 1.36 sg, respectively. The average density of the heavy and the light fluid was calculated to 1.36

sg. Figure 132 shows the four parts of the fluid. As shown, the colours of the fluid differ from each other. Number 1 and 2 have a lighter colour, implying that they probably have higher densities than the other two. However, looking at the measured densities shows that it is not the case. The density of number 4 is equal to the density of number 1 and number 2 has practically the same density as well. The one that stands out is number 3 with a density of 1.26 sg. The densities were measured three times for each part, and the average values were calculated.



Figure 132: The four parts in cups

6 SUMMARY AND DISCUSSION

In the following sections the results from the simulation study and experimental investigations are compared and discussed.

6.1 Simulation Study

In this section the results from the COMSOL simulations are discussed. Table 20 shows the maximum and minimum density, and the total density difference after 10 hours. Table 21 presents the length of the mixing zone after 1, 5 and 10 minutes and the maximum speed of the fluids in both upward and downward direction.

Table 20: Max. and min. density and density difference

Case	Max. density	Min. density	Total density difference	Total change in density difference
Reference	1.39 sg	1.30 sg	0.09 sg	82 %
Density difference 1	1.31 sg	1.24 sg	0.07 sg	80 %
Density difference 2	1.22 sg	1.18 sg	0.04 sg	80 %
Viscosity difference 1	1.39 sg	1.30 sg	0.09 sg	82 %
Viscosity difference 2	1.40 sg	1.30 sg	0.10 sg	80 %
Well size difference 1	1.37 sg	1.32 sg	0.05 sg	90 %
Well size difference 2	1.40 sg	1.30 sg	0.10 sg	80 %

Table 21: Length of mixing zone and max. speed of fluids

Case	Length of mixing zone after 1 minute	Length of mixing zone after 5 minutes	Length of mixing zone after 10 minutes	Max. speed downward direction	Max. speed upward direction
Reference	155 m	1020 m	-	0.13 m/s	0.16 m/s
Dens. diff. 1	80 m	640 m	1410 m	0.08 m/s	0.27 m/s
Dens. diff. 2	60 m	460 m	1000 m	0.07 m/s	0.18 m/s
Visc. diff. 1	150 m	1060 m	-	0.13 m/s	0.20 m/s
Visc. diff. 2	150 m	1020 m	-	0.13 m/s	0.30 m/s
Well size diff. 1	100 m	940 m	-	0.12 m/s	0.70 m/s
Well size diff. 2	80 m	520 m	1120 m	0.07 m/s	0.152 m/s

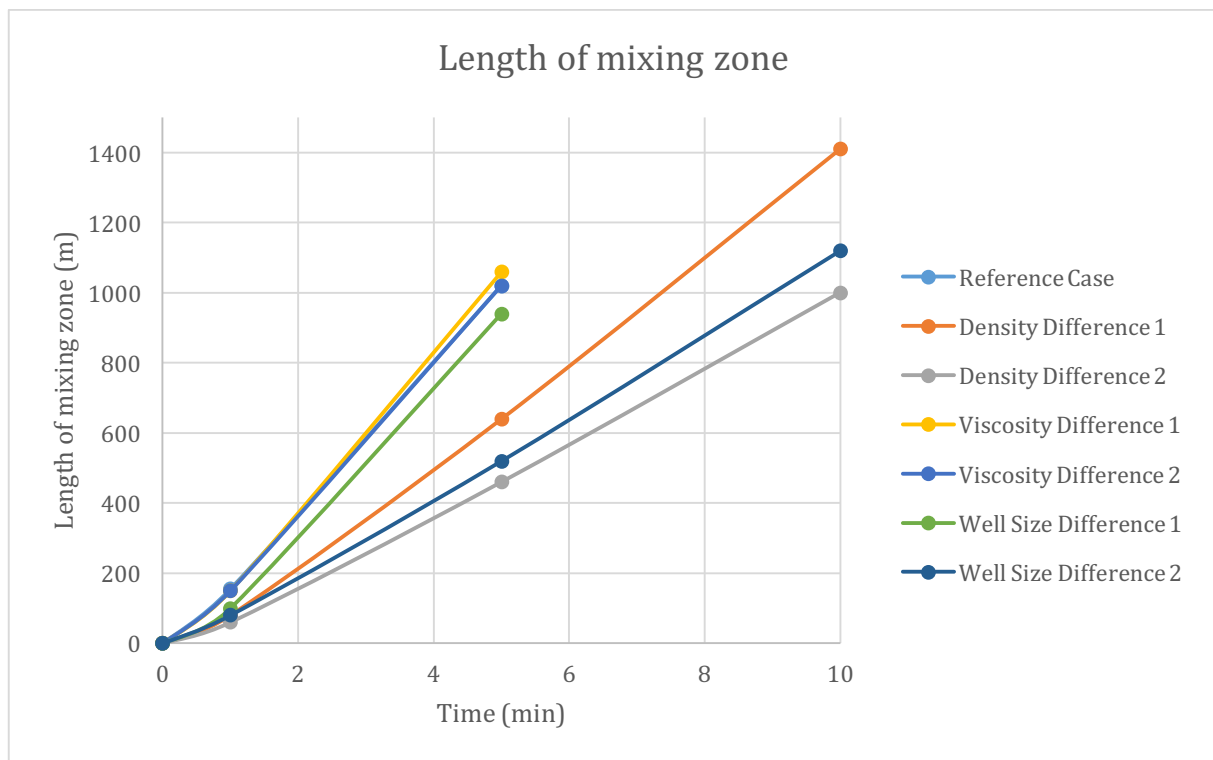


Figure 133: Length of mixing zone COMSOL simulation

Figure 133 presents a plot of the development of the length of the mixing zone in time for all 7 simulation cases. As shown on the plot, the density difference case 2 provides

the least growing mixing zone, followed by well size different case 2. The reference case, viscosity difference case 1 and 2, and well difference case 1 show approximately the same development of the mixing zone. The density difference case 1 is located between well difference case 1 and 2.

All the cases show a linear development of the mixing zone. The viscosity difference case 1 has the steepest line, implying the fastest growing mixing zone of all cases. Density difference case 2 shows the slowest growing mixing zone. According to the plot it may seem like the development of the length of the mixing zone will take some time to stabilize. The length of the mixing zone will probably grow until it equals the length of the fluid column as long as the fluid column is within a reasonable length. The question is how long it will take before the the length of the mixing zone is equal to the length of the fluid column.

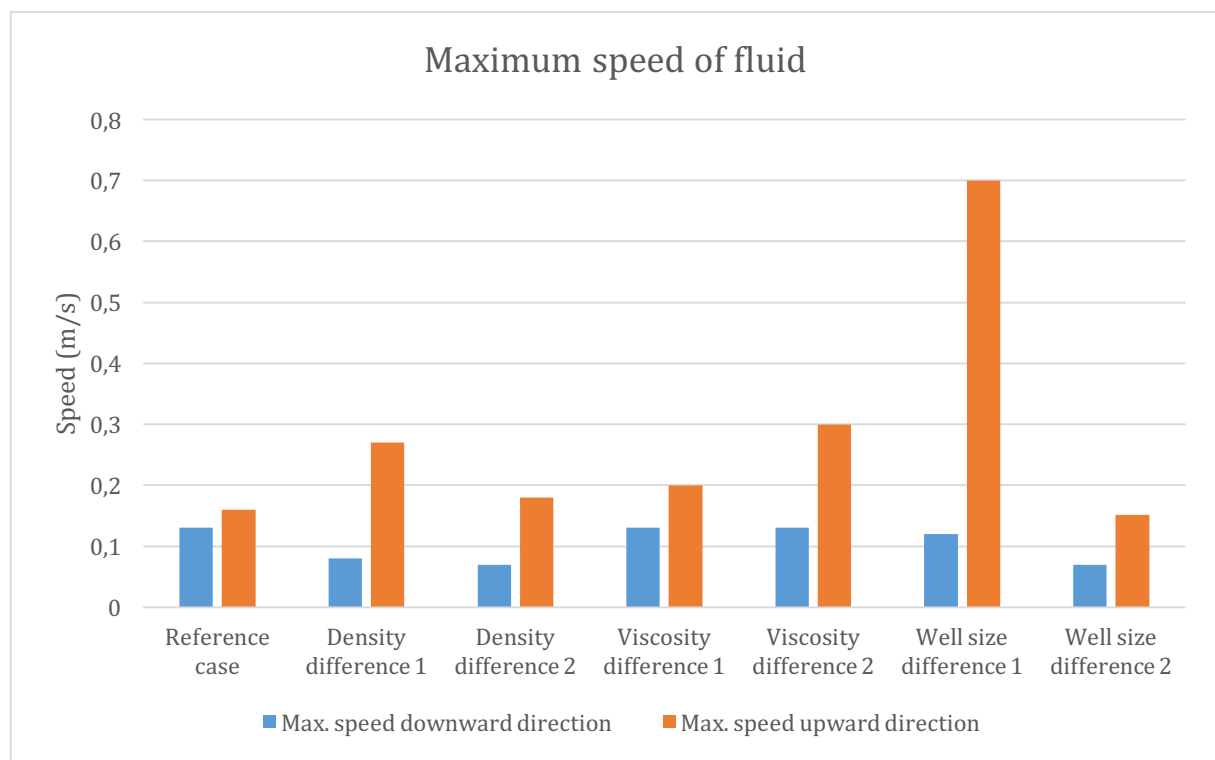


Figure 134: Maximum speed of fluid COMSOL simulation

Figure 134 presents the maximum speed in both upward and downward direction during 10 hours for all 7 simulation cases. All the velocities in the downward direction were interpreted at the interface, while the velocities in the upward direction were

located either on the top or on the bottom of the fluid column. Well size difference case 1 is clearly standing out with the highest speed calculated during the simulation. Density difference case 1 and viscosity difference 2 also have relatively high velocities in downward direction. The lowest velocities in downward direction were calculated during simulation of density difference case and well size difference case 2. Well size differenced case 2 has the lowest velocity in upward direction with a value of 0.152 m/s.

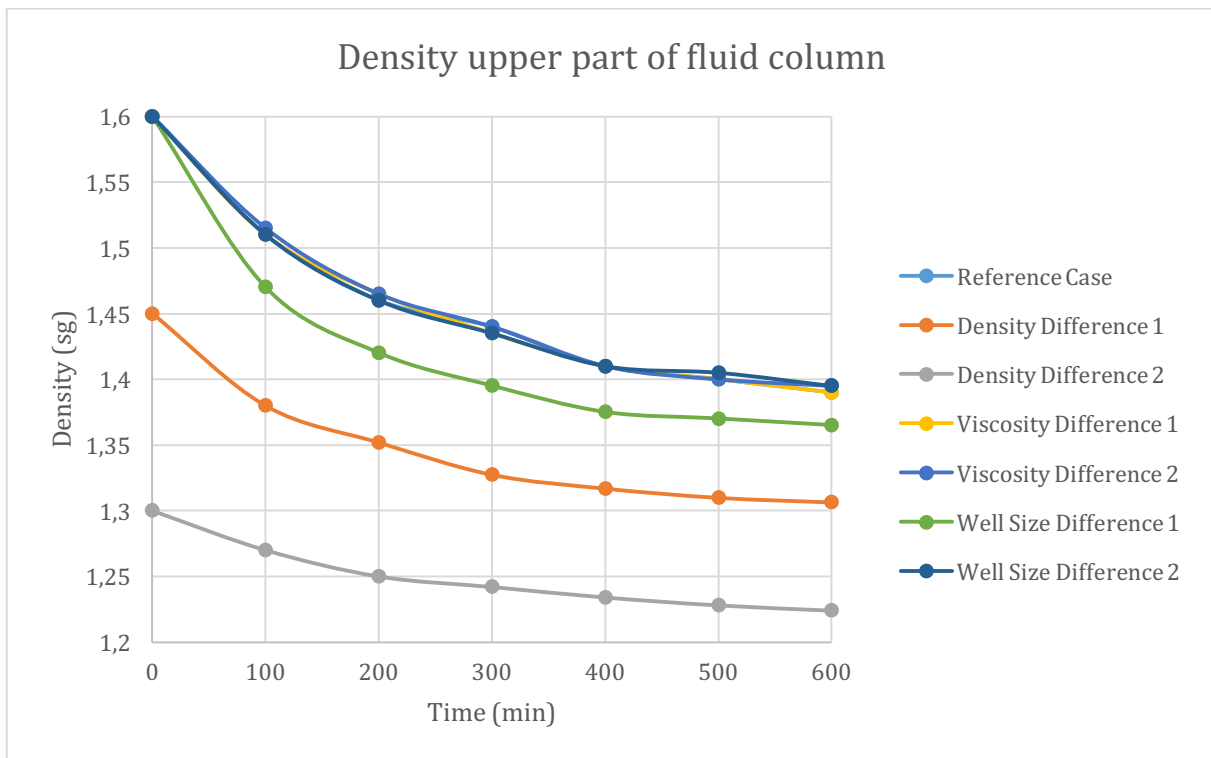


Figure 135: Density upper part of fluid column

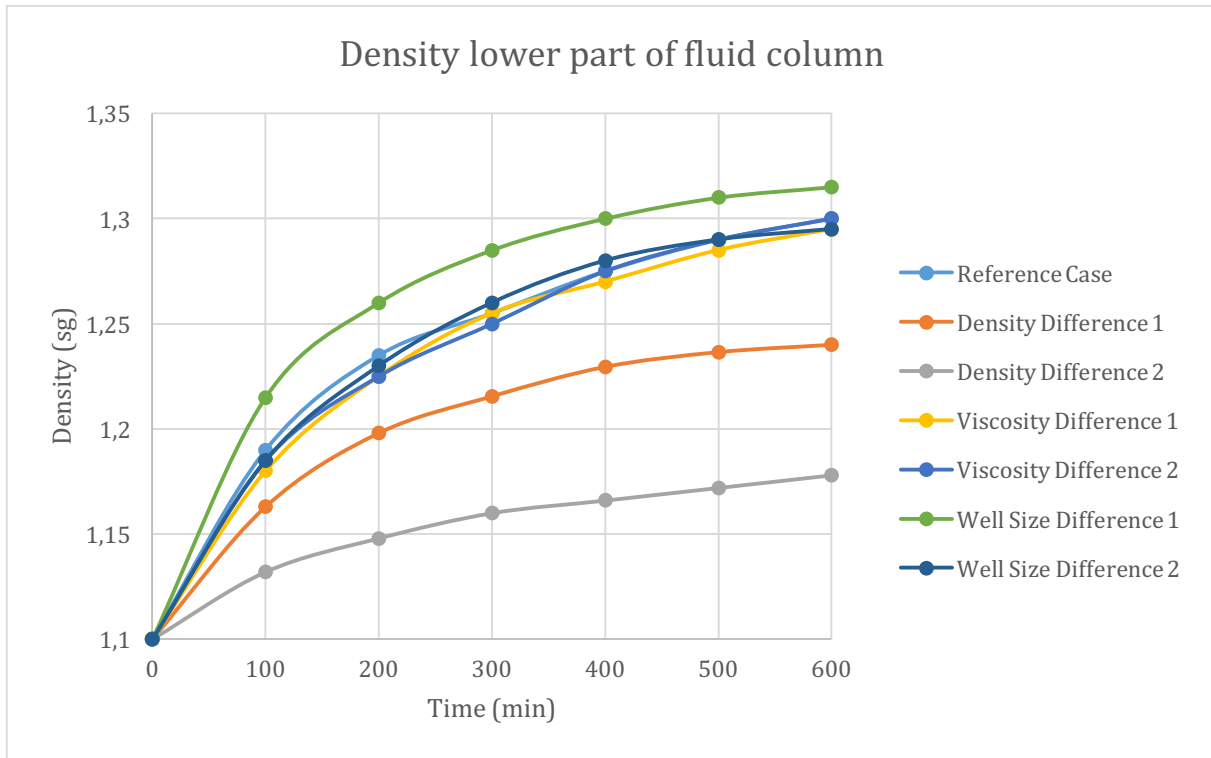


Figure 136: Density lower part of fluid column

Figure 135 and 136 present plots of the development of the densities in the upper and lower part of the fluid column, respectively. In all simulation cases the light fluids have the same density at start of simulation, as can be seen in figure 136. Figure 135 shows that both density difference cases have different densities at start of simulation than the rest of the simulations. The trends of the graphs are relatively alike and the lines flat out as time goes by. Well size difference case 1 differs from the other cases. The density in the upper part decreases faster and the density in the lower part increases faster than the densities in the other cases. After 10 hours the density difference is equal to 0.05 sg. Density difference case 2 obtained a density difference of 0.04 sg after 10 hours, but the densities of the heavy and light fluid were, respectively, 1.30 sg and 1.10 sg, giving a density difference of 0.20 sg at start. This gives an 80 % change in density variation, while the density variation in the well size difference case 1 had a 90 % change. The reference case, viscosity difference case 1 and 2, and well size difference case 2 had practically the same trend line for the density development in both parts of the fluid column.

6.1.1 Reference Case

The values for the parameters for the reference case were chosen from some of Reelwell's own parameters. The reference case provided a mixing zone with length of 155 meters after 1 minute and 1020 meters after 5 minutes. After 10 minutes the length of the mixing zone is beyond the length of the fluid column. The maximum speed during the 10 hours was calculated to 0.16 m/s. The reference case shows a relative rapid development of the length of mixing zone compared to some of the other cases.

The development of the density in the fluid column, presented in Figure 135 and 136, shows a logarithmic development. During 10 hours the density in the upper part of the fluid column decreases from 1.60 sg to 1.39 sg, and the density in the lower part of the fluid column increases from 1.10 sg to 1.30 sg. The density difference between the upper and lower part decreases from 0.50 sg to 0.09 sg, corresponding to a change of 82 %.

6.1.2 Effect of Density

The first density difference case had a heavy fluid with density 1.45 sg and a light fluid with density 1.10 sg. Thus, it was only the heavy fluid that had different density from the densities in the reference case. Compared to the reference case the density difference case 1 had a slower development of the length of the mixing zone. After 1 minute the length of the mixing zone in the reference case was equal to 155 meters, while the density difference case 1 had a mixing zone with length of 80 meters. During 10 minutes the length of the mixing zone in the reference case had reached beyond the length of the fluid column of 1500 meters. At the same time the mixing zone of the density difference case 1 had increased to a length of 1410 meters. The mixing zone in density difference case 2 developed a length of 60 meters after 1 minute and a length of 1000 meters after 10 minutes. Hence, a smaller density difference between the heavy and the light fluid provides a slower development of the mixing zone of the fluids.

The development of the mixing zone may also be related to the speed of the fluids in the fluid column. The maximum velocity of the reference case was calculated to 0.16 m/s, while the maximum velocities of the density difference case 1 and 2 were 0.27 m/s and 0.18 m/s. All the velocities were calculated in the upward direction. One should think

that the velocities in the density difference cases had smaller values than the reference case due to slower mixing zone development. Maybe the reference case had a total velocity higher than any of the velocities calculated in the density difference cases in a different time step than presented in this thesis. Or maybe the maximum velocity calculated in the fluid column is not so much related to the development of the mixing zone as one should think.

Looking at the density development in the fluid column, the lines for the reference case and the density difference cases have a quite similar development. The difference between the densities of the heavy and the light fluid in the reference case is 0.50 sg at start and 0.09 sg at the end of the simulation. This corresponds to a change of 82 %. The density variations for the density difference case 1 and 2 were respectively 0.35 sg and 0.20 sg. After 10 hours the density variations had decreased to 0.07 sg and 0.04 sg for case 1 and 2, respectively, corresponding to a change of 80 % for both cases. This implies that the reference case actually had the highest relative change in density variation between the two fluids.

6.1.3 Effect of Viscosity

In the viscosity difference cases the viscosity for both fluids were changed in both cases compared to the reference case. In the first case the viscosity difference is equal to 12 cP and for the second case the viscosity difference is equal to 1 cP. The viscosity difference for the reference case is equal to 5 cP. The length of the mixing zone after 1 minute is 155 meters for the reference and 150 meters for both viscosity difference cases. After 5 minutes the reference case and viscosity difference case 2 had a mixing zone with length of 1020 meters, and the length of the mixing zone for the viscosity difference case 1 was equal to 1060 meters. The length of the mixing zone after 10 minutes was beyond the length of the fluid column. The maximum velocities of the fluids are quite similar for both the reference case and the two viscosity difference cases. The viscosity difference between the heavy and the light fluid seems to have a small effect on the development of the mixing zone and the velocity of the fluids, as shown in figure 133 and 134.

As can be seen from figure 135 and 136 the development of the density in the fluid column is practically equal for the reference case and the two viscosity difference cases, implying that change in viscosity difference may have little effect on the development of density.

6.1.4 Effect of Well Size

The size of the well was changed to a larger diameter in the first case and a smaller diameter in the second case. The differences between the radius of the well size in the reference case and the radius of the well size in the well size difference case 1 and 2 are equal to 0.0735 meters and 0.0515 meters, respectively. The length of the mixing zone for the first well difference case was calculated to 100 meters after 1 minute, and for the second case it was found to be 80 meters. After 5 minutes the length of the mixing zone for the first case was equal to 940 meters and 520 meters for the second case. During 10 minutes the length of the mixing zone for the first case had reached the length of the fluid column. The mixing zone for the second case was calculated to 1120 meters after 10 minutes. The development of the length of the mixing zone for the first well difference case is quite similar to the reference case. The second well size difference case, however, shows a more modest development.

The maximum velocity of the well difference case 1 was calculated to 0.70 m/s, which is the highest velocity calculated of all simulation cases. The highest velocity calculated for the second well difference case was found to 0.152 m/s, which constitutes a difference of 0.548 m/s between the maximum velocities. According to these cases it may seem like the length of the mixing zone is related to the maximum velocity. The well difference case 1 has a rapid development of the mixing zone and also a high maximum velocity.

The plots in figure 135 and 136 show that the well difference case 2 has a quite similar density development as the reference case. Case 1, on the other hand, displays a faster change in density. During 10 hours the density difference between the fluids in the upper and lower part of the fluid decrease from 0.50 sg to 0.05 sg, corresponding to a change of 90 %. This is the highest density difference change of all simulation cases. From the simulations of the well difference size cases it seems like a larger well

diameter may speed up both the development of the mixing zone and the development of density in time. A slightly smaller diameter may have the opposite effect and decelerate the development of the length of the mixing zone, but may not have so much effect on the development of the density of the fluid column.

6.1.5 Summary

The results from the simulations show that the parameters that have the highest effect on the development of the length of mixing zone compared to the reference case, are density and well size. The lower density difference between the heavy and the light fluid, and the smaller well size diameter, the slower development of the mixing zone. Changing the viscosity of the fluids seems to have no or very little effect on the development of the mixing zone. The development of the mixing zone depends on several parameters, including gravity. A fluid with higher density will be exposed to a higher gravity force than a fluid with less density. Thus, when the density of the heavy fluid decreases, the gravity force acting on the fluid will decrease resulting in a slower mixing process.

Figure 134 shows that the maximum velocities for the various simulations are not so different from each other, except from well difference case 1. The radius of the well in this case was set to 0.2 meters, while the reference case had a radius of 0.1265 meters. Both of these may be typical sizes for a well. Due to decrease in casing diameter as the depth of the well increases during drilling of a well, the well size varies. As the size of the well decreases, the development of the mixing zone decelerates, implying that the mixing process may be fastest on top of the well.

According to the simulations in COMSOL the viscosity difference between the fluids have no or small effect on the development of the mixing zone and the development of the density during 10 hours. However, COMSOL does not take gel properties into account when simulation the HOL principle. Gel properties are important for drilling fluids and may have effect on the development of the mixing zone.

6.2 Experimental Work

This section discusses the results from the experiments and how the parameters affect the development of the mixing zone.

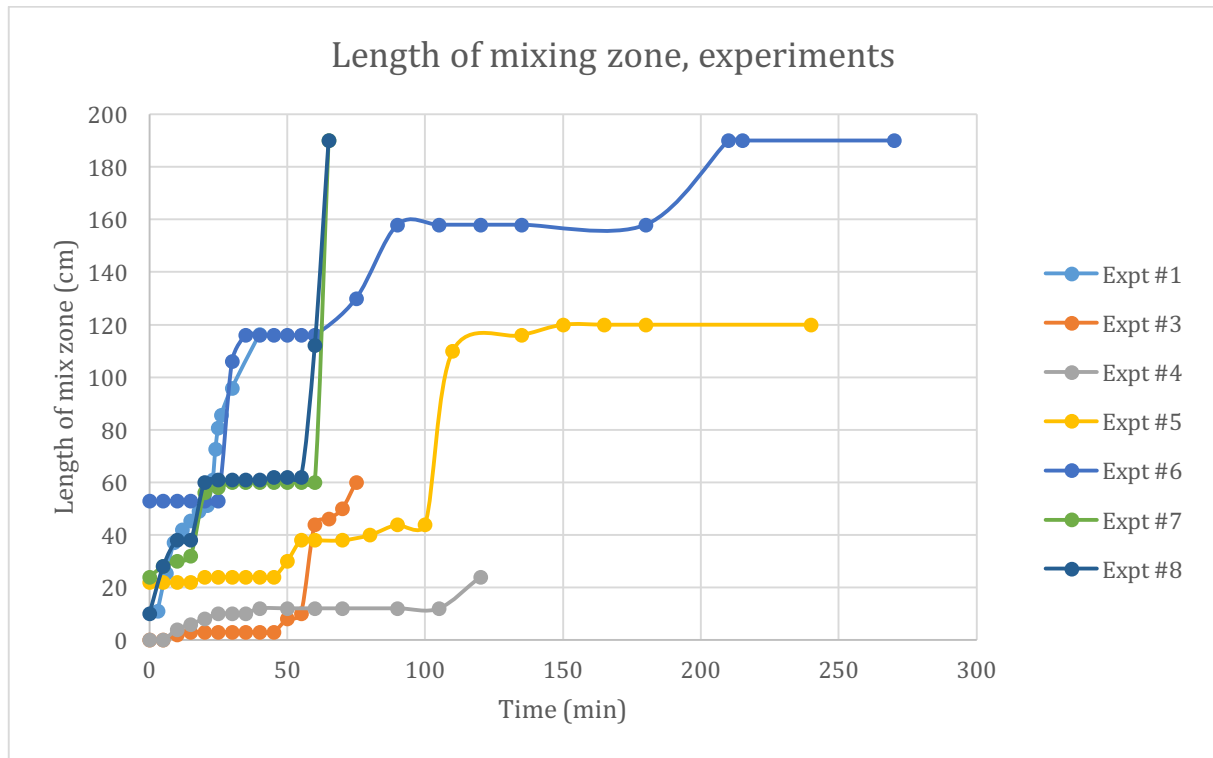


Figure 137: Length of mixing zone, experiments

Figure 137 presents the lengths of the mixing zone for all eight experiments in the same plot. As mentioned in the previous chapter and shown in the figure, the experiments were conducted at different time periods. Experiment #4 shows the most modest development. The length of the mixing zone in experiment #5 has a significant increase after 100 minutes and then it stabilizes at a length of 120 cm. In experiment #6, #7 and #8 the length of the mixing zone reached the length of the entire fluid column. For experiment #7 and #8 this length was measured when the inner pipe was rotated. It was first then it was possible to observe the light fluid on the top and the heavy fluid on the bottom of the pipe. The mixing zone in experiment #1 shows a smooth, but steep, increase.

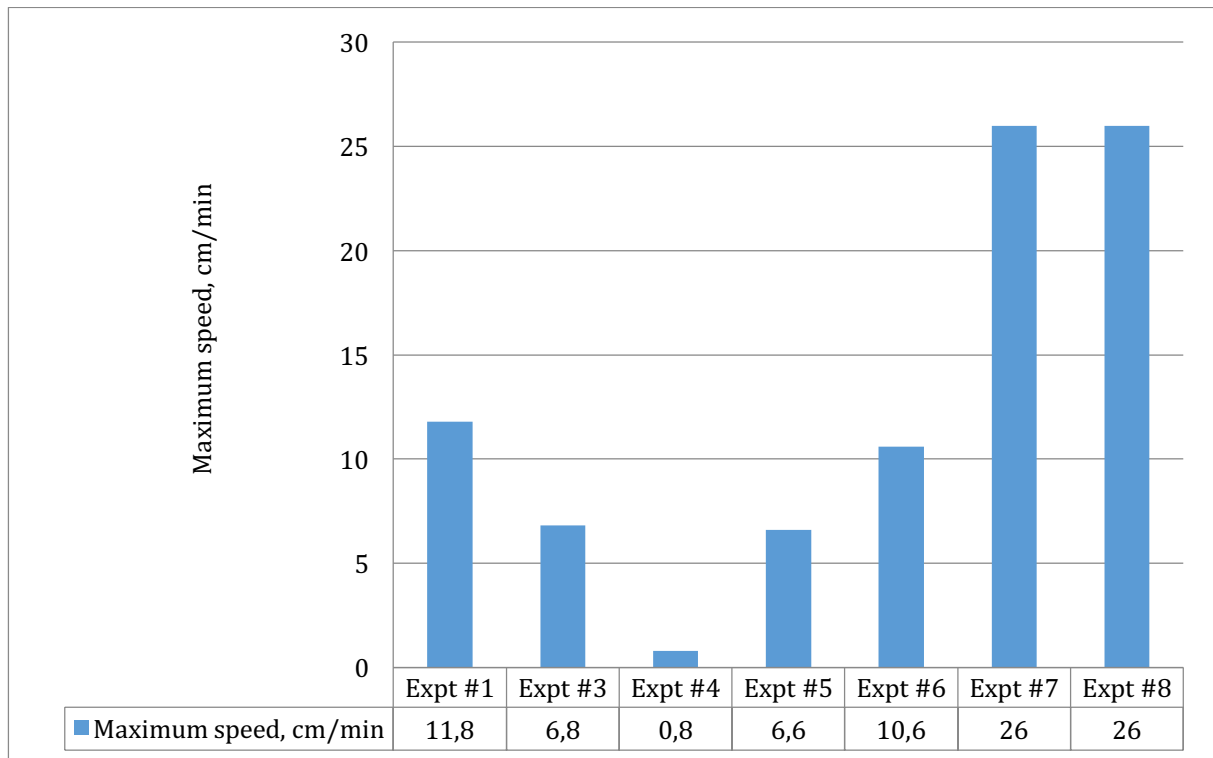


Figure 138: Maximum speed, experiments

Figure 138 presents the maximum speed measure in each experiment. It is clear that experiment #7 and #8 have the highest velocities. Figure 137 shows that the mixing zone in both of these experiments had a significant increase after approximately 1 hour and this is the reason for the high velocities. The lowest maximum speed was found in experiment #4. This is also the experiment where the mixing zone had the most modest development. A fast growing mixing zone gives high velocities.

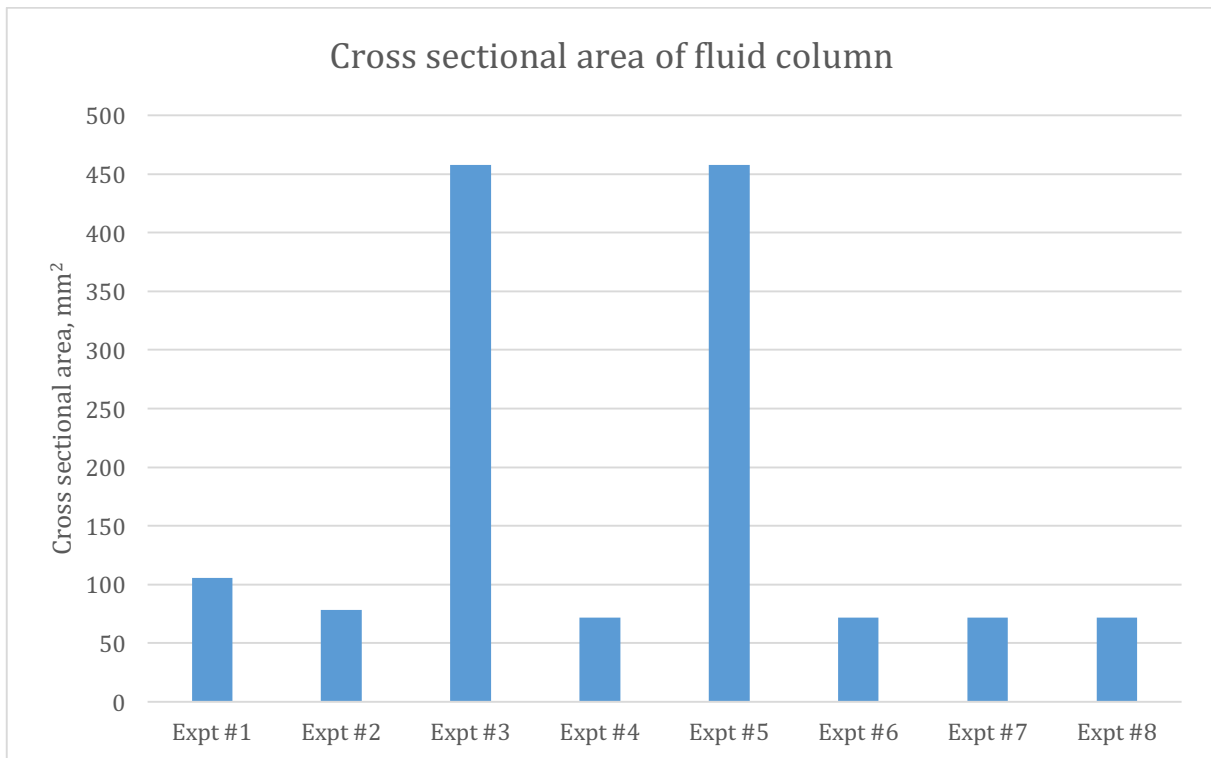


Figure 139: Cross sectional area of fluid column

Figure 139 presents a plot of the cross sectional area of the fluid column in all of the eight experiments. Experiment #3 and #5 stand out with a much larger cross sectional area than the other experiments. In experiment #1 there was used a slightly larger pipe than experiment #2, #4, #6, #7 and #8. In these experiments there as used the same outer pipe, but for experiment #2 there was not used an inner pipe. This gives a slightly larger cross sectional area for the fluid column.

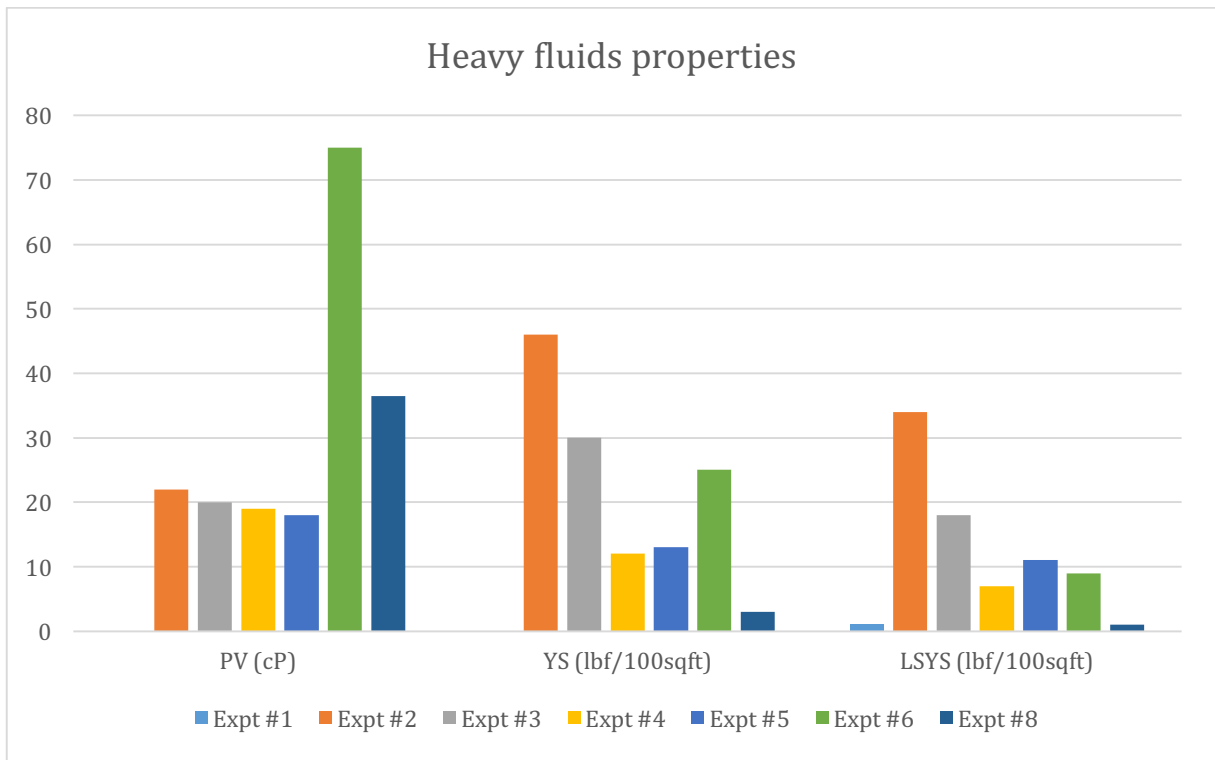


Figure 140: Heavy fluids properties

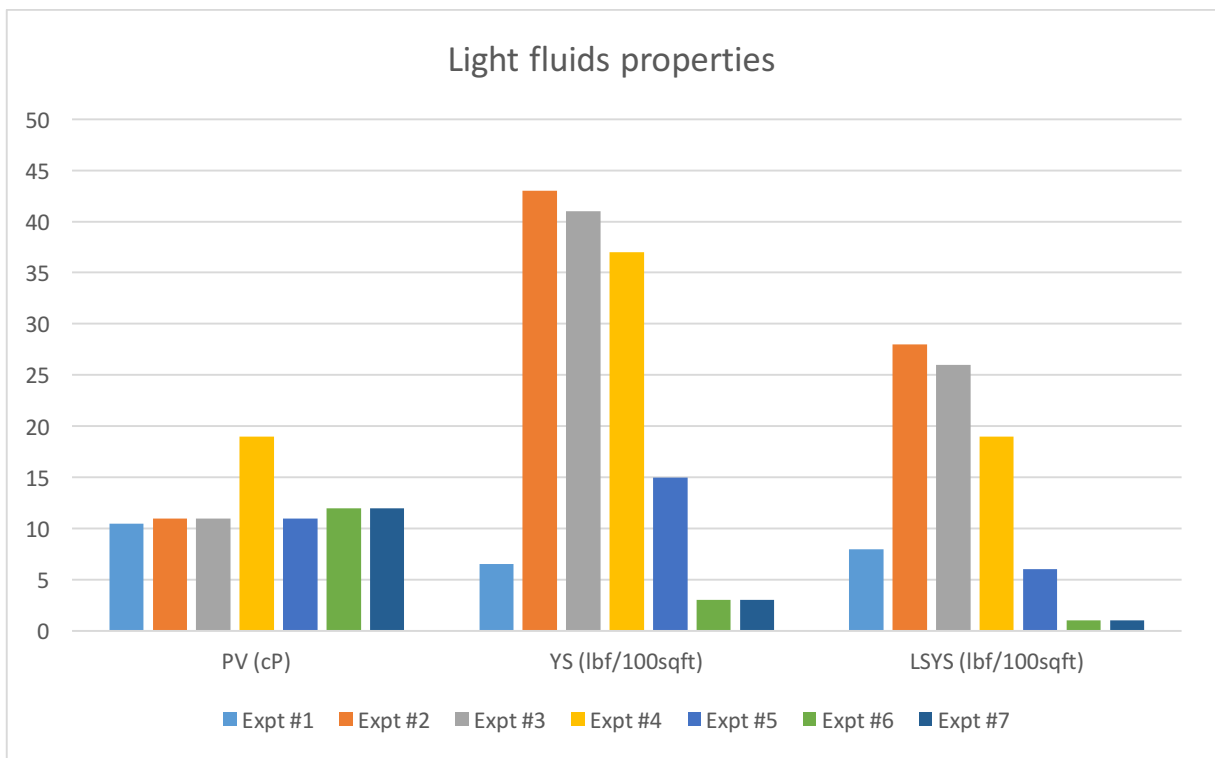


Figure 141: Light fluids properties

Figure 140 presents the fluid properties of the heavy fluids in all experiments, except experiment #7, and figure 141 presents the fluid properties for the light fluids in all experiments, except experiment #8. The rheology properties for the heavy fluid in experiment #7 and the light fluid in experiment #8 were not measured. In the experiments with a stable and measurable mixing zone (does not reach the top and/or bottom of the pipe), the fluids had relatively high gel properties, i.e. high LSYS value. Experiment #2 has the highest LSYS value for both the heavy and the light fluids. Due to the high gel strength the fluids formed into gel, making it impossible for them to blend. Thus, there was not measured any mixing zone in this experiment. The fluids in experiment #2 show high values in yield strength which may indicate that they tend to mix poorly. The cross sectional area of the fluid column was relatively small which may also be a contributing factor to the mixing process.

The mixing zone in experiment #1 had a relative smooth and gradual development. The rheology properties had quite low values compared to the other fluids, and may be the reason for the easy mixing of the fluids. The cross sectional area of the fluid column was measured to 78.5 mm², which is quite small. The formation of clusters of the heavy fluid in the light fluid may be because of a higher yield strength and LSYS of the light fluid. A possible explanation might be that the heavy fluid had to gather enough weight, i.e. force to pass through the light fluid. The heavy fluid was observed on the bottom of the pipe after almost half an hour. If the experiment had proceeded for a longer time period, the mixing zone would probably grow further after 40 minutes.

The fluids in experiment #3 had relatively high yield strength, especially the light fluid. These fluids provided a modest development of the mixing zone as shown in Figure 137, despite the large cross sectional area. The inner pipe had to be rotated for the fluids to mix better. This may imply that rotation weakens the yield strength of the fluids, and the fluids blend easier. The plastic viscosities of the fluids had quite ordinary values compared to the fluids in the other experiments.

Experiment #4, which showed the least development of the mixing zone, had a light fluid with high rheology property values compared to the other fluids. The fluid properties of the heavy fluid were average compared to the other fluids. The fluids did not mix until

the inner pipe was rotated. This may be due to the high yield strength of the light fluid. The cross sectional area of the fluid was measured to 71.5 mm², which is not very large. This may contribute to a poor mixing.

The rheology properties of the fluids in experiment #5 are quite regular compared to the other fluids, but a large cross sectional area. The fluids had a modest mixing until 100 minutes. The heavy fluid was observed on the bottom of the pipe, and the length of the mixing zone got a sudden leap from 44 cm to 110 cm. The heavy fluid was most likely sinking through the light fluid without the possibility of being observed from the outside. It is possible that the light fluid had risen further up through the heavy fluid without being observed.

The mixing zones in experiment #6, #7 and #8 reached a length equal to the pipe. The fluids in these experiments were oil based muds, all with relatively low rheology values. The exceptions are the plastic viscosity and yield strength of the heavy fluid in experiment #6. The fluid columns in these experiments had all the same cross sectional area. The inner pipes were rotated in all three experiments, which made the fluids mix better and it was easier to observe the extent of the mixing zone. As seen in figure 137, the maximum velocities for the mixing zone in experiment #7 and #8 are quite large. This is due to the sudden increase in the length of the mixing zone when the inner pipe was rotated. Oil based muds do not form into gel structure as easily as water based muds, and this may be one of the main reasons for the rapid mixing of the fluids in experiment #6, #7 and #8.

Due to visual measuring of the mixing zone in the experiments, there may be uncertainties. Fluids may rise or sink near the centre of the pipe which makes it impossible to observe the movement of the fluid and thus measure the length of the mixing zone. This may be the reason for the sudden increase in length and the high velocities.

6.3 Summary

As seen from the simulations in COMSOL, the density and the well size were the most contributing factors to the development of the mixing zone. Smaller density difference had most effect on the length of the mixing zone. Larger well contributed to a high maximum speed of the fluids and a smaller well reduced the length of the mixing zone. The cases were simulated for a period of ten hours, which results in a huge amount of time steps. Only a few of these were chosen to study and the results may have been much more accurate if all the time steps were studied. That would probably give the opportunity of measuring maximum velocity and development of mixing zone better. This may be an option for further studies, in addition to improvement of the model in COMSOL.

Yield strength, LSYS, gel properties, rotation force and friction from pipe wall are factors that were not taken into account. The only parameters that were contributing to the development of the mixing zone are density, plastic viscosity, interfacial tension, well size and diffusion coefficient. The diffusion coefficient was constant in all simulation cases, and does not affect the comparison of the various cases to the reference case. For some of the simulations there was reported a bug making the time show wrong values. There may also be other bugs in the model that is not verified and may affect the simulations results. This is difficult to verify, and it is probably only COMSOL support team that is capable of confirming any bugs. It is therefore difficult to determine whether the model is trustworthy and reliable or not. The COMSOL model in this thesis may be one of very few of its kind for a scenario with the HOL solution, and may have some improvements.

The results from the COMSOL simulations show that the mixing zone accelerates during the first hour while experiments prove otherwise. This may indicate that the model does not show a realistic scenario, at least not during the first hour. As observed in the figures of the screenshots of the surface concentration, it was during the first hour unrealistic values for the concentrations at the colour chart. This may imply that the model is trying to stabilize during the first hour, and may be the reason for the acceleration of the mixing zone. After 1 hour the speed of the mixing zone is decelerating, as it should.

According to the experiments yield strength and LSYS were two of the most contributing factors to the development of the mixing zone. High LSYS values give high gel properties resulting in stiffer fluids which mix poorly. Rotation of an inner pipe may contribute to a better mixing of the fluids. Both plastic viscosity and cross sectional area of the fluid column seems to have little effect on the mixing process between heavy and light fluids. Interfacial tension and friction from the pipe walls may have effect on the movement of the fluids. Neither of them were taken into consideration in this thesis, but this could be a topic for further studies.

Referring to section Appendix C, there is a proposal for avoiding a mixing zone between the heavy and light fluid. The experiment describes the use of a fluid plug between a heavy and a light fluid. This is not relevant if a mixing zone is desirable, but may be a solution were no contact between the fluids is necessary. It is possible for further studies for this solution if this is of interest.

7 CONCLUSION

This work covers theoretical and experimental studies of the HOL solution. For the numerical simulations, the COMSOL multiphysics software was used. For the experimental work, a simple arrangement was built for testing, including various fluids, operational parameters, fluid rheology properties, densities and model well sizes. The results are summarized as follows.

The COMSOL simulation study:

- A lower density difference between heavy and light fluid and/or a smaller wellbore reduces the speed of the mixing development.
- A larger wellbore size has shown an increasing effect on the maximum velocity of the fluids.
- Both increased and reduced viscosity difference between heavy and light fluid seem to have no or little effect on the development of the length of the mixing zone.

The experimental investigations provide the following results:

- The mix phenomenon of the fluid systems having high LSYS indicate a stable HOL interface. This fluid property reflects a stronger internal structure of the fluid system, which is associated with stiffer fluid of high gel strength.
- Fluids with high yield strength and a high LSYS have shown a poorly mixing property, i.e. a small or no mixing zone.
- Based on the observation above, the concept of fluid plug is introduced. This is to be placed between the heavy fluid and the light fluid, and could be a solution for Reelwell if no mixing is desired.
- Rotation of inner pipe may result in better and more even mixing of the fluids, but it is difficult to determine if the rotation has an effect on the development of the mixing zone and/or the velocity of the fluids.

Due to a software bug in some of the COMSOL simulations it is be difficult to determine the reliability of the model. However, the simulations show a reasonable result, which together with experiments, may give a fair picture of the mixing process between a

heavy and a light fluid. Both simulations and experiments demonstrate that various parameters may affect the development of the mixing zone.

Further studies may investigate the HOL solution with variation of other parameters such as interfacial tension, friction of inner wall of outer pipe, friction of outer wall of inner pipe and diffusion constant. These studies may also include investigation of fluid plug between heavy and light fluid, preventing the fluids from mixing.

REFERENCES

- [1] Walker, M. & Molloy, R., *Sakhalin-1: Technologies to Efficiently Drill and Develop Resources While Expanding the ERD Envelope*. Moscow, World Petroleum Congress 2014, p. 4.
- [2] Reelwell, *Technology description*, retrieved from: <http://www.reelwell.no/Technology/Description> (13.01.16)
- [3] Vandvik, E. A., *Experimental investigation at heavy light interface mixture of Reelwell ERD*. Master's Thesis, University of Stavanger, June 2014
- [4] Hurum, M., *Extended Reach Drilling using RDM – Heavy Over Light solution. Stability and control of the well annulus fluid*. Master's Thesis, University of Stavanger, June 2015
- [5] Reelwell homepage, retrieved from: <http://www.reelwell.no> (14.01.2016)
- [6] Vestavik, O., Egorenkov, M., Schmalhorst, B., Falcao, J.: *Extended Reach Drilling – new solution with a unique potential (SPE/IADC 163463)*. SPE/IADC Drilling Conference and Exhibition, Amsterdam, The Netherlands, 2013
- [7] Vestavik, O., Kerr, S., Brown, S.: *Reelwell Drilling Method (SPE/IADC 119491)*. SPE/IADC Drilling Conference and Exhibition, Amsterdam, The Netherlands, 2009
- [8] Douglas, J.F., Gasiorek, J.M., Swaffield, J.A., Jack, L.b., *Fluid Mechanics*, Fifth edition, 2005, p. 10-11
- [9] The Physics Classroom, *Newton's Law of Universal Gravitation*, retrieved from: <http://www.physicsclassroom.com/class/circles/Lesson-3/Newton-s-Law-of-Universal-Gravitation> (18.01.2016)

- [10] Barnes, H. A., *Viscosity*, Institute of Non-Newtonian Fluid Mechanics, University of Wales, 2002
- [11] Evje, S., Fjelde, K. K., *Hybrid Flux-Splitting Schemes for a Two-Phase Flow Model*. Journal of Computational Physics 175, 2002
- [12] Encyclopædia Britannica, *Convection*, retrieved from: <http://www.britannica.com/science/convection> (26.01.2016)
- [13] COMSOL Multiphysics Cyclopedia, *What is Diffusion?*, retrieved from: <https://www.comsol.com/multiphysics/what-is-diffusion> (04.05.2016)
- [14] Atkins P., Paula, J. de, *Atkins' Physical Chemistry*, 8th ed., chapter 21, Oxford University Press, 2006
- [15] PetroWiki, *Interfacial Tension*, retrieved from: http://petrowiki.org/Interfacial_tension (01.02.2016)
- [16] B. Aadnøy, I. Cooper, S. Miska, R. Mitchell and M. Payne, *Advanced Drilling and Well Technology*. Richardson, TX: Society of Petroleum Engineers, 2009
- [17] Ochoa, M. V., *Analysis of Drilling Fluid Rheology and Tool Joint Effect to Reduce Errors in Hydraulics Calculations*, PhD Thesis, Texas A&M University, August 2006.
- [18] *Sarat Chandra Kuchibhatla // Experimental Investigation Of The Effect Of Initial Conditions On Rayleigh-Taylor Instability Master Of Science Thesis August 2010*
- [19] Reckinger, S., *Direct Numerical Simulation of Rayleigh-Taylor Instability Preliminary Examination Research Presentation*, 2009

- [20] Li, X. L., Jin, B. X., Glimm, J., *Numerical Study for the Three-Dimensional Rayleigh-Taylor Instability through the TVD/AC Scheme and Parallel Computation*, revised January 1996
- [21] COMSOL Multiphysics version 5.2 (2016), *COMSOL Multiphysics, Help User's Guide*.
- [22] COMSOL Multiphysics Cyclopedia, *Navier-Stokes Equations*, retrieved from: <https://www.comsol.com/multiphysics/navier-stokes-equations> (14.06.2016)
- [23] COMSOL Multiphysics software
- [24] COMSOL Multiphysics Cyclopedia, *Diffusion Coefficient*, retrieved from: <https://www.comsol.com/multiphysics/diffusion-coefficient> (03.05.2016)
- [25] Dhatt, G., Lefrancois, E., Touzot, G., *Finite Element Method*, John Wiley & Sons, 2012
- [26] COMSOL, *COMSOL Blog: Meshing Considerations for Linear Static Problems*, retrieved from: <https://www.comsol.com/blogs/meshing-considerations-linear-static-problems/> (20.05.2016)

APPENDIX A SIMULATION RESULTS

A-1 Results Reference Case

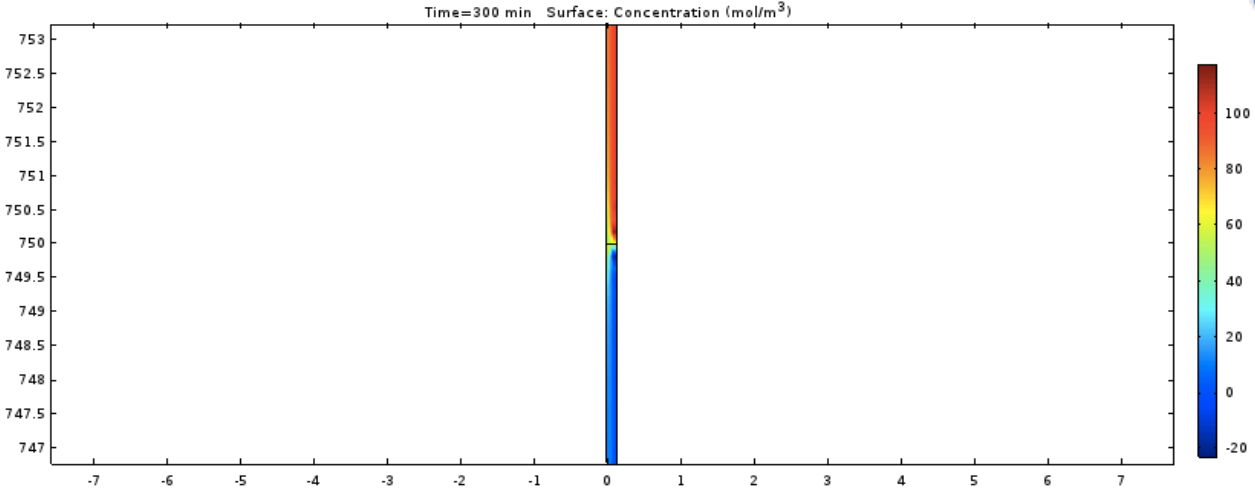


Figure A- 1: Surface concentration reference case, after 5 minutes

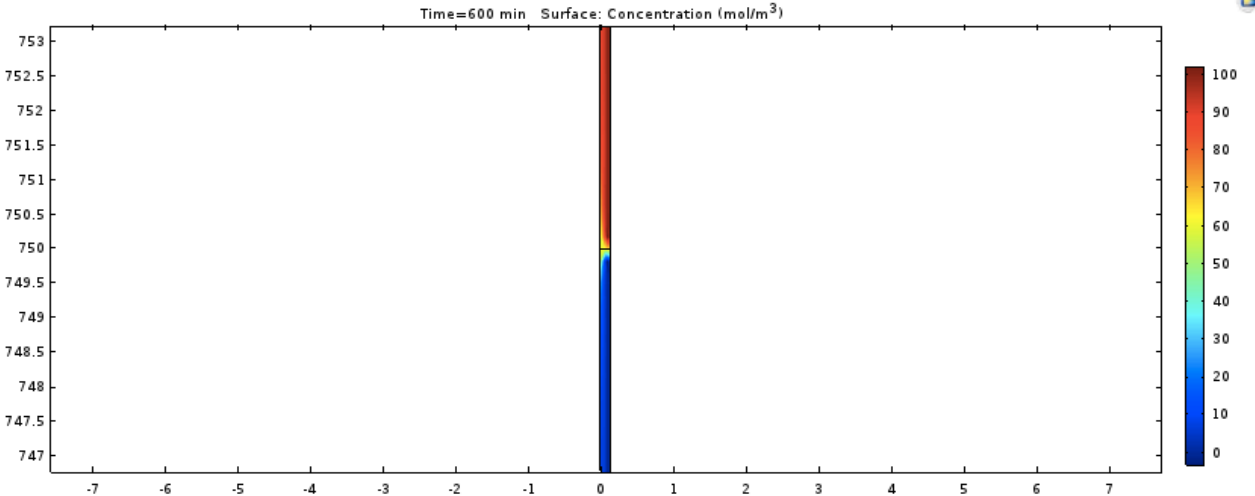


Figure A- 2: Surface concentration reference case, after 10 minutes

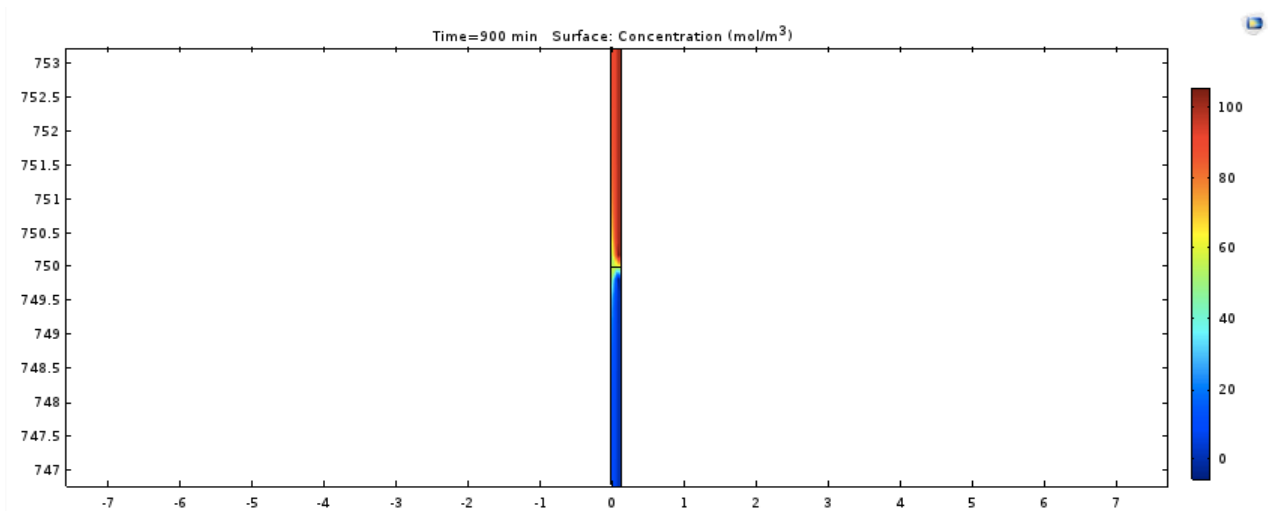


Figure A- 3: Surface concentration reference case, after 15 minutes

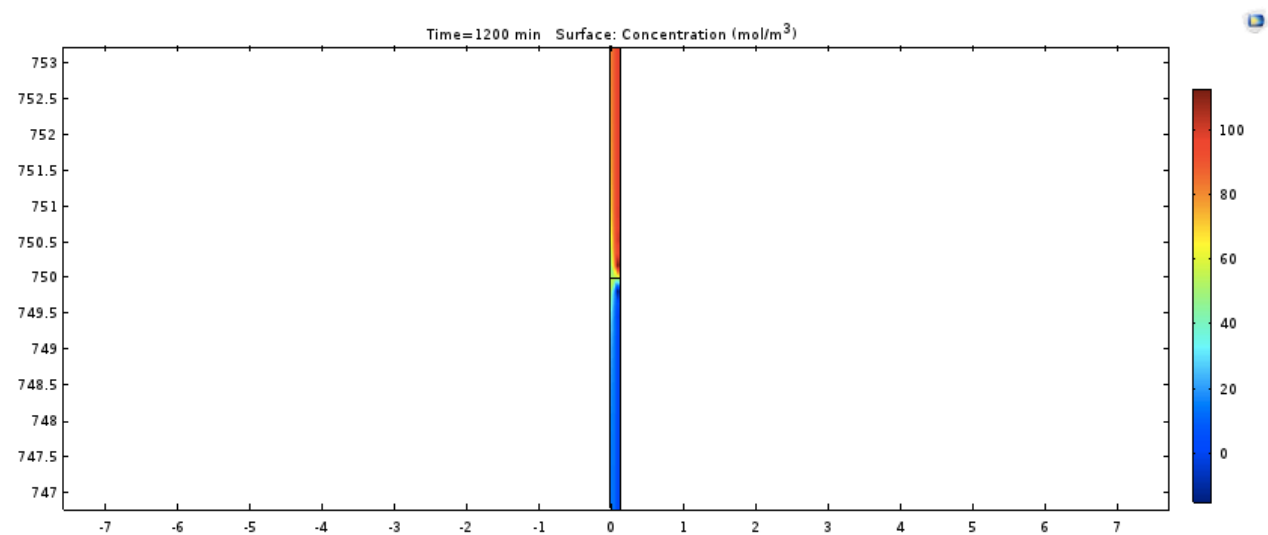


Figure A- 4: Surface concentration reference case, after 20 minutes

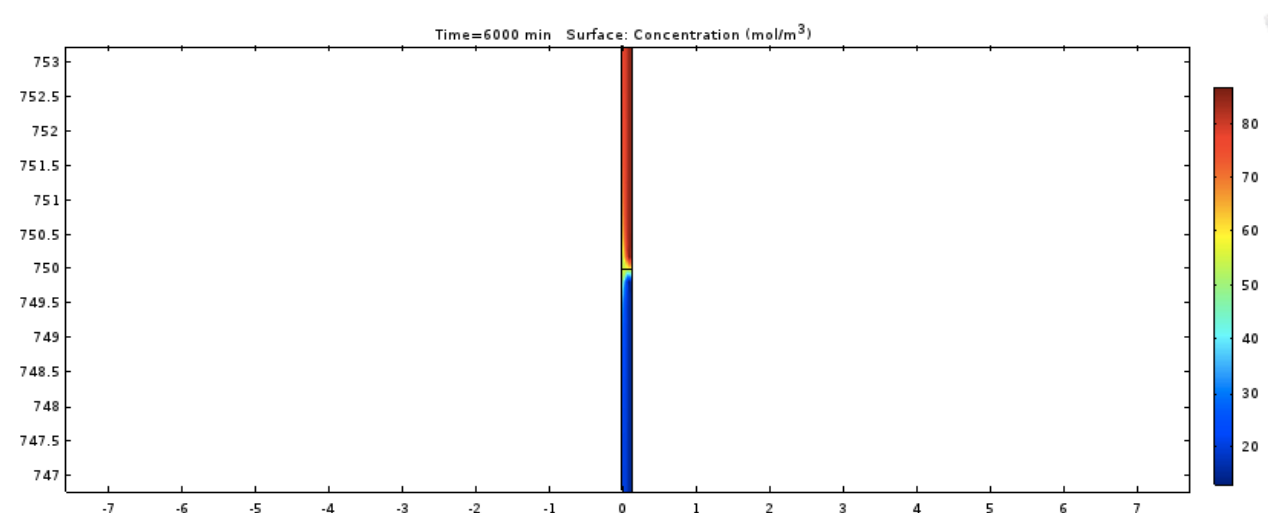


Figure A- 5: Surface concentration reference case, after 100 minutes

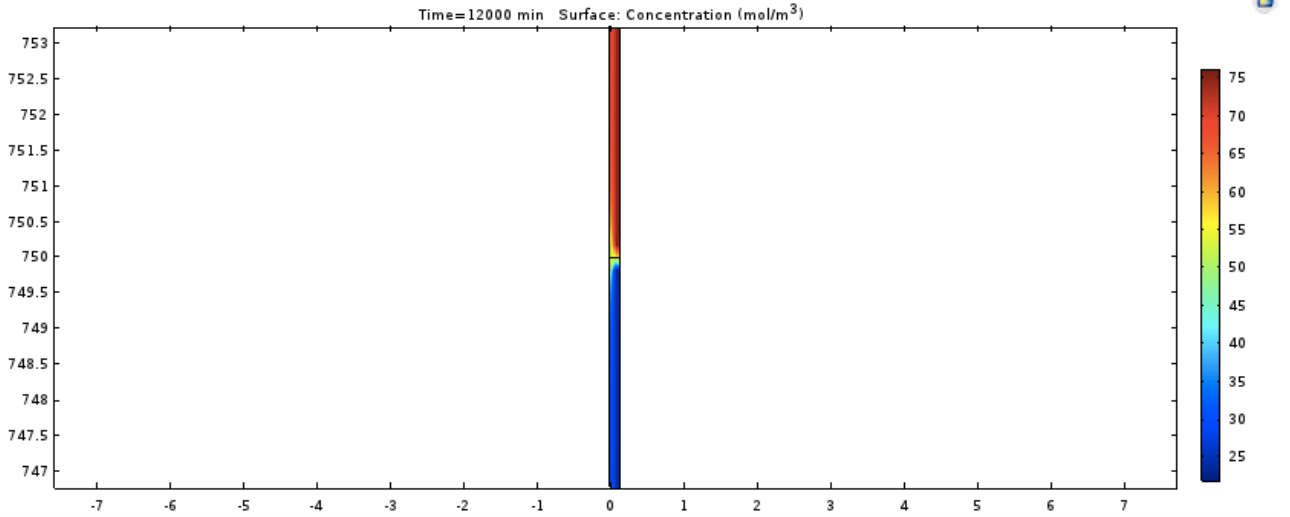


Figure A- 6: Surface concentration reference case, after 200 minutes

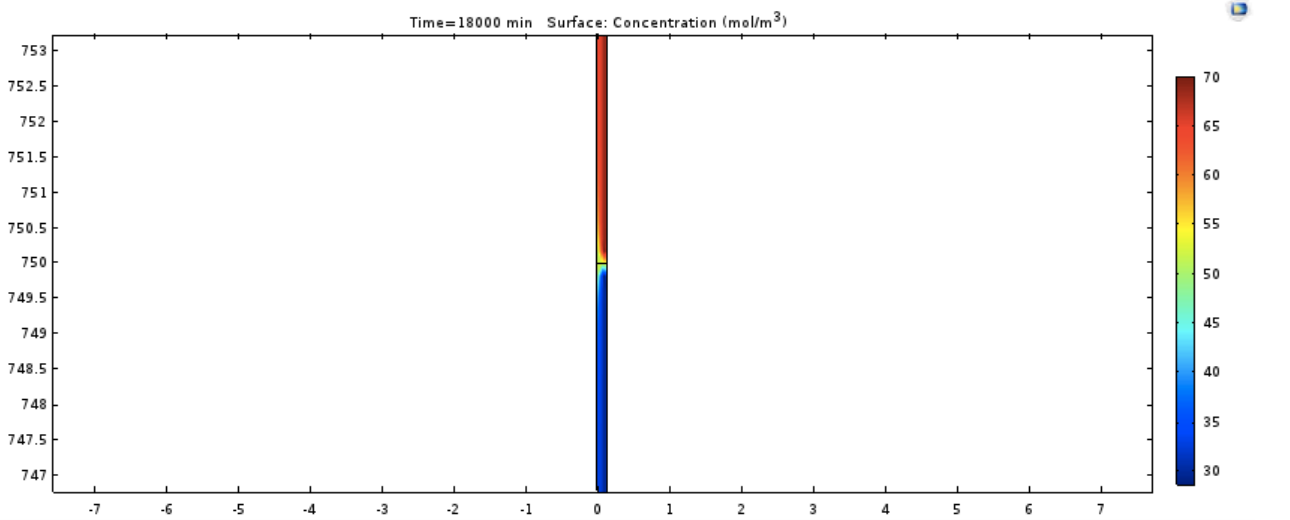


Figure A- 7: Surface concentration reference case, after 300 minutes

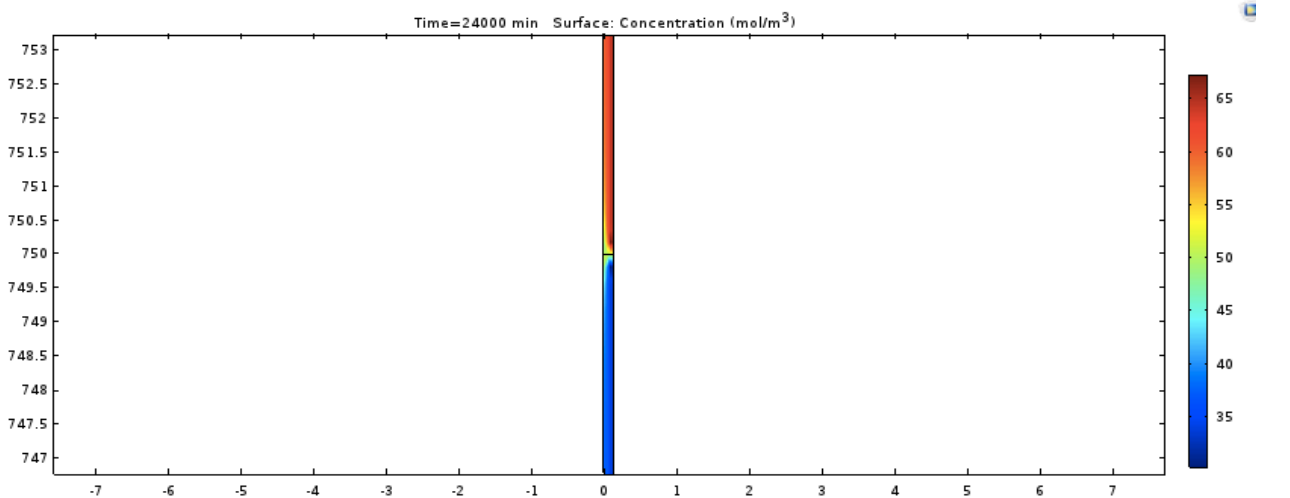


Figure A- 8: Surface concentration reference case, after 400 minutes

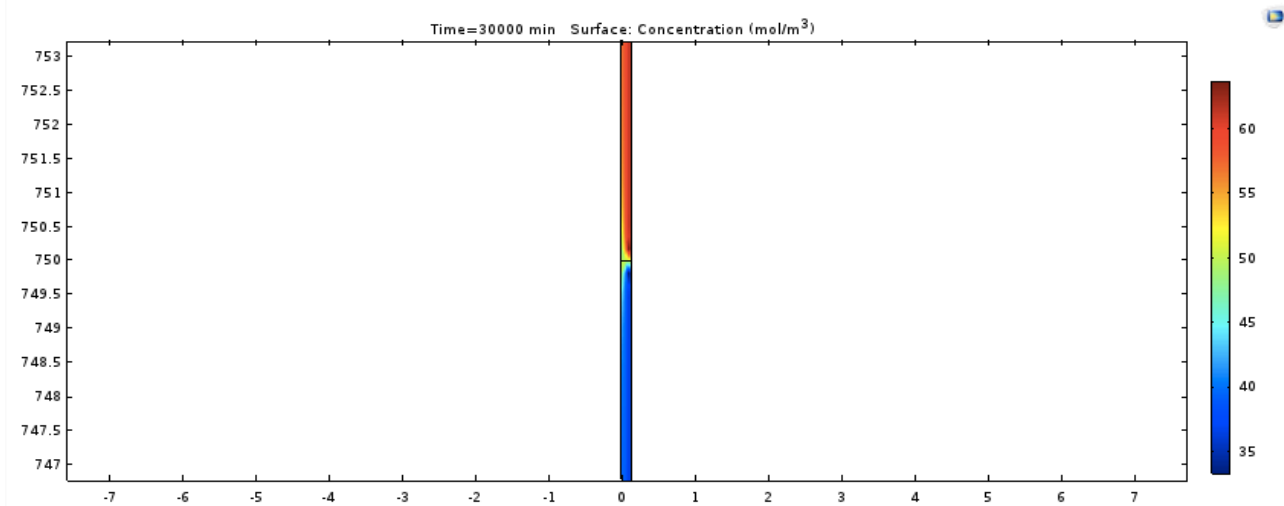


Figure A- 9: Surface concentration reference case, after 500 minutes

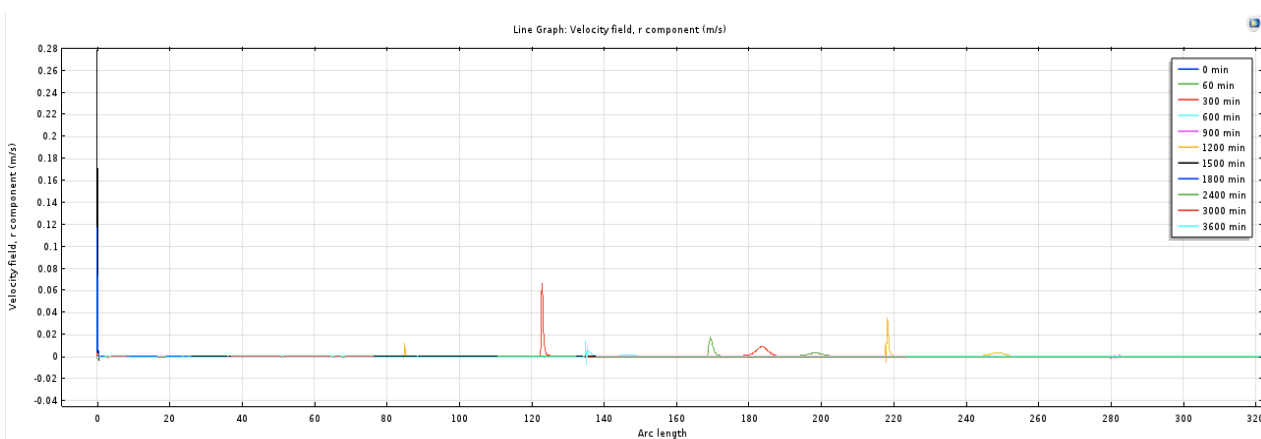


Figure A- 10: Line graph velocity field on bottom of fluid column, reference case, during 1 hour

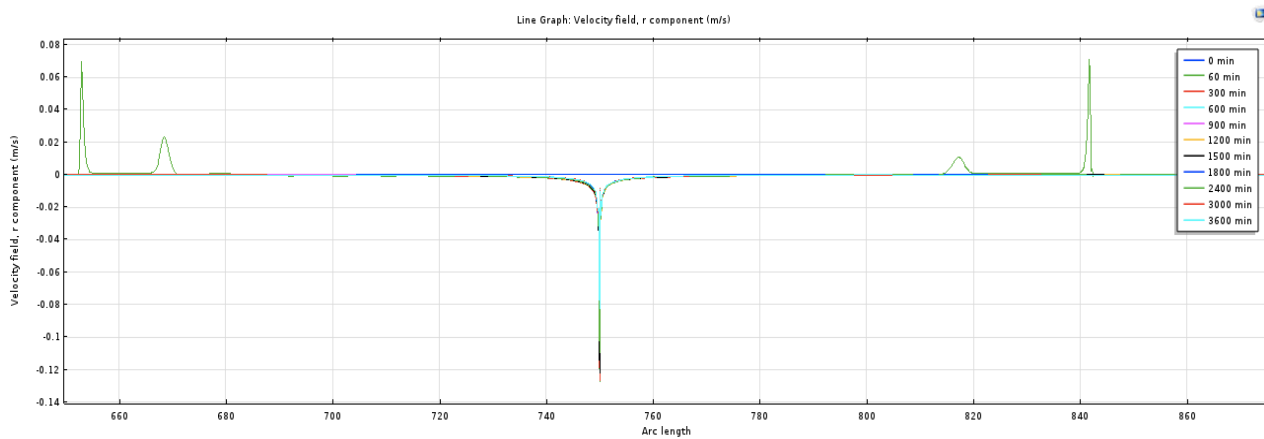


Figure A- 11: Line graph velocity field at interface, reference case, during 1 hour

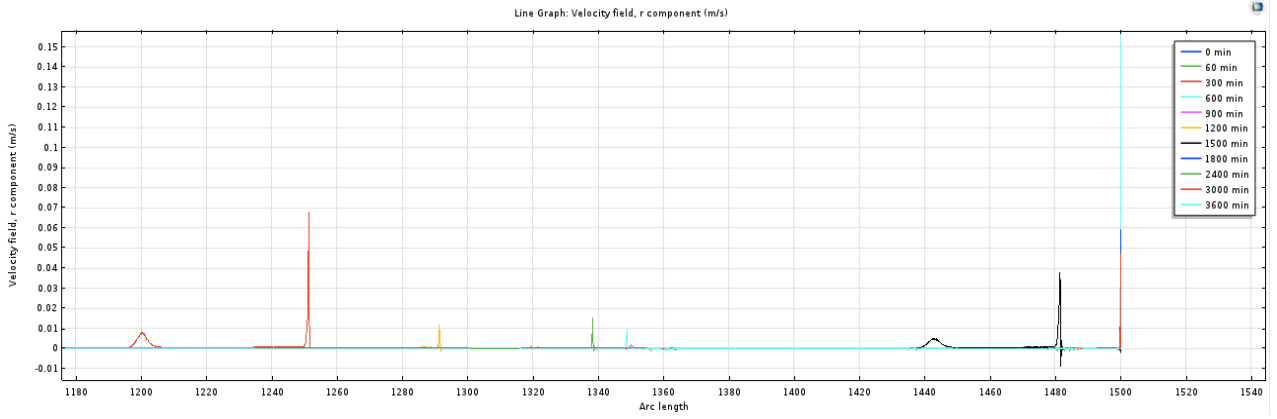


Figure A- 12: Line graph velocity field on top of fluid column, reference case during 1 hour

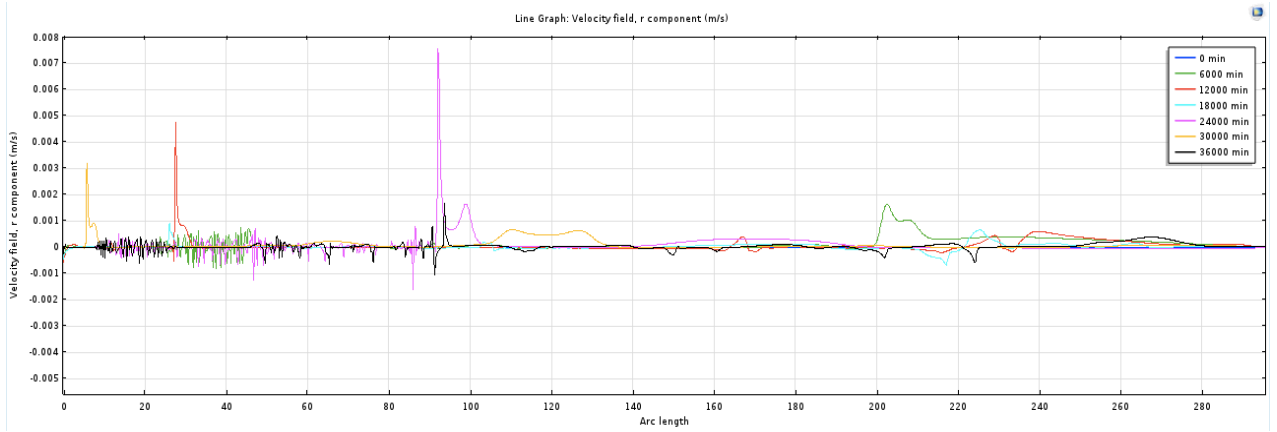


Figure A- 13: Line graph velocity field on bottom of fluid column, reference case, during 10 hours

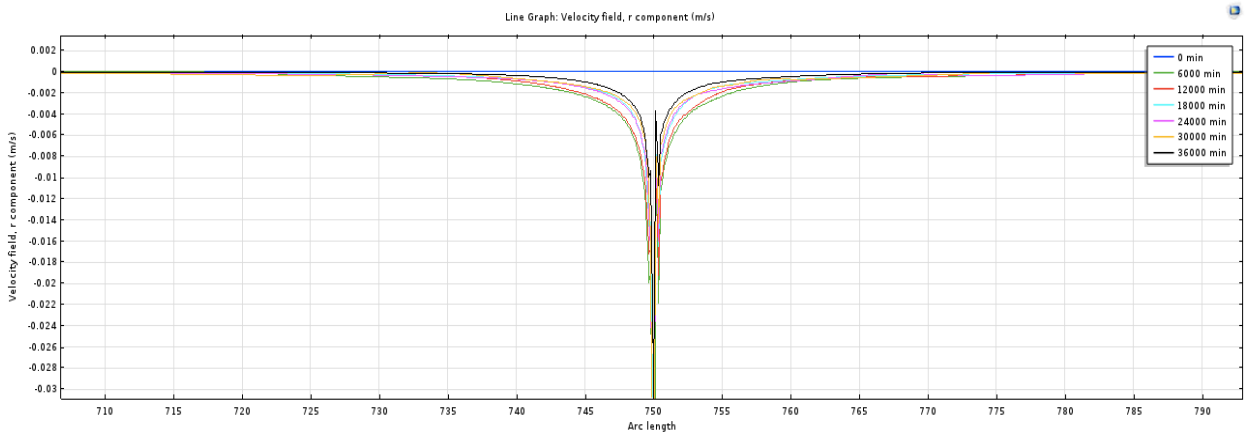


Figure A- 14: Line graph velocity field at interface, reference case, during 10 hours

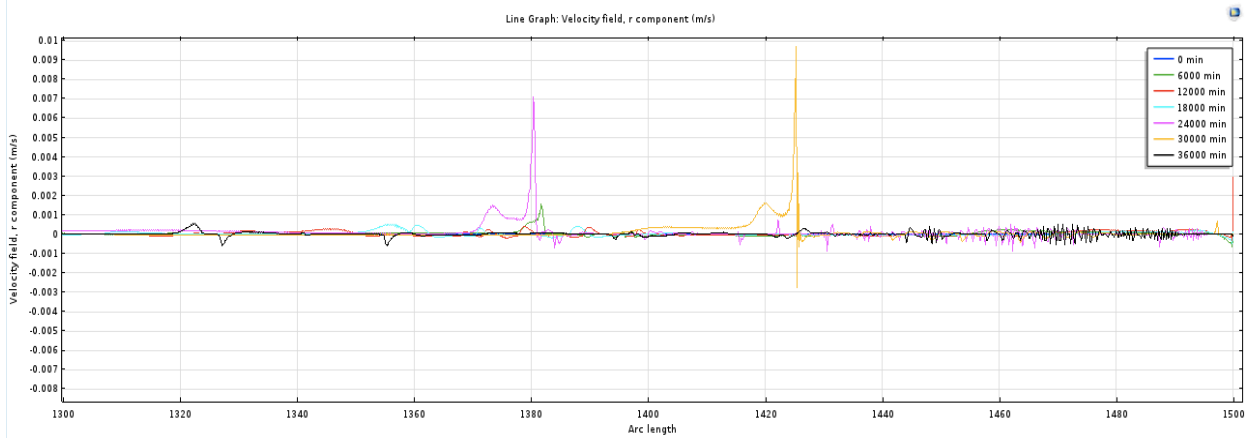


Figure A- 15: Line graph velocity field on top of fluid column, reference case, during 10 hours

A-2 Effect of Density

A-2.1 Density Difference 1

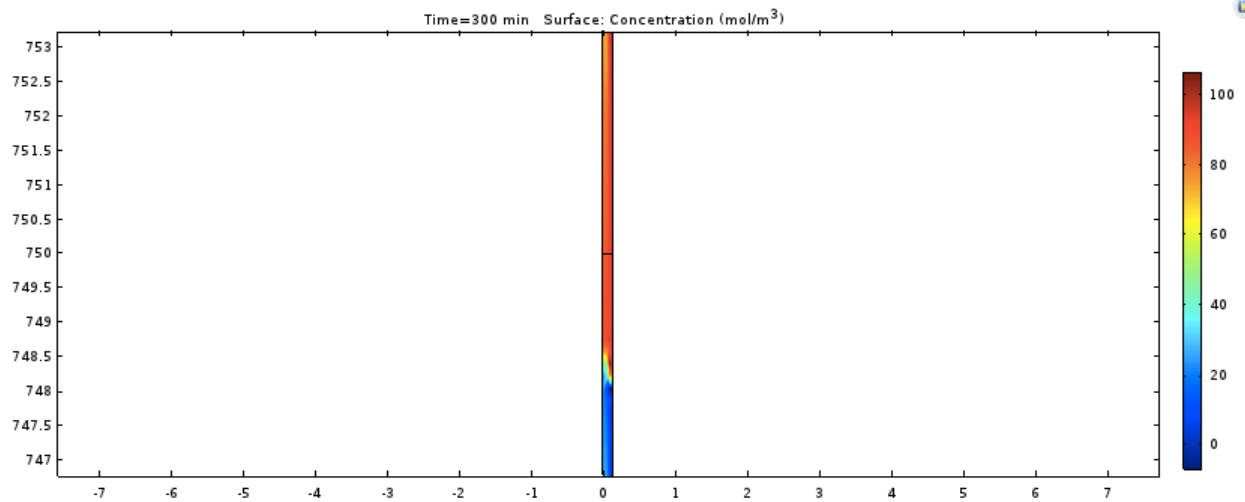


Figure A- 16: Surface concentration, density difference 1, after 5 minutes

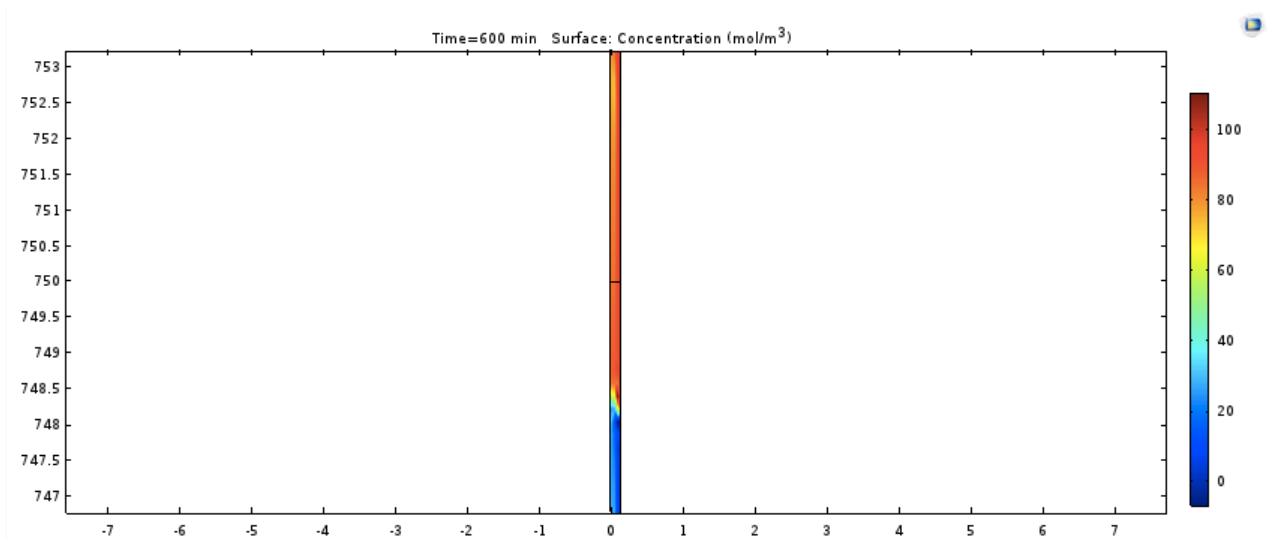


Figure A- 17: Surface concentration, density difference 1, after 10 minutes

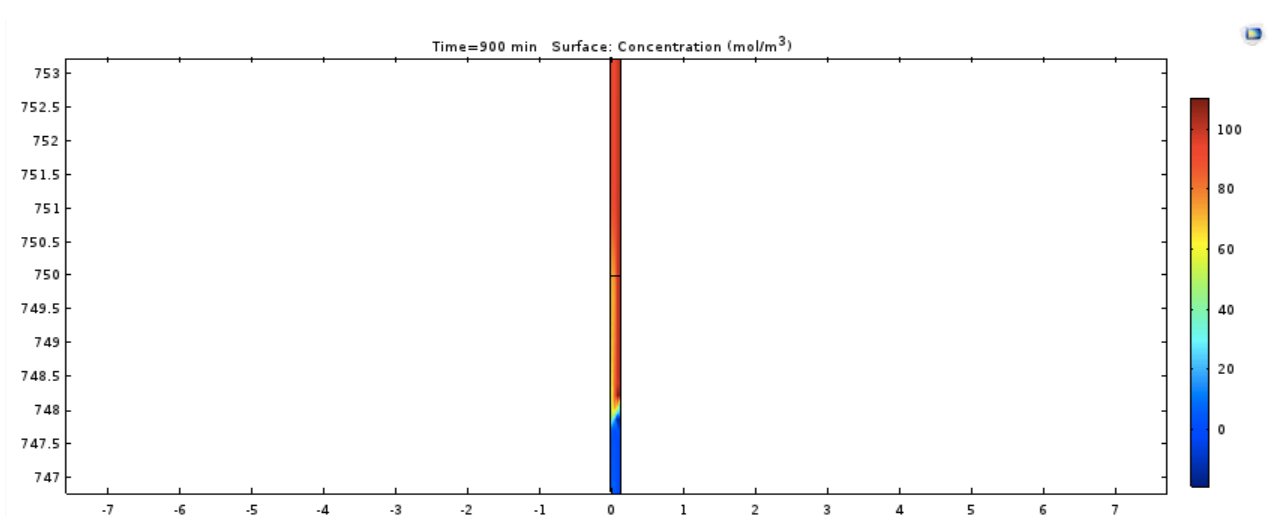


Figure A- 18: Surface concentration, density difference 1, after 15 minutes

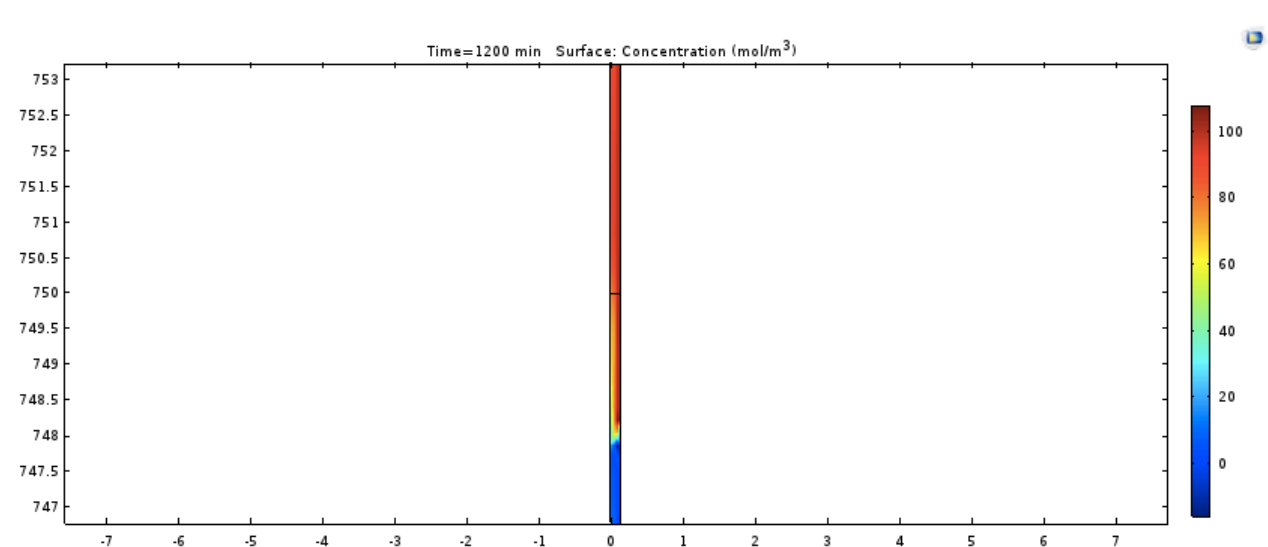


Figure A- 19: Surface concentration, density difference 1, after 20 minutes

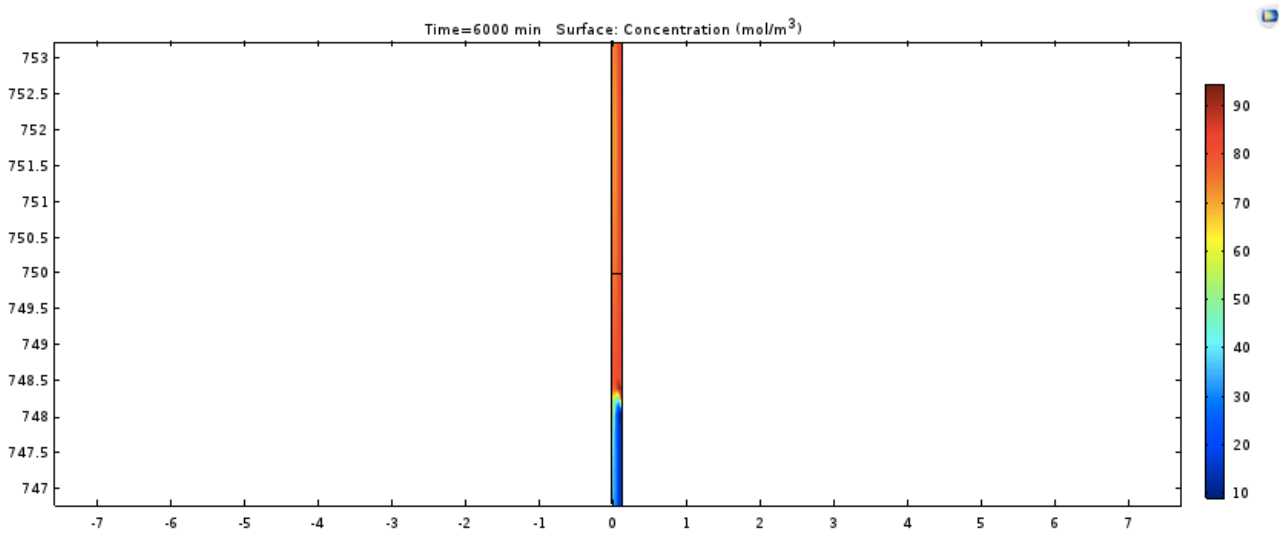


Figure A- 20: Surface concentration, density difference 1, after 100 minutes

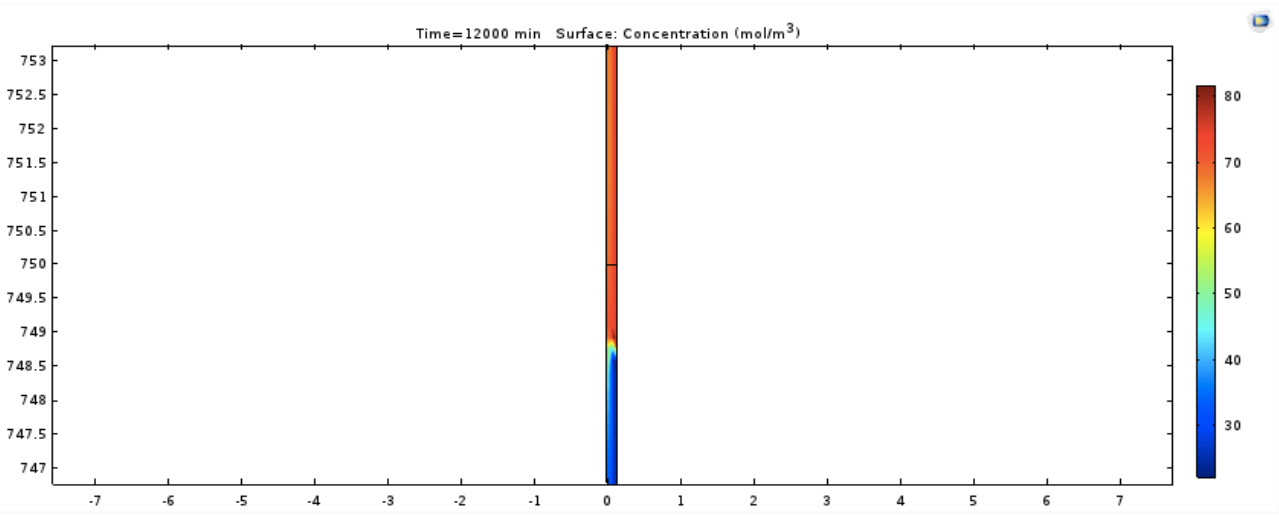


Figure A- 21: Surface concentration, density difference 1, after 200 minutes

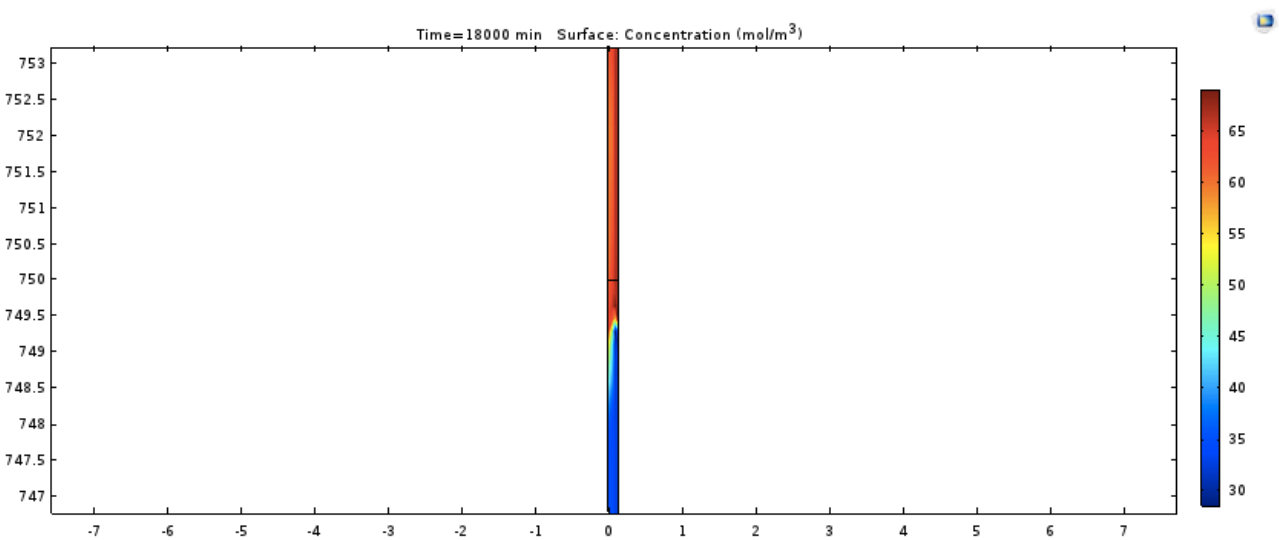


Figure A- 22: Surface concentration, density difference 1, after 300 minutes

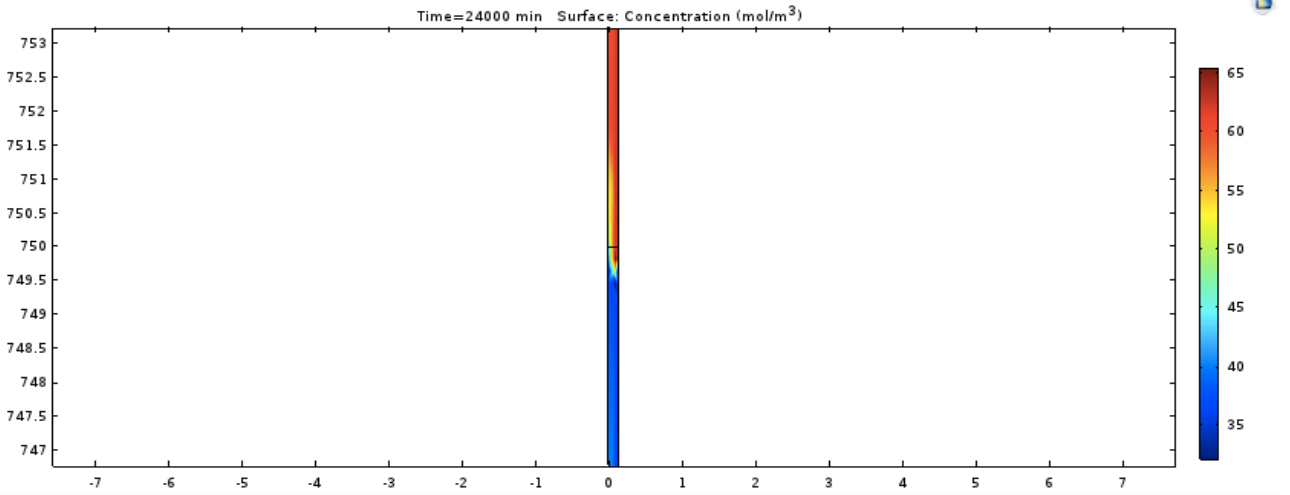


Figure A- 23: Surface concentration, density difference 1, after 400 minutes

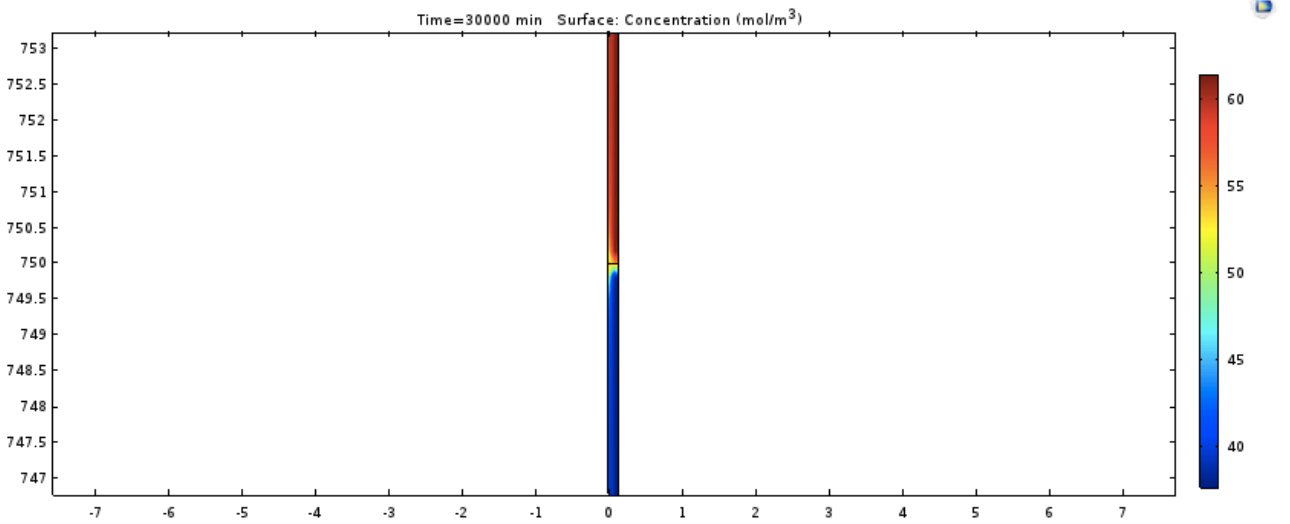


Figure A- 24: Surface concentration, density difference 1, after 500 minutes

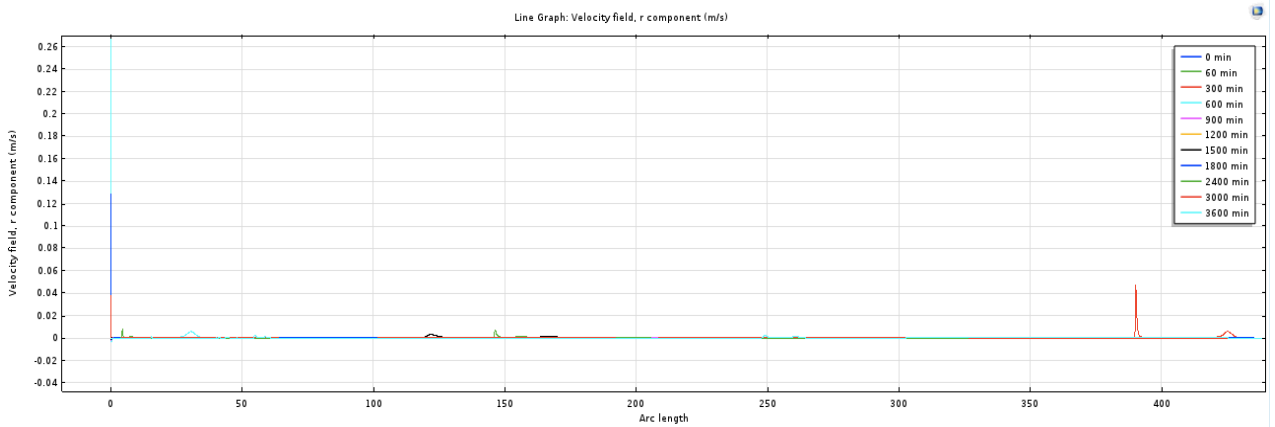


Figure A- 25: Line graph velocity field on bottom of fluid column, density difference 1, during 1 hour

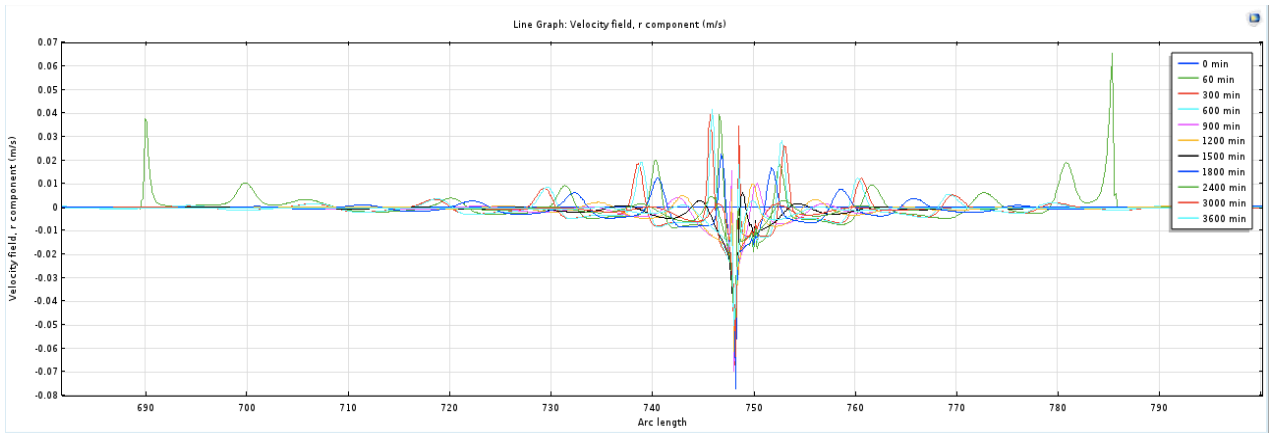


Figure A- 26: Line graph velocity field at interface, density difference 1, during 1 hour

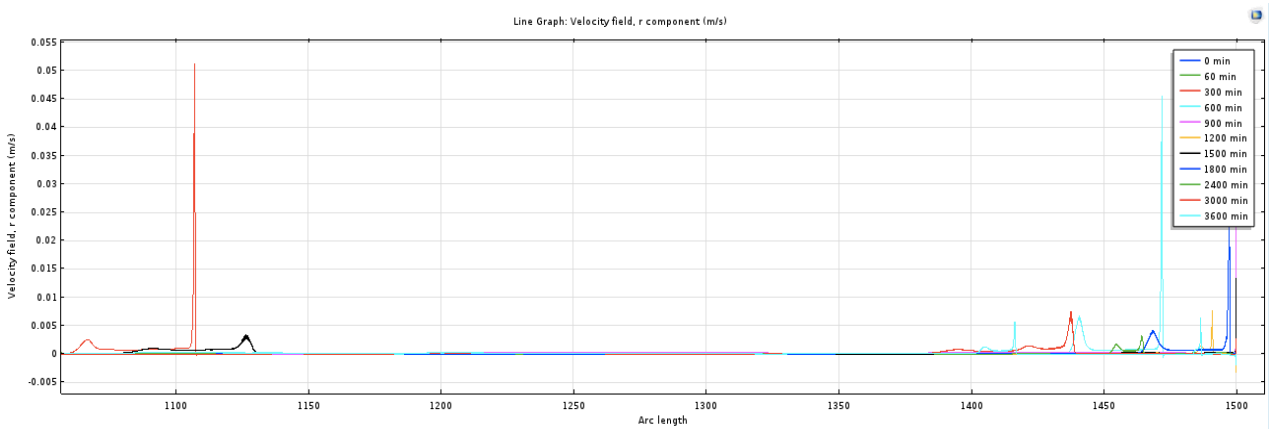


Figure A- 27: Line graph velocity field on top of fluid column, density difference 1, during 1 hour

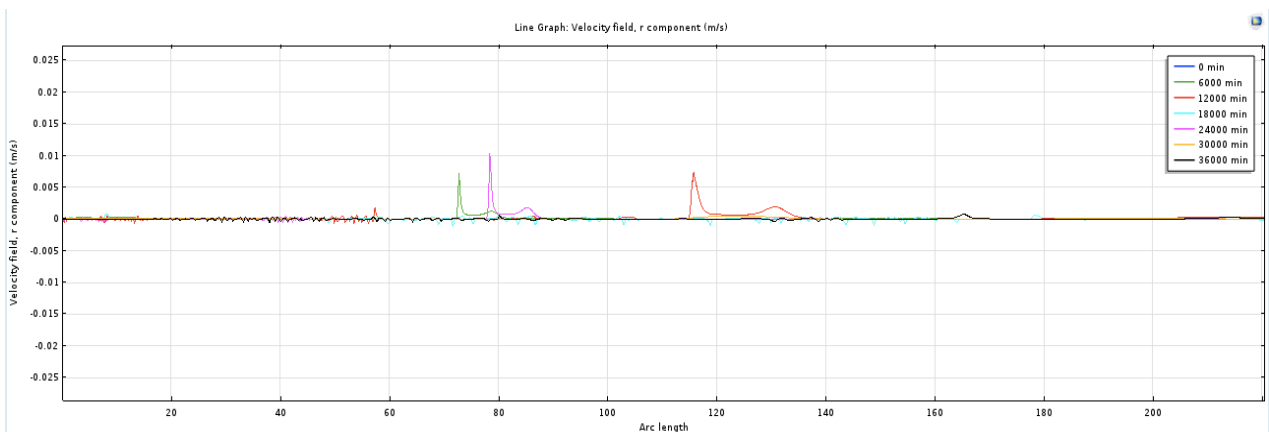


Figure A- 28: Line graph velocity field on bottom of fluid column, density difference 1, during 10 hours

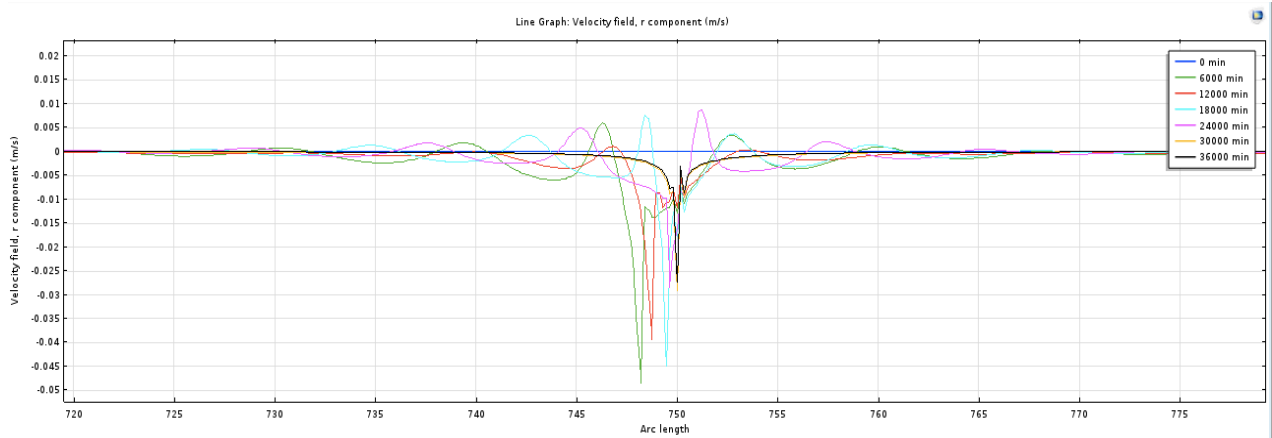


Figure A- 29: Line graph velocity field at interface, density difference 1, during 10 hours

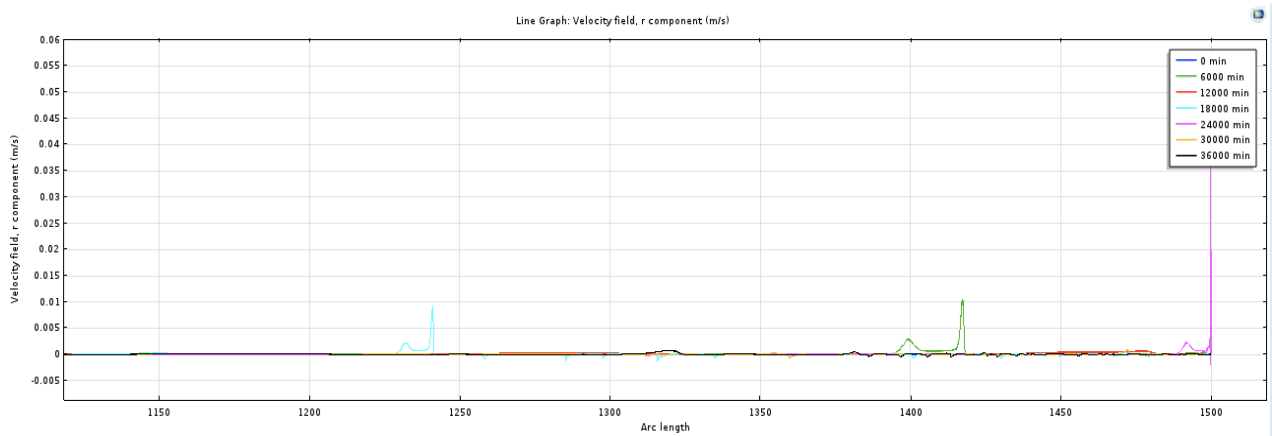


Figure A- 30: Line graph velocity field on top of fluid column, density difference 1, during 10 hours

A-2.2 Density Difference 2

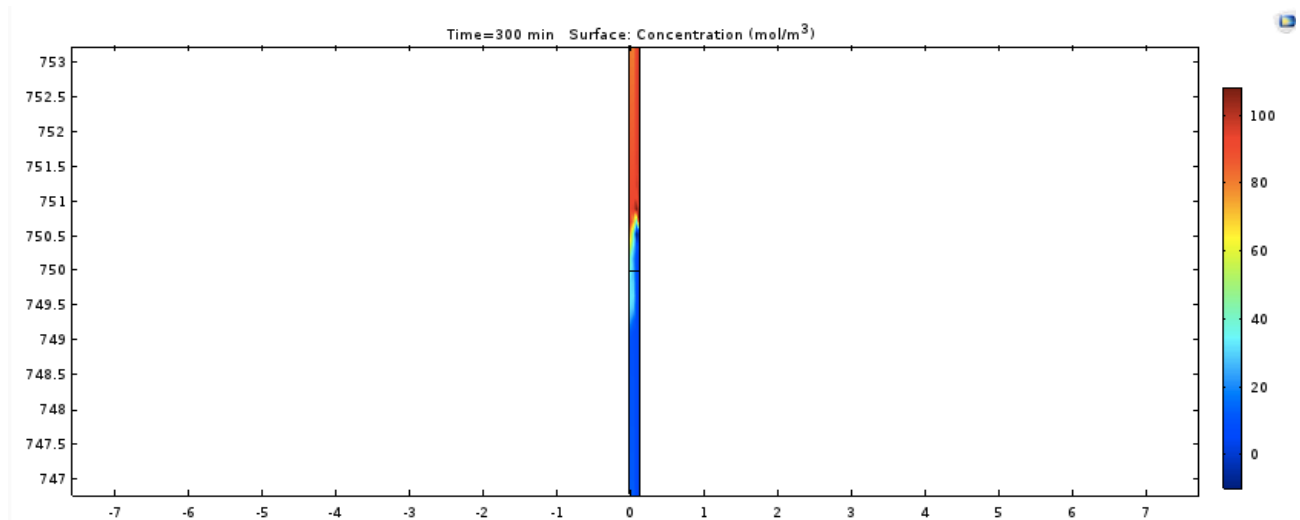


Figure A- 31: Surface concentration, density difference 2, after 5 minutes

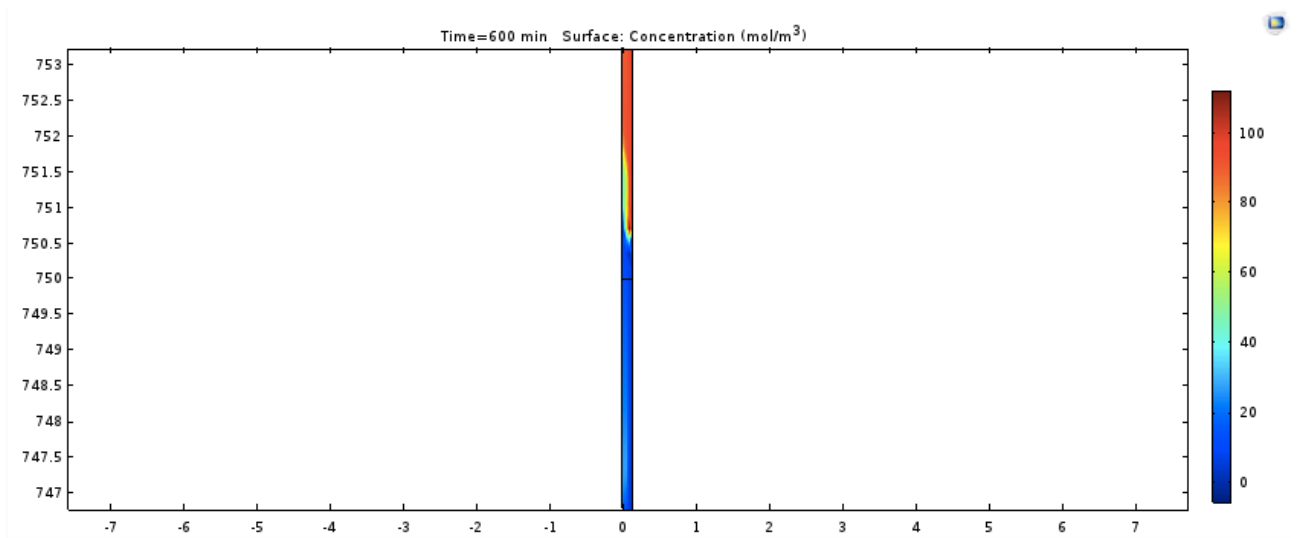


Figure A- 32: Surface concentration, density difference 2, after 10 minutes

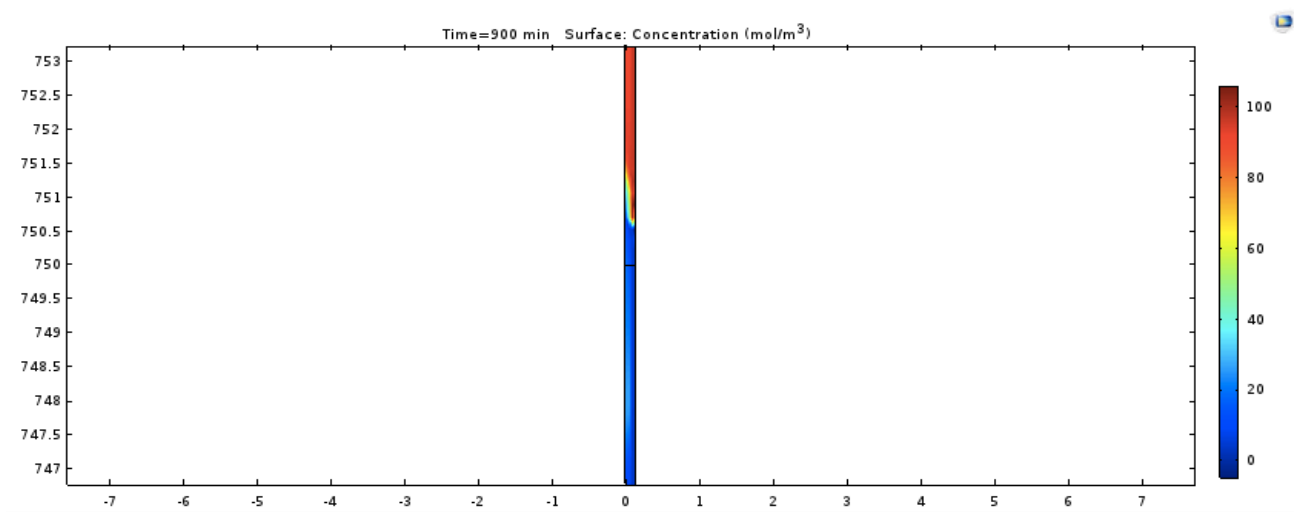


Figure A- 33: Surface concentration, density difference 2, after 15 minutes

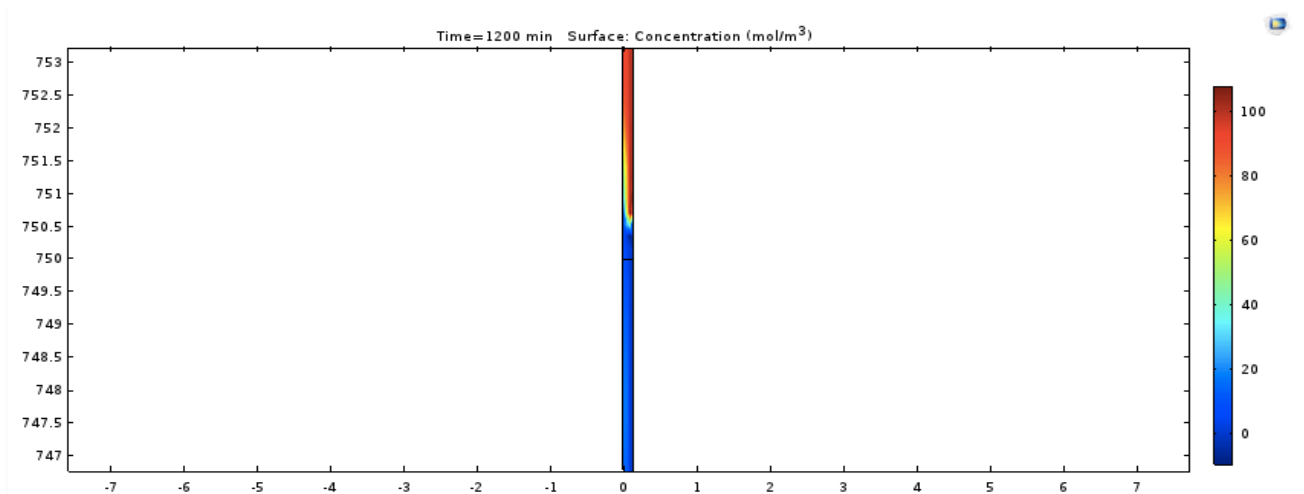


Figure A- 34: Surface concentration, density difference 2, after 20 minutes

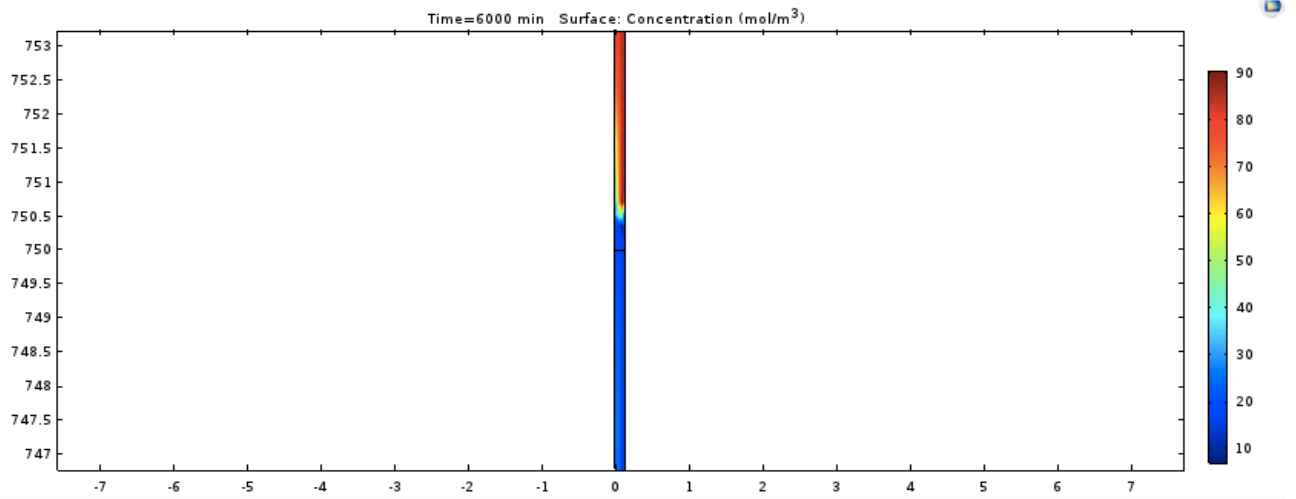


Figure A- 35: Surface concentration, density difference 2, after 100 minutes

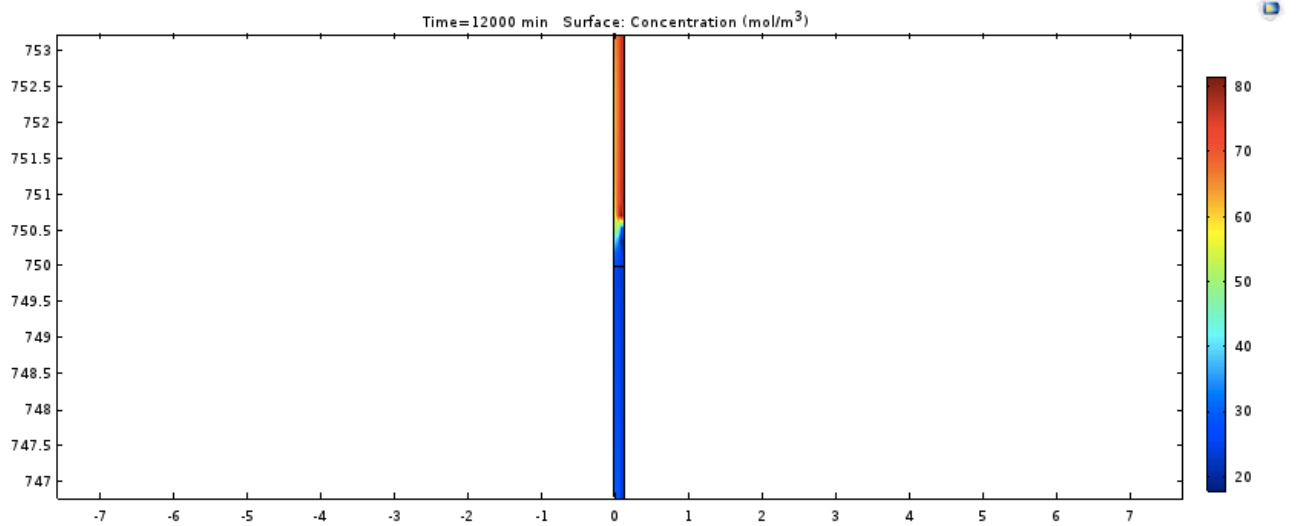


Figure A- 36: Surface concentration, density difference 2, after 200 minutes

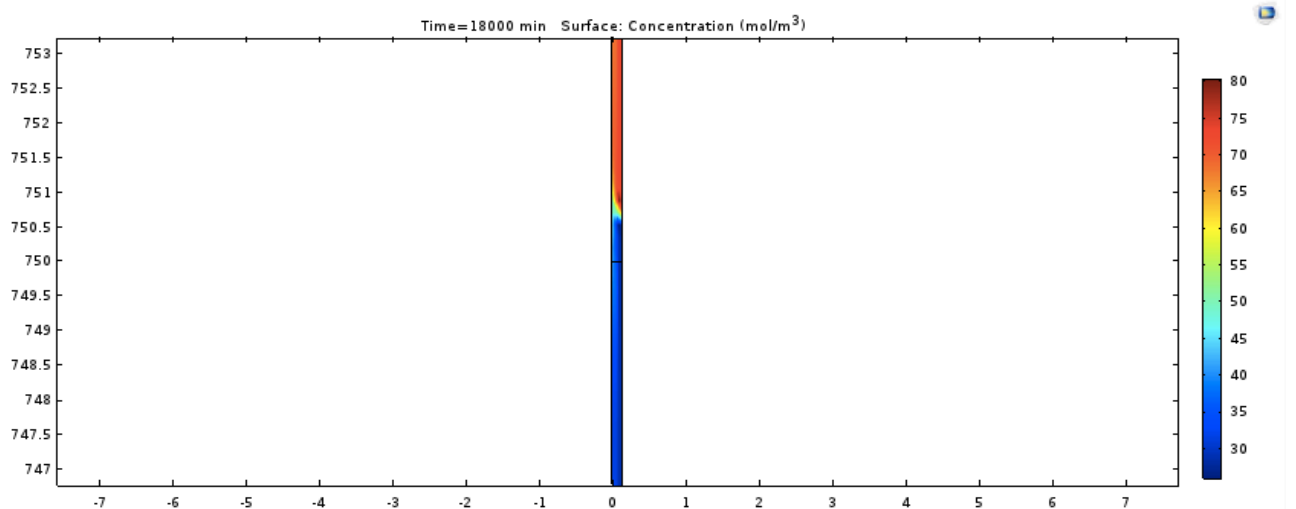


Figure A- 37: Surface concentration, density difference 2, after 300 minutes

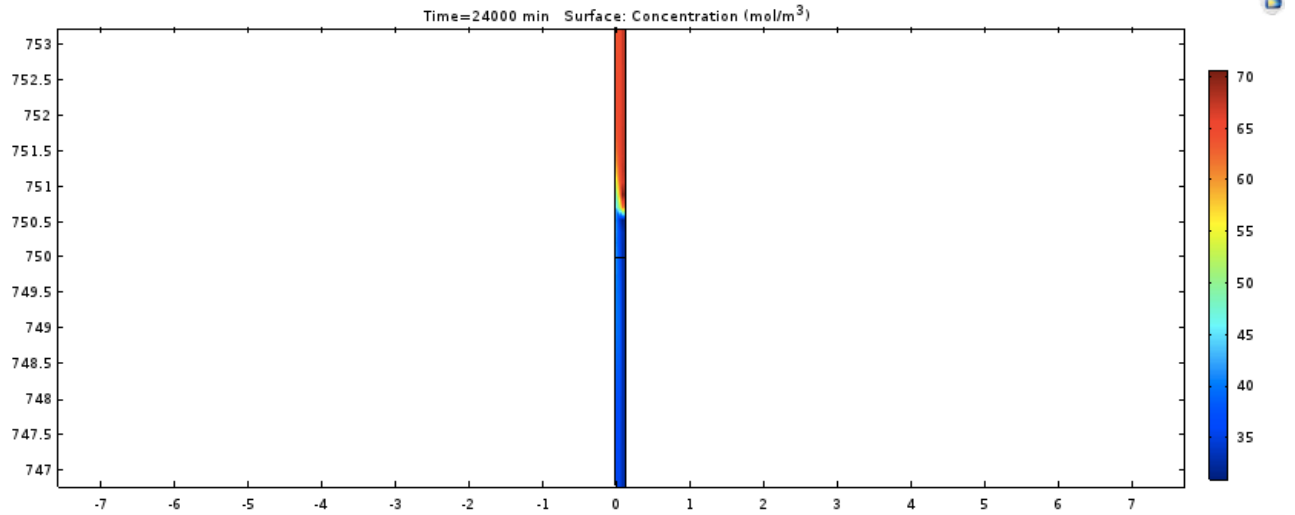


Figure A- 38: Surface concentration, density difference 2, after 400 minutes

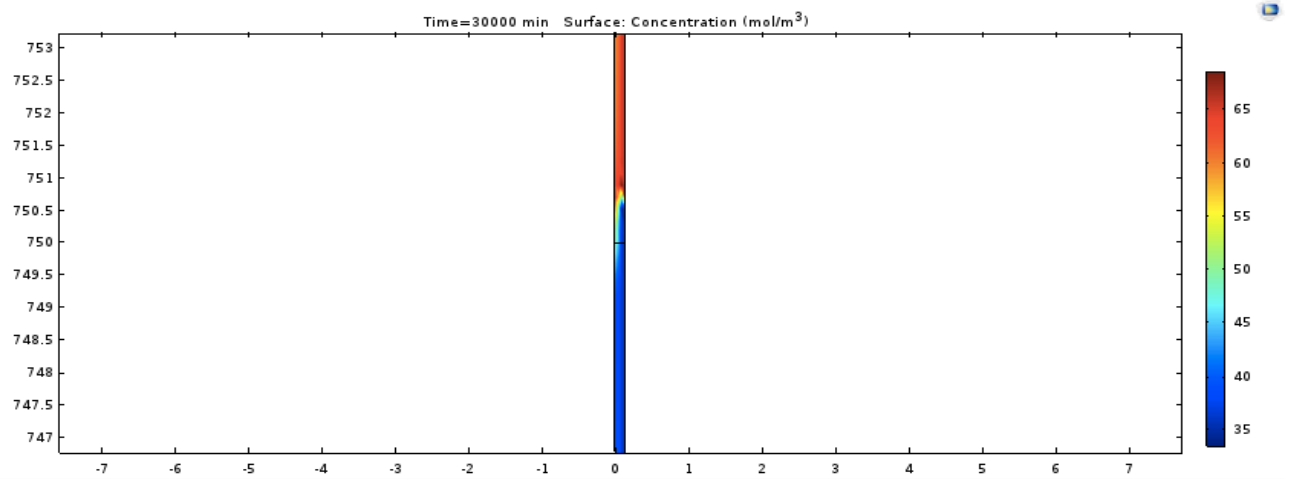


Figure A- 39: Surface concentration, density difference 2, after 500 minutes

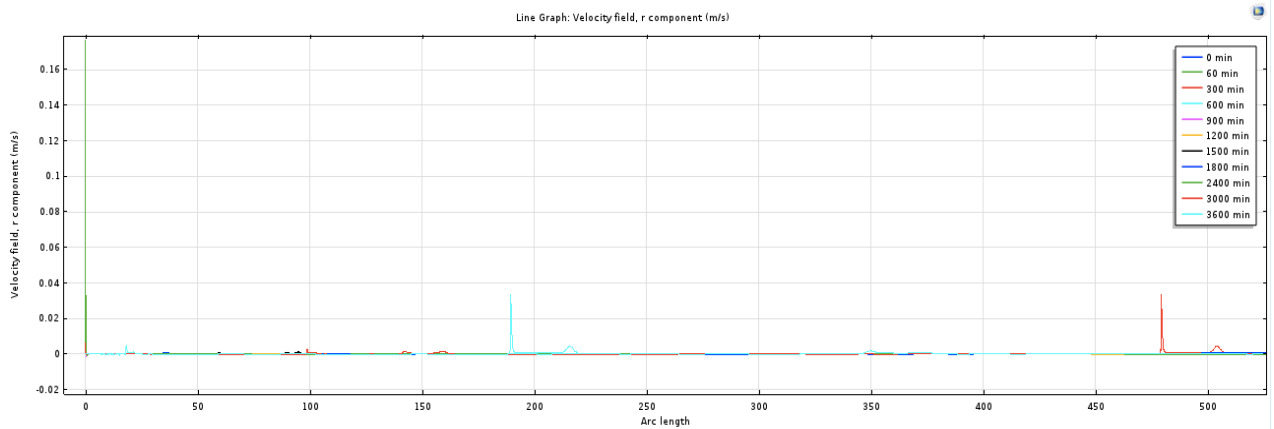


Figure A- 40: Line graph velocity field on bottom of fluid column, density difference 2, during 1 hour

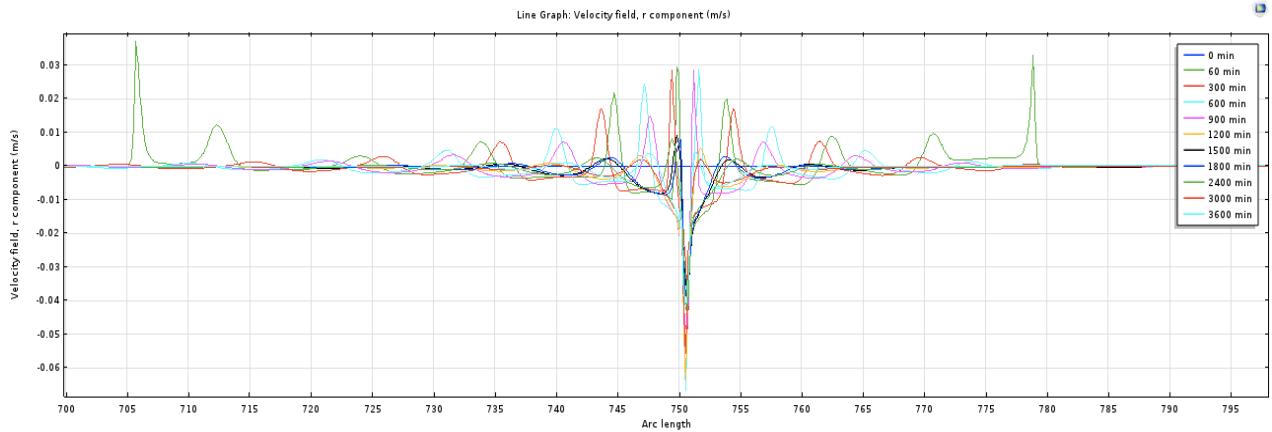


Figure A- 41: Line graph velocity field at interface, density difference 2, during 1 hour

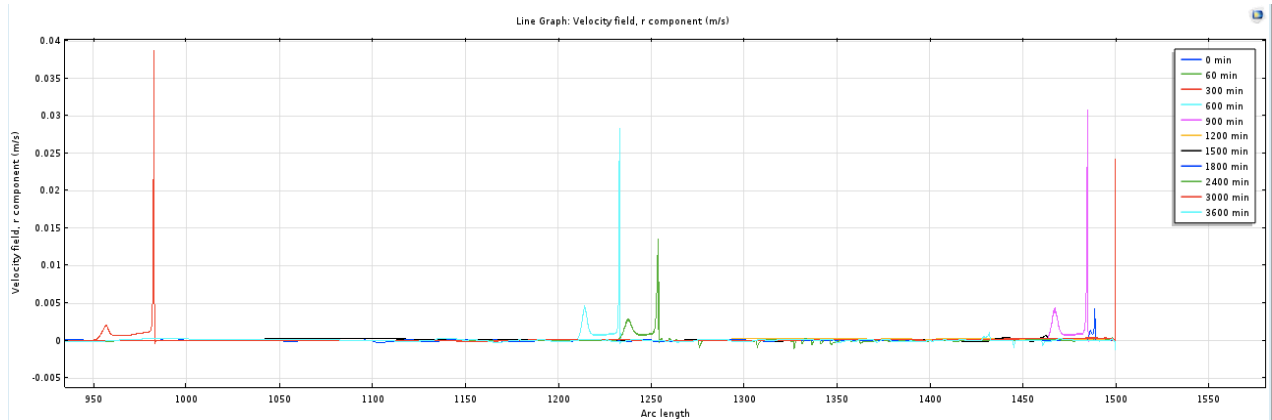


Figure A- 42: Line graph velocity field on top of fluid column, density difference 2, during 1 hour

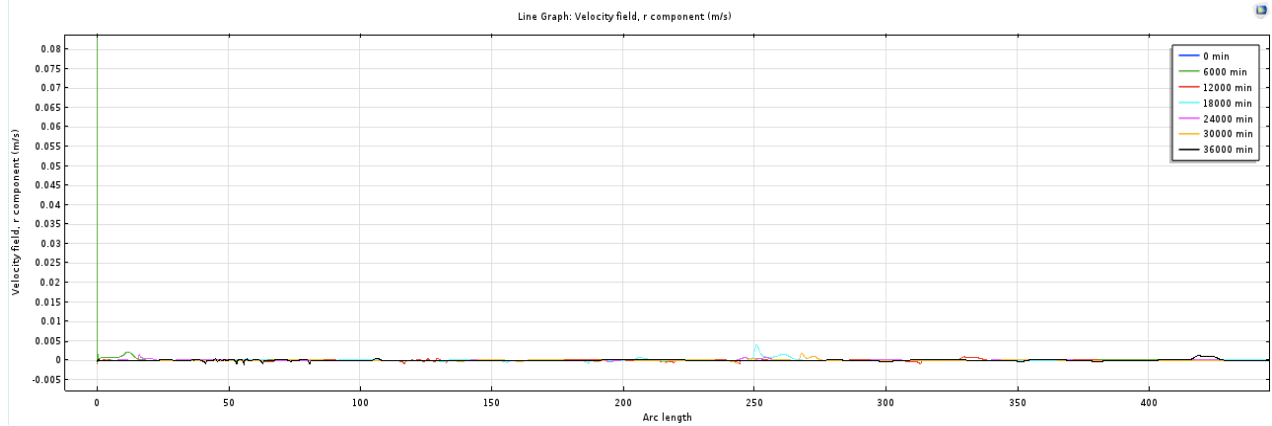


Figure A- 43: Line graph velocity field on bottom of fluid column, density difference 2, during 10 hours

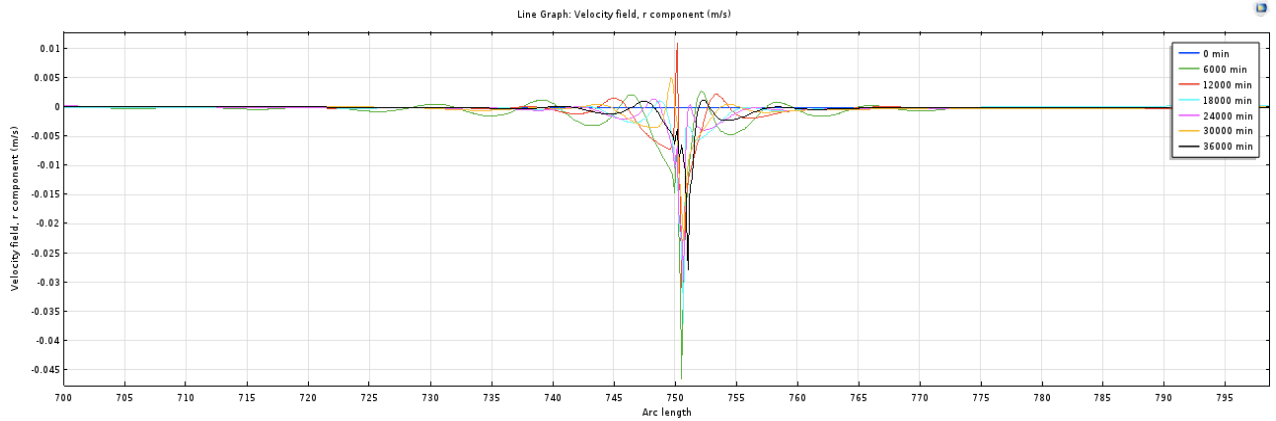


Figure A- 44: Line graph velocity field at interface, density difference 2, during 10 hours

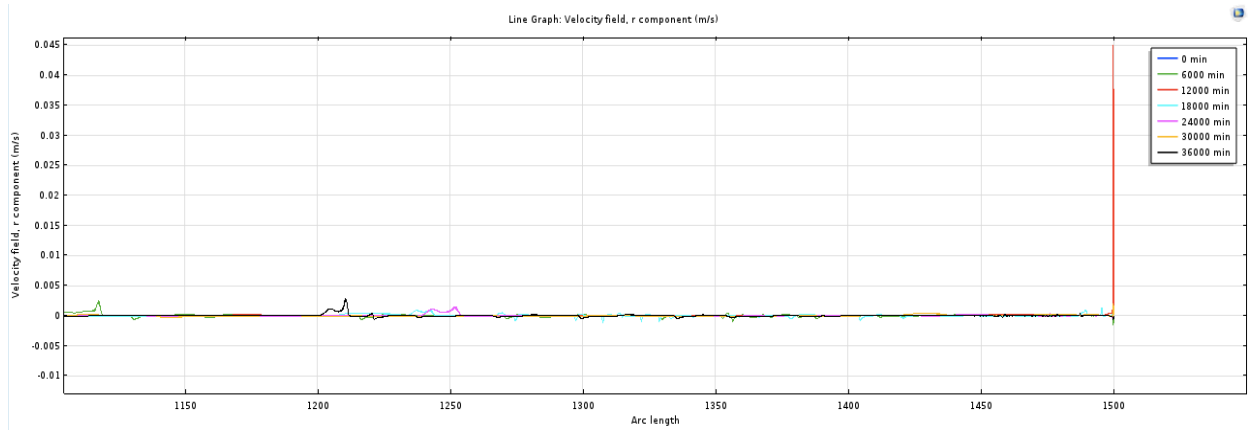


Figure A- 45: Line graph velocity field on top of fluid column, density difference 2, during 10 hours

A-3 Effect of Viscosity

A-3.1 Viscosity Difference 1

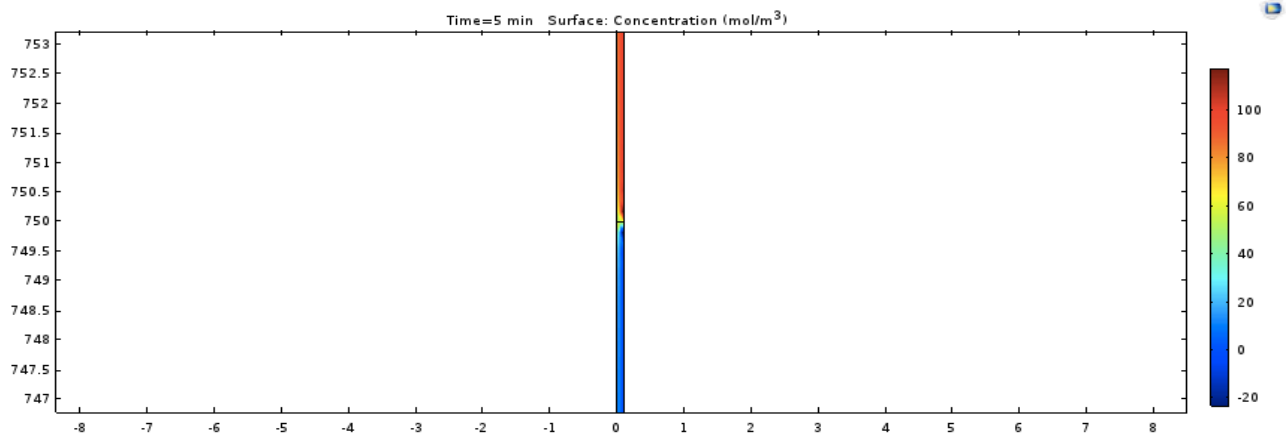


Figure A- 46: Surface concentration, viscosity difference 1, after 5 minutes

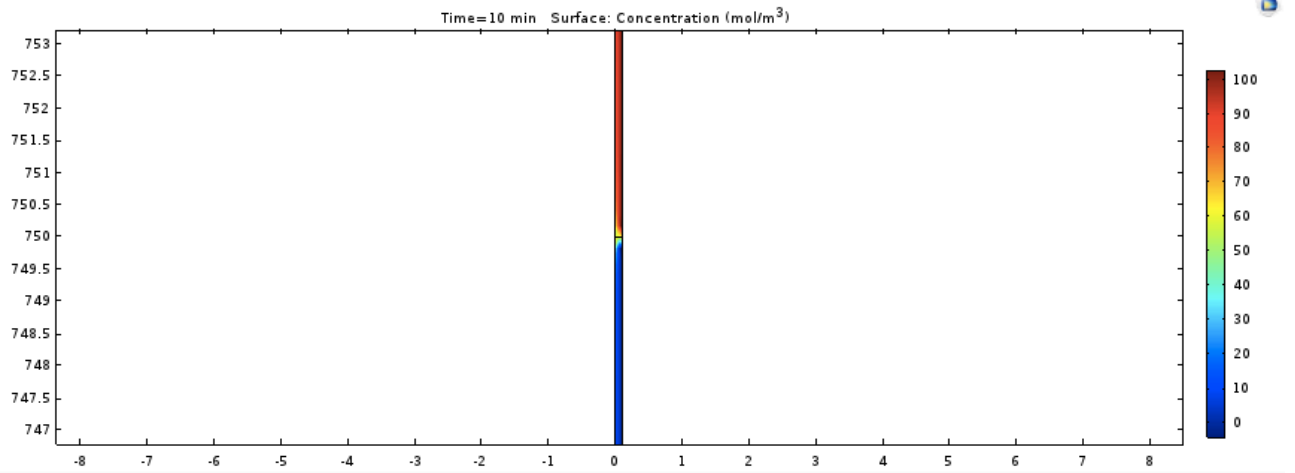


Figure A- 47: Surface concentration, viscosity difference 1, after 10 minutes

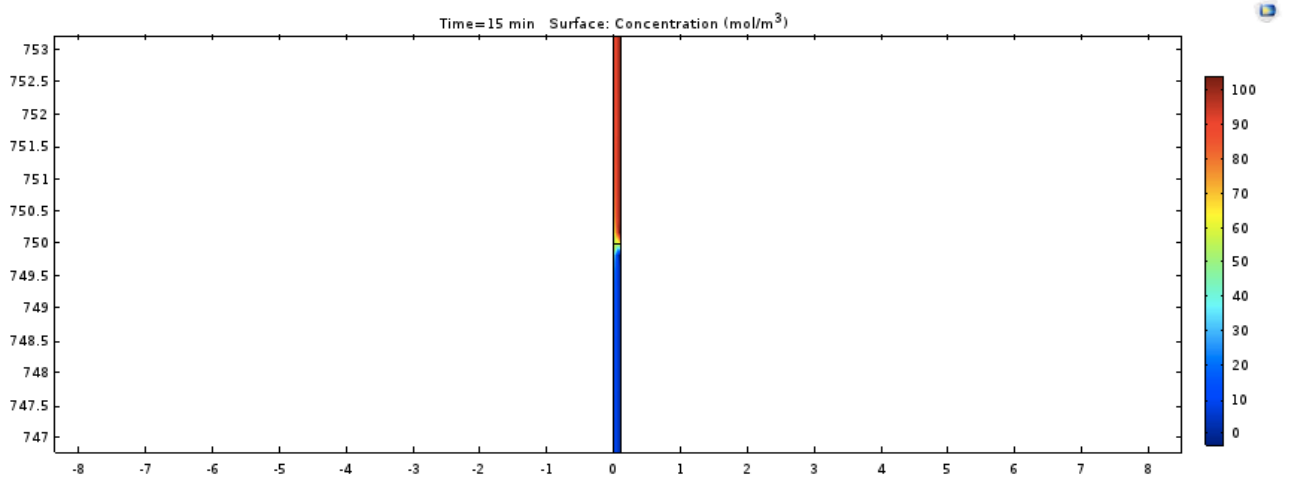


Figure A- 48: Surface concentration, viscosity difference 1, after 15 minutes

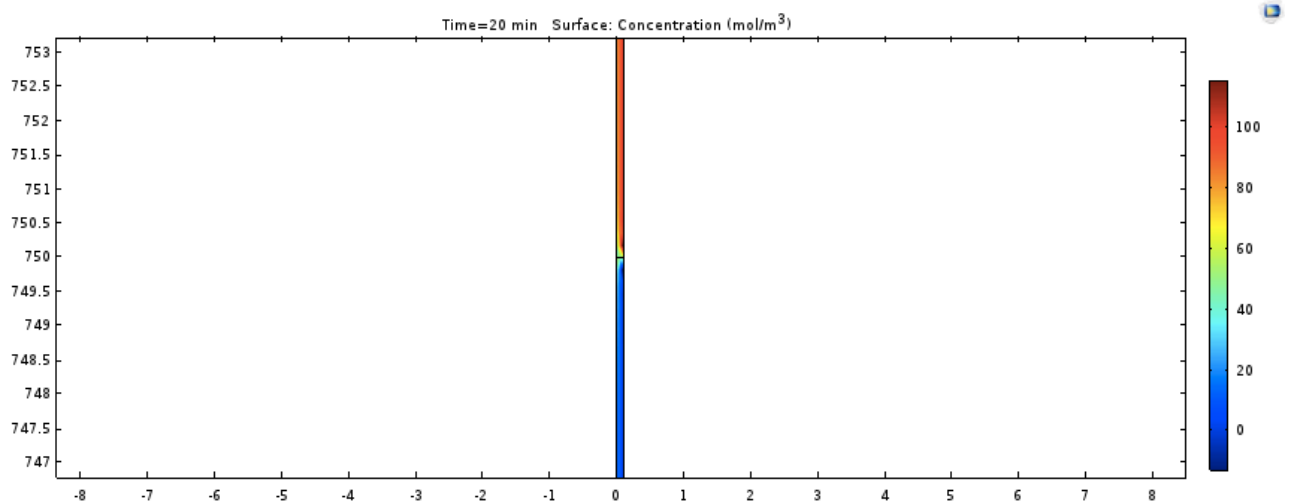


Figure A- 49: Surface concentration, viscosity difference 1, after 20 minutes

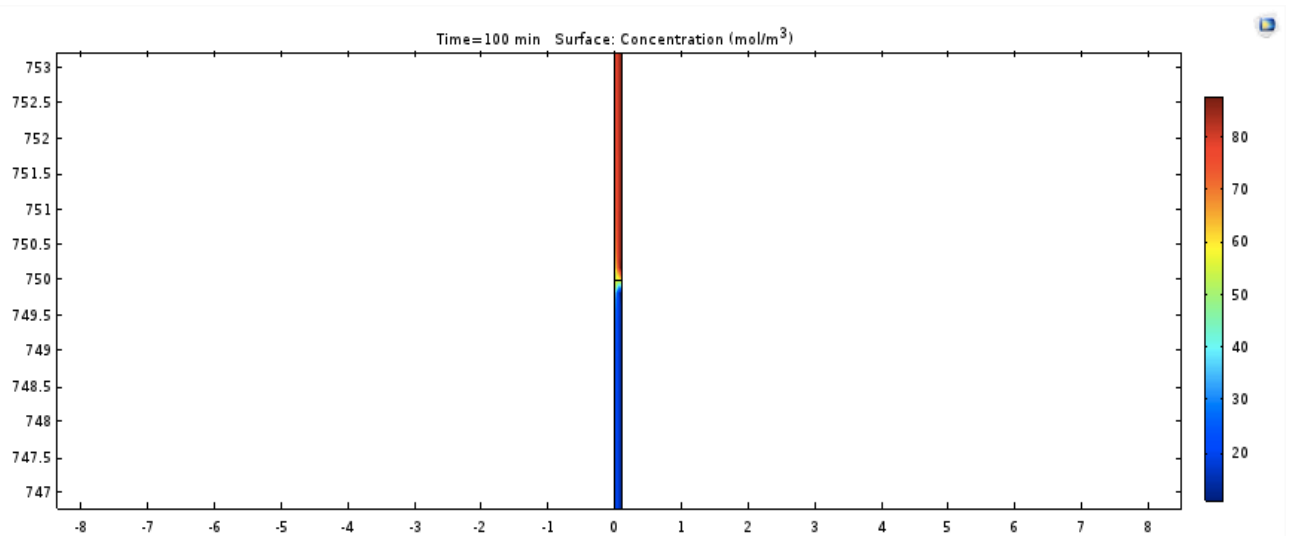


Figure A- 50: Surface concentration, viscosity difference 1, after 100 minutes

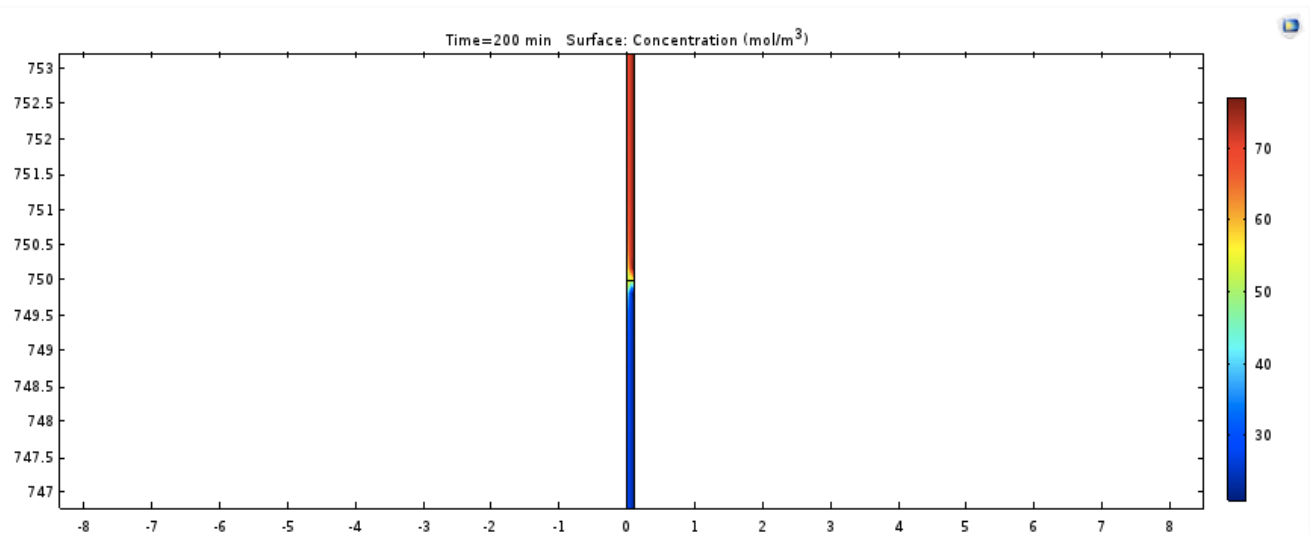


Figure A- 51: Surface concentration, viscosity difference 1, after 200 minutes

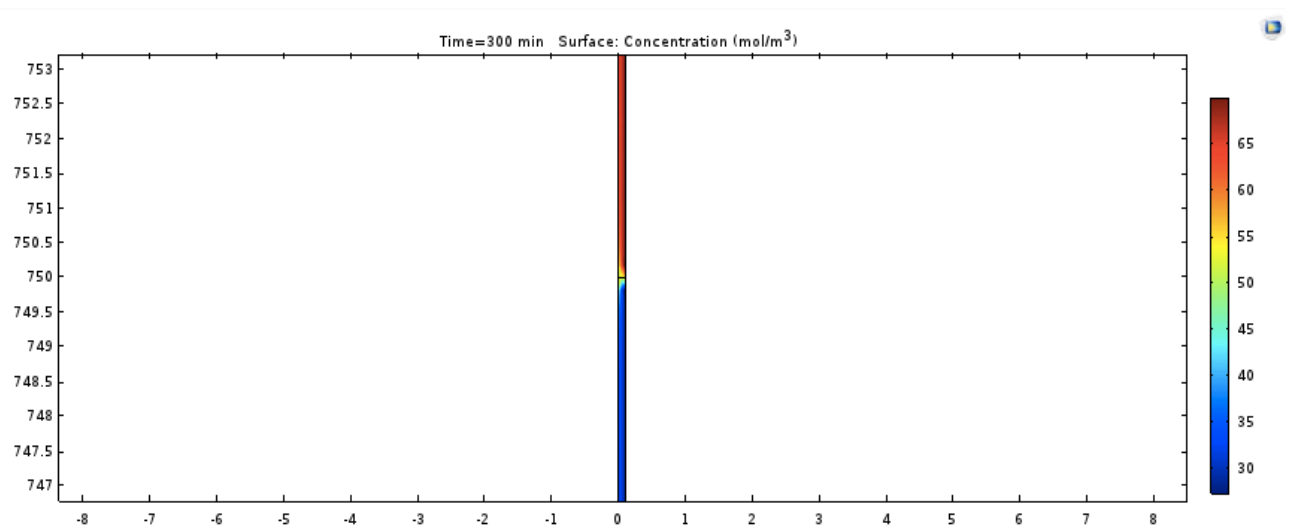


Figure A- 52: Surface concentration, viscosity difference 1, after 300 minutes

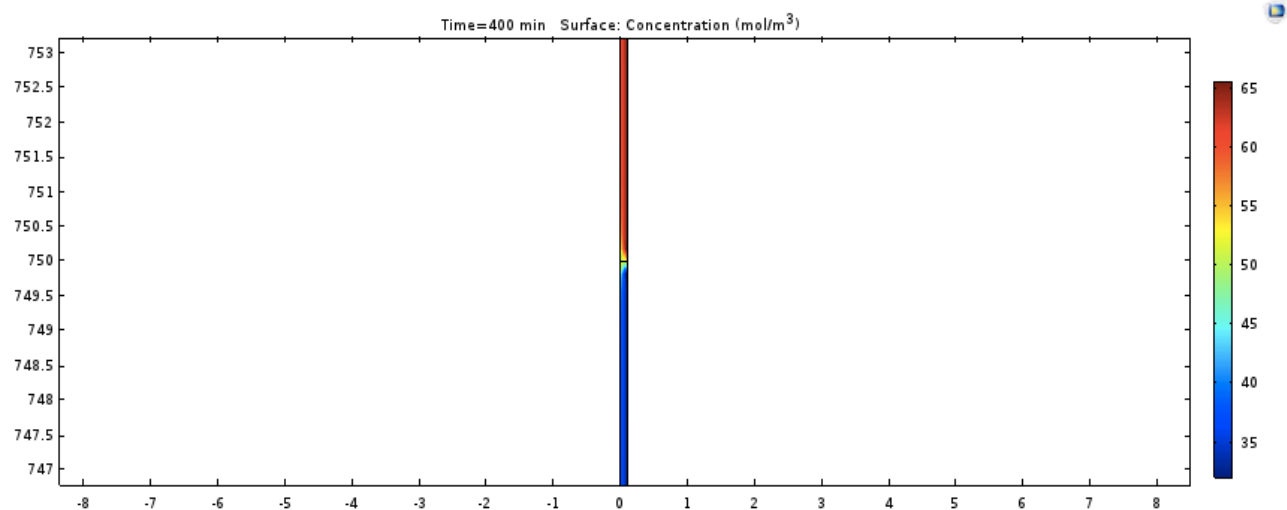


Figure A- 53: Surface concentration, viscosity difference 1, after 400 minutes

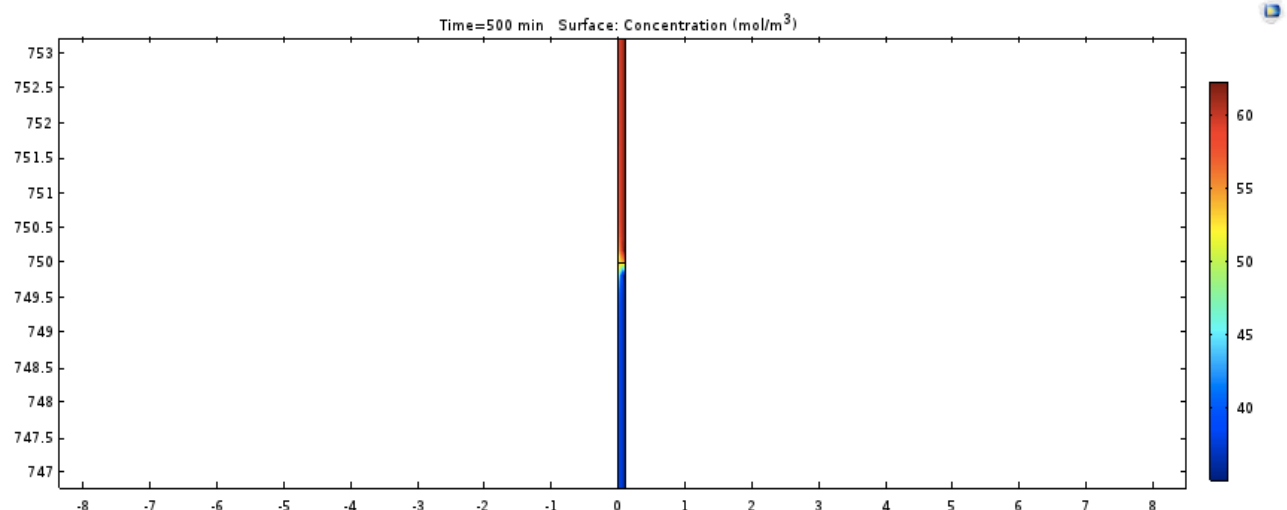


Figure A- 54: Surface concentration, viscosity difference 1, after 500 minutes

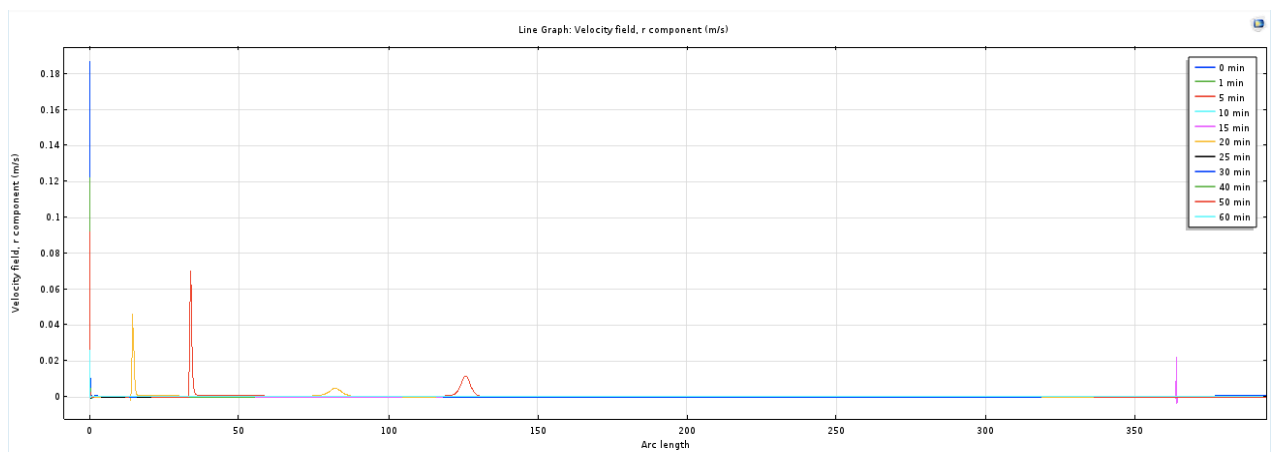


Figure A- 55: Line graph velocity field on bottom of fluid column, viscosity difference 1, during 1 hour

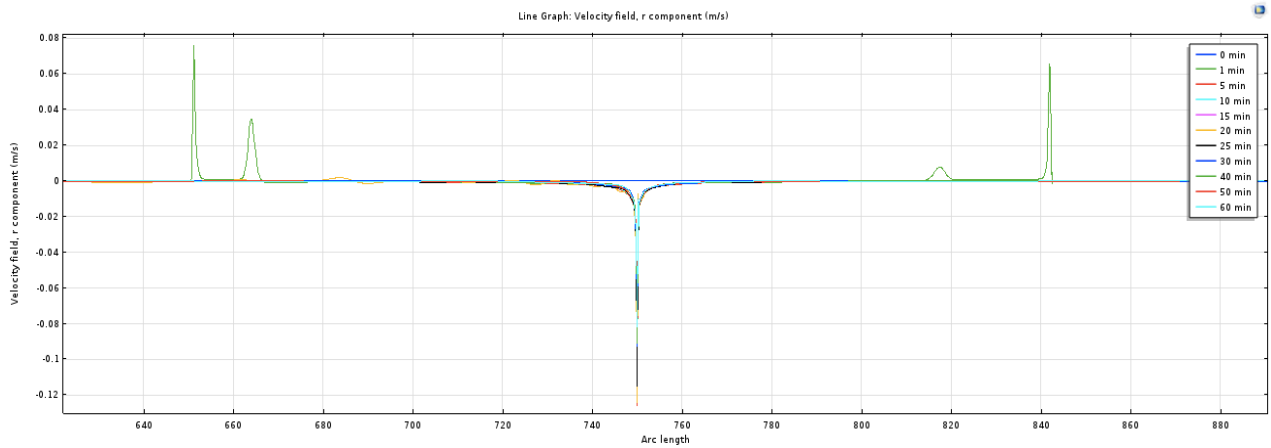


Figure A- 56: Line graph velocity field at interface, viscosity difference 1, during 1 hour

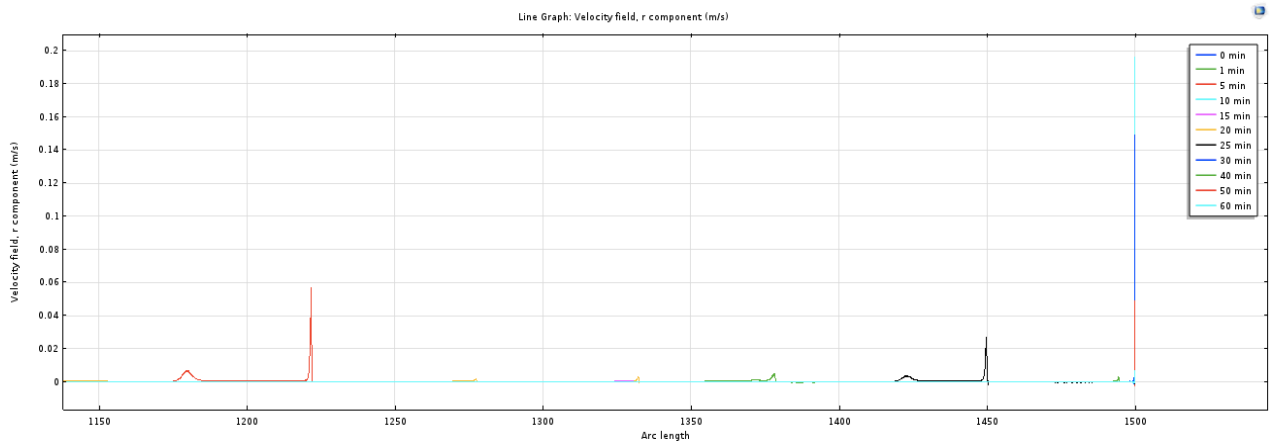


Figure A- 57: Line graph velocity field on top of fluid column, viscosity difference 1, during 1 hour

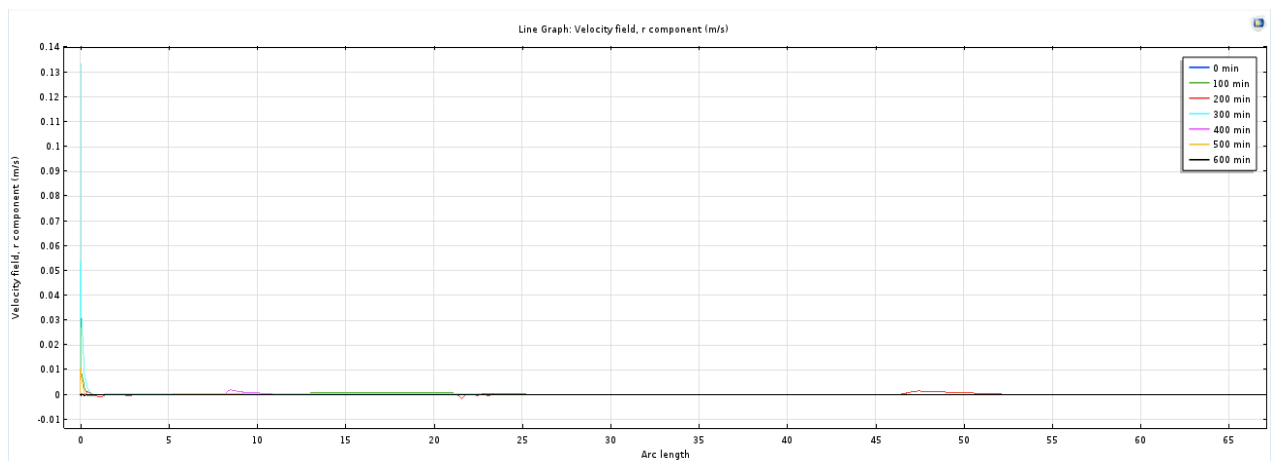


Figure A- 58: Line graph velocity field on bottom of pipe, viscosity difference 1, during 10 hours

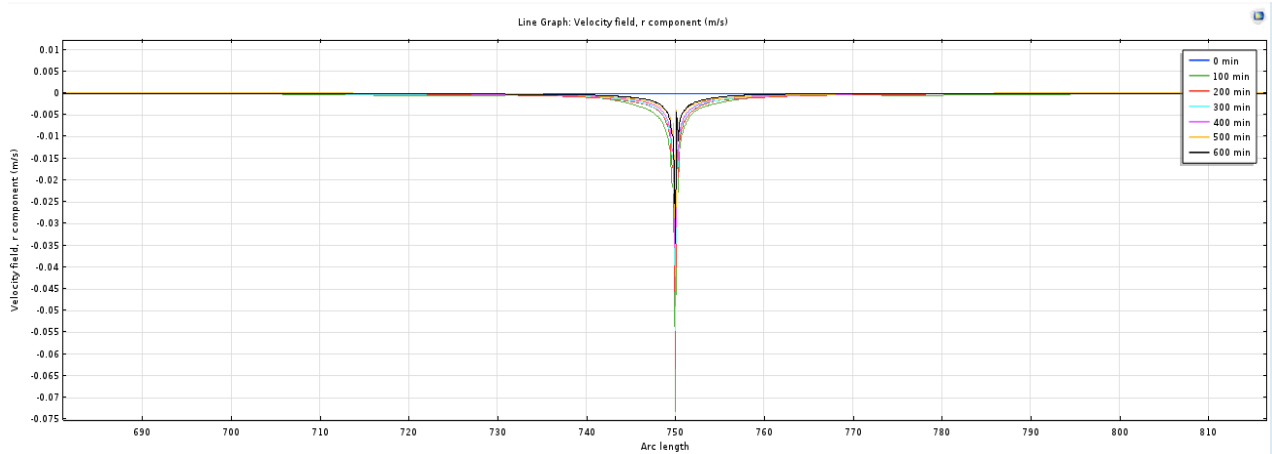


Figure A- 59: Line graph velocity field at interface, viscosity difference 1, during 10 hours

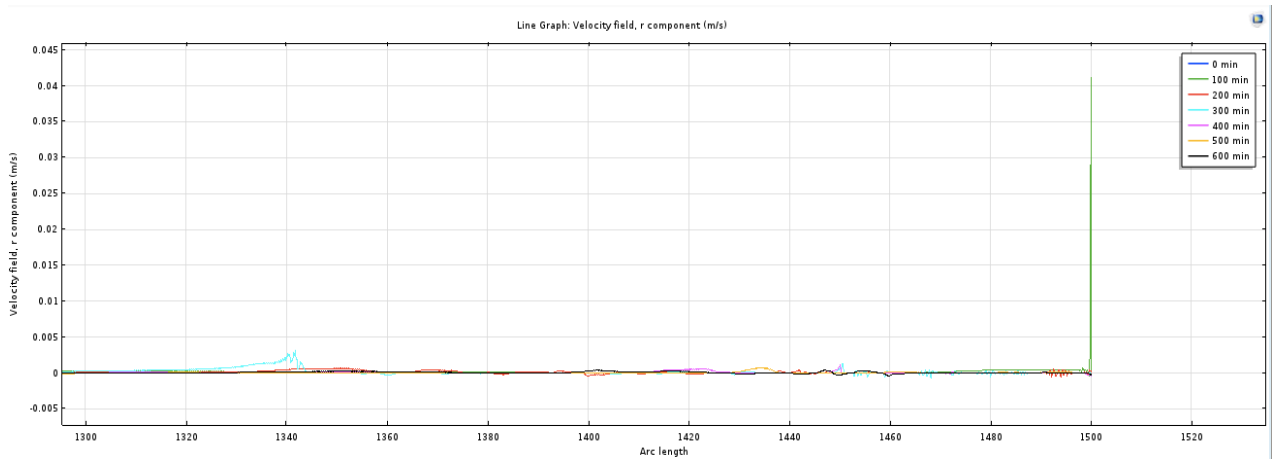


Figure A- 60: Line graph velocity field at top of fluid column, viscosity difference 2, during 10 hours

A-3.2 Viscosity Difference 2

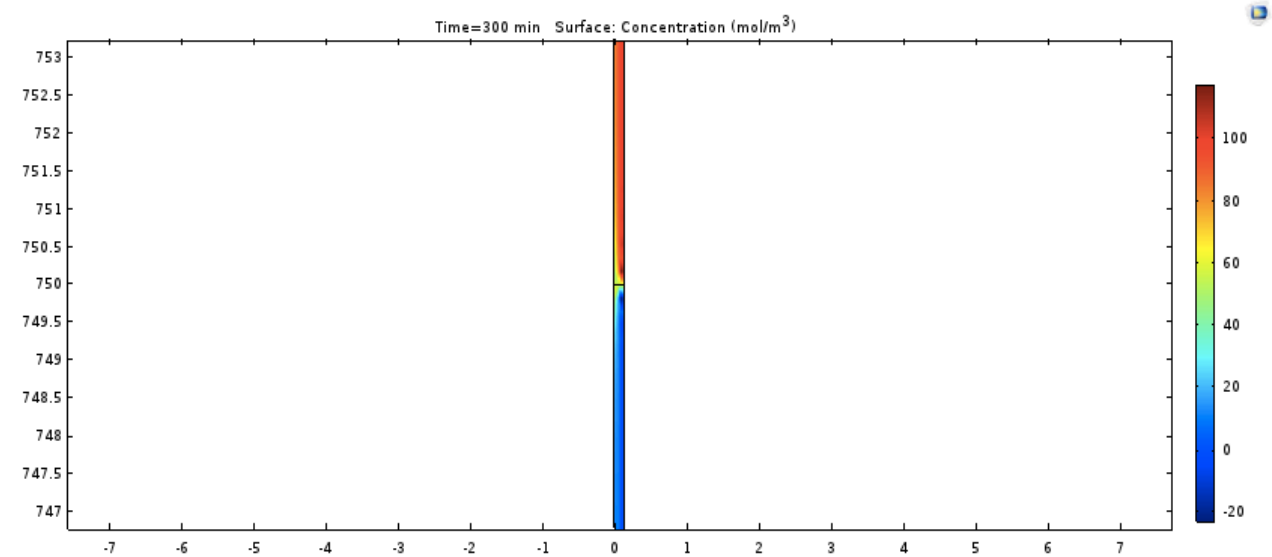


Figure A- 61: Surface concentration, viscosity difference 2, after 5 minutes

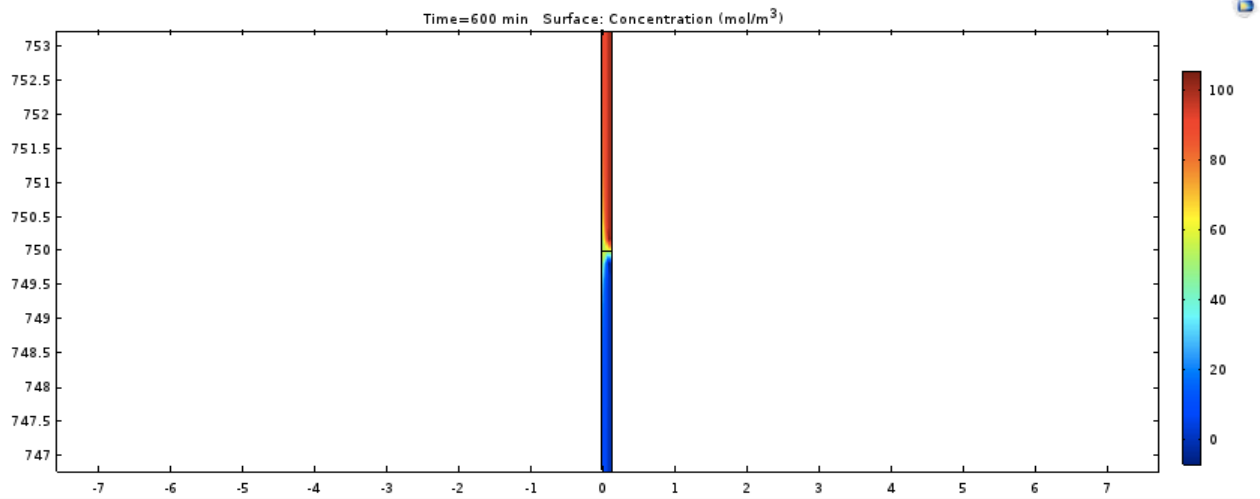


Figure A- 62: Surface concentration, viscosity difference 2, after 10 minutes

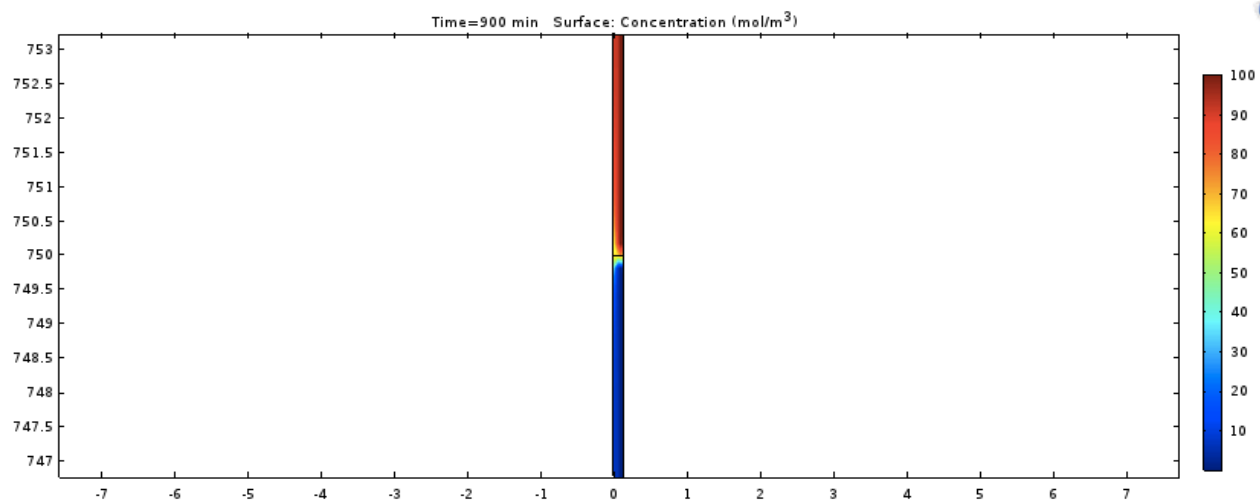


Figure A- 63: Surface concentration, viscosity difference 2, after 15 minutes

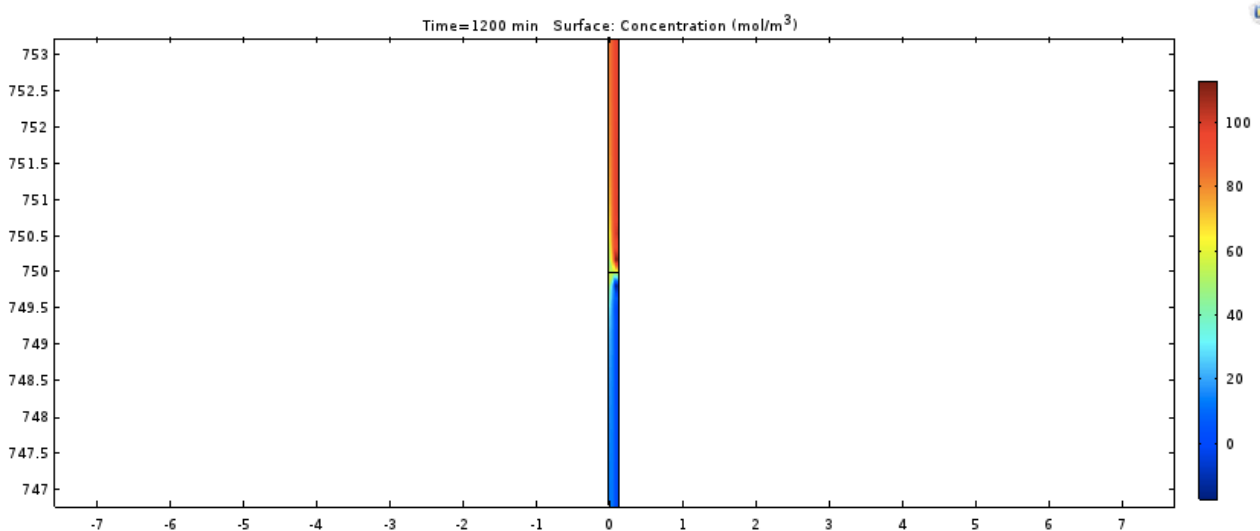


Figure A- 64: Surface concentration, viscosity difference 2, after 20 minutes

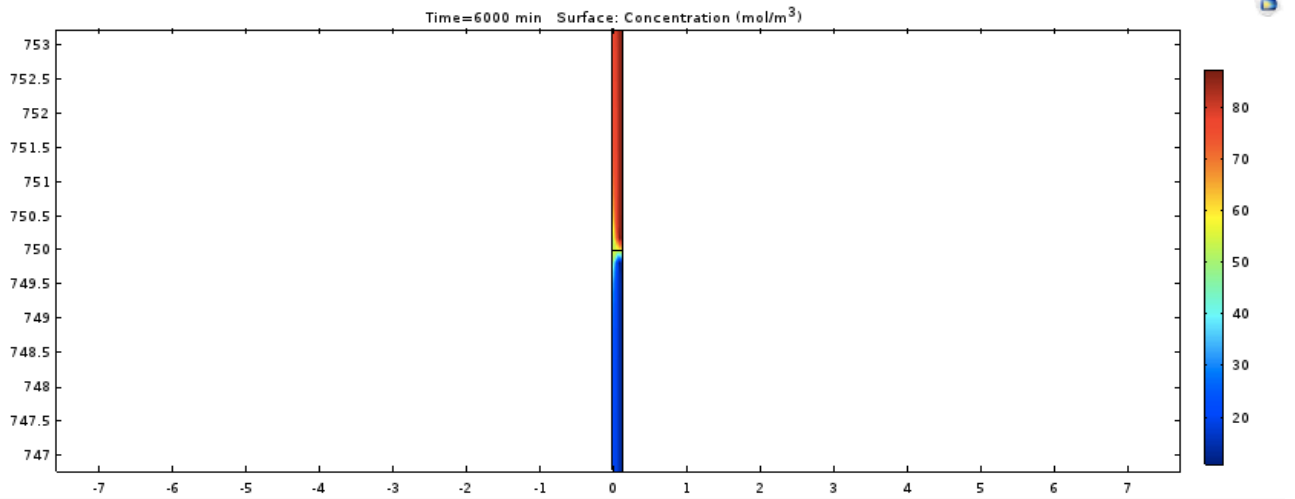


Figure A- 65: Surface concentration, viscosity difference 2, after 100 minutes

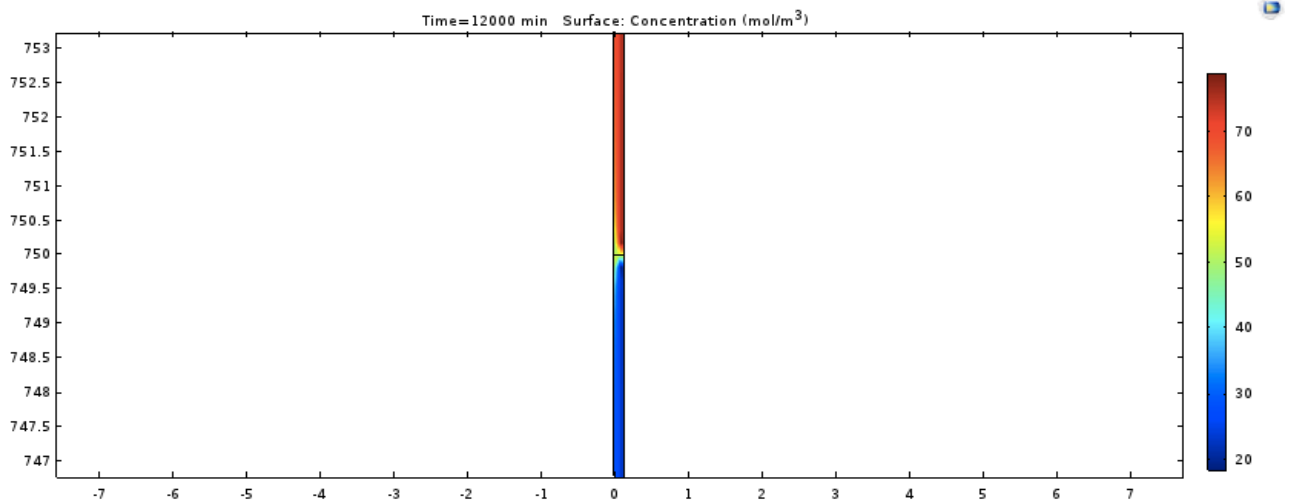


Figure A- 66: Surface concentration, viscosity difference 2, after 200 minutes

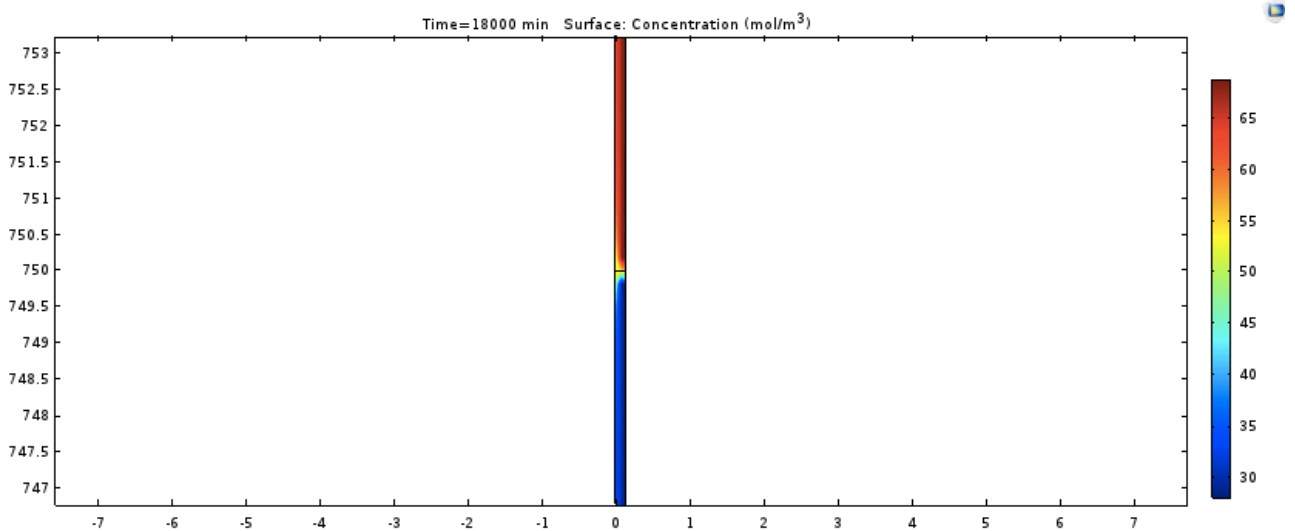


Figure A- 67: Surface concentration, viscosity difference 2, after 300 minutes

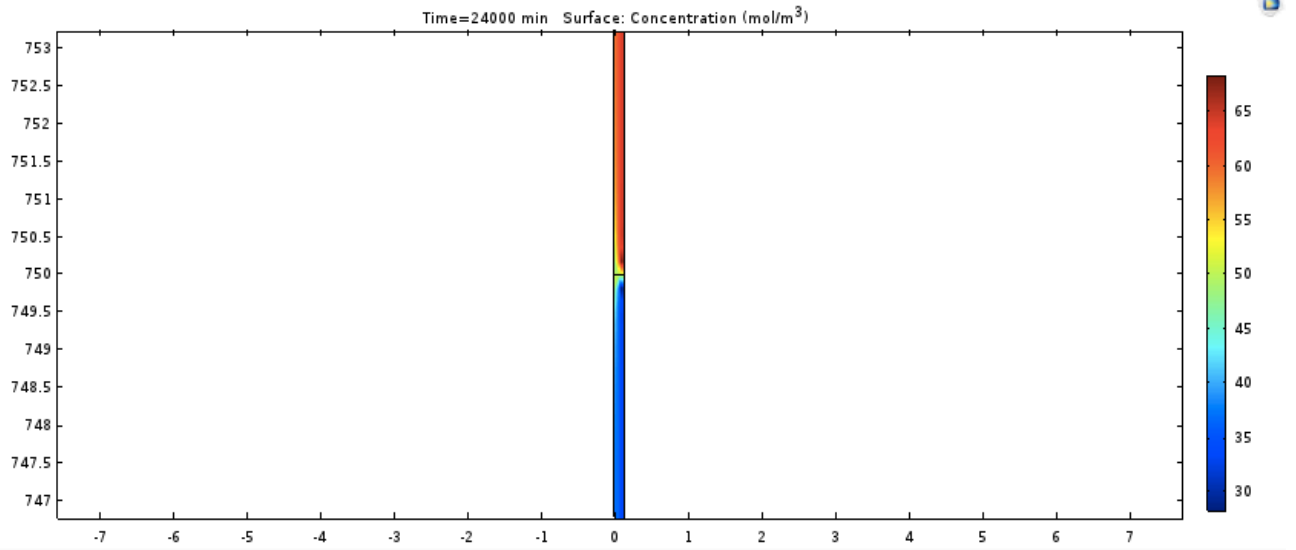


Figure A- 68: Surface concentration, viscosity difference 2, after 400 minutes

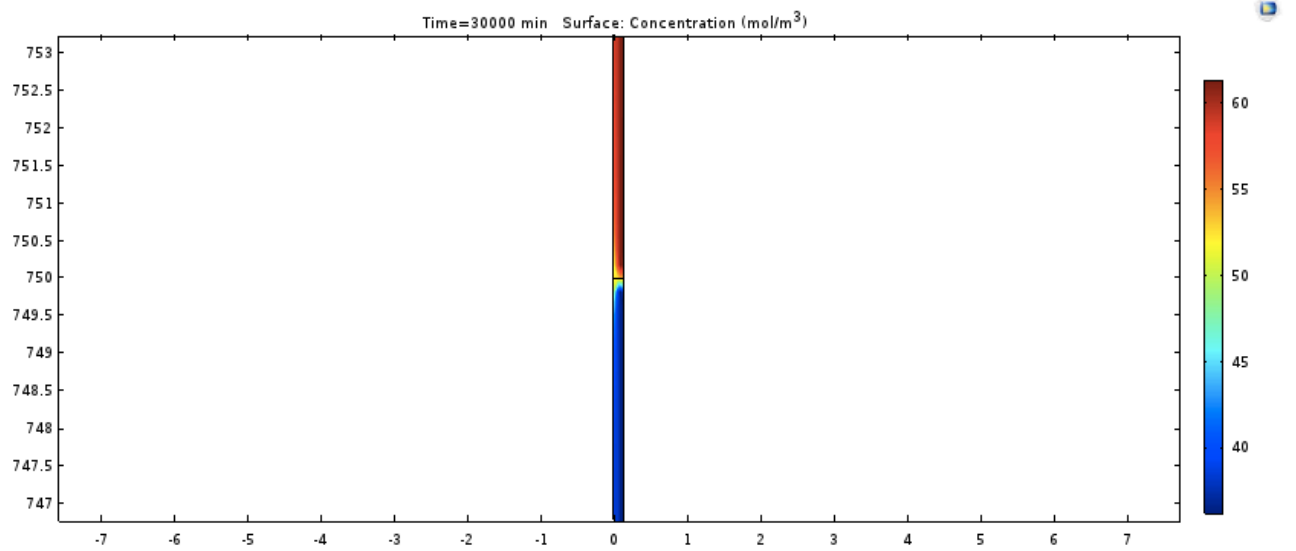


Figure A- 69: Surface concentration, viscosity difference 2, after 500 minutes

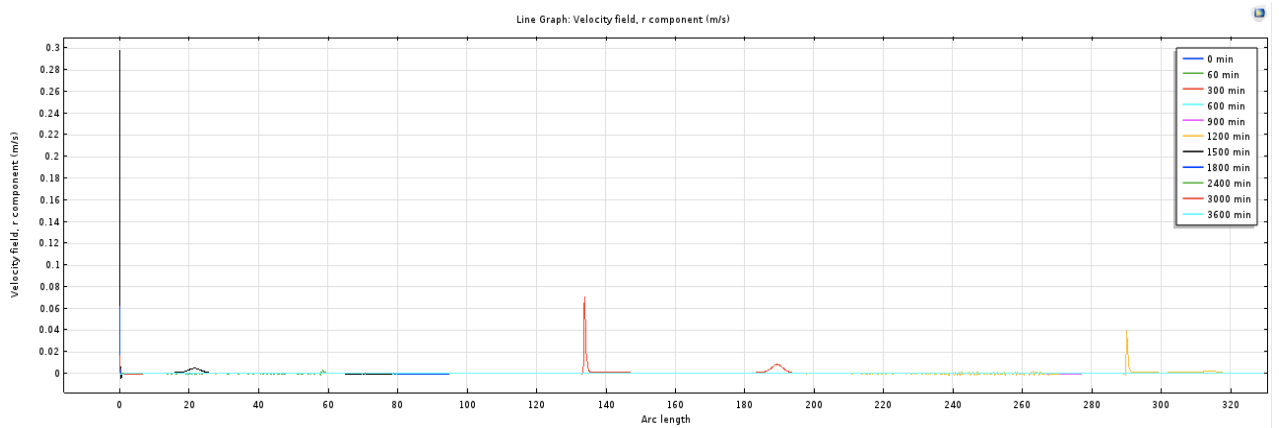


Figure A- 70: Line graph velocity field on bottom of fluid column, viscosity difference 2, during 1 hour

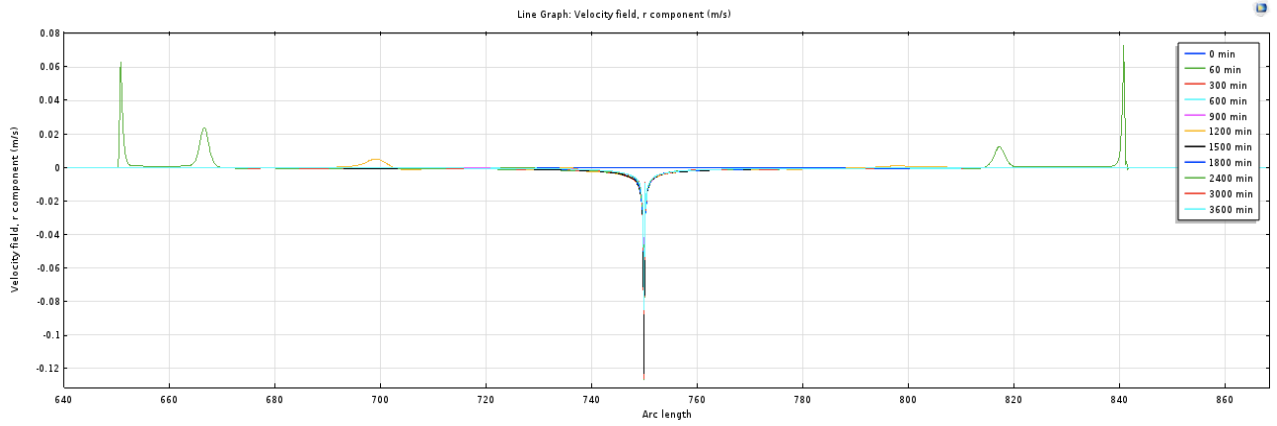


Figure A- 71: Line graph velocity field at interface, viscosity difference 2, during 1 hour

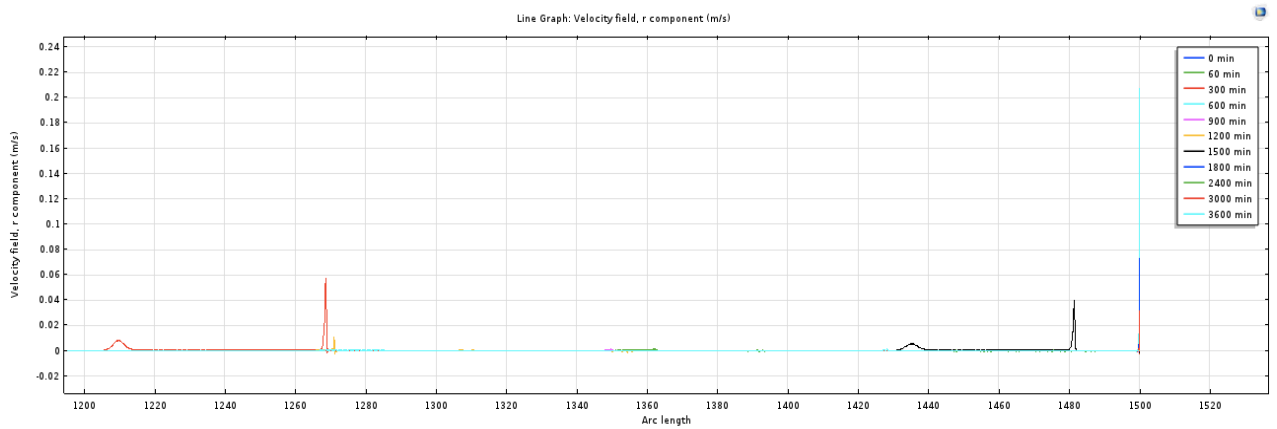


Figure A- 72: Line graph velocity field on top of fluid column, viscosity difference 2, during 1 hour

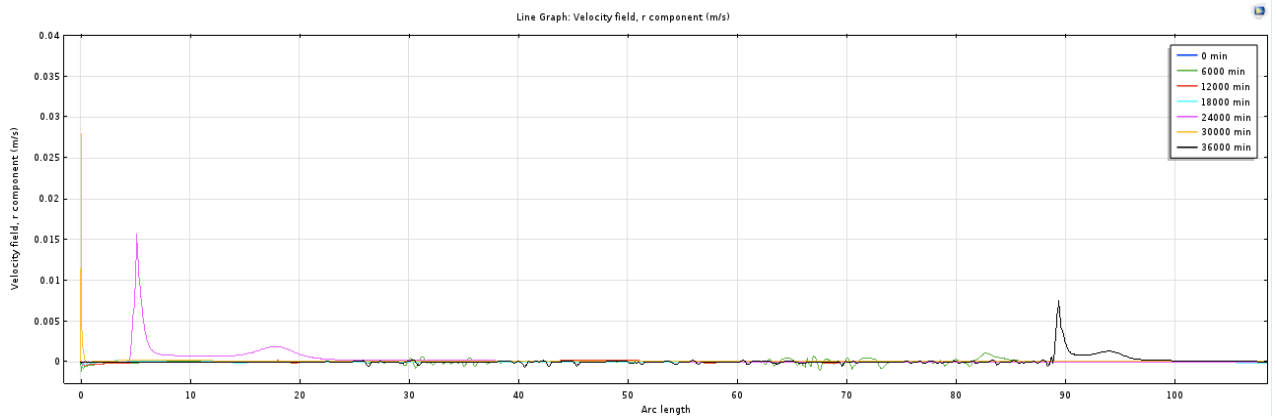


Figure A- 73: Line graph velocity field on bottom of fluid column, viscosity difference 2, during 10 hours

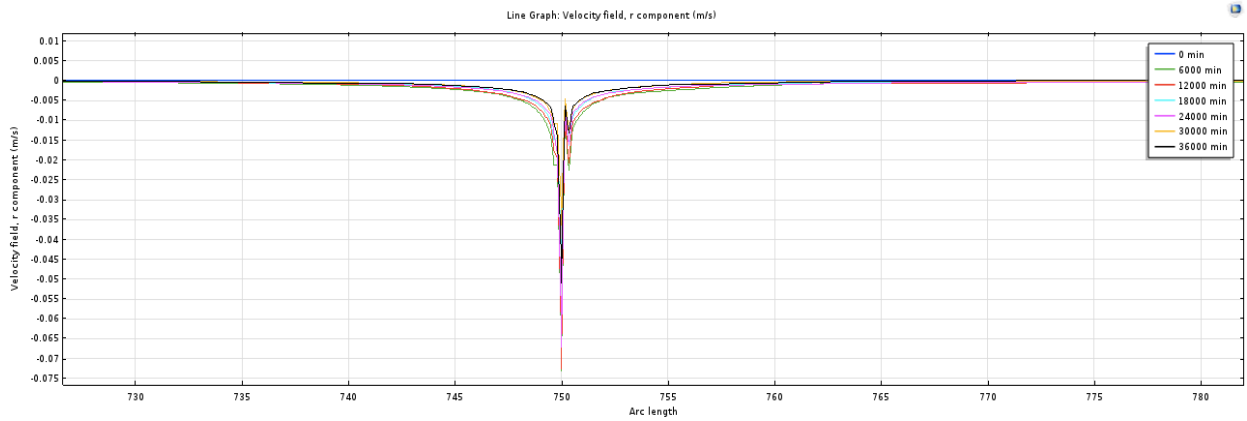


Figure A- 74: Line graph velocity field at interface, viscosity difference 2, during 10 hours

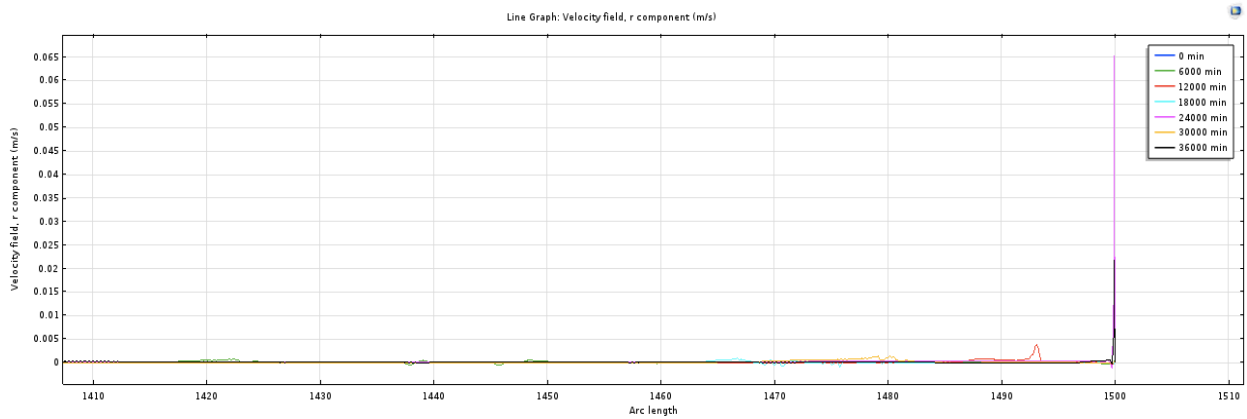


Figure A- 75: Line graph velocity field on top of fluid column, viscosity difference 2, during 10 hours

A-4 Effect of Well Size

A-4.1 Well Size Difference 1

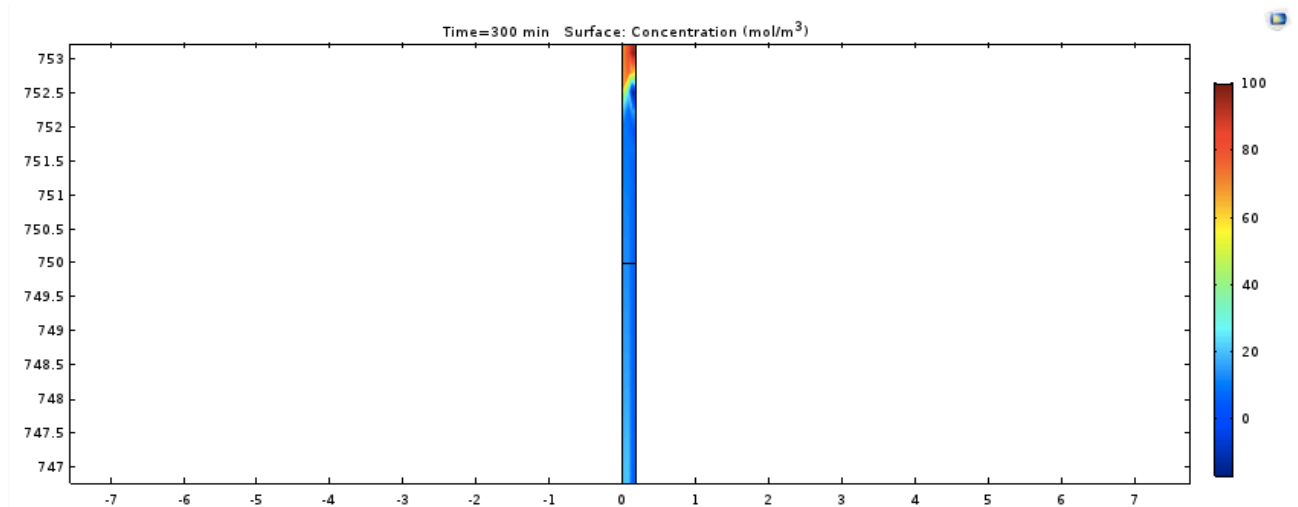


Figure A- 76: Surface concentration, well size difference 1, after 5 minutes

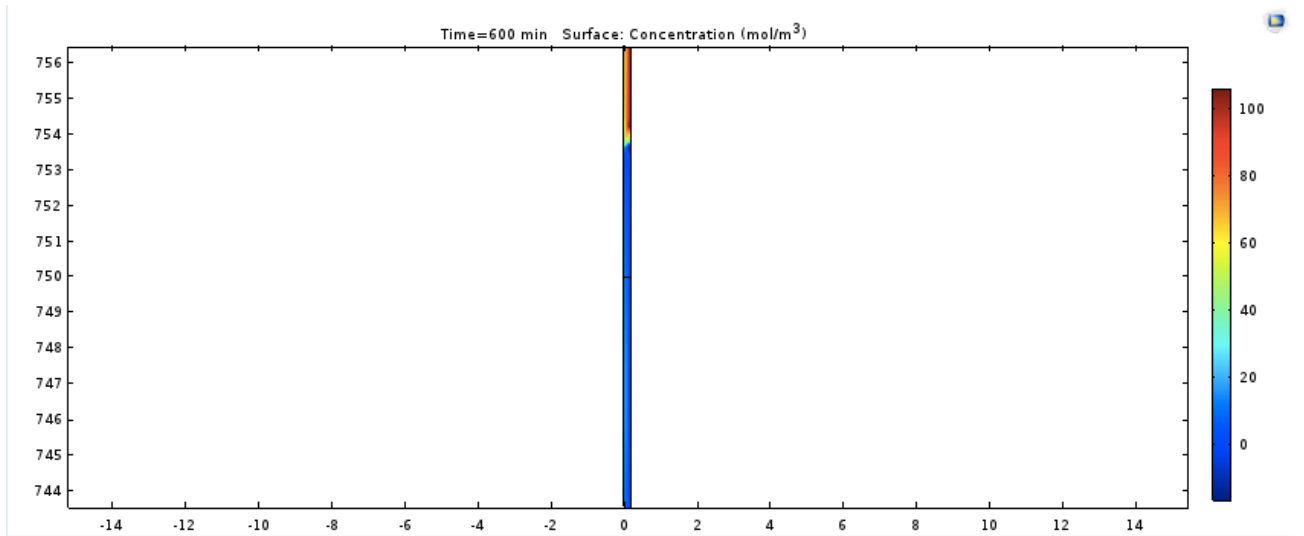


Figure A- 77: Surface concentration, well size difference 1, after 10 minutes

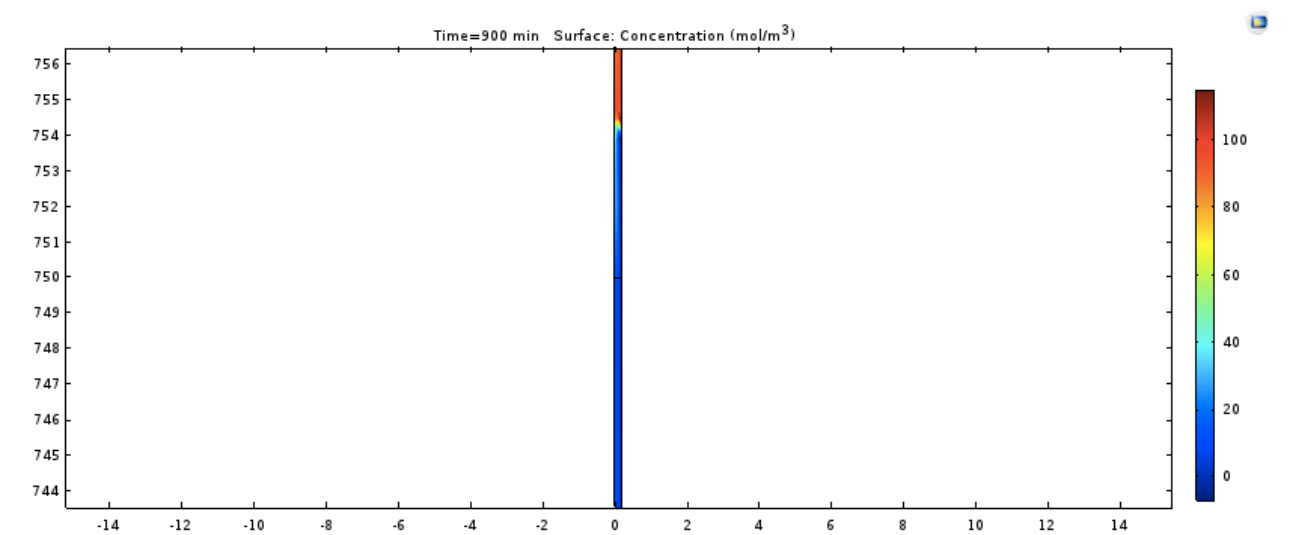


Figure A- 78: Surface concentration, well size difference 1, after 15 minutes

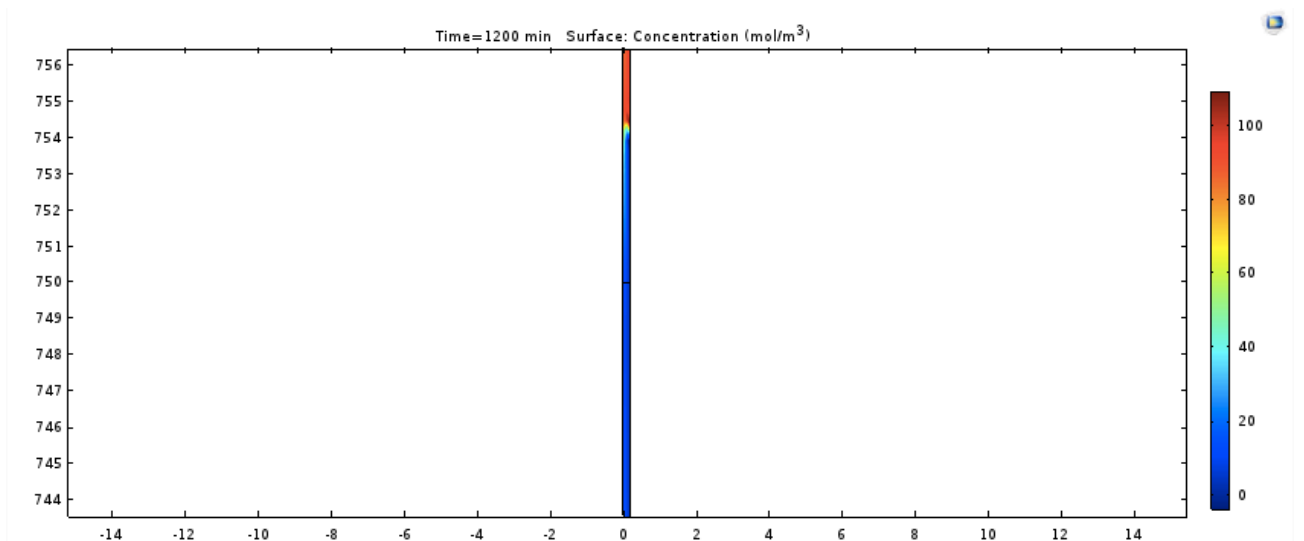


Figure A- 79: Surface concentration, well size difference 1, after 20 minutes

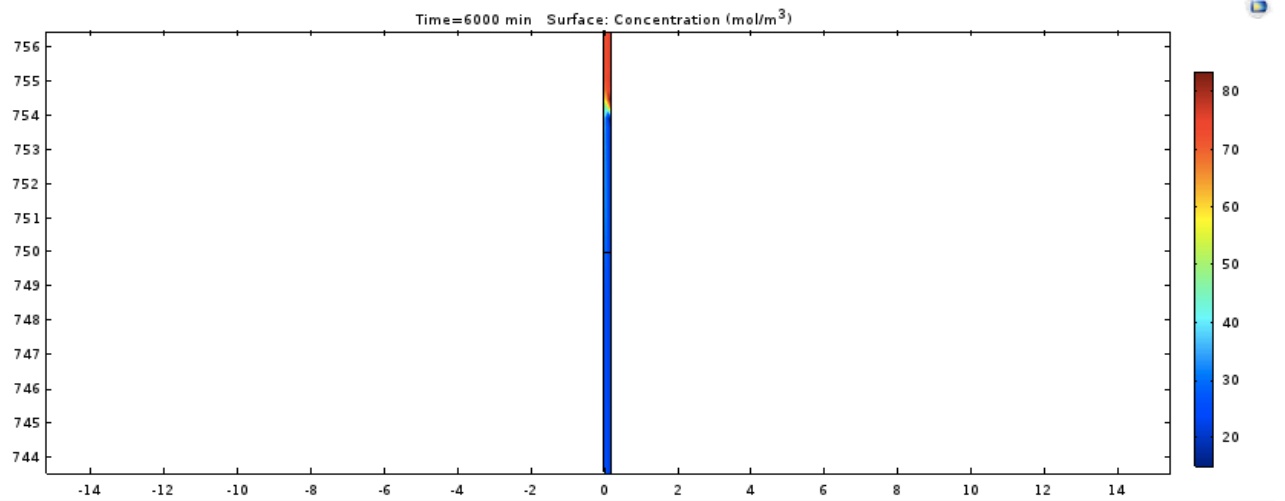


Figure A- 80: Surface concentration, well size difference 1, after 100 minutes

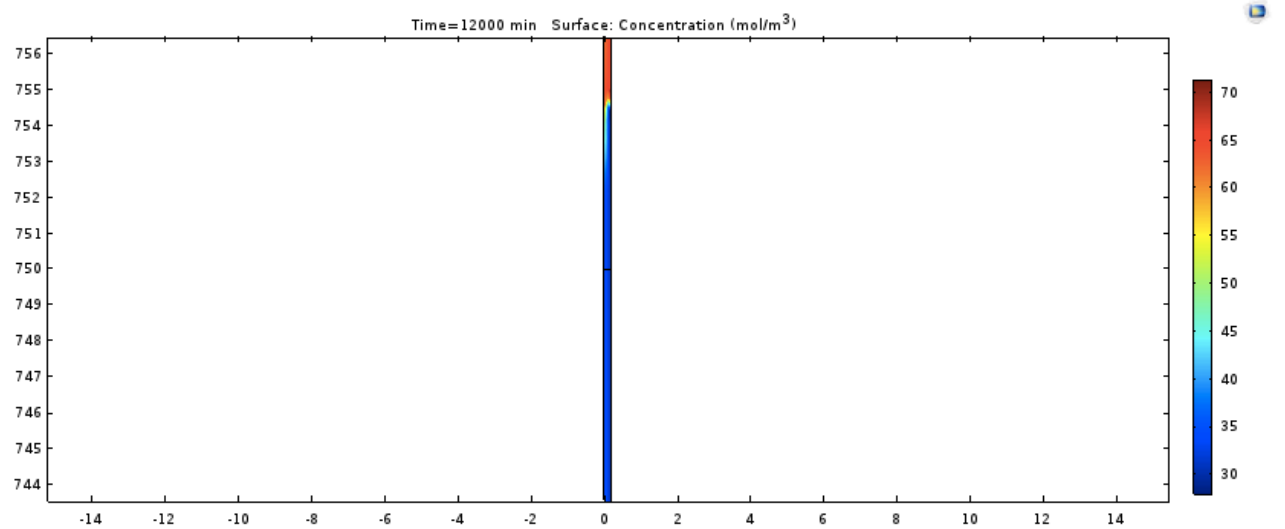


Figure A- 81: Surface concentration, well size difference 1, after 200 minutes

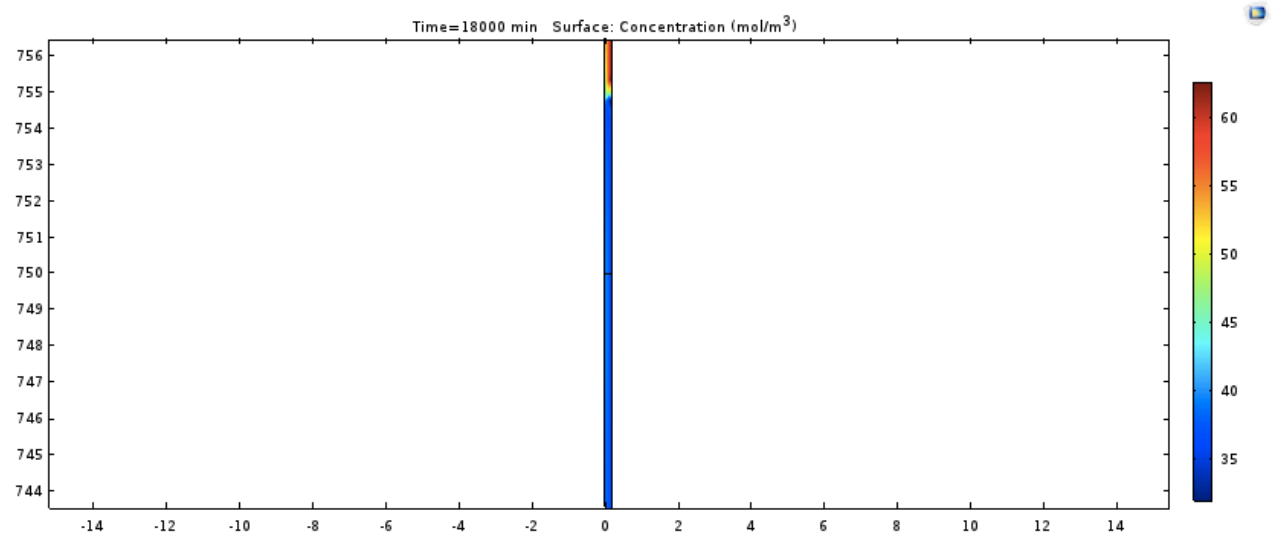


Figure A- 82: Surface concentration, well size difference 1, after 300 minutes

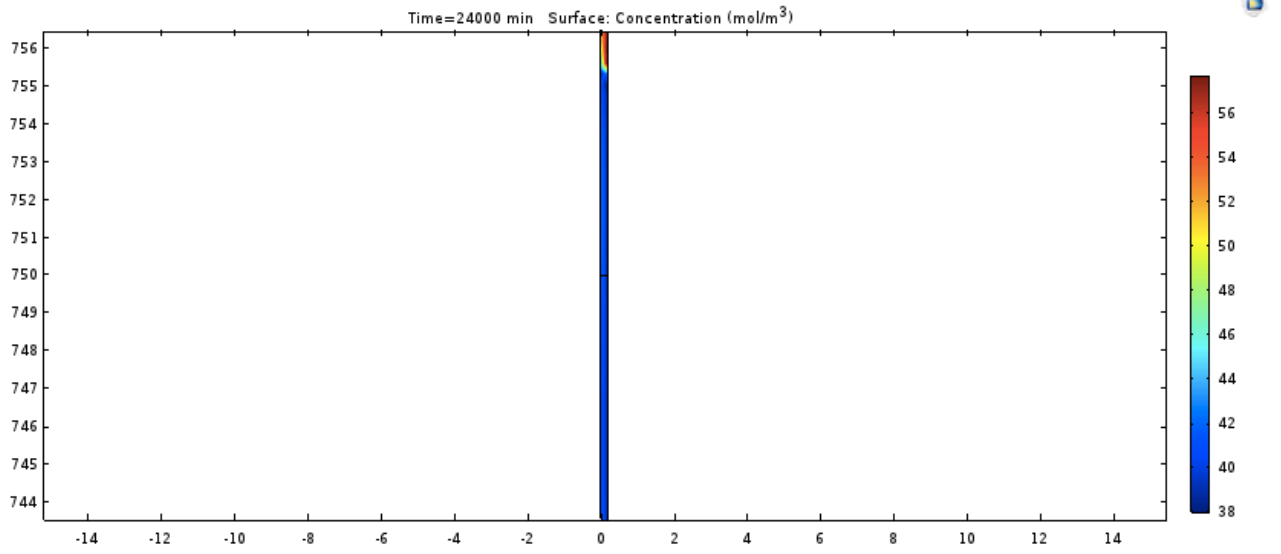


Figure A- 83: Surface concentration, well size difference 1, after 400 minutes

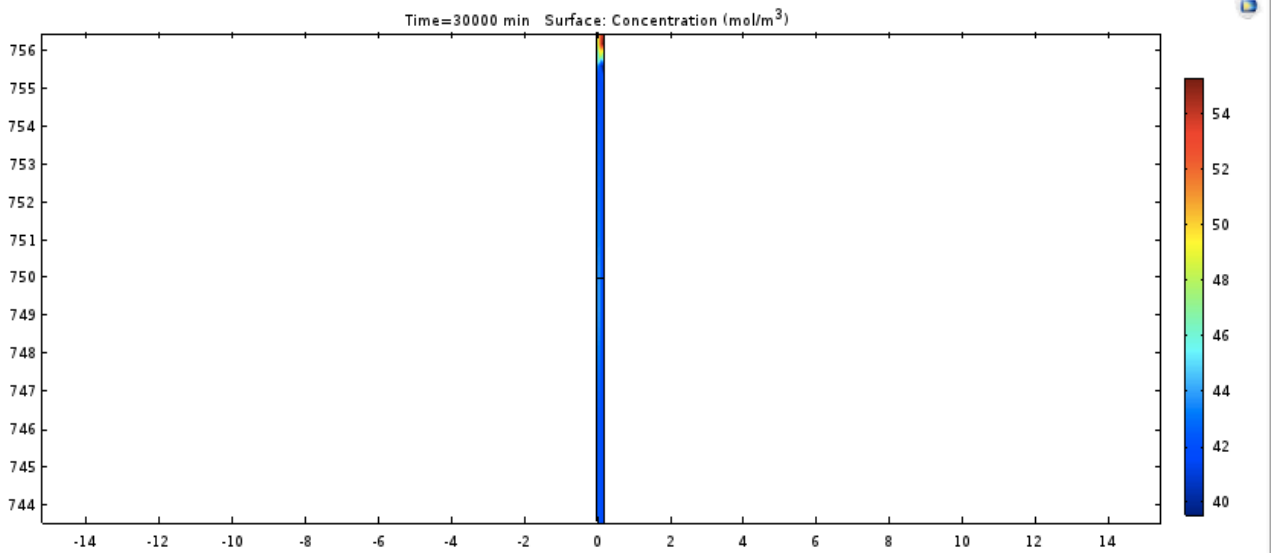


Figure A- 84: Surface concentration, well size difference 1, after 500 minutes

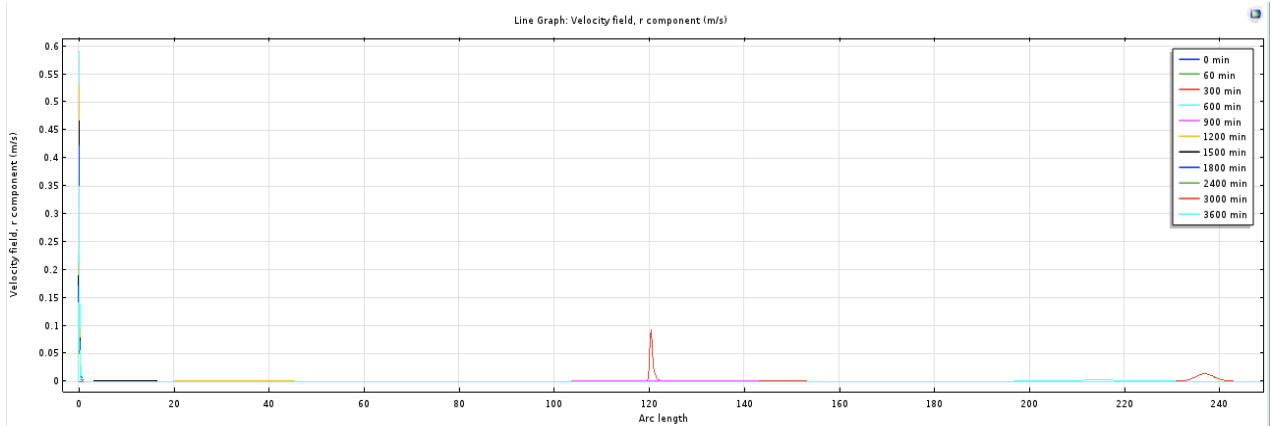


Figure A- 85: Line graph velocity field on bottom of fluid column, well size difference 1, during 1 hour

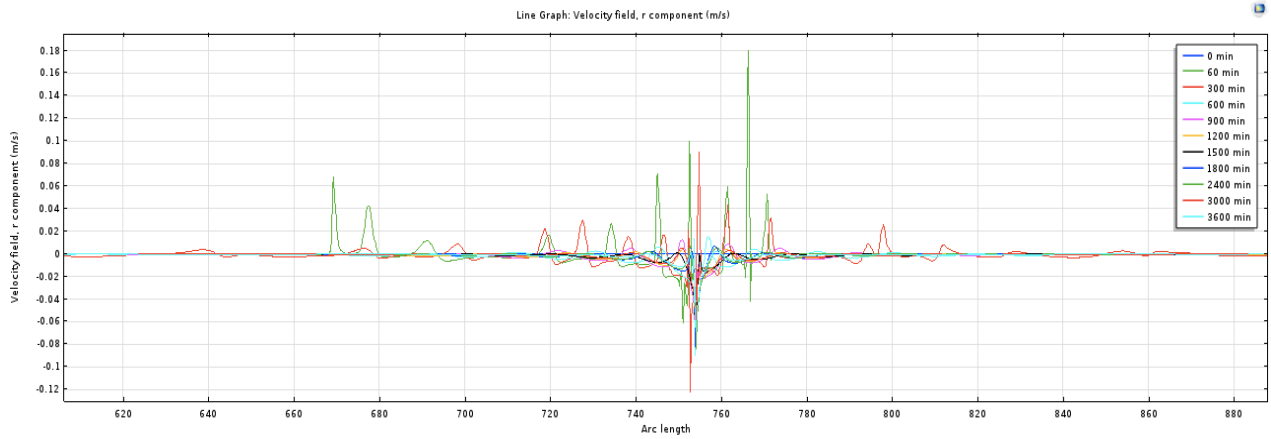


Figure A- 86: Line graph velocity field at interface, well size difference 1, during 1 hour

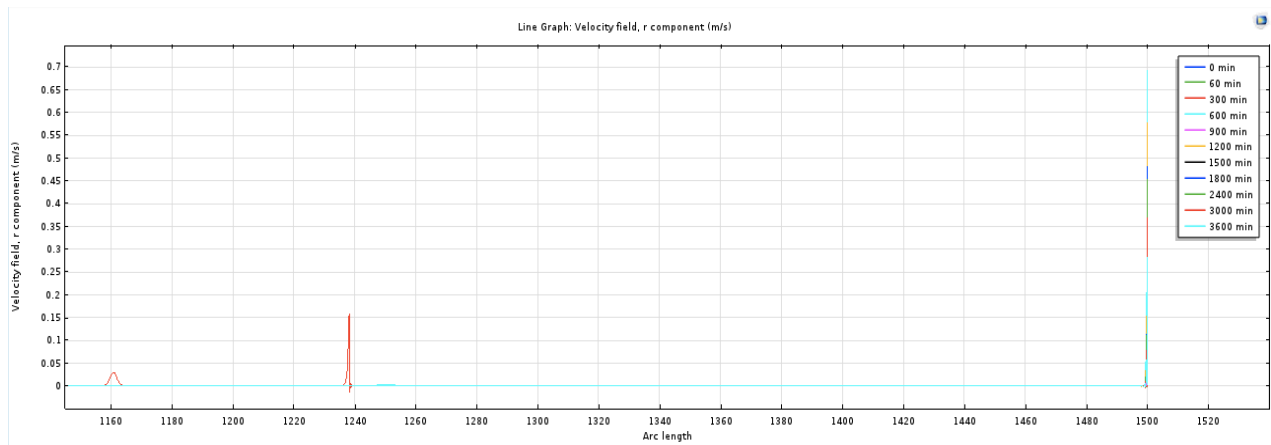


Figure A- 87: Line graph velocity field on top of fluid column, well size difference 1, during 1 hour

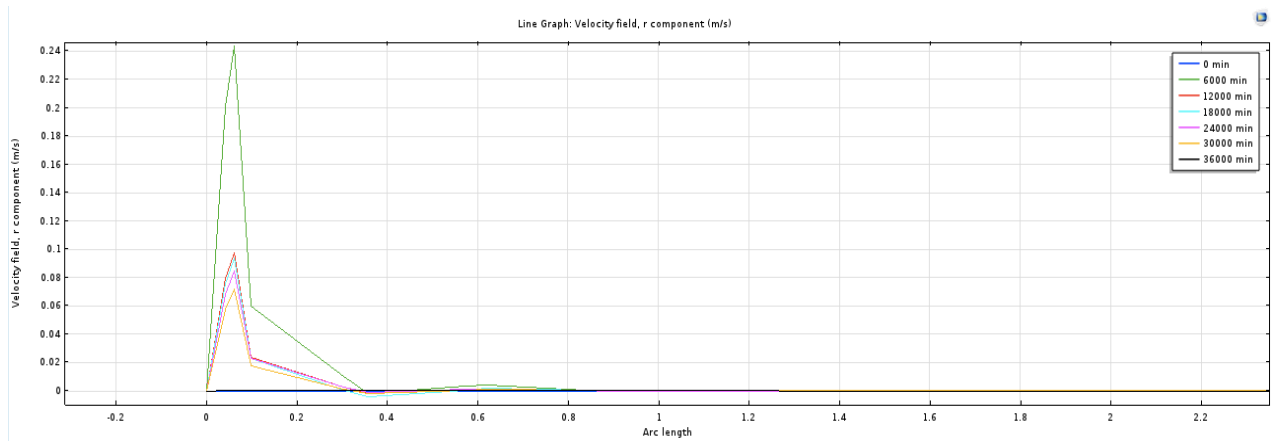


Figure A- 88: Line graph velocity field on bottom of fluid column, well size difference 1, during 10 hours

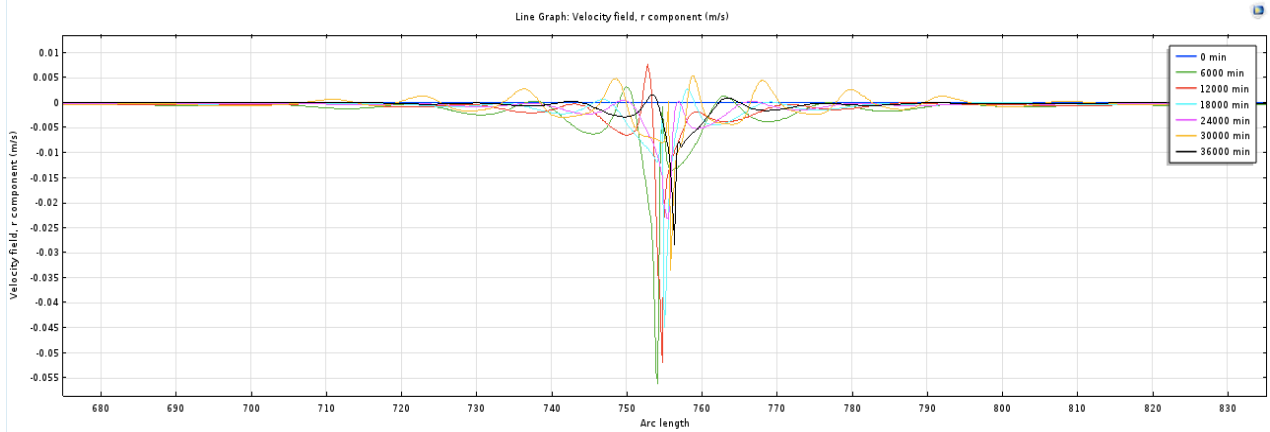


Figure A- 89: Line graph velocity field at interface, well size difference 1, during 10 hours

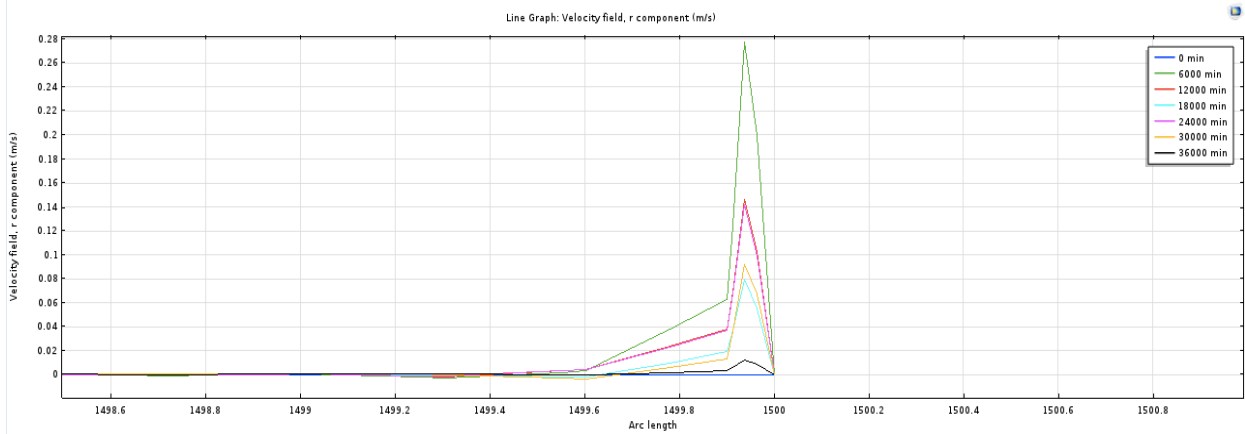


Figure A- 90: Line graph velocity field on top of fluid column, well size difference 1, during 10 hours

A-4.2 Well Size Difference 2

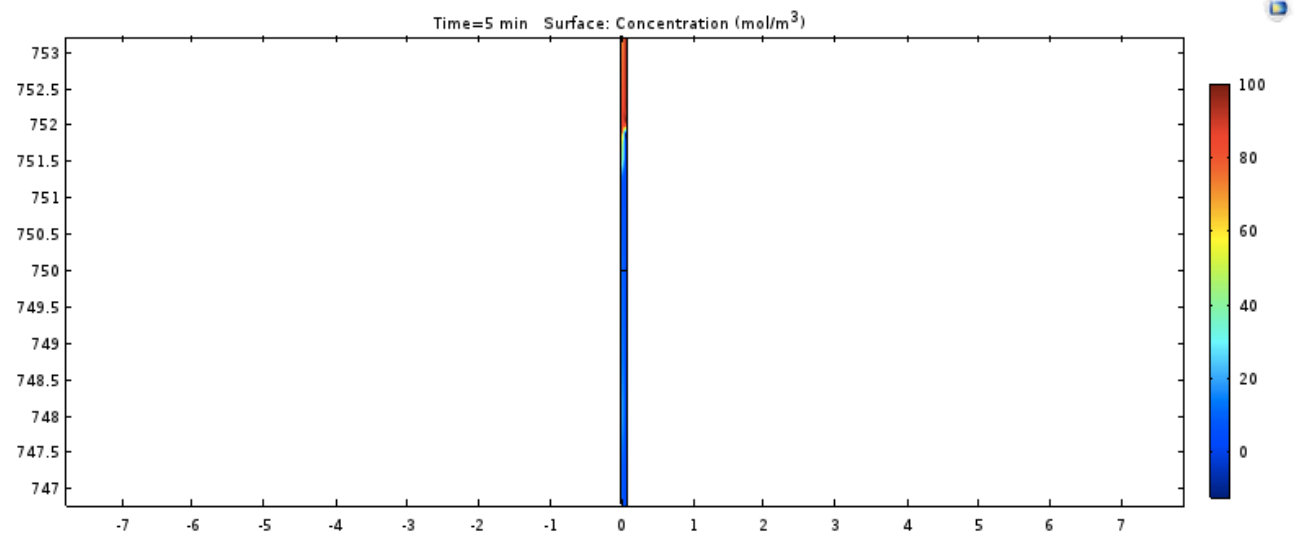


Figure A- 91: Surface concentration, well size difference 2, after 5 minutes

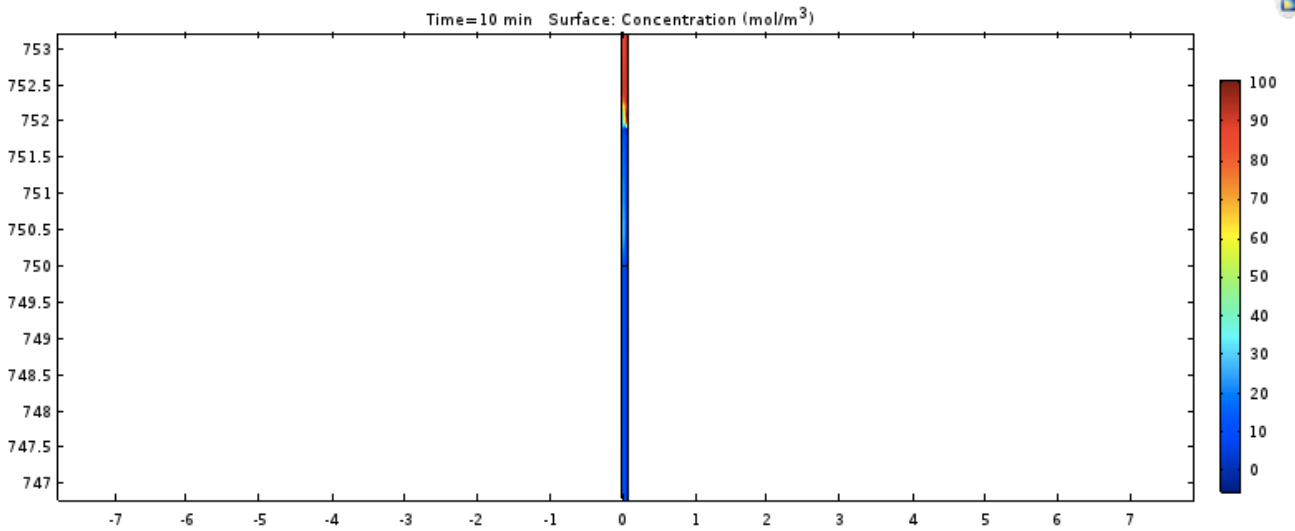


Figure A- 92: Surface concentration, well size difference 2, after 10 minutes

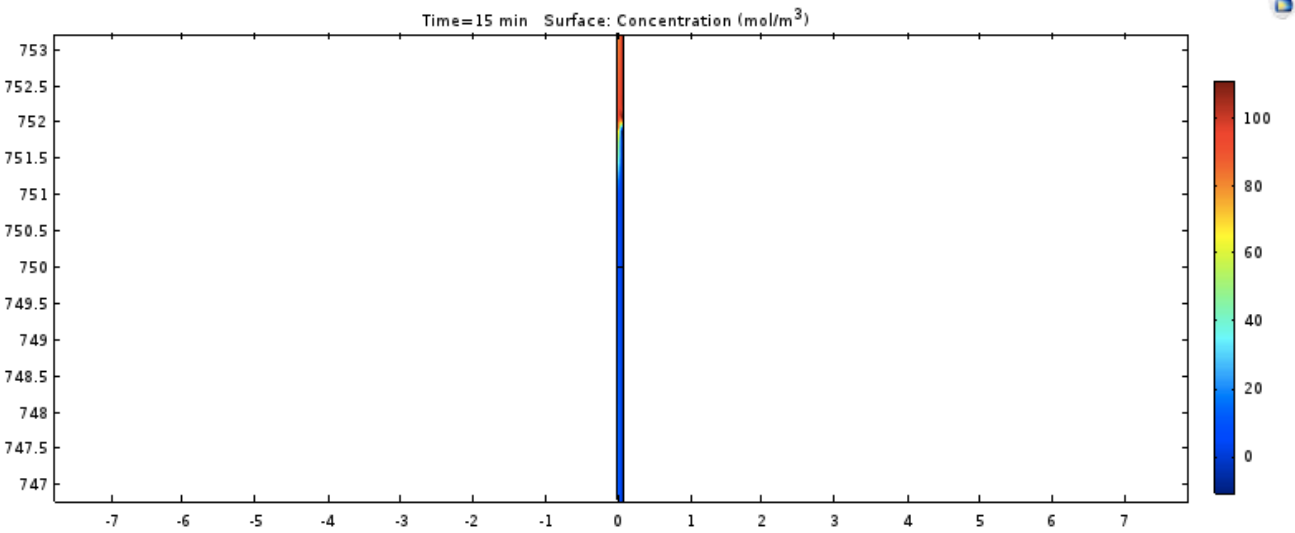


Figure A- 93: Surface concentration, well size difference 2, after 15 minutes

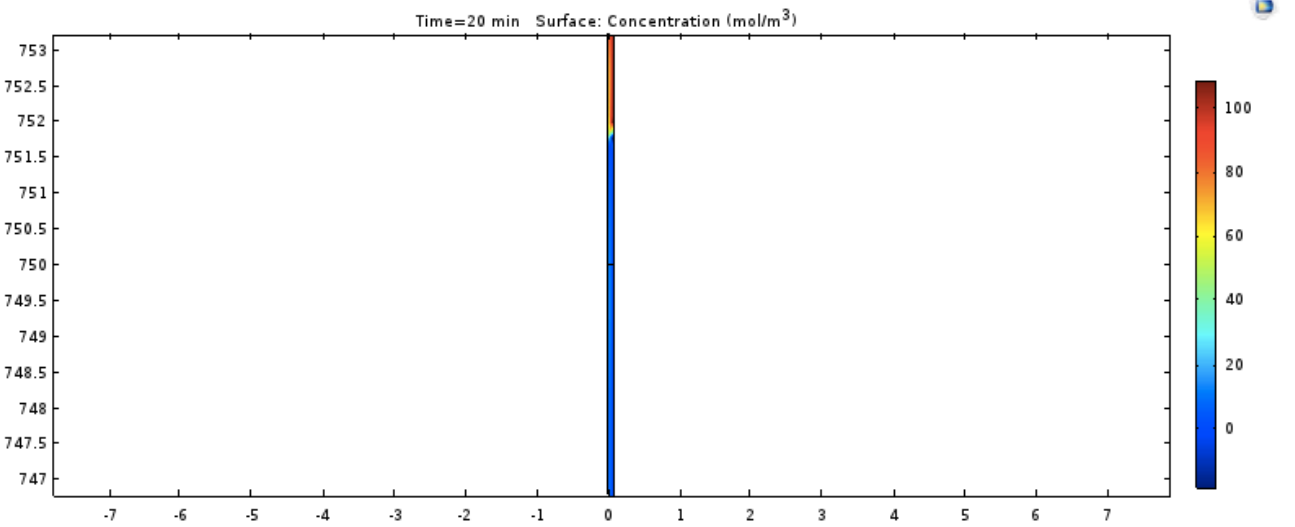


Figure A- 94: Surface concentration, well size difference 2, after 20 minutes

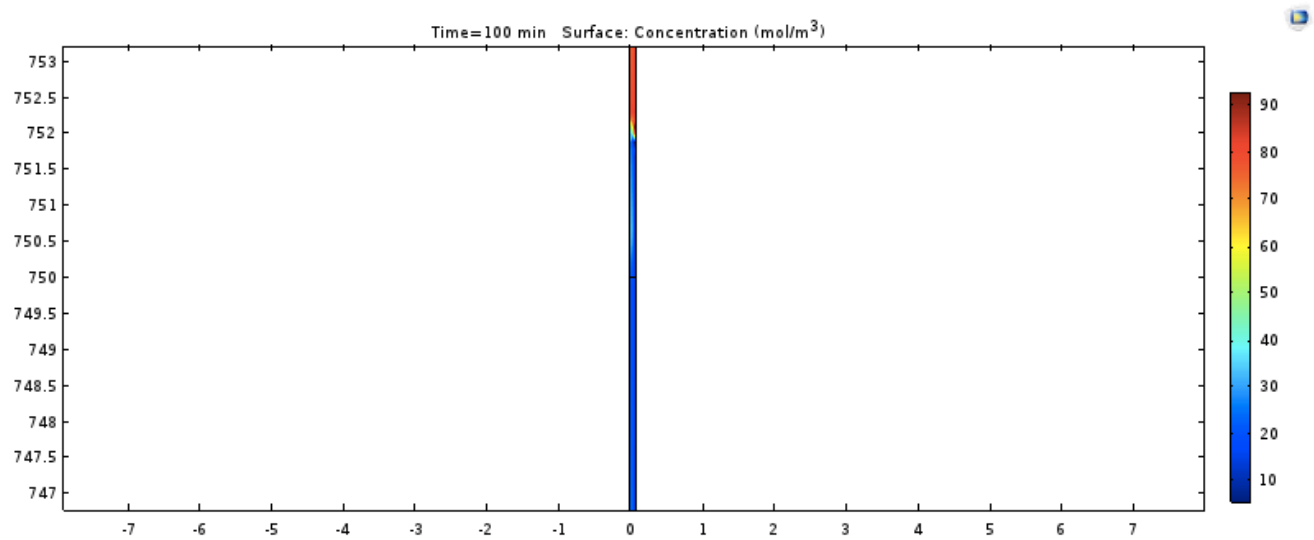


Figure A- 95: Surface concentration, well size difference 2, after 100 minutes

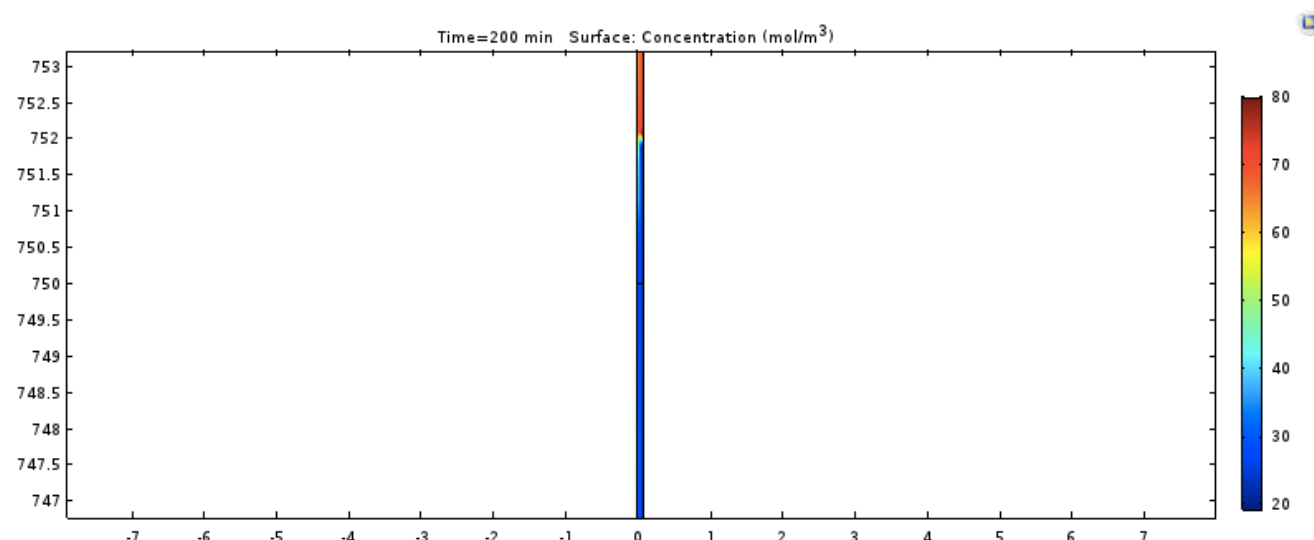


Figure A- 96: Surface concentration, well size difference 2, after 200 minutes

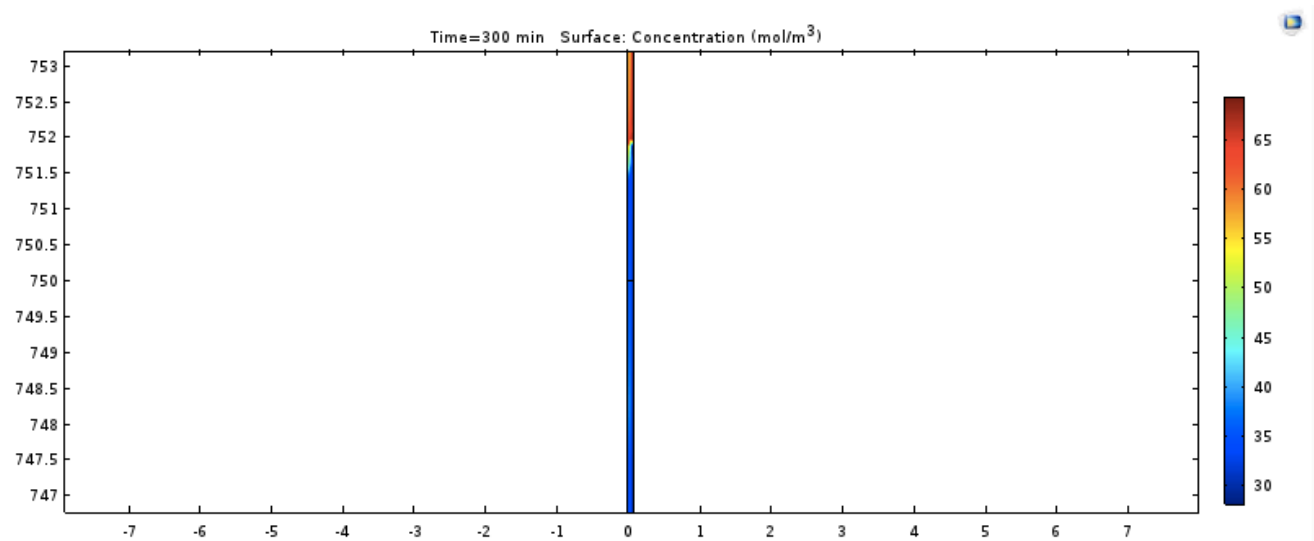


Figure A- 97: Surface concentration, well size difference 2, after 300 minutes

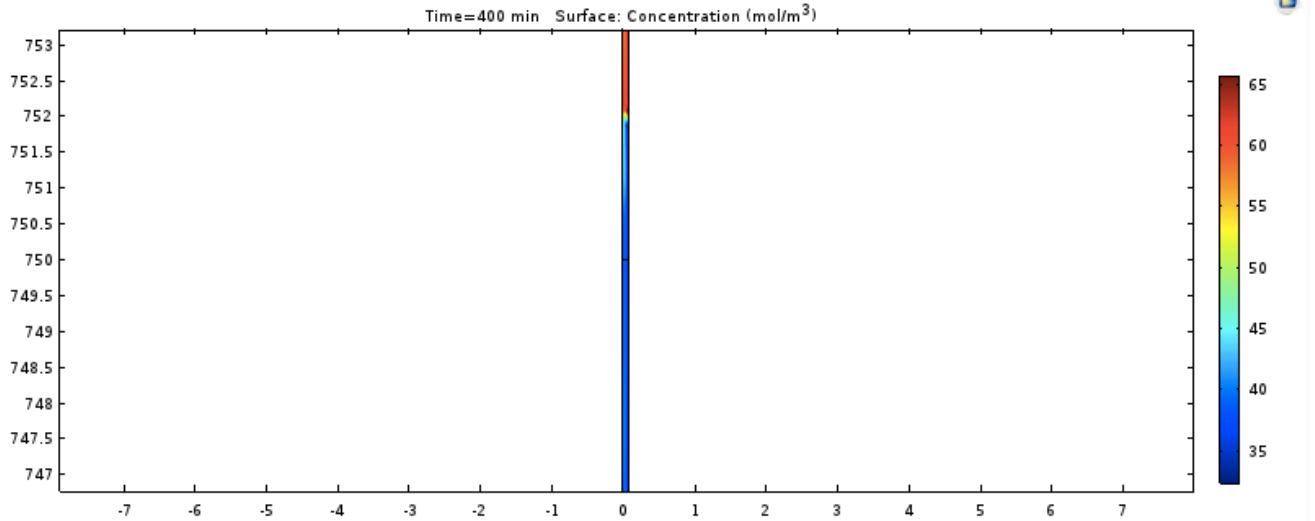


Figure A- 98: Surface concentration, well size difference 2, after 400 minutes

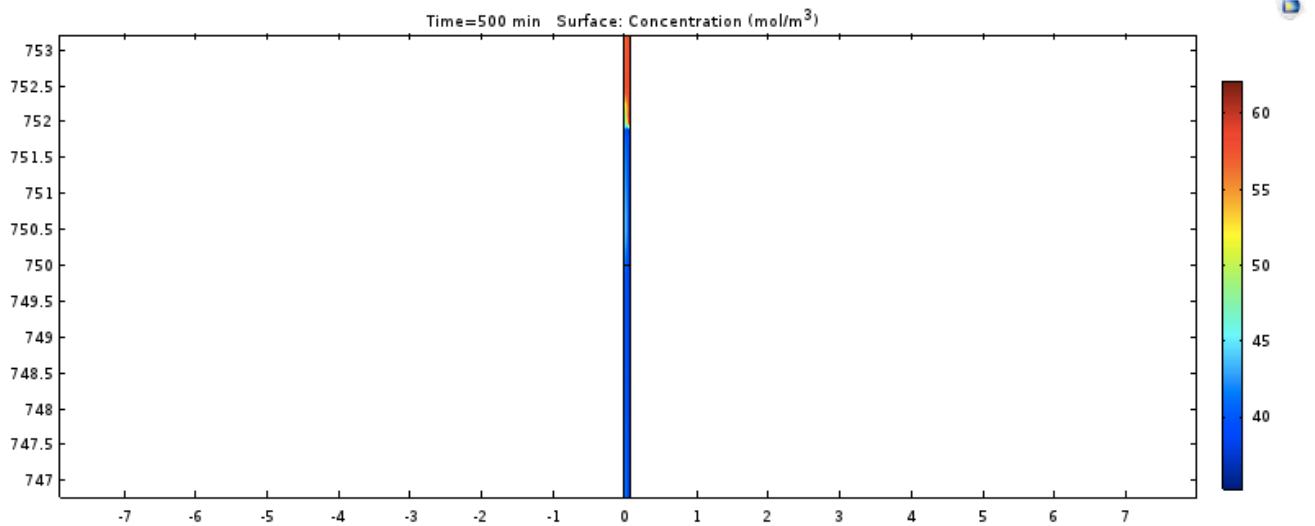


Figure A- 99: Surface concentration, well size difference 2, after 500 minutes

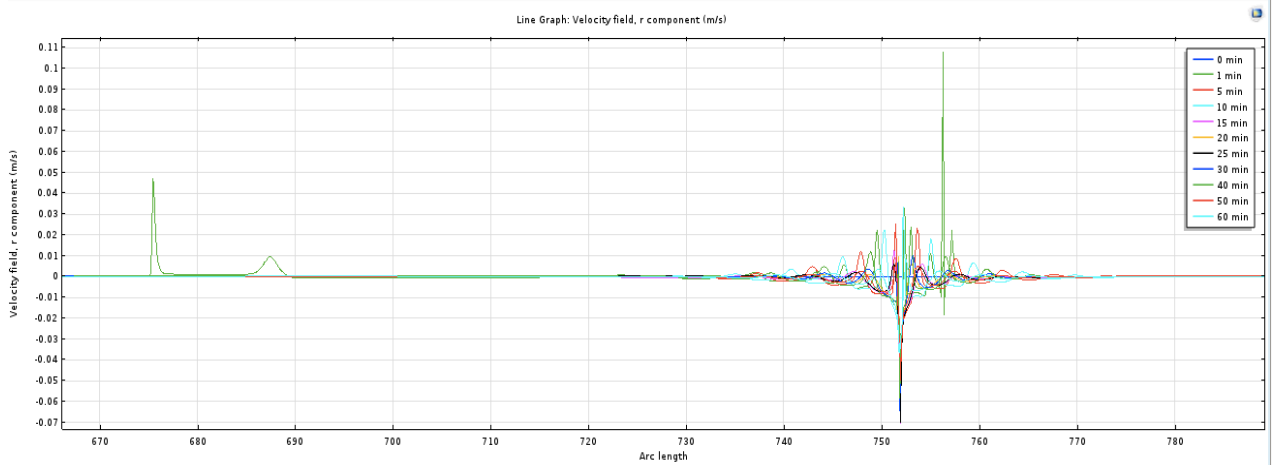


Figure A- 100: Line graph velocity field at interface, well size difference 2, during 1 hour

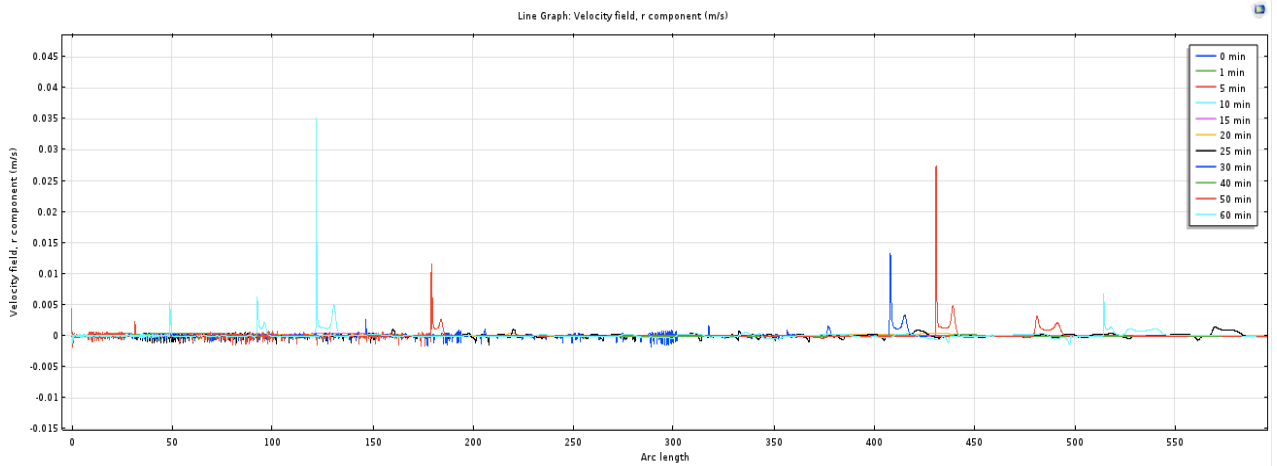


Figure A- 101: Line graph velocity field on bottom of fluid column, well size difference 2, during 1 hour

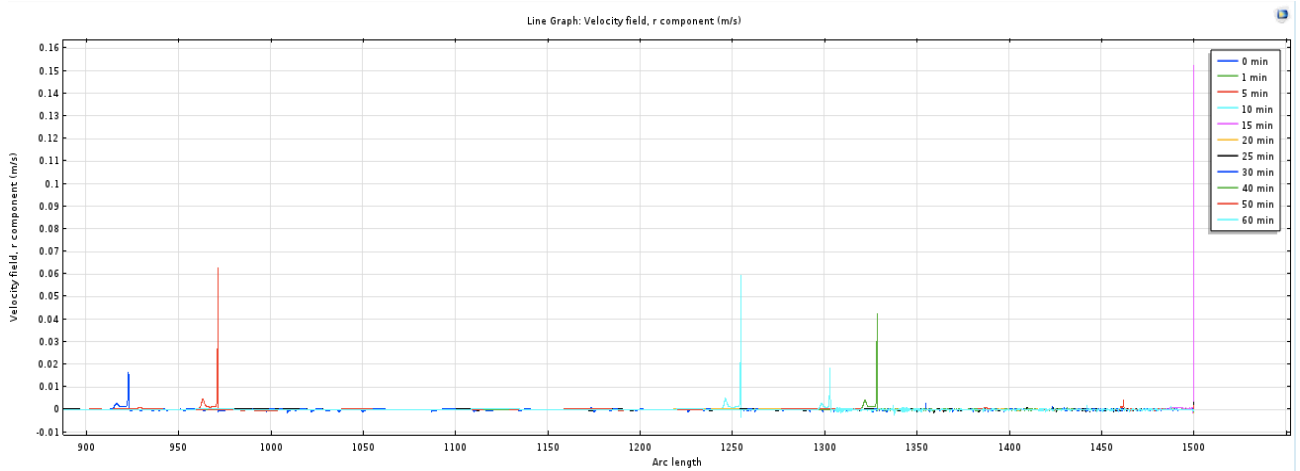


Figure A- 102: Line graph velocity field on top of fluid column, well size difference 2, during 1 hour

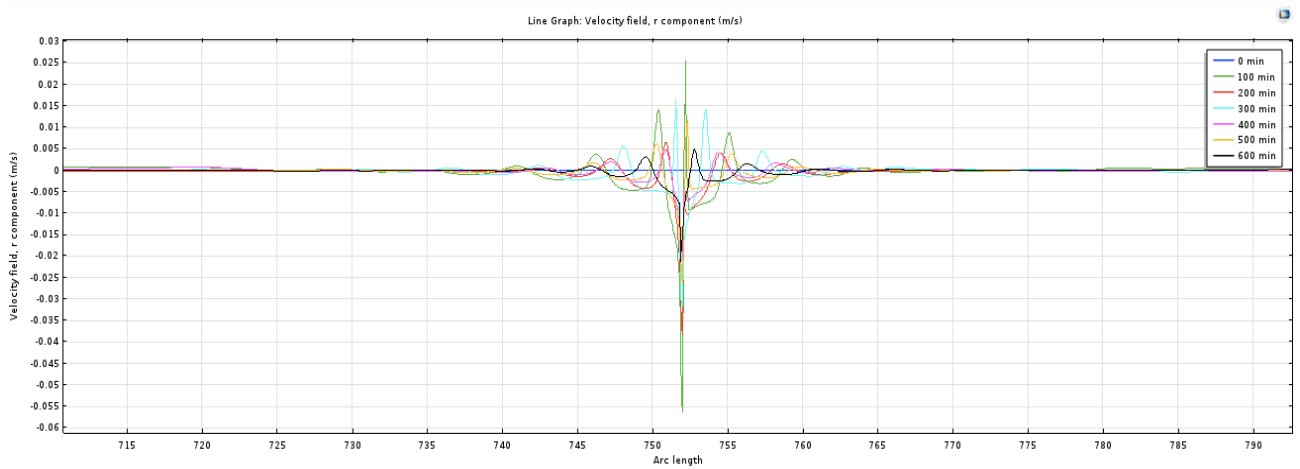


Figure A- 103: Line graph velocity field at interface, well size difference 2, during 10 hours

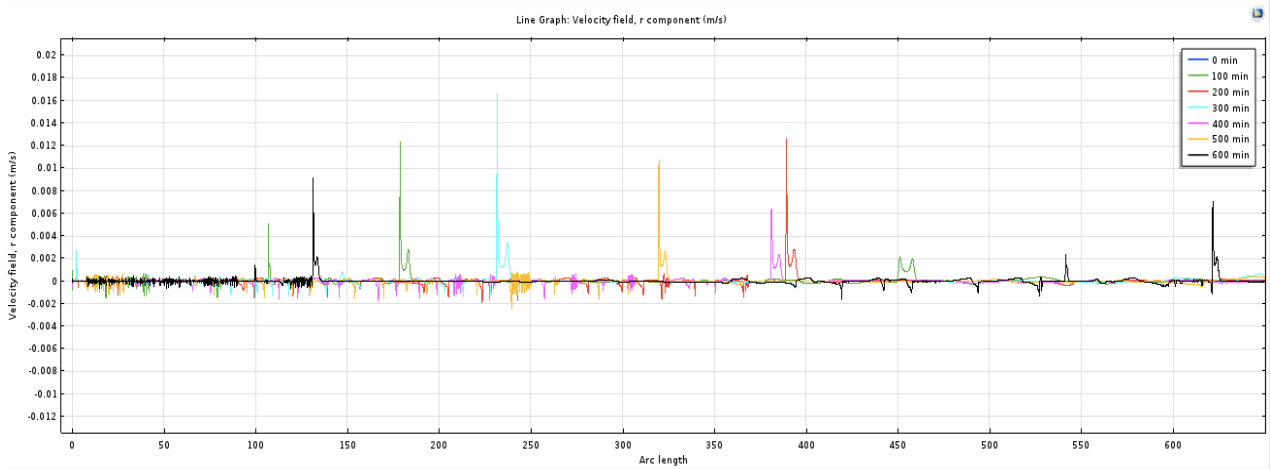


Figure A- 104: Line graph velocity field on bottom of fluid column, well size difference 2, during 10 hours

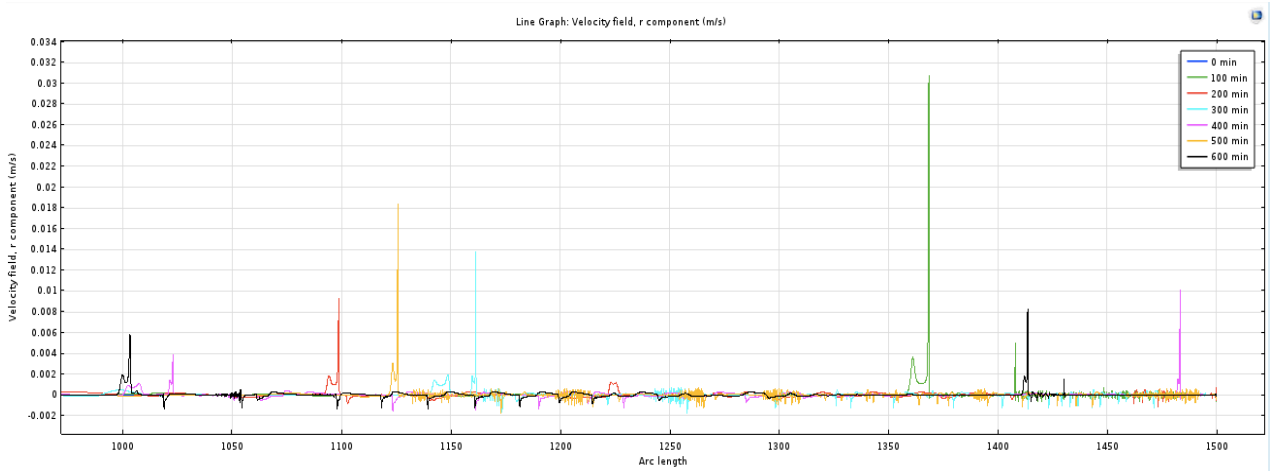


Figure A- 105: Line graph velocity field on top of fluid column, well size difference 2, during 10 hours

APPENDIX B EXPERIMENTS

B-1 Experiment #1

Table B- 1: Rheology properties, experiment #1

RPM	Heavy fluid	Light fluid
600	>300	27.5
300	>300	17
200	224	14.5
100	113	12
60	68	11
30	34	10
6	7	9
3 (gel)	4	8.5

Table B- 2: Length of mixing zone, experiment #1

Time (min)	Length of mixing zone (cm)
3	11.1
6	25.5
9	37.1
12	42.0
15	45.4
18	48.9
21	51.1
23	60.9
24	72.7
25	80.7
26	85.5
30	95.9
40	116.3

B-2 Experiment #2

Table B- 3: Rheology properties, experiment #2

RPM	Heavy fluid	Light fluid
600	90	65
300	68	54
200	58	49
100	47	42
60	43	38
30	39	34
6	34	28
3 (gel)	34	28

B-3 Experiment #3

Table B- 4: Rheology properties, experiment #3

RPM	Heavy fluid	Light fluid
600	70	63
300	50	52
200	42	47
100	32	40
60	28	36
30	24	33
6	20	28
3 (gel)	19	27

Table B- 5: Length of mixing zone, experiment #3

Time (min)	Length of mixing zone (cm)
0	0
5	0
10	2
15	3
20	3
25	3
30	3
35	3
40	3
45	3
50	8

55	10
60	44
65	46
70	50
75	60

B-4 Experiment #4

Table B- 6: Rheology properties, experiment #4

RPM	Heavy fluid	Light fluid
600	50	75
300	31	56
200	25	48
100	18	38
60	14	33
30	11	29
6	7	21
3 (gel)	7	20

Table B- 7: Length of mixing zone, experiment #4

Time (min)	Length of mixing one (cm)
0	0
5	0
10	4
15	6
20	8
25	10
30	10
35	10
40	12
50	12
60	12
70	12
90	12
105	12
120	24

B-5 Experiment #5

Table B- 8: Rheology properties, experiment #5

RPM	Heavy fluid	Light fluid
600	49	37
300	31	26
200	25	21
100	18	15
60	16	12
30	13	10
6	11	6
3 (gel)	11	6

Table B- 9: Length of mixing zone, experiment #5

Time (min)	Length of mixing zone (cm)
0	22
5	22
10	22
15	22
20	24
25	24
30	24
35	24
40	24
45	24
50	30
55	38
60	38
70	38
80	40
90	44
100	44
110	110
135	116
150	120
165	120
180	120
240	120

B-6 Experiment #6

Table B- 10: Rheology properties, experiment #6

RPM	Heavy fluid	Light fluid
600	175	37
300	100	15
200	73	10
100	45	6
60	33	4
30	23	3
6	11	2
3 (gel)	10	1.5

Table B- 11: Length of mixing zone, experiment #6

Time (min)	Length of mixing zone (cm)
0	53
5	53
10	53
15	53
20	53
25	53
30	106
35	116
40	116
45	116
50	116
55	116
60	116
75	130
90	158
105	158
120	158
135	158
180	158
210	190
215	190
270	190

B-7 Experiment #7

Table B- 12: Length of mixing zone, experiment #7

Time (min)	Length of mixing zone (cm)
0	24
5	28
10	30
15	32
20	56
25	58
30	60
35	60
40	60
45	60
50	60
55	60
60	60
65	190

B-8 Experiment #8

Table B- 13: Rheology properties, experiment #8

RPM	Heavy fluid
600	76
300	39.5
200	27
100	15
60	10
30	5.5
6	2
3 (gel)	1.5

Table B- 14: Length of mixing zone, experiment #8

Time (min)	Length of mixing zone (cm)
0	10
5	28
10	38
15	38
20	60
25	61
30	61
35	61
40	61
45	62
50	62
55	62
60	112
65	190

APPENDIX C PLUG EXPERIMENT

Method for Stabilization of Reelwell’s HOL Fluids

This report presents the development and testing of fluid “plug” idea.

A-C.1 Introduction

This draft report presents a method to create a stable heavy over light interface. The concept was developed based on Rayleigh-Taylor’s instability phenomenon and the idea is tested through experimental works.

It is a natural phenomenon that the heavy over light instability is governed by change in density and pressure gradient at the interface. From the literature it is reviewed that the height of the mix zone development is proportional to the Atwood number and the square of time with proportionality constant, called alpha which describe the rate of mix. When the Atwood number is positive, the interface is instable and when it is zero or nearly zero the interface will be stable.

$$h = \alpha A g t^2 \quad (\text{A-C.1})$$

$$A = \frac{\rho_H - \rho_L}{\rho_H + \rho_L} \quad (\text{A-C.2})$$

A-C.2 Theory

Figure C-1 illustrates the Rayleigh-Taylor heavy over light instability sequence. Figure C-1 (a) is the condition at $t = 0$ and Figure C-1 (b) is at some time t , which creates instability. During figure C-1 (c), the instability creates spike, bubble and droplets.

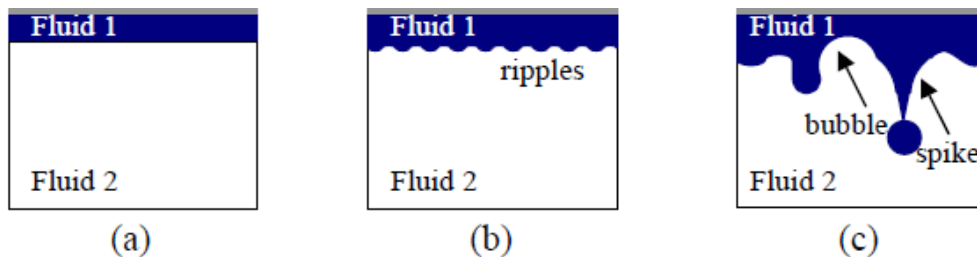


Figure C- 1: Rayleigh-Taylor heavy over light instability sequence

A-C.2.1 Settling velocity for solid particle

As can be seen from the figure, the bubble act like a solid since it consists of barite. The bubble is suspended in the fluid 2 system. For this particle to be in suspension, the viscosity of the fluid should be higher. This phenomenon can be described by Stokes law.

$$V_s = \frac{gd_p^2(\rho_p - \rho_s)}{18\mu_{eff}} \quad (A-C.3)$$

where

- d_p is the particle diameter
- ρ_p is particle density (heavy fluid)
- ρ_s is fluid density
- μ_{eff} is effective apparent viscosity
- g is acceleration due to gravity

A-C.2.2 Idea to create stable heavy over light

From Equation A-C.3, we can learn that particle settle at lower velocity if the fluid viscosity is higher. Therefore, in order to hold bubbles of the heavy fluid in suspension, the lighter fluid should have a higher viscosity. Since we cannot modify the lighter fluid of Reelwell to a have a higher viscosity, we need to insert a fluid “plug” which separates the heavy (Reelwell) from the light (Reelwell). This fluid acts as spacer.

To fit the Stokes law for our fluid system, by analogy, Equation A-C.3 can be modified as

$$V_s = \frac{gd_p^2(\rho_H - \rho_L)}{18\mu_{Light}} \quad (A-C.4)$$

where

- d_p is the particle diameter
- ρ_H is particle density (heavy fluid)
- ρ_L is light fluid density
- μ_{Light} is effective apparent viscosity of light fluid
- g is acceleration due to gravity

A-C.3 Experiment

The idea presented in section A-C.2.2 will be tested here. The heavy and light fluids are typical Reelwell fluids. The heavier fluid has a density of 1.75 sg and 1.6 sg (from Master's Thesis of Magne Hurum [4]). The lighter fluid was obtained from the left over from experiment from Master's Thesis of Eirik A. Vandvik [3], which has a density of 1.375 sg. The second light has a density of 1.285 sg.

Two experiments were performed

- Heavy/Plug/Light = 1.6/1.075/1.375 sg
- Heavy/Plug/Light = 1.75/1.075/1.285 sg

A-C.3.1 Viscometer measured data drilling fluids

Figure A-C.2 shows the measured viscometer data of Heavy (1.75 sg), plug (1.075 sg) and light (1.285 sg) fluid. As can be seen, the yield strength of the plug is very high.

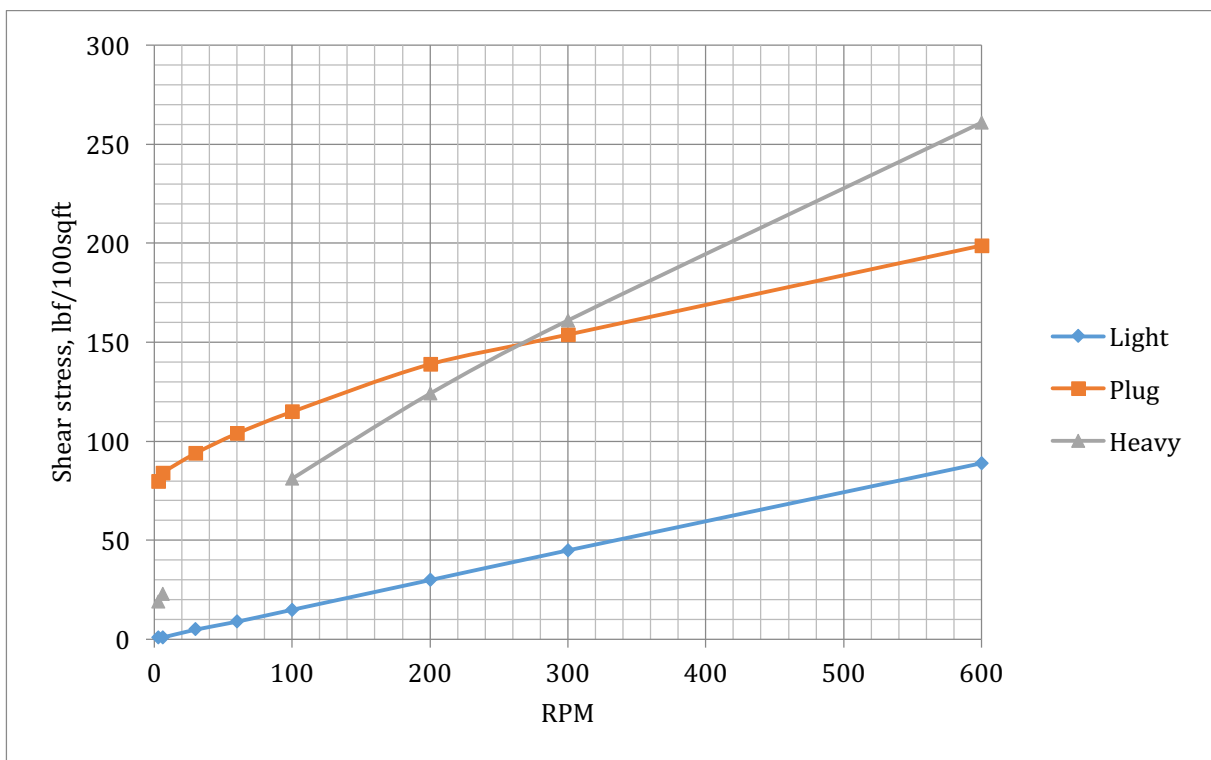


Figure C- 2: Viscometer data of the fluid systems

A-C.3.2 Viscosity and physical properties of drilling fluids

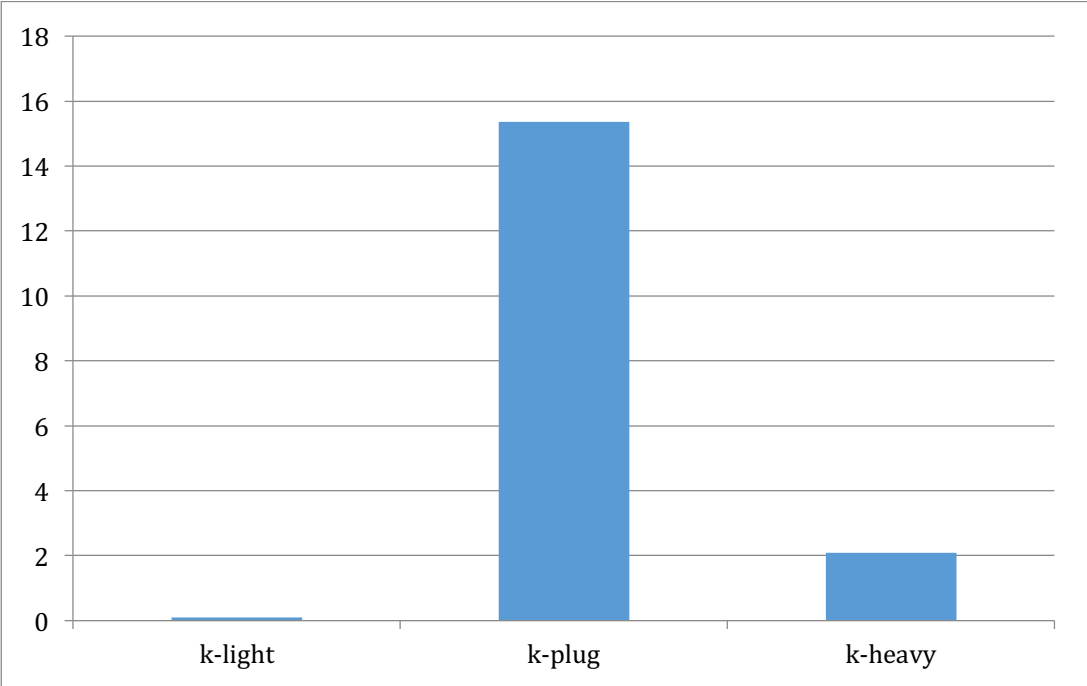


Figure C- 3: Comparisons of consistency index

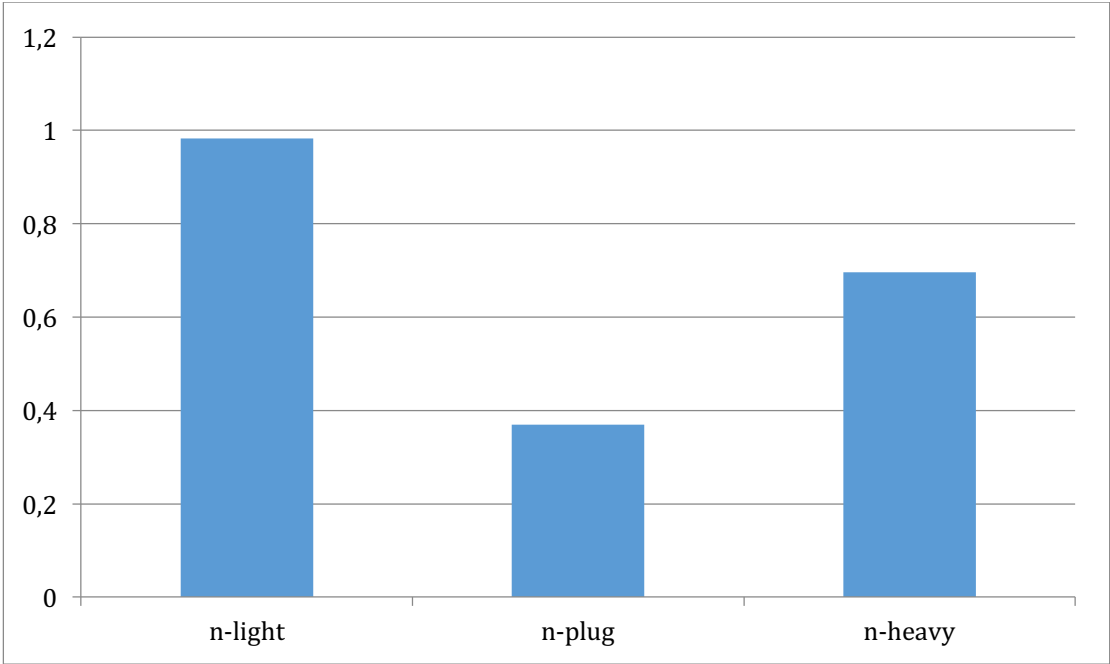


Figure C- 4: Comparisons of flow index

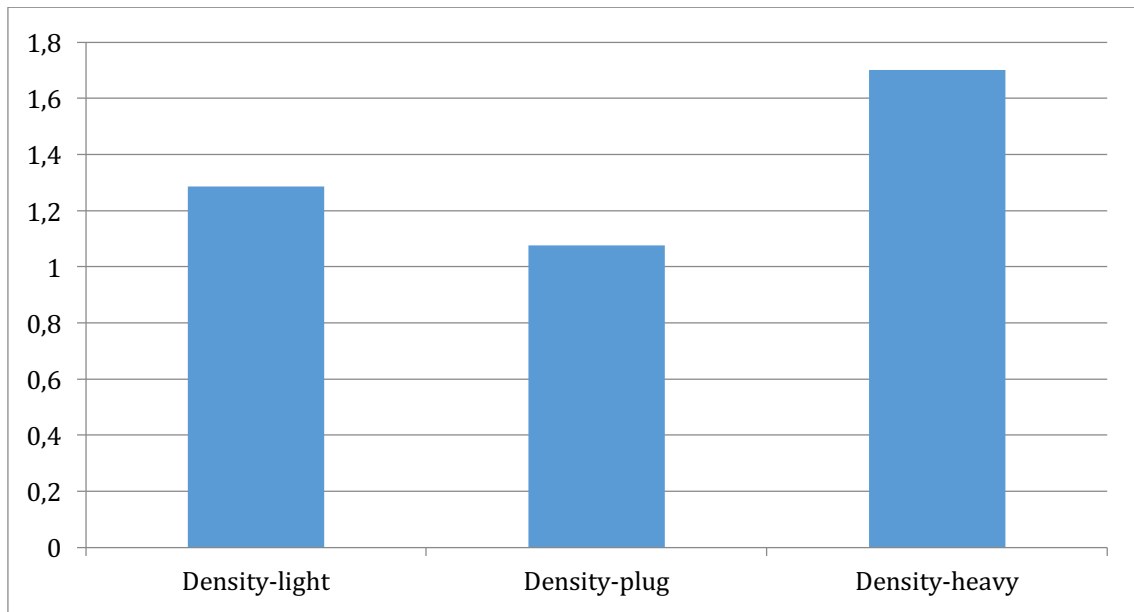


Figure C- 5: Comparisons of density

As can be seen, the LSYS describes the gel strength of the fluid system, which has something to do with the suspension of heavy fluid. The plug LSYS is five times higher than the heavy fluid and hence can create a stable interface. Unlike the Atwood number, the gel strength contrast is also one of the parameters that control the stability of the heavy/over light interface.

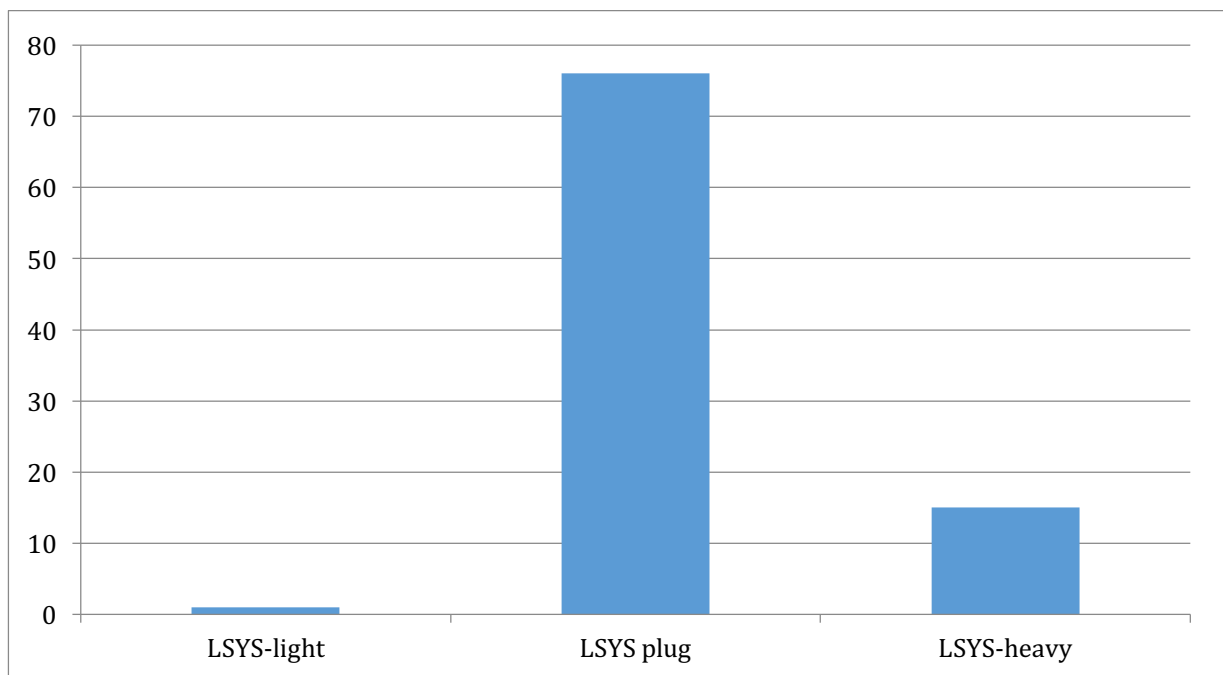
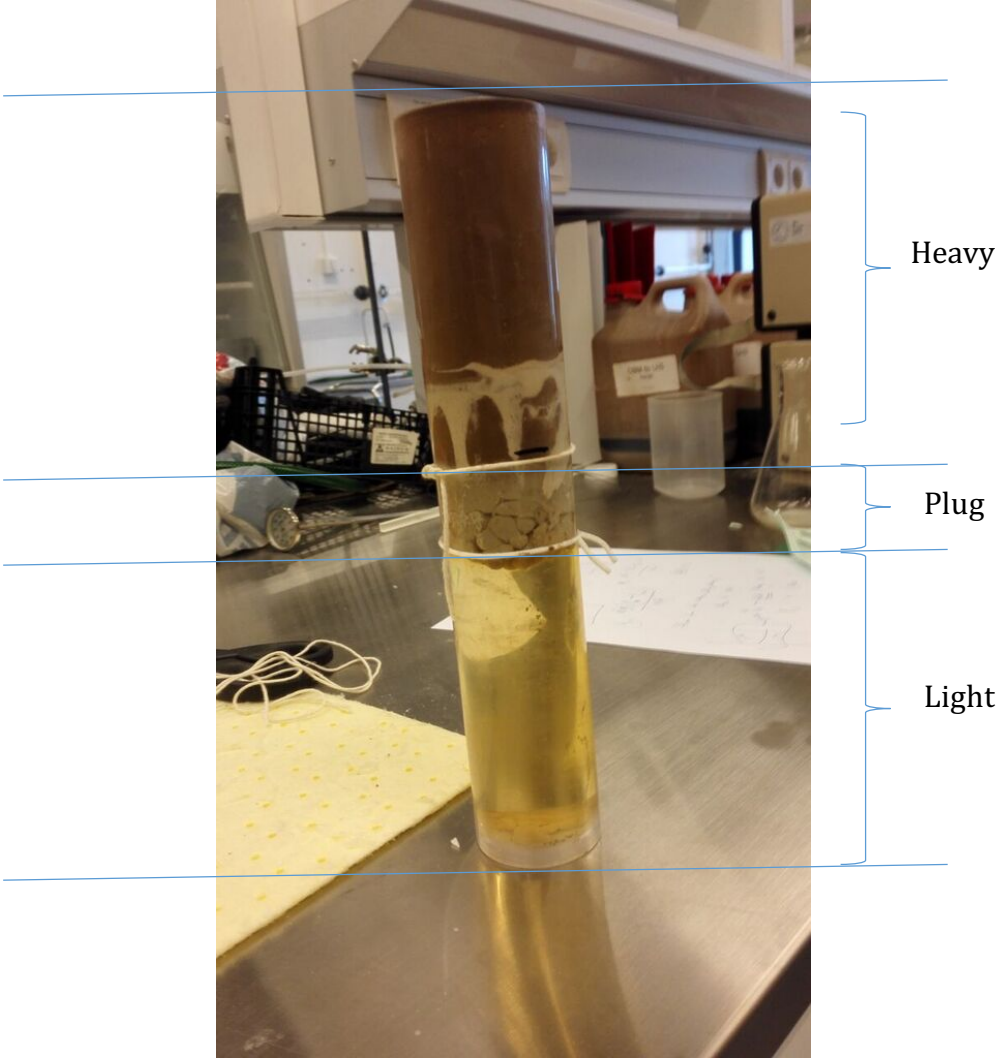


Figure C- 6: Comparisons of Lower Shear Yield Strength

A-C.4 Results

A-C.4.1 Heavy over light stability of system 1

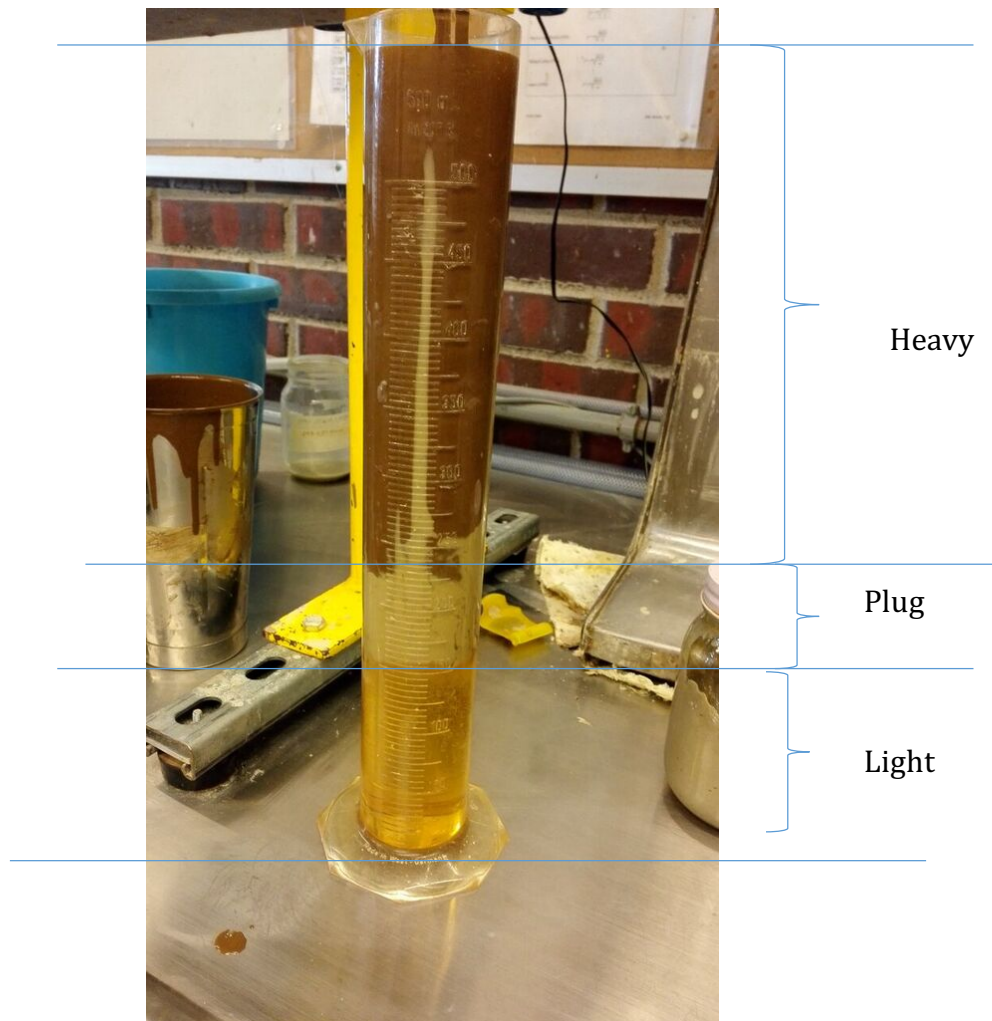
System 1= Heavy/Plug/Light = 1.6/1.075/1.375 sg



Observation: The system was stable during 24 hours. The plug had no leak path so that the heavy and the light were stable

A-C.4.2 Heavy over light stability of system 2

System 2 = Heavy/Plug/Light = 1.75/1.075/1.285 sg



Observation: Due to leak path, after 24 hours the light fluids penetrates through the plug.

A-C.5 Summary

The result shows that the presence of fluid plug, which has higher gel strength and lower density, will help stabilizing the heavy fluid. If this is interesting results, it is desirable to test very well formulated industry spacer (Halliburton's) to learn more about the behavior of fluid "plug" between the heavy/light of the Reelwell fluid. For this we want to have

- a spacer having the property of fluid plug presented in section A-C.3.1
- a spacer, which is commonly used for cement operation

APPENDIX D LIST OF FIGURES

Figure 1: Illustration of an envelope of drilled ERD [1].....	1
Figure 2: Reelwell Drilling Method [2].....	2
Figure 3: Heavy over Light solution in horizontal section.....	3
Figure 4: Research methods.....	4
Figure 5: Schematic of the arrangement for the Reelwell Drilling Method.....	6
Figure 6: Relationship between viscosity, shear stress and shear rate for a Newtonian fluid	11
Figure 7: Examples of relationship between viscosity, shear stress and shear rate for a non-Newtonian fluid.....	11
Figure 8: An illustration of density mix as a function of volume fraction.....	12
Figure 9: Rotation of drill pipe in wellbore	15
Figure 10: Forces affecting the fluids at the interface	17
Figure 11: Hydrodynamics simulation of the Rayleigh-Taylor instability	18
Figure 12: Model Builder in COMSOL	22
Figure 13: Defining the size of the fluid column in COMSOL	23
Figure 14: 2D Axisymmetric option in COMSOL Multiphysics®.....	23
Figure 15: Parameters in COMSOL.....	24
Figure 16: Dividing the rectangle/fluid column into two pieces in COMSOL.....	25
Figure 18: Variables expressions in COMSOL	25
Figure 19: Four different types of elements used for 3D modelling in COMSOL	28
Figure 20: Meshing at the interface (left) and at the boundaries; at the top (in the middle) and at the bottom (to the right), and along the pipe wall.....	29
Figure 20: Boundary condition in COMSOL	29
Figure 21: Physics interfaces in COMSOL	30
Figure 22: Surface concentration of reference case at start of simulation.....	33
Figure 23: Surface concentration of reference case after 1 minute.....	33
Figure 24: Surface concentration of reference case after 1 hour.....	34
Figure 25: Surface concentration of reference case after 10 hours.....	34
Figure 26: Line Graph Concentration Reference Case after 0, 1, 5, 10, 15, 20, 25, 30, 40, 50 and 60 minutes	36

Figure 27: Line Graph Concentration Reference Case after 0, 100, 200, 300, 400, 500 and 600 minutes.....	37
Figure 28: Concentration fluid column, Reference case	38
Figure 29: Line Graph Velocity field Reference Case after 0, 1, 5, 10, 15, 20, 25, 30, 40, 50 and 60 minutes	40
Figure 30: Line Graph Velocity field Reference Case after 0, 100, 200, 300, 400, 500 and 600 minutes.....	41
Figure 31: Density fluid column vs. time, Reference Case	43
Figure 32: Surface concentration of Density Difference 1 at start.....	45
Figure 33: Surface concentration of Density Difference 1 after 1 minute	45
Figure 34: Surface concentration of Density Difference 1 after 1 hour	46
Figure 35: Surface concentration of Density Difference 1 after 10 hours	46
Figure 36: Line Graph Concentration Density Difference 1 after 0, 1, 5, 10, 15, 20, 25, 30, 40, 50 and 60 minutes	48
Figure 37: Line Graph Concentration Density Difference 1 after 0, 100, 200, 300, 400, 500 and 600 minutes.....	49
Figure 38: Concentration fluid column, Density Difference case 1	50
Figure 39: Line Graph Velocity field Density Difference 1 after 0, 1, 5, 10, 15, 20, 25, 30, 40, 50 and 60 minutes	52
Figure 40: Line Graph Velocity field Density Difference 1 after 0, 100, 200, 300, 400, 500 and 600 minutes.....	53
Figure 41: Density fluid column vs. time, Density Difference 1.....	55
Figure 42: Surface concentration of Density Difference 2 at start.....	56
Figure 43: Surface concentration Density Difference 2 after 1 minute	57
Figure 44: Surface concentration Density Difference 2 after 1 hour	57
Figure 45: Surface concentration Density Difference 2 after 10 hours.....	58
Figure 46: Line Graph Concentration Density Difference 2 after 0, 1, 5, 10, 15, 20, 25, 30, 40, 50 and 60 minutes	59
Figure 47: Line Graph Concentration Density Difference 2 after 0, 100, 200, 300, 400, 500 and 600 minutes.....	60
Figure 48: Concentration fluid column, Density Difference case 2.....	61
Figure 49: Line Graph Velocity field Density Difference 2 after 0, 1, 5, 10, 15, 20, 25, 30, 40, 50 and 60 minutes	63

Figure 50: Line Graph Velocity field Density Difference 2 after 0, 100, 200, 300, 400, 500 and 600 minutes.....	64
Figure 51: Density fluid column, vs. time, Density Difference 2.....	66
Figure 52: Surface Concentration at start, Viscosity Difference 1.....	68
Figure 53: Surface Concentration after 1 minute, Viscosity Difference 1.....	68
Figure 54: Surface Concentration after 1 hour, Viscosity Difference 1.....	69
Figure 55: Surface Concentration after 10 hours, Viscosity Difference 1.....	69
Figure 56: Line Graph Concentration Viscosity Difference 1 after 0, 1, 5, 10, 15, 20, 25, 30, 40, 50 and 60 minutes.....	71
Figure 57: Line Graph Concentration Viscosity Difference 1 after 0, 100, 200, 300, 400, 500 and 600 minutes.....	72
Figure 58: Concentration fluid column, Viscosity Difference case 1.....	73
Figure 59: Line Graph Velocity field Viscosity Difference 1 after 0, 1, 5, 10, 15, 20, 25, 30, 40, 50 and 60 minutes.....	75
Figure 60: Line Graph Velocity field Viscosity Difference 1 after 0, 100, 200, 300, 400, 500 and 600 minutes.....	76
Figure 61: Density fluid column vs. time, Viscosity Difference 1.....	78
Figure 62: Surface concentration Viscosity Difference 2 at start.....	79
Figure 63: Surface concentration Viscosity Difference 2 after 1 minute.....	79
Figure 64: Surface concentration Viscosity Difference 2 after 1 hour.....	80
Figure 65: Surface concentration Viscosity Difference 2 after 10 hours.....	80
Figure 66: Line Graph Concentration Viscosity Difference 2 after 0, 1, 5, 10, 15, 20, 25, 30, 40, 50 and 60 minutes.....	82
Figure 67: Line Graph Concentration Viscosity Difference 2 after 0, 100, 200, 300, 400, 500 and 600 minutes.....	83
Figure 68: Concentration fluid column, Viscosity Difference case 2.....	84
Figure 69: Line Graph Velocity field Viscosity Difference 2 after 0, 1, 5, 10, 15, 20, 25, 30, 40, 50 and 60 minutes.....	86
Figure 70: Line Graph Velocity field Viscosity Difference 2 after 0, 100, 200, 300, 400, 500 and 600 minutes.....	87
Figure 71: Density fluid column vs. time, Viscosity Difference 2.....	89
Figure 72: Surface concentration Well Size Difference 1 at start.....	91
Figure 73: Surface concentration Well Size Difference 1 after 1 minute.....	91

Figure 74: Surface concentration Well Size Difference 1 after 1 hour	92
Figure 75: Surface concentration Well Size Difference 1 after 10 hours	92
Figure 76: Line Graph Concentration Well Size Difference 1 after 0, 1, 5, 10, 15, 20, 25, 30, 40, 50 and 60 minutes	94
Figure 77: Line Graph Concentration Well Size Difference 1 after 0, 100, 200, 300, 400, 500 and 600 minutes.....	95
Figure 78: Concentration fluid column, Well Size Difference case 1.....	96
Figure 79: Line Graph Velocity field Well Size Difference 1 after 0, 1, 5, 10, 15, 20, 25, 30, 40, 50 and 60 minutes	98
Figure 80: Line Graph Velocity field Well Size Difference 1 after 0, 100, 200, 300, 400, 500 and 600 minutes.....	99
Figure 81: Density fluid column vs. time, Well Size Difference 1.....	101
Figure 82: Surface Concentration Well Size Different 2 at start	102
Figure 83: Surface Concentration Well Size Different 2 after 1 minute.....	102
Figure 84: Surface Concentration Well Size Different 2 after 1 hour.....	103
Figure 85: Surface Concentration Well Size Different 2 after 10 hours.....	103
Figure 86: Line Graph Concentration Well Size Difference 2 after 0, 1, 5, 10, 15, 20, 25, 30, 40, 50 and 60 minutes	105
Figure 87: Line Graph Concentration Well Size Difference 2 after 0, 100, 200, 300, 400, 500 and 600 minutes.....	106
Figure 88: Concentration fluid column, Well Size Difference case 2.....	107
Figure 89: Line Graph Velocity field Well Size Difference 2 after 0, 1, 5, 10, 15, 20, 25, 30, 40, 50 and 60 minutes	109
Figure 90: Line Graph Velocity field Well Size Difference 2 after 0, 100, 200, 300, 400, 500 and 600 minutes.....	110
Figure 91: Density fluid column vs. time, Well Size Difference 2.....	112
Figure 92: General experimental setup.....	114
Figure 93: Syringe for measuring 10 ml of fluid	116
Figure 94: Digital scale for weighing fluid	116
Figure 95: Rheology properties, experiment #1	118
Figure 96: Length of mixing zone, experiment #1	119
Figure 97: Speed of mixing zone, experiment #1	120
Figure 98: Pictures experiment #1 after 0, 20 and 30 minutes.....	121

Figure 99: Rheology properties, experiment #2	122
Figure 100: Pictures experiment #2 at start, after 1 hour and after 24 hours	123
Figure 101: Experiment #2, fluids in test glass at start and after 24 hours.....	124
Figure 102: Rheology properties, experiment #3	125
Figure 103: Length of mixing zone, experiment #3.....	127
Figure 104: Speed of mixing length, experiment #3	127
Figure 105: Pictures, experiment #3, at start and after 2 hours.....	128
Figure 106: Pictures, experiment #3, with rotation at start and after 30 minutes.....	128
Figure 107: Rheology properties, experiment #4	129
Figure 108: Length of mixing zone, experiment #4.....	131
Figure 109: Speed of mixing zone, experiment #4.....	131
Figure 110: Pictures, experiment #4, at start and after 1 hour	132
Figure 111: Pictures, experiment #4, after 1 hour of rotation.....	132
Figure 112: Rheology properties, experiment #5	133
Figure 113: Length of mixing zone, experiment #5.....	135
Figure 114: Speed of mixing zone, experiment #5.....	135
Figure 115: Pictures, experiment #5, at start and after 35 minutes	136
Figure 116: Pictures, experiment #5, after 1 hour and 50 minutes	136
Figure 117: Rheology properties, experiment #6	137
Figure 118: Length of mixing zone, experiment #6.....	139
Figure 119: Speed of mixing zone, experiment #6.....	140
Figure 120: Pictures, experiment #6, at start, after 30 minutes and after 90 minutes..	140
Figure 121: Pictures, experiment #6, at start of rotation	141
Figure 122: Pictures, experiment #6, after 1 hour of rotation (4,5 hours of experiment)	141
Figure 123: Heavy fluid on the bottom of the pipe, experiment #7	143
Figure 124: Length of mixing zone, experiment #7.....	144
Figure 125: Speed of mixing zone, experiment #7.....	144
Figure 126: Pictures, experiment #7, at start, after 1 hour and after 5 minutes of rotation	145
Figure 127: Dividing fluid column in 4 parts.....	147
Figure 128: Length of mixing zone, experiment #8.....	148
Figure 129: Velocity of mixing zone, experiment #8	148

Figure 130: Pictures, experiment #8, at start.....	149
Figure 131: Pictures, experiment #8, at start of rotation and 5 minutes after rotation	149
Figure 132: The four parts in cups.....	150
Figure 133: Length of mixing zone COMSOL simulation.....	152
Figure 134: Maximum speed of fluid COMSOL simulation.....	153
Figure 135: Density upper part of fluid column.....	154
Figure 136: Density lower part of fluid column.....	155
Figure 137: Length of mixing zone, experiments.....	160
Figure 138: Maximum speed, experiments.....	161
Figure 139: Cross sectional area of fluid column.....	162
Figure 140: Heavy fluids properties.....	163
Figure 141: Light fluids properties.....	163

APPENDIX E LIST OF TABLES

Table 1: Parameters for the reference case.....	31
Table 2: Parameters for simulation of density difference in COMSOL.....	44
Table 3: Parameters for simulation of viscosity difference in COMSOL.....	67
Table 4: Parameters for simulation of well size difference in COMSOL.....	90
Table 5: Parameters in the experiments.....	117
Table 6: Fluid parameters, experiment #1.....	118
Table 7: Additives of the fluids in experiment #2.....	121
Table 8: Fluid parameters, experiment #2.....	122
Table 9: Additives of the fluids in experiment #3.....	125
Table 10: Fluid parameters, experiment #3.....	125
Table 11: Additives of the fluids in experiment #4.....	129
Table 12: Fluid parameters, experiment #4.....	130
Table 13: Additives of the fluids in experiment #5.....	133
Table 14: Fluid parameters, experiment #5.....	134
Table 15: Additives of the light fluid in experiment #6.....	137
Table 16: Fluid parameters, experiment #6.....	138
Table 17: Fluid parameters, experiment #7.....	142
Table 18: : Additives of the heavy fluid in experiment #8.....	146
Table 19: Fluid properties, experiment #8.....	146
Table 20: Max. and min. density and density difference.....	151
Table 21: Length of mixing zone and max. speed of fluids.....	152

